Frontiers in Science and Engineering
International Journal

Edited by The Hassan II Academy of Science and Technology of Morocco

Earth, Water and Oceans, Environmental Sciences

View of reefal limestone cliff at Sakhrat Mohammed-Ben-Brahim (Oued-Cherrat), assigned to Lower Emsian.

Devonian to Lower Carboniferous stratigraphy and facies of the Western Moroccan Meseta : Implications for palaeogeography and structural interpretation

Ralph Thomas Becker, Ahmed El Hassani and Zhor Sarah Aboussalam
(Guest Editors)

ACADEMY Press MA

Volume 10 - Number 1 - 2020

Frontiers in Science and Engineering

International Journal

Edited by The Hassan II Academy of Science and Technology of Morocco

Editorial board

Frontiers in Science and Engineering

International Journal

Volume 10 - Number 1 - 2020

Edited by The Hassan II Academy of Science and Technology of Morocco

Devonian to Lower Carboniferous stratigraphy and facies of the Western Moroccan Meseta : Implications for palaeogeography and structural interpretation

Ralph Thomas Becker, Ahmed El Hassani and Zhor Sarah Aboussalam
(Guest Editors)

Special issue dedicated to the memory of late
Jean-Michel DERCOURT

February 2020

Dépôt légal : 2012 PE 0007
ISSN : 2028 - 7615

ACADEMY Press MA

Email : fse@academiesciences.ma
www.academiesciences.ma/fse/

Layout by : AGRI-BYS S.A.R.L
Printed by : Imprimerie LAWNE
11, rue Dakar, 10040 - Rabat

In memoriam

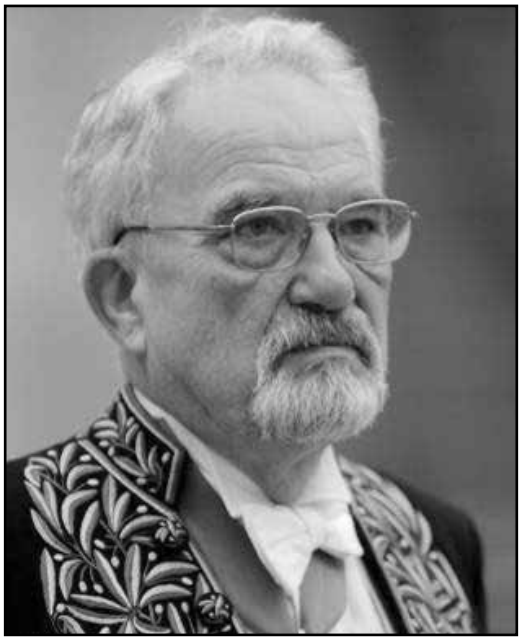

Jean Dercourt (11 mars 1935 - 22 mars 2019)

The Hassan II Academy of Science and Technology dedicates this special issue to the memory of the late Professor Jean-Michel DERCOURT, who passed away on March 23, 2019. He was Honorary Secretary of the Academy of Science (France), Emeritus Professor at Pierre and Marie Curie University (Paris), and since 2005 Associate Member of the Hassan II Academy within the College of Science and Technology, Environment, Earth and Sea. His Majesty King Mohammed VI - may God protect Him - appointed Professor Dercourt as member of the Academy Foundation Commission.

Professor Dercourt will be remembered for his invaluable contributions to the activities of the Hassan II Academy of Science and Technology.

Contents

WELCOME TO FSE

Frontiers in Science and Engineering, an International Journal edited by The Hassan II Academy of Science and Technology, uses author-supplied PDFs for all online and print publication.

The objective of this electronic journal is to provide a platform of exchange of high-quality research papers in science and engineering. Though it is rather of wide and broad spectrum, it is organized in a transparent and simple interactive manner so that readers can focus on their direct interest.

All papers are submitted to the normal peer-review process. Publication criteria are based on :

i) Novelty of the problem or methodology and problem solving, ii) Salience of the approach and solution technique, iii) Technical correctness and outputs, iv) Clarity and organization.

Papers are first reviewed by the Executive Board Director who receives the paper and, if relevant in terms of the overall requirements, it is then proposed to one of the most appropriate associate editors on the field who will select 2 to 3 expert reviewers. Electronic printing will allow considerable time savings for submission delays which will be reduced drastically to less than three to six months. Prospective authors are therefore invited to submit their contribution for assessment while subjected to similar quality criteria review used in paper journals.

Authors are notified of acceptance, need for revision or rejection of the paper. It may be noted that papers once rejected cannot be resubmitted. All the details concerning the submission process are described in another section. This electronic journal is intended to provide :

- the announcement of significant new results,
- the state of the art or review articles for the development of science and technology,
- the publication of proceedings of the Academy or scientific events sponsored by the Academy,
- the publication of special thematic issues.

So that the scientific community can :

- promptly report their work to the scientific community,
- contribute to knowledge sharing and dissemination of new results.

The journal covers the established disciplines, interdisciplinary and emerging ones. Articles should be a contribution to fundamental and applied aspects, or original notes indicating a significant discovery or a significant result.

The topics of this multidisciplinary journal covers amongst others : Materials Science, Mathematics, Physics, Chemistry, Computer sciences, Energy, Earth Science, Biology, Biotechnology, Life Sciences, Medical Science, Agriculture, Geosciences, Environment, Water, Engineering and Complex Systems, Science education, Strategic and economic studies, and all related modeling, simulation and optimization issues, etc. ...

Once, a certain number of papers in a specific thematic, is reached, the Academy might edit a special paper issue in parallel to the electronic version.

Prof. Dr. Driss Ouazar
FSE Executive Director

FORWORD

On the occasion of the Solemn Plenary session of the Hassan II Academy of Science and Technology on the general theme «*Natural heritage and sustainable development*», The College of Science and Technology of Environment, Earth and Sea dedicates this volume of "*Frontiers in Science and Engineering*" to the scientific community in order to share the latest data on the Western Moroccan Meseta geology, particularly on an essential part of the Paleozoic era that is the Devonian and the Lower Carboniferous.

This document will focus on : «***New data** on Devonian to Lower Carboniferous stratigraphy and facies of the Western Moroccan Meseta Implications for palaeogeography and structural interpretation* » and includes results and interpretations of research undertaken by a joint Moroccan-German team in the framework of a partnership between the Mohammed V University of Rabat (Morocco) and the Westphalian Wilhelms-University of Muenster (Germany), within the framework of an agreement between the CNRST (Morocco) and the DFG (Germany). This cooperation has been extended beyond the period allocated to it and now represents more than twenty years of cooperation. It brought together more than thirty specialists from around the world (Moroccans, Europeans and Americans) and constitutes a model of successful group work in Earth Science.

Concerning the project itself, as the first and major step, it was planned to document, characterize and analyze with highest stratigraphic resolution the depositional and faunal history of so far poorly studied Middle Devonian (Eifelian) to Lower Carboniferous (Tournaisian) sections of the Western Moroccan Meseta and of a few Palaeozoic windows within the Atlas Mountains. These represent tectonically complex, different structural zones and sedimentary basins of Hercynian Morocco. It was not expected or required to cover all sections in this rather large region, but the concentration on representative and fossiliferous key sections for each block enabled a meaningful overview of the whole region. In several cases, revisions and more detailed re-sampling of previously published sections took place.

The given time (Devonian-Lower Carboniferous) interval was chosen since it includes sufficiently fossiliferous strata and since it allows to follow the Eovariscan developments from the time before reef complexes were established on specific blocks until the time when rather poorly fossiliferous, thick, flyschoid clastics started to prevail in the whole region, as sign of the beginning of the main phase of Variscan orogeny.

Cooperating specialists from Germany and France provided identifications of various fossil groups, such as brachiopods, trilobites, rugose and tabulate corals, stromatoporids, ostracods, bivalves, and palynomorphs. This continued long-term cooperations, for example in the frame of the IUGS International Subcommission on Devonian stratigraphy.

The biostratigraphic investigations required some taxonomic revisions, the first description of faunas, especially of new and rare forms, and an improved correlation of different biozone systems. Our high-resolution dating of sediments and Eovariscan tectonic movements as well as interbasinal correlations are based on

conodonts, ammonoids, miospores, event (sedimentology/microfacies, stable isotopes) and sequence stratigraphy. In this context, several aspects were especially important:

- The development and correlation of regional zonal schemes with the established international zonations (for example, for the dating of facies changes, periods of condensation, and discontinuities).

- Reworking units, such as conglomerates, synsedimentary breccias and chaotic olistolites, their composition (lithological type, abundance, and sorting of components), texture, and the time range of reworked clasts and faunas needed to be elucidated with the best available precision.

- Biostromal and biohermal complexes of specific areas (their faunal composition, microfacies, palaeoecology, age, and cyclicity).

The tectonic setting of the studied sections is generally known but detailed structural features (macro- and microscopic; local style of folding and faulting, analyses of tectonic transport directions) were needed. Such expertise was important in order to evaluate the palinspastic configuration of outcrops and studied blocks, especially of allochthonous complexes embedded in Carboniferous flysch facies.

Another focus was on strata that correlate with the established fine global event succession, in order to provide data on their regional/local expression and characteristics. As known from pelagic successions of the Anti-Atlas, France, Carnic Alps, or Germany (e.g., Buggisch et al. 2006, Kaiser et al. 2006, 2008), carbon isotope stratigraphy of carbonate matrix is now an important tool in Devonian event stratigraphy. New faunal data sets can be used for palaeobiogeographic comparison within Hercynian Morocco, and between the latter and the Tafilalt, Maider and Dra Valley regions of the Anti-Atlas.

A wealth of new biostratigraphic data provided an improved overview of the timing and regional extent of Eovariscan movements. Taking into consideration the post-sedimentary tectonic dislocations, the study aims at the production of a dynamic palaeogeographical model at substage or even biozonal time resolution. Comparisons with the Tafilalt, Maider, and Dra Valley areas, which regional history is now much better known, enabled to compare the structural history of the stable cratonic NW Gondwana and of the southern margin of the Hercynides at the time of craton margin disintegration (Wendt ١٩٨٥). In this context, the Devonian facies development at the Anti-Atlas/Atlas boundary (e.g., Skoura and Tindjad-Tinerhir areas) deserves special attention.

The results of these studies will be presented in a series of three documents and it will concern the following areas:

Part 1 : Oued Cherrat area (sections of Aïn Khira, Aïn Dakhla, Aïn-Al-Aliliga, and Aïn-as-Seffah); allochthonous Mrirt area (sections of Gara de Mrirt and Anajdam); and Imouzer du Kandar area (Middle Atlas Basement).

Part 2 : Rabat-Tiflet area (Chabet El Harcha, Oued Tiflet), Oulmes area (sections of Aïn Jemaa, Ta'araft, Moulay Hassane, and Bou Alzaz); Azrou area (sections of Jebel ben Arab, Bab El Ari, and Bou Ighial); Khenifra area (sections of Ziyyar and Jbel Tabainout).

Part 3: Ben Ahmed area (sections of Boudouda, Oued Aricha, Zwair); Rehamna area (sections of Mechra Ben Abbou, and Foum El Mejez); Jebilet area (sections Jaidet East, and Mzoudia/Jebel Ardouz); Skoura/South Atlas area (sections of Taliouine, Tizi n'Ourthi, and Asserhmo).

Prof. Dr. Ahmed El Hassani
Associate Editor
Director of the College '*Science and Technology of Environment, Earth and Sea*'
Hassan II Academy of Science and Technology

Contributors:

Dr. Zhor Sarah Aboussalam, Institut für Geologie und Paläontologie, WWU Münster, Corrensstraße 24, D-48149 Münster, Germany; taghanic@uni-muenster.de

Prof. Dr. Ralph Thomas Becker, Institut für Geologie und Paläontologie, WWU Münster, Corrensstraße 24, D-48149 Münster, Germany; rbecker@uni-muenster.de

M.Sc. Stephan Eichholt, Institut für Geologie und Paläontologie, WWU Münster, Corrensstraße 24, D-48149 Münster, Germany; stephan.eichholt@outlook.de

Prof. Dr. Ahmed El Hassani, Institute Scientifique, Mohammed V University of Rabat, Avenue Ibn Batouta, 10106 Rabat, Morocco; ahmed.elhassani@um5.ac.ma

Dr. Sven Hartenfels, Institut für Geologie und Mineralogie, Universität zu Köln, Zülpicher Straße 49a, D-50674 Köln, Germany; shartenf@uni-koeln.de

M.Sc. Stephan Helling, Institut für Geologie und Paläontologie, WWU Münster, Corrensstraße 24, D-48149 Münster, Germany; stephanhelling@uni-muenster.de

Priv.-Doz. Dr. Heiko Hüneke, Ernst-Moritz-Arndt-Universität Greifswald, Domstr. 11, D-17489 Greifswald, Germany; hueneke@uni-greifswald.de

M.Sc. Julia Richter, Institut für Geologie und Paläontologie, WWU Münster, Corrensstraße 24, D-48149 Münster, Germany

Acknowledgements:

Our joint German-Moroccan (DFG-CNRST Maroc) research project on the Devonian to basal Carboniferous of the Moroccan Meseta would have been impossible without the assistance and close cooperation with a wide range of persons, either from Münster or from various Moroccan research institutions, or without the advice by Devonian specialists on various fossil groups. Our special thanks go to (in alphabetical order):

Lukas Afhüppe (Münster): Student assistant, conodont sample processing.

Prof. Dr. Lahssen Baidder (UH2-Casablanca): Field work, special guidance to the Skoura and Tinerhir regions and in the Anti-Atlas, structural and regional geology, general stratigraphy, student field trip leader.

Dr. El Moustafa Benfrika (UH2-Casablanca): Field work in the Oued Cherrat-Ben Slimane, Coastal Block, and Tiflet regions, conodont biostratigraphy.

Dr. Denise Brice (Lille): Devonian and Carboniferous brachiopods.

Traudel Fährenkemper (Münster): Graphics/illustrations.

Dr. Helga Groos-Uffenorde (Göttingen): Devonian ostracods.

Christoph Hartkopf-Fröder (Krefeld): Field work, palynology.

Dr. U. Jansen (Frankfurt a. M.): Devonian brachiopods.

Pia Kain (Münster): Thin sections.

Dr. Fouad El Kamel (UH2-Casablanca): Field work in the Mdakra, Rehamna and Jebilet regions.

Eva Kuropka (Münster): Conodont sample processing.

Davina Mathijssen (Münster): Conodont sample processing.

Dr. Andreas May (Unna): Corals and stromatoporids.

Gerd Schreiber (Münster): Thin sections and goniatite preparations.

M. Sc. Klaus Schwermann (Münster): Devonian shark teeth.

M.Sc. Sören Stichling (Münster/Krefeld): Field work and reef facies.

Prof. Dr. Abdelfatah Tahiri (UM5-Rabat): Field work in the Oulmes-Fes regions.

Dr. Dieter Weyer (Berlin): Devonian deep-water Rugosa.

Devonian to Lower Carboniferous stratigraphy and facies of the Moroccan Meseta: implications for palaeogeography and structural interpretation – a project outline

R. Thomas BECKER & Ahmed EL HASSANI

1. Introduction

1.1. Devonian stratigraphy

The Devonian was the first system in which all chronostratigraphic units (series and stages) were formally defined, producing a stable time frame work for detailed international and interdisciplinary correlation (e.g., BECKER et al. 2012, 2020). This also applies to the main part (Tournaisian, Viséan) of the Lower Carboniferous (e.g., DAVYDOV et al. 2012). The most significant fossil groups that provide an international high-resolution subdivision of time are conodonts and ammonoids for the pelagic facies realm, conodonts, brachiopods and trilobites for the neritic realm, and miospores for terrestrial settings and for nearshore clastic sediments with high terrigeneous influx. There are both regional and global zonation schemes, which supplement each other. Together with other modern stratigraphic techniques, such as Devonian global event, isotope, and sequence stratigraphy, it is now possible to establish precise time frameworks for fossiliferous sedimentary successions, which lie far beyond the past research (Fig. 1). This can now be applied to regions with difficult outcrop conditions and strong tectonic overprinting, where stratigraphic progress has been slow. One such example is the Moroccan Meseta, which, in terms of Devonian-Carboniferous stratigraphy, has long remained in the shadow of the Anti-Atlas (e.g., EL HASSANI & TAHIRI, Eds., 1999; EL HASSANI, Ed., 2004; BECKER et al., Eds., 2013; HARTENFELS et al., Eds., 2018). The eastern Anti-Atlas is famous for its internationally celebrated geological heritage (e.g., EL HASSANI et al. 2017), but, as presented in this volume, there are equally important and fossil-rich localities in the Western Meseta and Middle Atlas basement.

1.2. Devonian plate tectonics

The Devonian plate tectonic configuration has been controversial for a long time and this applies especially to the latitudinal position of Gondwana and Laurussia (= Laurentia + Baltica + Avalonia) and to the width of the oceanic system between both supercontinents, variably named as western part of the Prototethys, Palaeotethys, or the Variscan Oceans (FRANKE et al. 2017). The widely used term Rheic Ocean applies only to a specific part within the dynamic system; it closed during the Emsian, which was followed by the opening of the Rhenohercynian Ocean (e.g., FRANKE 2000). Whilst palaeomagnetic data and reconstructions (e.g., VAN DER VOO 1990; BACHTADSE et al. 1987; TAIT et al. 2000; NANCE et al. 2012) postulated a very wide Devonian ocean, palaeobiogeographic comparisons between cratonic Gondwana and Laurussia (e.g., ROBARDET et al. 1990; MCKERROW et al. 2000; GOLONKA 2007; NAZIK & GROOS-UFFENORDE 2016), suggest a narrow ocean, as depicted first in the Devonian continent distribution of HECKEL & WITZKE (1979). Occurrences of calcareous contourite deposits in strongly condensed deeper-water

settings (HÜNEKE 2006, 2007) agree with close-fit palaeogeographic reconstructions. Based on the close similarity of German and Meseta Givetian reefs, EICHHOLT & BECKER (2016) suggested a ca. 3.000 km wide (N-S) "Variscan Sea". It had no oceanic crust in a wide archipelago of crustal blocks and islands (BECKER et al. 2016d) ranging from the Moroccan Meseta in the South to a ribbon of southern European microplates. These were represented, for example, by the Betic Cordillera and Catalonia of Spain, Menorca, Sardinia, Sicily, and Calabria, as well as the Rif and Kabylie areas, which were then situated more easterly than today ("Palaeo-Adria" belt of FRANKE et al. 2017). Clearly, the Meseta faunas and facies developments play a significant role in this plate tectonic debate.

The Devonian plate configuration is not only crucial for the geodynamic understanding of the Variscan Oceans and later orogeny, but critical for the reconstruction of global palaeoclimate, oceanic currents (e.g., BALBUS 2015), and paleobiogeography, including, for example, the early dispersal of tetrapods and freshwater biota (e.g., YOUNG 1981, 2003 BLIECK et al. 2007). Both equivocal and crucial is the Devonian plate tectonic position of Morocco. Many reconstructions (e.g., HOUSE 1975; NEUGEBAUER 1988, SIMANCAS et al. 2006; GOLONKA 2007, VON RAUMER et al. 2009; PÉREZ-CACÉRES et al. 2017) place it slightly or far to the west of Iberia, directly facing the Appalachian belt. Other authors (e.g., HECKEL & WITZKE 1979; ZIEGLER 1989; MCKERROW et al. 2000; MATTE 2001) place the Moroccan Meseta just to the south of the southern European Variscides. The latter view is strongly supported by palaeobiogeographic similarities (e.g. ROBARDET et al. 2000; EICHHOLT & BECKER 2016) and the trans-Variscan tracing of thin marker units from the Meseta Devonian to southern France. An important example is given in our chapter on the Mrirt sucession (see BECKER et al. 1997; BECKER & HOUSE 2000a).

1.3. Prototethys palaeogeography

A better understanding of the western Prototethys evolution can be reached by a much finer (in terms of time resolution) and dynamic comparison of facies, faunal, floral, and palaeogeographic characteristics of its southern and northern shelf areas. These are preserved in the moderately deformed, fossiliferous, southern (= Meseta, SE Portugal) and northern external Variscides. An improved understanding of the varied and complex sedimentary and faunal successions of the Meseta is the key to understand the dynamics of a seaway, which controlled the East-West moving oceanic water masses and, in the form of stepping stones, the North-South migration of biota. Rather enigmatic and incompatible with the sedimentary and palaeobiogeographic record (e.g., ROBARDET et al. 1990; ROBARDET 2003; ERNST & RODRÍGUEZ 2010) are Devonian maps with a position of Morocco far to the east and completely outside of the southern European/Variscan realm (e.g. DALZIEL et al. 1994, COCKS & TORSVIK 2002).

1.4. Devonian synsedimentary tectonics

The Middle Devonian to Lower Carboniferous was the time when Eovariscan tectonic events occurred throughout the Variscan oceans. This led to distinctively different sedimentary and palaeoecological patterns on separate, often closely adjacent crustal blocks, microplates, and on the marginal shelf sees. However, the lack of precise biostratigraphic dating for such movements and re-sedimentation events hampered palaeogeographic and structural reconstructions. Even further, it has been claimed (TRIBOVILLARD et al. 2004; AVERBUCH et al. 2005) that Eovarican tectonics played a major role as a trigger mechanism for major marine eutrophication

events, such as the Kellwasser Events near the Frasnian-Famennian boundary. This can be tested (and rejected) based on the precise dating of Eovariscan uplift and erosion episodes and their relationships in time and space with the Kellwasser Beds, which are partly well-developed in the Meseta.

There are links between synsedimentary tectonics and palaeobiogeography. More equal facies and biota across the ocean system can be expected in times of tectonic quiescence, when similar depositional conditions could spread over large areas and when faunal exchanges were not limited by deep and wide troughs or subaerial arc barriers. Fluctuating biodiversity gradients and peaks of endemism, for example of (sub)tropical shallow-water corals, ammonoids, and conodonts, are good indicators of stable or changing latitudinal and climatic differences. The Meseta localities provide insights into latitudinally intermediate but tectonically influenced ecosystems at the southern margin of the palaeotropics.

1.5. The Meseta Variscides

As part of the southern Variscides, Hercynian Morocco includes the strongly tectonized Palaeozoic successions north of the more or less stable cratonic part of NW Gondwana, the Anti-Atlas, which experienced only moderate Upper Carboniferous folding and faulting (e.g., BURKHARD et al 2006; TOTO et al. 2007). Sedimentary successions of the Moroccan Meseta and of small tectonic windows within the Atlas Mountains or at its southern margin (Skoura region) are overlain by flat lying Mesozoic and Cenozoic strata. Widespread granites are related to post-Variscan (Cenozoic) volcanism (MICHARD 1976). There was considerable post-Variscan crustal shortening in the High Atlas since the Miocene (GOMEZ et al. 2000). Syn- and postsedimentary tectonic movements (e.g., PIQUE & MICHARD 1989; EL HASSANI & TAHIRI, Eds., 1994, 2000) resulted in a very complex framework of structural units (e.g., PIQUE & MICHARD 1981; PIQUE 1994; MICHARD et al. 2010), each with a distinctive faunal and synsedimentary tectonic history. There are both autochthonous and allochthonous units, including nappes and large olistostromes, that experienced significant westward displacement and re-embedding during the "middle" Carboniferous peak of deformation. The Western Meseta clearly belong to an extensional tectonic regime, from the basal Devonian well into the Carboniferous (e.g., PIQUE 1975; BEAUCHAMP & IZART 1987; OUANAIMI et al. 2019). However, Famennian metamorphism and compression has been suggested for the Midelt area (Middle Atlas; e.g., PIQUE & MICHARD 1981). Towards the Anti-Atlas in the South, there is no evidence for a significant terrane or facies boundary at the tectonically complex southern Variscan Front (e.g., JEANETTE & PIQUE 1981; BAIDDER et al. 2008; FERONI et al. 2010; RYTINA et al. 2013; Sub-Meseta Zone of MICHARD et al. 2010).

A wide range of previous research dealt with post-sedimentary tectonic styles, the main structural framework, and tectonic models (summaries in PIQUE & MICHARD 1981, 1989; PIQUE 1994, 2001; EL HASSANI & TAHIRI, Eds., 1994; EL HASSANI et al. 2003; MICHARD et al. 2008, 2010). However, former attempts to reconstruct the Devonian to Tournaisian palaeogeographic evolution suffered badly from the lack of adequate biostratigraphic data and poor international correlation of successions. Examples are the rough stratigraphic columns in HOEPFFNER et al. (2005; subsequently recycled in other summary papers) and the many uncertainties recognized in stratigraphic reviews, such as EL HASSANI & BENFRIKA (1995, 2000) and KAISER et al. (2007). A few modern (bed-by-bed) studies and high-resolution biostratigraphic data are available for some sections and restricted time intervals.

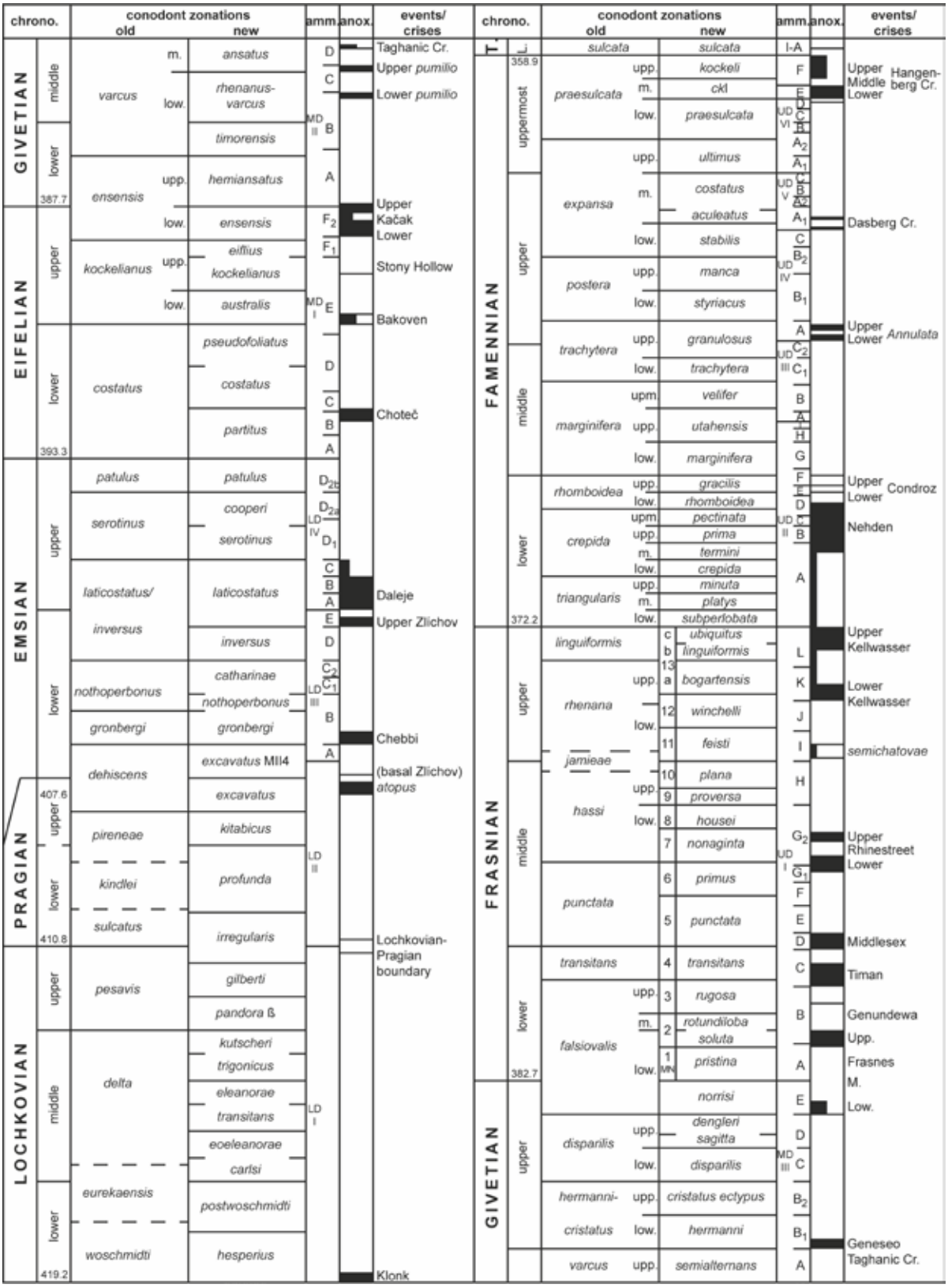

Fig. 1: Devonian chrono-, bio- (conodonts, ammonoid zonal key), and event stratigraphy.

But for the majority of successions, previous biostratigraphic data were imprecise, poorly documented, based on incipient, widely spaced sampling, or require a revision of taxonomy and zonal assignments according to the current state of the art. Our studies intended to overcome these shortcomings, involving also specialists for

other fossil groups, and by concentrating on key sections for individual structural units. The applied schemes for chrono-, bio- (conodonts, ammonoids), and event stratigraphy are shown in Fig. 1. A wealth of new stratigraphic and biofacies results is presented in chapters that include as many details as possible, such as bed-by-beds section logs, abundant outcrop photos, range charts, fossil and microfacies plates. A refined picture of palaeogeography and of Eovariscan movements in time and space will emerge when the data from all individual successions are combined and correlated.

2. Structural units of the Meseta Palaeozoic

2.1. Main tectonic and palaeogeographic zones

The Moroccan Meseta is constituted by the Palaeozoic Plateau and its flat lying cover between the Atlas system and Rif mountains (Figs. 2-3). The Middle Atlas divides this domain into two areas:

The **Western Meseta** is located approximately between the cities of Rabat, Taza, Marrakesh and Essaouira. There are three major Palaeozoic zones (massifs), the Massif Central, Rehamna, and Jebilet, and some outcrops in the small valleys of the Atlantic coastal rivers (e.g., at the Oued Oum-er-Rbia). These massifs are separated by Mesozoic and Cenozoic areas, the Khouribga and Gantour Phosphate plateau, Doukkala, and Chaouïa. Despite this cover, it is possible to establish stratigraphic and structural correlations and to reconstruct a common Palaeozoic history.

The **Eastern Meseta** consists also of Palaeozoic regions and a Mesozoic-Cenozoic cover, but outcrops are smaller than those of the western part. It is composed of the Midelt area, and the areas of Zekkara, Jorf Ouezzène, Jerada Debdou, and Mekkam. The small outcrop make correlations more difficult.

The Palaeozoic basement of the **Middle Atlas** is poorly exposed in small tectonic windows, for example at Immouzer-du-Kandar S of Fez (e.g., CHARRIÈRE & RÉGNAULT 1989; our new chapter). Reworked Neoproterozoic and Lower Palaeozoic rocks, especially magmatic pebbles and the Devonian facies development, differ significantly from other Meseta regions but there are some similarities with the nappes of the eastern Central Meseta.

The principle palaeogeographic configuration of the Meseta began in the upper Silurian, followed by the earliest Hercynian tectonic movements. Early Devonian sedimentation continued in most regions conformably from the Silurian (Pridoli). The transition is characterized by a strong increase of calcareous deposition related to a decreasing amount of terrigenous supply from the West African Craton in the South. This was accompanied by climatic warming due to the motion of northeast Gondwana into a warmer, southern subtropic position.

Three palaeogeographic zones are distinguished in the Moroccan Meseta. A western carbonate platform zone (Western Meseta) was subdivided during the Lower and Middle Devonian into several calcareous ridges and adjacent, deeper-water troughs with shales and rare calcareous intercalations. Biostromes and bioherms grew along the borders of tectonically uplifted and emerged areas. A second, transitional zone, corresponding to eastern parts of the Central Moroccan Massif, is characterized by differentiated facies in allochthonous and autochthonous series. Reef growth was rather localized. The third zone, the Eastern Meseta, shows turbiditic and pelagic sedimentation with siliciclastics derived both from distant African shields and from emerged areas (e.g., ACOTTO et al. 2018).

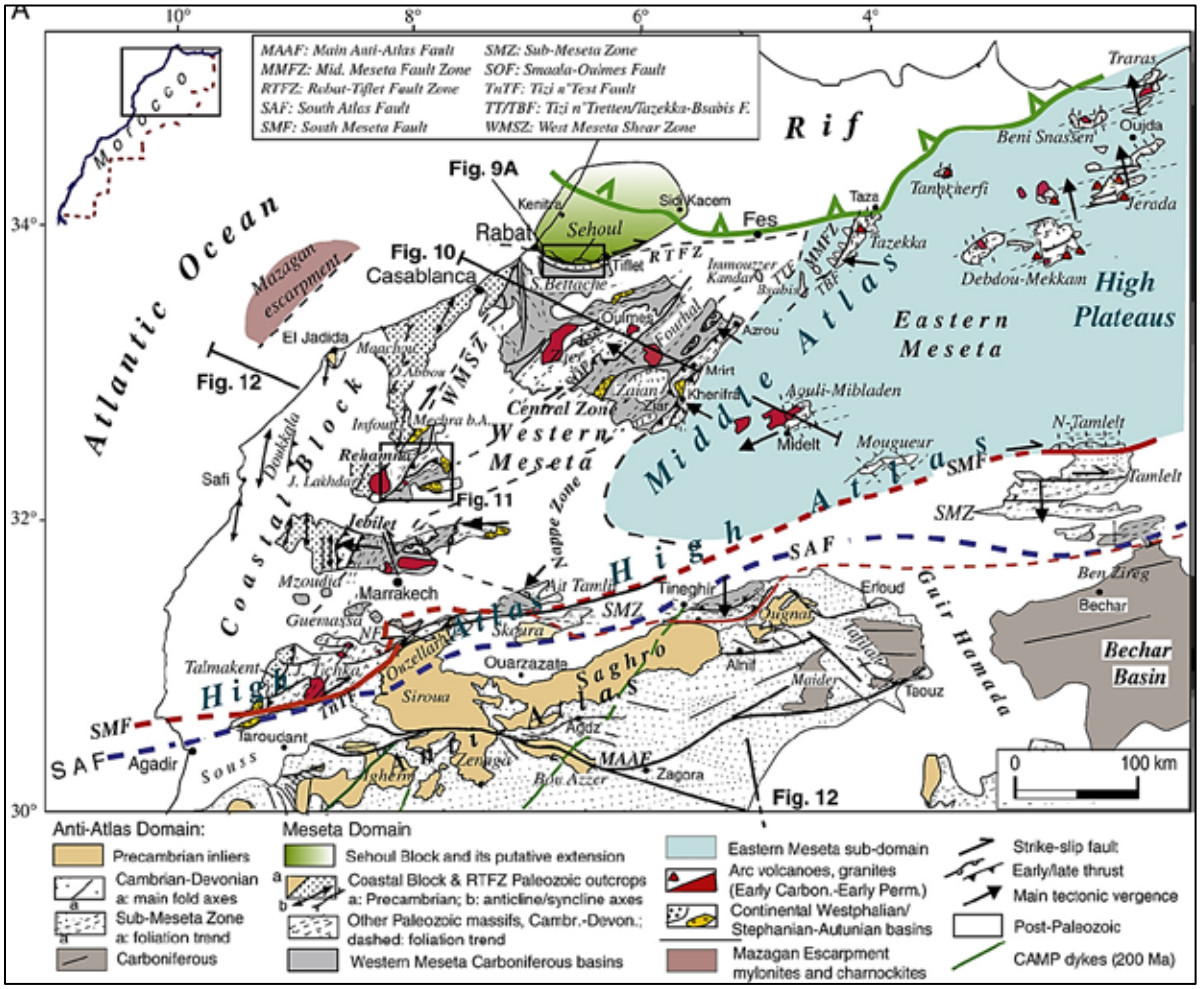

Fig. 2: The Meseta Domain and adjacent Anti-Atlas foreland; structural map of the Variscan Meseta Domain, from MICHARD et al. (2008, fig. 3.16), modified after PIQUE & MICHARD (1989), OUANAIMI & PETIT (1992), HOEPFFNER et al. (2005), BAIDDER et al. (2008), SOULAIMANI & BURKHARD (2008), MICHARD et al. (2010), and TAHIRI et al. (2010). White: Mesozoic–Cenozoic cover.

2.2. Investigated sedimentary-tectonic units of the Western Meseta

The Western Meseta is characterized by folding and metamorphic events of the Upper Carboniferous main Hercynian/Variscan orogeny. However, Eovariscan folding (Upper Tournaisian, "Eovariscan 2 Events of MICHARD et al. 2008) is observed in the eastern Azrou–Khenifra Basin and affected Cambrian–Ordovician formations. This suggests an initial continuity with the Eastern Meseta (MICHARD et al. 2010). In the northern part, the Sehoul Block is regarded as a Caledonian block (e.g., PIQUÉ, 1979; EL HASSANI, 1991) but the re-dating of its granitoids showed that this terrane was affected by Famennian (367 ma), not Silurian magmatism (TAHIRI et al. 2010). It does not include Devonian sediments and, therefore, was not re-studied during our project.

Various authors, who have worked in the Palaeozoic of the Meseta, agreed to divide it into distinctive sedimentary-structural units. Their Devonian and Lower Carboniferous stratigraphy has been reviewed by ZAHRAOUI (1994), FADLI (1994a, 1994b), EL HASSANI & BENFRIKA (1995, 2000). The following regions were part of our project (Figs. 2-5):

2.2.1. Coastal block ("Môle côtier")

It is located in the western part of the western Meseta and includes Palaeozoic

outcrops W of the Western Meseta Shear Zone (PIQUE et al. 1980), such as the coastal plateau and western parts of the Rehamna and Jebilet massifs. The successions consist mainly of Cambrian to Upper Devonian sediments. Carboniferous outcrops were discovered only in boreholes of the Doukkala Basin, which is a Silurian–Devonian basin beneath the Mesozoic cover (ECHARFAOUI et al. 2002). Deformation occurred during the Main Variscan-Phase, which gives in this region large open folds (at kilometer scale), with locally low cleavage development in the fold-axis. This moderately deformed zone extends southward up to the westernmost High Atlas Palaeozoic Massif (CORNÉE, 1989). We logged and re-sampled the Oulad Abbou (Douar Zrahna) section (EL KAMEL 2004), concentrating on the dating of Middle Devonian reef drowning phases and overlying deeper-water Upper Devonian strata.

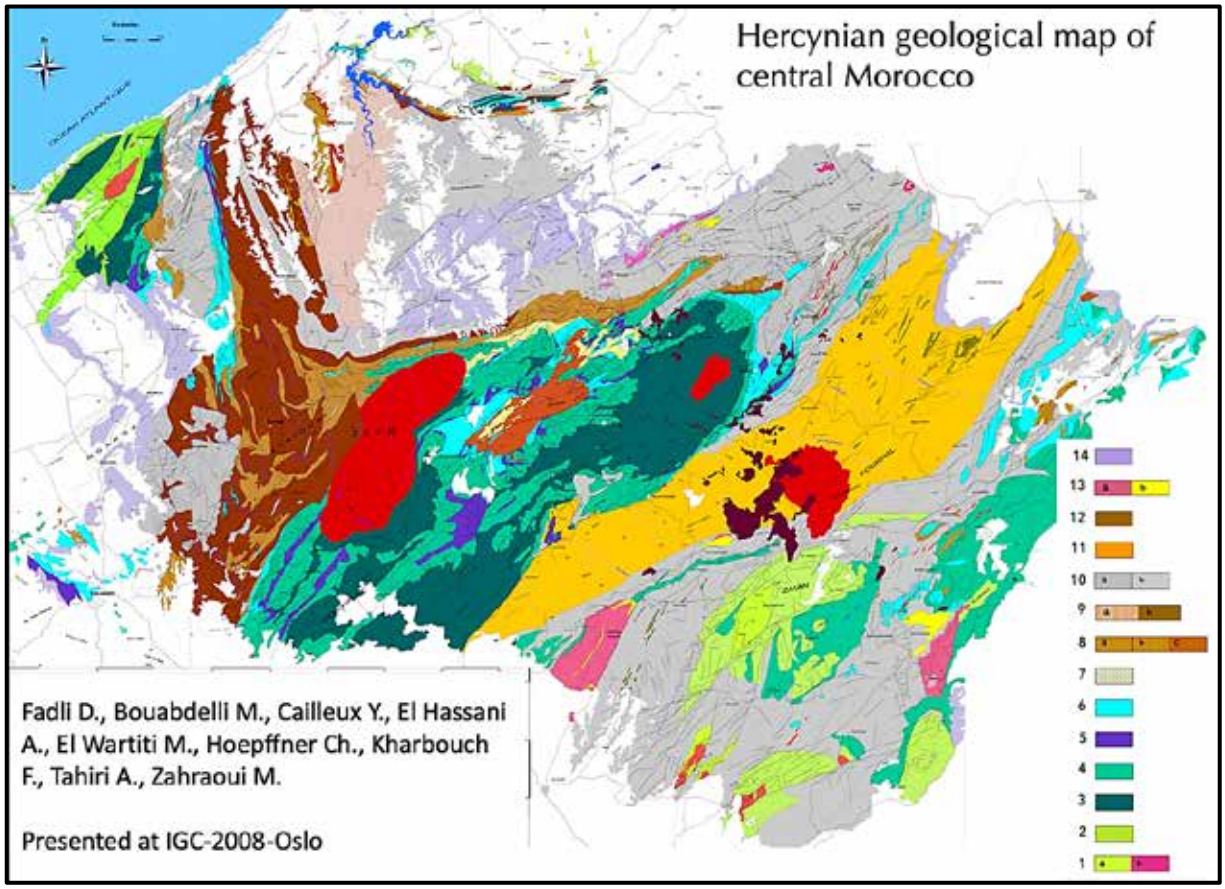

Fig. 3: Hercynian Geological map of Central Morocco (FADLI et al., 2008): 1. Cambrian (a: grauwackes, siltstones and quartzites; b: trachyandesites and rhyolites); 2. Cambrian-Ordovician (Zain quartzites and Phyllades of Sehoul Block); 3. Lower Ordovician; 4. Upper Ordovician; 5. Silurian; 6. Lower-Middle Devonian; 7. Undifferentiated Devonian; 8. Upper Devonian and Tournaisian; 9. Lower Visean ; 10. Middle, Upper Visean and lower Namurian; 11. upper Namurian – lower Westphalian ; 12. upper Westphalian ; 13. Stephanian – Permian ; 14. Triassic.

2.2.2. Rabat-Tiflet Zone

The Rabat-Tiflet Zone is a narrow band in tectonic contact with the Sehoul block (Fig. 6). It includes the so-called "Taicha Granite", which was attributed to the Ordovician by CHARLOT et al. (1973). TAHIRI et al. (2010) recalculated the age of this supposed Caledonian granite as 609 ± 4 Ma in age, and, consequently, re-interpreted it as Precambrian basement. The Devonian is represented in western part of the Rabat-Tiflet Zone by fossiliferous Lochkovian to Emsian strata of

the Oued Bou Regreg region, which have been studied by numerous authors (last review and detailed conodont biostratigraphy by BENFRIKA et al. 2007). We concentrated in our project on the Devonian and Lower Carboniferous of Chabat-el-Harcha (EL HASSANI 1991) and on the Tiflet region (Oued Tiflet and the reefal limestones of the Tiflet Quarry).

2.2.3. Sidi Bettache Basin

This basin was defined by PIQUÉ (1979, 1981). It stretches SSE of the Rabat-Tiflet Zone (Fig. 4) and comprises a thick, partly flyschoid, siliciclastic Famennian to Tournaisian succession. Only some intervals are rich in fossils. We concentrated on these, for example on the goniatite-rich Tournaisian of Aïn Hallaouf/Aïn Aouda (S of Rabat; BOLLELI et al. 1953) and on the conodont-bearing limestones at Sidi Jilali and Sidi Radi (see IZART & VIESLET 1988).

2.2.4. Oued Cherrat Zone

The Oued Cherrat is a narrow, ca. N-S running Devonian outcrop band that forms the western border of the Sidi-Bettache Basin (Fig. 7). It follows a palaeogeographical ridge and is best characterized by its Emsian and Givetian, economically important reef limestones. Eovariscan reworking, reef destruction, and re-deposition were very prominent. The first chapter of this volume deals with a detailed review and many new data concerning its biostratigraphy and synsedimentary tectonic movements. We concentrated, from North to South, on four successions: Aïn Khira, Aïn-ad-Dakhla to Cakhrat-ach-Chleh, Aïn-Al-Aliliga to Cakhrat Mohammed ben Brahim, and Aïn-as-Seffah.

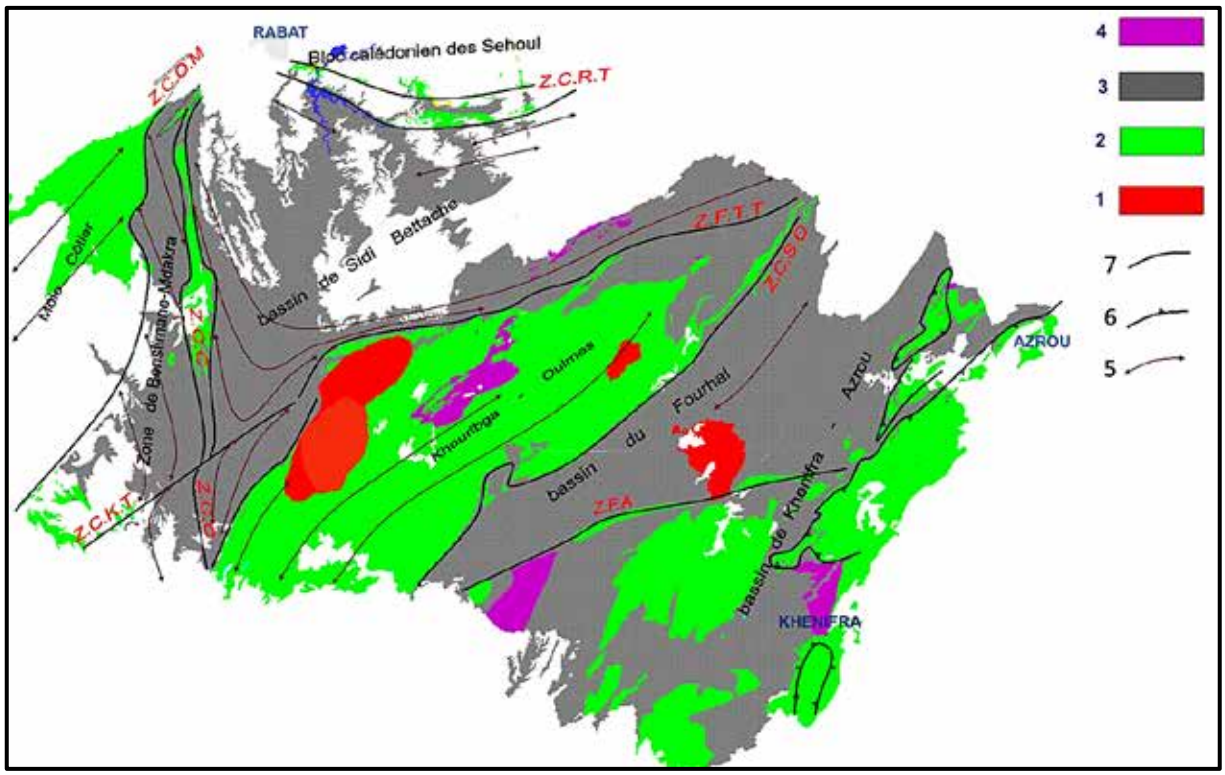

Fig. 4: General structural map of Central Morocco (in FADLI et al. 2008): 1. Variscan granites, 2. Cambrian to Middle Devonian, 3. Carboniferous basins (Upper Devonian to lower Westphalian), 4. Continental sediments (upper Westphalian to Permian), 5. Axial direction of major folds, 6. Thrust contacts, 7. Main Faults.

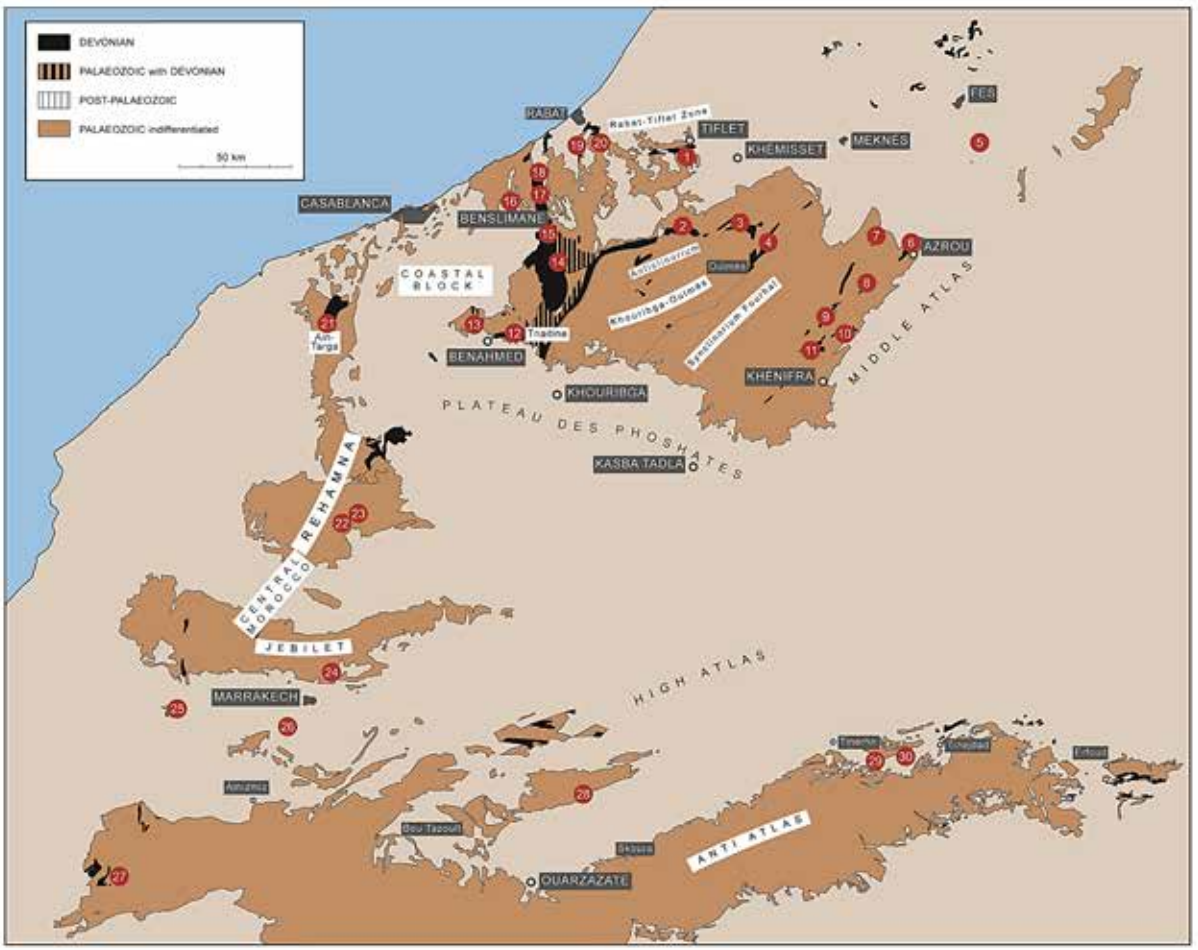

Fig. 5: Geographic position of sampled Meseta/Atlas regions. **1**. Rabat-Tiflet Zone, **2**. Tiddas region, **3**. Oulmes region, **4**. El Hammam Block, **5**. Immouzer-du-Kandar, **6**. Azrou, **7**. Jebel ben Arab, **8**. Bou Khedra-Bou Trou, **9**. Mrirt autochthon at Dechra Ait Abdallah, **10**. Mrirt allochthon, **11**. Khénifra region, **12**. Oued Aricha, **13**. Western Mdakra Massif, Benhamed region, **14**. Khatouat Massif (Jennabia, Biar Setla), **15**. Al Attamna, **16**. Ben Slimane Region, **17-18**. Oued Cherrat Zone, **19**. Western Sidi Bettache Basin (Aïn Aouda), **20**. Central Sidi Bettache Basin (Sidi Jilali, Sidi Radi), **21**. Coastal Block (Oulad Abbou), **22**. Western Rehamna (Mechra-ben-Abbou region), **23**. Eastern Rehamna (Foum-el-Mejez), **24**. Eastern Jebilet, **25**. Western Jebilet (Jebel Ardouz), **26**. Mzoudia (El Moussira), **27**. Western High Atlas (Talmakent), **28**. Skoura region just S of High Atlas, **29**. Tinerhir region, Southern Variscan Front, **30**. Tinejdad allochthon (Bou Tisdafine SW, Oued Ferkla).

2.2.5. Ben Slimane region

Devonian outcrops are more restricted in the basin of Ben Slimane, which lies just W of the Oued Cherrat (Fig. 7). We re-studied two areas, the Lower Devonian and ammonoid-rich uppermost Famennian just South of Ben Slimane (near Aous bel Fassi/Chaabat Hamira), and, to the North, the Lower Devonian limestones of Bled Besbass (ZAHRAOUI 1991).

2.2.6. Al Attamna

The Al Attamna region lies just S of the Oued Cherrat (Figs. 3, 7) and is characterized by a continuation of its general facies and by the re-appearance of thick Emsian and Givetian reefs. We re-sampled two sections: of BENFRIKA & BULTYNCK (2003), Sidi Ahmed Lemdoun and Sidi Mohammed Smaine (see EICHHOLT & BECKER 2016), with a second focus on Eovariscan breccia beds.

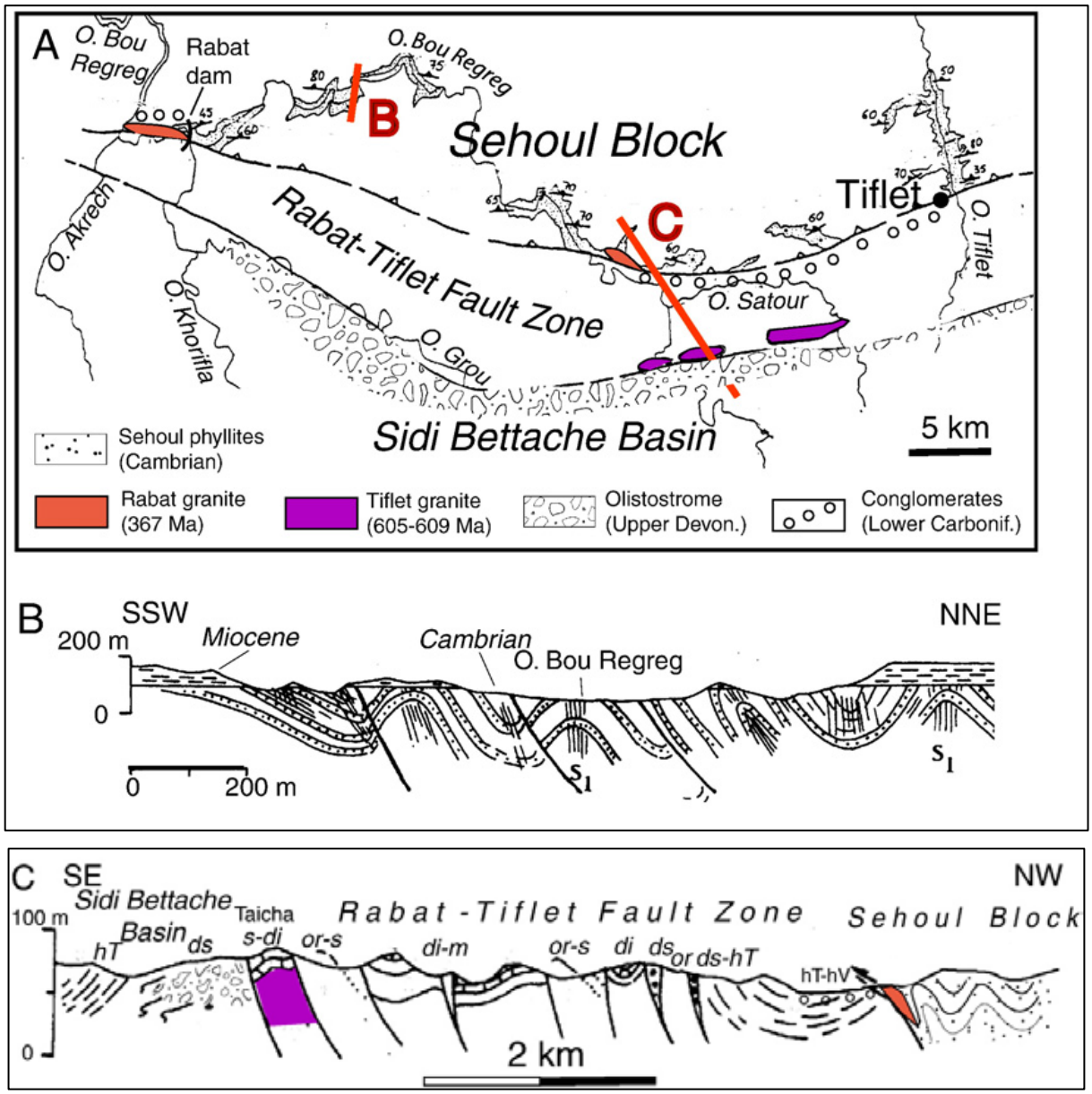

Fig. 6: The Sehoul Block and Rabat–Tiflet Fault Zone (RTFZ) in the eponymous regions, after EL HASSANI (1994a, 1994b), modified after TAHIRI et al. (2010) who use the name of "Bou Regreg Corridor" for the RTFZ. **A.** Sketch map with location of B–C cross-sections. **B.** Cross-section within the Sehoul Block. **C.** Cross-section of the RTFZ. S1: metamorphic foliation; or: Ordovician; s: Silurian; di, dm, ds: Lower, Middle, Upper Devonian; hT: Tournaisian; hV: Visean.

2.2.7. Khatouat Massif

The tectonically complex Palaeozoic of the Khatouat Massif lies East of the Al Attamna and forms the southern continuation of the Sidi Bettache Basin (FADLI 1990; Figs. 3, 5). Siliciclastics dominate but there are strongly tectonized and largely reworked Middle Devonian reefs, which we studied at Jennabia and Biar Settla (EICHHOLT & BECKER 2016). Eovariscan conglomerates and olistolites are wide-spread, for example at Chabet-el-Baya S of the Al Attamna reefs (FADLI 1990, 1994a).

2.2.8. Benhamed region

The Devonian and LowerCarboniferous of the Benhamed region (Figs. 3-5), the western and southern parts of the Mdakra Massif ("Chaouï sud"), has somewhat been neglected since the pioneer monograph by

TERMIER & TERMIER (1951). We logged and re-sampled the pelagic, ammonoid-rich Famennian basin of the Oued Aricha (NE of Benhamed) and the deeper-water Givetian to Frasnian of Dhar Cheikh el Mfaddel, Zwayir, and Boudouda (NNW of Benhamed). In the latter section, neritic limestone with rich foraminifers overlying Eovariscan breccias proved to be of Viséan age (det. P. COZAR). The Lower Devonian, including thick Emsian reefs, requires more work.

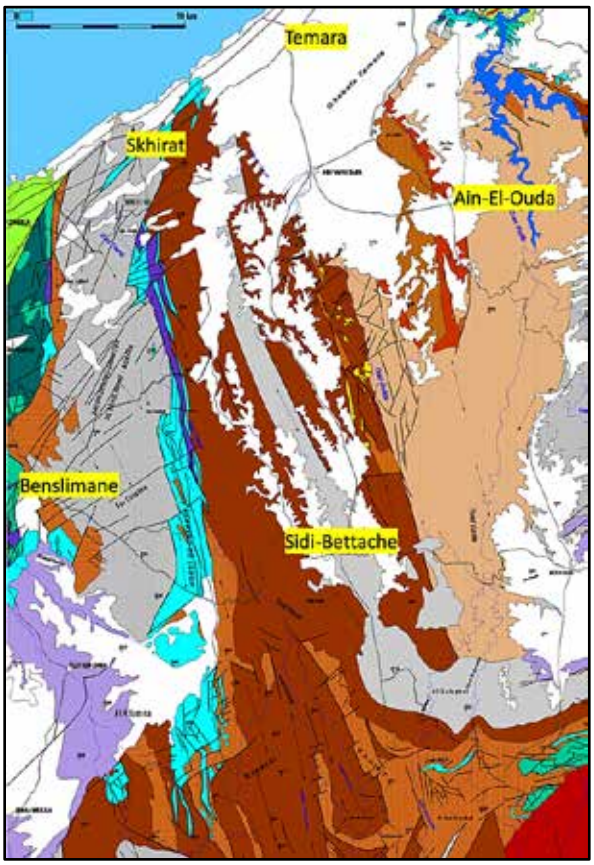

Fig. 7: Geology of the Benahmed, Ben Slimane, Oued Cherrat, Al Attamna, and western Sidi Bettache Basin regions (FADLI et al., 2008); 1. Cambrian (a: grauwackes, siltstones and quartzites; b: trachyandesites and rhyolites); 2. Cambrian-Ordovician (Zain quartzites and Phyllades of Sehoul Block); 3. Lower Ordovician; 4. Upper Ordovician; 5. Silurian; 6. Lower-Middle Devonian; 7. Undifferentiated Devonian; 8. Upper Devonian and Tournaisian; 9. Lower Visean ; 10. Middle, Upper Visean and lower Namurian; 11. upper Namurian – lower Westphalian ; 12. upper Westphalian ; 13. Stephanian – Permian ; 14. Triassic.

2.2.9. Zaer Ridge

Devonian is exposed in the northwestern limb of the Khouribga-Oulmes Anticlinorium, East of the Sidi Bettache Basin, along the ENE to NE Zaer fault strip (ZAHRAOUI, 1991). This zone extends from Sibara in the Southwest to the South of Tiddas (Fig. 8). Lower and Middle Devonian rocks appears mostly as tectonic lenses or redeposited blocks within thick Famennian-Tournaisian breccia and olistolite units (CHAKIRI & TAHIRI 2000). Strata in these outcrops are folded and affected by regional metamorphism, to which a contact metamorphism is superposed on the northwestern side of Zaer Granite (Fig. 8). We conducted some new work on the stratigraphy and microfacies in the most easily accessible outcrops of Sidi Ahroun (= Jebel Hadid, S of Tiddas, e.g., ALBERTI 1969).

2.2.10. Oulmès Zone

The Devonian to the NNW of Oulmès belongs to the northern part of the Khourigba-Oulmès Anticline (Fig. 8). It is characterized by alternating neritic and fully pelagic sediments, with an important Givetian-lower Frasnian reefal episode (GENDROT 1970). Our detailed logging and sampling concentrated on the Eifelian-Frasnian, on the well-exposed Devonian-Carboniferous transition of Aïn Jemaa (KAISER et al. 2007), and on the adjacent, goniatite-rich Bou Keziam section (COGNEY 1967). Thick, Lower Carboniferous (pre-Viséan) Eovariscan breccias were studied on the northern slope of Aïn Jemaa ridge, at Ta´araft.

2.2.11. El Hammam Zone

The Devonian exposed around the small track up to Moulay El Hassane sanctuary, NE of Oulmès, was first summarized by COGNEY (1967). It belongs to a different structural and facies unit, for example without reefs, the El

Hamman Zone (TAHIRI & HOEPFFNER 1988; TAHIRI 1994). We logged and sampled the Middle-Upper Devonian pelagic facies (LAZREQ 1990), which yielded a new, unique, small-sized Frasnian ammonoid fauna. The Frasnian-Famennian transition is exposed, too.

The El Hamman Zone continues for quite some distance to the NNW and reaches the Bou Alzaz region SW of Meknes (TAHIRI & LAZREQ 1988; LAZREQ 1999). There, we conducted limited new field work, with some sampling for conodont, microfacies, and brachiopods in the Lower/Middle Devonian of Ayn Azza (= Bou Alzaz-South). We noted the rare occurrence of transported reefal corals in the Givetian.

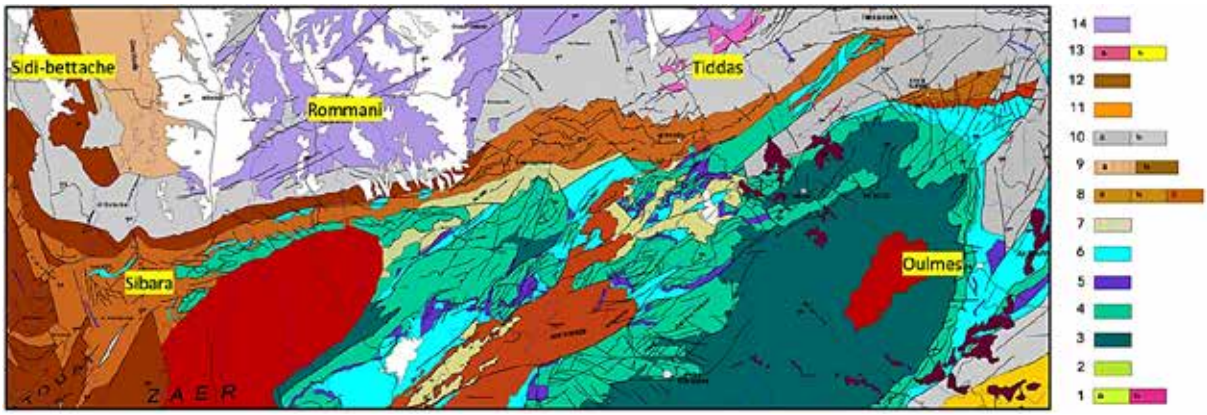

Fig. 8: Geological map of the Zaer Ridge (FADLI et al., 2008): 1. Cambrian (a: grauwackes, siltstones and quartzites; b: trachyandesites and rhyolites); 2. Cambrian-Ordovician (Zain quartzites and Phyllades of Sehoul Block); 3. Lower Ordovician; 4. Upper Ordovician; 5. Silurian; 6. Lower-Middle Devonian; 7. Undifferentiated Devonian; 8. Upper Devonian and Tournaisian; 9. Lower Visean ; 10. Middle, Upper Visean and lower Namurian; 11. upper Namurian – lower Westphalian ; 12. upper Westphalian ; 13. Stephanian – Permian ; 14. Triassic.

2.2.12. Azrou-Khénifra Basin; Azrou area

According to BOUABDELLI & PIQUÉ (1990), the "Azrou-Khénifra Carboniferous Basin" (Fig. 9) developed an internal thrust front that overlaps the eastern Meseta of Morocco, with west vergence. At the end of the Devonian, the basin was bound by two NE-SW running, deep transcurrent faults. These authors defined a dextral shear zone, where the sedimentation was controlled by lateral movements of synsedimentary faults and tilting blocks. The Upper Devonian–Lower Carboniferous period is characterized by sedimentary breaks, olistostromes and gravity nappes that were embedded in upper Visean-Namurian shales. Even if we are not yet sure about the origin of the gravitationally transported material, the existence of entire series within nappes allows us to elaborate relatively complete stratigraphic studies. The faunal content and facies development provide important clues concerning the relationship with autochthonous Meseta and Anti-Atlas regions.

In the Azrou Nappe, in the close vicinity of Azrou, facies changes and the conodont stratigraphy of Devonian outcrops were first studied in detail by BOHRMANN & FISCHER (1985). We re-sampled their localities Bou Ighial and Bab-el-Ari at even finer resolution, with some focus on the numerous Eovariscan breccia beds.

Further to the SW, we restudied and sampled the Devonian of Bou Khedra (Bou Khadra, e.g., BOUABDELLI 1994), which ends with an angular unconformity between Emsian limestones and (Upper?) Tournaisian

shales. It provides important evidence for the Eovariscan 2 Phase of MICHARD et al. (2008).

2.2.13. Ziar-Mrirt Nappe

The Ziar-Azrou Nappe overlaps in the NW the Azrou Nappe (Fig. 9). Our second detailed chapter provides a review and many new stratigraphic, faunal and microfacies data for the allochthonous Devonian and basal Carboniferous East and South of Mrirt, with a focus on the sections Anajdam (e.g., LAZREQ 1999) and Gara de Mrirt (= Bou Ounebdou; e.g., LAZREQ 1999; WALLISER et al. 2000; BECKER & HOUSE 2000a).

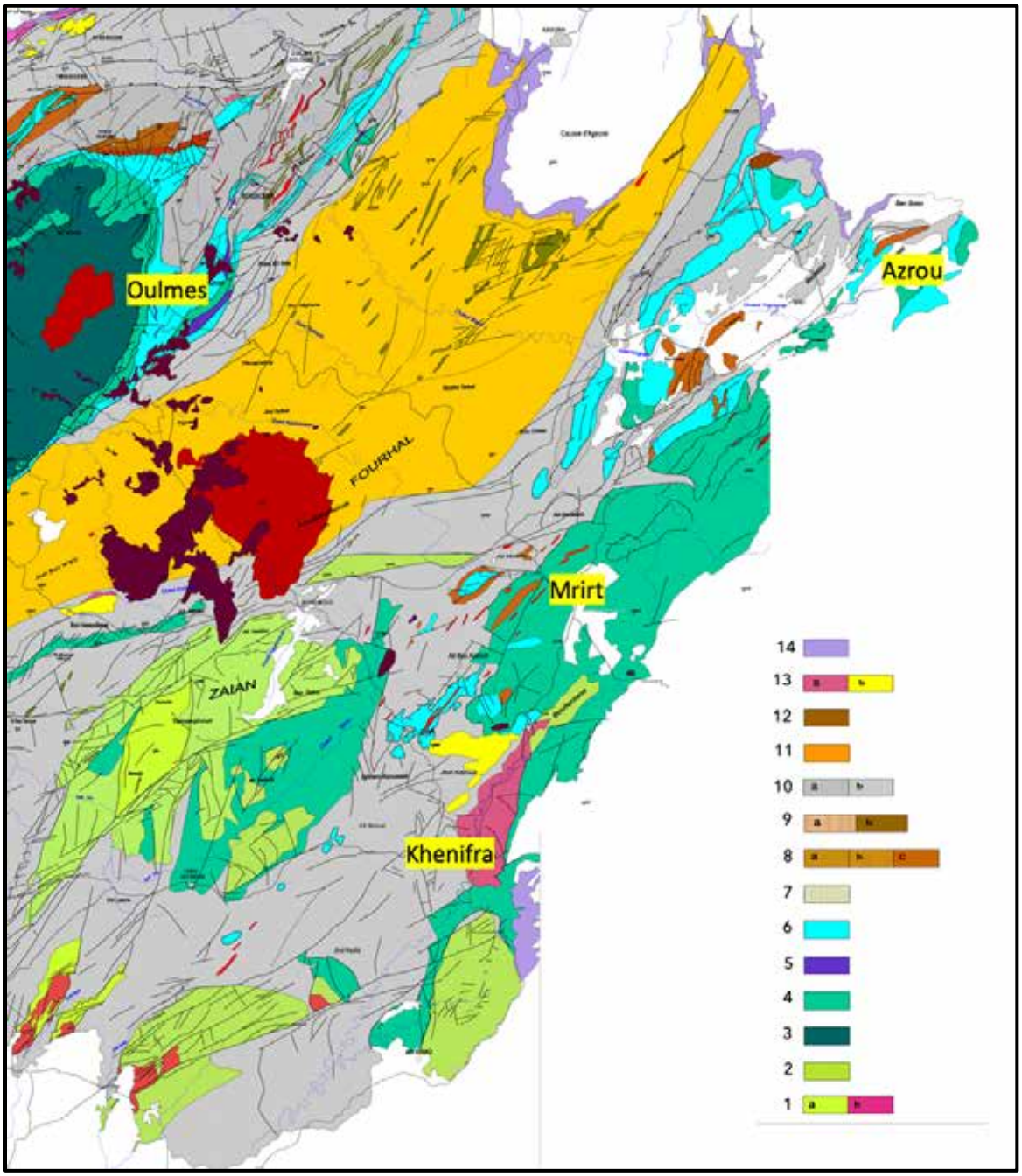

Fig. 9: Geological map of the eastern part of Central Morocco (Azrou-Khenifra Basin; FADLI et *al*., 2008): 1. Cambrian (a: grauwackes, siltstones and quartzites; b: trachyandesites and rhyolites); 2. Cambrian-Ordovician (Zain quartzites and Phyllades of Sehoul Block); 3. Lower Ordovician; 4. Upper Ordovician; 5. Silurian; 6. Lower-Middle Devonian; 7. Undifferentiated Devonian; 8. Upper Devonian and Tournaisian; 9. Lower Visean; 10. Middle, Upper Visean and lower Namurian; 11. upper Namurian – lower Westphalian; 12. upper Westphalian; 13. Stephanian – Permian; 14. Triassic.

Further to SE, large allochthonous Devonian outcrops re-appear in the Ziar (Ziyyar) region (e.g., WALLISER et al. 1995). We conducted bed-by-bed sampling for conodonts, foraminifers, and microfacies in the Emsian to Frasnian and middle-upper Famennian intervals. We dated precisely local unconformities, Eovarican slumping units, and also focused on global event intervals, such as the Kellwasser Crises, *Annulata* and Dasberg Events.

Principally the same Devonian facies and faunas re-appear as clasts in massive Upper Viséan olistolites, which belong to the thick flysch succession above the shallow-water limestones of the Jebel Tabainout (e.g., MULLIN et al. 1976). This unit lies outside the Ziar-Azrou Nappe and belongs to the Kasba Tadla-Azrou Anticline.

2.2.14. Western Azrou-Khénifra Basin

There are numerous fossiliferous Devonian outcrops to the W of the Ziar-Mrirt Nappe, from the Jebel Bouchot to the Dechra-Aït-Abdallah (or Agarad-n-Azdaït) region, W/NW of Mrirt (Fig. 9). Pioneer stratigraphic work on the Palaeozoic was done by TERMIER & TERMIER (1970) and TERMIER et al. (1975). The successions are also part of allochthonous units (nappes) but they reflect a complex palaeogeography in terms of biofacies and floras (GROBE 1997) that differs significantly from the Azrou and Ziar-Mrirt sections. For example, there a thick reefs and important plant shales (e.g., PRESTIANNI et al. 2012). So far, we concentrated on sections with reefs (Awajgal, Amdawar) and took spot samples from Famennian strata (e.g., at Titar Oumjel), in order to complement the unpublished M.Sc. Thesis of GROBE (1993).

2.2.15. Jebel ben Arab

Another distinctive Devonian succession, with yet another facies development, from pelagic Lower Devonian shales to a Middle Devonian turbidite basin, overlain by Upper Devonian sandstones, is exposed WNW of Azrou, at the Jebel ben Arab (Fig. 9). We logged and sampled the section published by LAZREQ (1990) in finer detail.

2.2.16. Middle Atlas Basement (Immouzer-du-Kandar)

Our third detailed chapter presented here deals with the unique Devonian at Immouzer-du-Kandar (Figs. 2, 5), a tectonic window into the Middle Palaeozoic of the Middle Atlas South of Fes. Our studies built on the previous research by CHARRIÈRE & RÈGNAULT (1989), CYGAN et al. (1990), and others.

2.2.17. Rehamna

In the Rehamna, Devonian formations are represented by variable facies in distinctive zones. Despite the studies by a range of geologists (e.g., MICHARD, Ed., 1982; EL HASSANI & EL KAMEL 2000; EL KAMEL 2004), the age of formations and the dating of facies changes and Eovariscan reworking and re-deposition episodes still lacked precision.

Our work concentrated on Mechra ben Abbou (GIGOUT 1951, 1955) and its fine reefs, overlain by Famennian quartzites with brachiopods, and on the supposedly contemporaneous non-reefal limestones of Foum-el-Mejez, which are followed by brachiopod-rich siltstones. Not very successful spot samples for conodonts and microfacies were taken in the Lower Devonian of Sakhra et Taïra to the SE, which is characterized by very early slumping and re-sedimentation events (EL KAMEL et al. 1992). In addition, we examined the reworked Palaeozoic blocks within the thick, supposedly "Autunian" conglomerates at Koudiat-ed-Diab (HOLLARD et al. 1982).

2.2.17. Jebilet: Eastern Jebilet

The Jebilet Massif is a tectonically complex Palaeozoic structure, which thick,

siliciclastic main parts reflect the opening of an Upper Devonian-Lower Carboniferous basin (DELCHINI et al. 2018). Fossiliferous Devonian strata are mainly exposed in the eastern Jebilet (e.g., Bou Marhara and Smaha). They correspond to Lower Devonian allochthonous or para-autochthonous series (HUVELIN 1977; TAHIRI 1982). The litho- and biofacies shares similarities with the Skoura region, especially in the presence of griotte limestones with rich upper Emsian goniatites (anarcestids), and with East Central Morocco (Azrou-Khenifra zone). We logged and sampled the Lochkovian to Emsian at Jaidet and examined the conglomeratic unconformity at the base of the overlying Viséan carbonate platform.

2.2.18. Mzoudia (Jebel Ardouz)

The western Jebilet Formations are exposed in the Skhirat Unit and mainly in Mzoudia (Jebel Ardouz). The Devonian belongs to a large thrust slice, which stratigraphy has been synthesized by TAHIRI (1982). However, our new data led to an important age revision for the reddish conglomerate at the base. The Eifelian-Givetian and Famennian strongly resemble the Mechra ben Abbou succession. However, there is only a relatively thin biostrome that was truncated by Famennian brachiopod-bearing white quartzites.

2.2.19. Haouz (El Moussira)

GAILLET (1986) suggested that a Middle Devonian to Tournaisian succession, with a reefal interval overlain by a siliclastic basin, is developed at El Moussira in the Haouz region S of Marrakesh. Based on rare conodonts, this claim could be firmly rejected by ABOUSSALAM et al. (2017), who documented top-Viséan conodonts from the supposed Middle Devonian. However, Famennian strata with conodonts occur within the Marrakesh city area (LAZREQ 2017), somewhat to the South of the main, W-E trending Jebilet outcrop belt

Fig. 10: Strongly dolomitized, stromatoporid or stromatolite "ghost" from the top of the Khemis-n´Ga Formation (probably lower Emsian).

Fig. 11: Post-sedimentary (?Eovariscan), polymict breccia encrusted unconformably and very locally on the Lower Devonian Khemis n`Ga carbonate platform (preserved in a minor depression on the main slope of the outcrop). Most particles are angular clasts of orange to reddish dolomites, partly with preserved crinoid remnants, sitting in a calcarenitic to dark and partly laminated limestone matrix (picture width = 25 cm).

2.2.20. Safi region

After an outcrop gap West of the western Jebilet margin, upper Silurian and Devonian limestones resurface from the post-Palaeozoic cover in the Safi region, at Khemis n´Ga (BEUN et al. 1992; BULTYNCK & SARMIENTO 2003). We re-sampled the rather thic, mostly coarse crinoidal limestones

(encrinites) but did not succeed to obtain new faunas and ages. However, we recognized domal-shaped, strongly dolomitzed, large (up to 50 cm) stromatoporids or stromatolites at the top (Fig. 10). In addition, we found a coarse, orange-reddish, post-sedimentary breccia (?Eovariscan) that truncated the neritic carbonate platform after it was uplifted. It is only very locally preserved and yielded no conodonts.

2.2.21. Western High Atlas

In the western High Atlas, there are several tectonic windows which expose Devonian strata, especially the Lower Devonian (e.g., CORNÉE 1989; CORNÉE et al. 1990). The age of most stratigraphic units is still only roughly established; conodont and microfacies data are still lacking. More at an exploration stage, we took some samples from bryozoan-rich, partly biostromal Emsian limestones at Souk Sebt Talmakant. A similar initial survey concerning allochthonous Devonian blocks at Ida ou Zal (DE KONINCK 1957) yielded black orthocerid limestones of unclear age, because they lack conodonts.

2.2.22. Skoura region

Since the initial study by ROCH (1939), the well-exposed and partly thick Devonian and Lower Carboniferous stratigraphy, faunas, and facies succession of the Skoura region (Fig. 5), NNE/NE of Ouarzazate, and at the southern foot of the High Atlas, remained very poorly studied. LAVILLE (1980) concentrated on the tectonics and microtectonics. The region belongs to the Sub Meseta (Fault) Zone of MICHARD et al. (2010: SMZ or SMFZ). It includes along strike consistent sedimentary successions that are non-cleaved and weakly deformed in the West and strongly tectonized in the East. The Lower/Middle Devonian facies and faunas strongly resemble the Anti-Atlas but there are also relationships with the eastern Jebilet (as said above). All sections show Eovariscan (Middle-Upper Devonian) breccias, as typical for Meseta sections. We logged and sampled three sections intensively, Taliouine (= Tiliouine), Tizi-n-Ourthi, and Asserhmo, partly within the Devonian countourite research project of H. HÜNEKE (Greifswald).

2.2.23. Tinerhir region

The Sub Meseta Fault Zone continues eastwards to the Tinerhir region (Fig. 5), where there was complex transpressional tectonics and nappe stacking (MICHARD et al. 1982; FERONI et al. 2010) marking the "Southern Variscan Front". The Devonian occurs as variably-sized olistolites and more massive, double reworked breccia units within the Lower Carboniferous (HINDERMEYER 1954, 1955; GRAHAM & SEVASTOPULO 2008). We sampled many individual clasts within the Taourirt n´Khellil Formation (RYTINA et al. 2013) as well as large individual olistolites (within the Aït Yalla Formation) and a breccia succession at Tikkedarine (western end of Tinerhir). This will enable a high-resolution reconstruction of Devonian sedimentation at the former Anti-Atlas/Meseta boundary. Clearly, there was no major facies and faunal break; the tectonic suture did not yet exist in Devonian time.

2.2.24. Tinejdad region

Another large isolated Devonian olistolite lies close to main road from Tinerhir to Tinejdad, but closer to the latter (locality named as Bou Tisdafine East). It differs considerably from the large lower Emsian olistolites to the West since it preserved internally a non-cleaved (Anti-Atlas-type), fine and fossiliferous Eifelian to Famennian succession. Important are trilobite-rich limestones, Givetian (Eovariscan) breccias, and a pristine Frasnian-Famennian boundary sequence.

Just to the NE of Tinejdad, the allochthonous Devonian of Oued Ferkla became within our project the subject of the M.Sc. study of P. D. WARD (WARD et al. 2013). Only preliminary results have been published so far. Further microfacies and tectonic studies are currently been conducted by A. TALIH (Rabat). The section is exceptional for its perfect preservation of the Kačak and *pumilio* Events and rich in agglutinating foraminifers. Whilst the Emsian to basal Givetian is weakly deformed and very similar to the Tafilalt, the Upper Devonian just to the North is very strongly cleaved, unfossiliferous, and was deposited in a turbiditic (flyschoid) basin.

Repository

The figured and listed fossils, with the exception of specimens shown in field photos, are deposited in the Geomuseum Münster, WWU, under the following collection numbers:

Brachiopods: B5B.15…
Cephalopods: B6C.53…
Conodonts: B9A.12…
Corals: B2C.56…
Ostracods: B7B.15…
Shark teeth: A1C.4…
Trilobites: B7A.11…

The Devonian of the Oued Cherrat Zone (Western Meseta) – review and new data

Ralph Thomas Becker, Zhor Sarah Aboussalam, Ahmed El Hassani, Stephan Eichholt & Stephan Helling

Fig. 1: View of massive lower Emsian reefal (biostromal) carbonates of the Dhar-es-Smene Formation (Cakhrat-ach-Chleh Member) at Mechra al Kraker just E of the Oued Cherrat, ca. at x = 351.1, y = 342.2, 12 km NE of Ben Slimane.

1. Introduction

The Oued Cherrat Zone is named after the N-S running and deeply incised Oued Cherrat valley, which follows a N-S running, synsedimentarily active fault and sheer zone beginning between Rabat and Casablanca in the western Central Massif (Pique et al. 1980; Fig. 2). In the W, it is delimited by the faults, which separate predominating Lower Devonian neritic to reefal carbonates from the siliciclastic Famennian and Lower Carboniferous of the Ben Slimane area. In the E follow the thick Famennian to Lower Carboniferous deposits of the Sidi Bettache Basin. Within the Oued Cherrat Zone, the succession ranges from the upper Silurian (Ludlow) to the basal Serpukhovian (Neqqazi et al. 2014). Chalouan & Hollard (1979) and Chalouan (1981) introduced a lithostratigraphic subdivision, which was refined by Aboussalam et al. (2013) and Eichholt & Becker (2016). Further lithostratigraphic terms are introduced here, mostly because intensive conodont sampling provided a refined time framework. The special significance of the Oued Cherrat Zone lies in their well-exposed and thick Lower (Emsian) and Middle (Givetian) reef complexes, which have been studied by several authors (e.g., Gendrot et al. 1969; Gendrot 1973, Zahraoui 1991; Cattanaeo et al. 1993; Eichholt & Becker 2016). Reefal limestones occur on both sides of the Oued

Cherrat valley and are of high economic significance (NAHRAOUI et al. 2012). This resulted in the creation of large, active, and fast expanding quarries that, unfortunately, destroy gradually some of the best outcrops. Equally significant are major Eovariscan block faulting and reworking events, which led to block tilting, erosion, and the re-deposition of partly very thick conglomerate and breccia units during specific phases of a long total interval (Givetian to Famennian), with activity peaks in the upper Givetian and middle/upper Famennian. Uplifted blocks were partly deeply eroded, exposing Lower Palaeozoic quartzites and magmatic rocks.

Our summary is based on new data for four different successions, from Aïn Khira (or Aïn El Khira) in the N, to Aïn Dakhla/Cahkrat-ach-Chleh and Aïn-al-Aliliga in the middle, and to Aïn-as-Seffah in the southern part of the reefal band. It re-appears further to the S, in the Al Attamna region (e.g., FADLI 1990; BENFRIKA & BULTYNCK 2003; EICHHOLT & BECKER 2016).

2. Research History

LECOINTRE (1926): Initial survey of the region, with a recognition of strata ranging from the upper Silurian to Lower Carboniferous limestones with "*Spirifer tornacensis"*.

ROCH (1950): Records of Emsian trilobites and spiriferids and of a rich Givetian fauna with stromatoporids, tabulate and rugose corals (including the colonial genus *Phillipsastrea*), and the index brachiopod *Stringocephalus*. On the eastern flank, the occurrence of *Archaeocalamites* in Upper Devonian clastics was noted.

HOLLARD (1967, fig. 4): Brief summary of the Oued Cherrat Devonian.

GENDROT et al. (1969): Initial study of reefal carbonates at two localities (Atiliga Syncline and "Sokrat Md. Ben Brahim" (= Cakhrat Mohammed-Ben-Brahim).

KERGOMARD (1970): Unpublished report on the Silurian-Devonian of the Western Meseta, with data for the Oued Cherrat, e.g., a section log for Aïn-al-Aliliga.

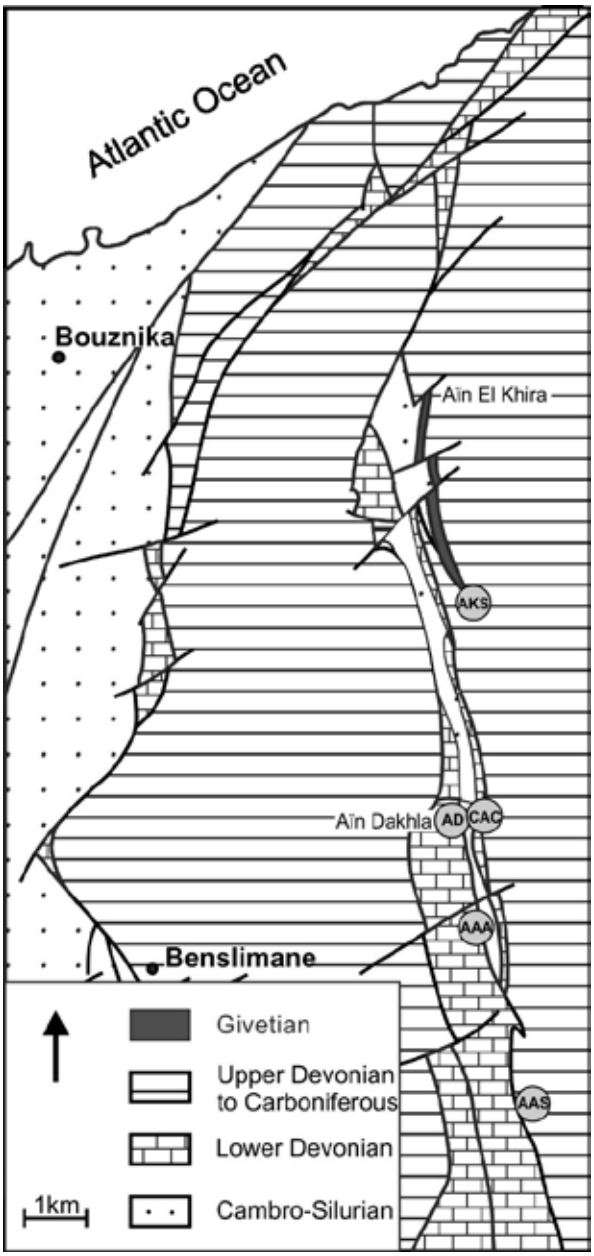

Fig. 2: Position of the four re-studied successions in the narrow Oued Cherrat Zone. **AKS** = Aïn Khira South, **AD** = Aïn Dakhla (W of the river) and CAC = Cakhrat-ach-Chlee (E of the river), **AAA** = Aïn-al-Aliliga, and **AAS** = Aïn-as-Seffah (EICHHOLT & BECKER 2016, fig. 2, redrawn from ZAHRAOUI 1991).

GENDROT (1973): Study on Devonian reefs in the Moroccan Meseta, including the Oued Cherrat.

KELLING & MULLIN (1975): Sedimentological analysis of coral- and brachiopod-bearing shallow-water carbonates, interpreted as Viséan tempestites.

CHALOUAN & HOLLARD (1979): Brief summary of Oued Cherrat lithostratigraphy, introducing numerous new formations.

PIQUE et al. (1980): Recognition of the Oued Cherrat as a distinctive tectonic unit within the wider Western Meseta Shear Zone.

CHALOUAN (1981): Detailed lithostratigraphy and faunal characteristics, providing geological cross-sections for five key successions.

RACHEBEUF (1990): Record of Lower Devonian chonetids from Aïn Dakhla.

ZAHRAOUI (1991, 1994a, 1994b): Summary of Oued Cherrat Silurian to Middle Devonian litho- and biostratigraphy.

CATTANEO et al. (1993): Comprehensive analysis of the Givetian reefal succession at Aïn Khira.

LAAMRANI ELIDRISSI (1993): Unpublished Diplom Thesis on the structural geology of the Bouznika-Cherrat region.

EL HASSANI (1994): Tectonics of the N-S trending Oued Cherrat-Oued Ikem band.

FADLI (1994a, 1994b): Summaries of Famennian to Viséan litho- and biostratigraphy of the Meseta, including the Oued Cherrat.

VACHARD et al. (1994): Description of fifteen species of foraminifers from the Givetian at Aïn Khira, including two new taxa, *Tubeporina (?) polydermoides* (Tuberitinidae) and *Palachemonella maroccana* (Issinellidae).

EL HASSANI & BENFRIKA (1995, 2000): Review of the Meseta Devonian, including a stratigraphic summary for the Oued Cherrat.

CASIER et al. (1997): Description of a rich (fifty species) Givetian ostracod fauna and its paleoecology from Aïn Khira.

BENFRIKA (1999): Description of the lower Emsian *Caudicriodus celtibericus* from Aïn al Quob at the southern end of the Oued Cherrat Devonian outcrop strip.

MAMET et al. (1999): Description of calcareous algae from the Oued Cherrat region, with the Emsian of Aïn Dhakla as the type locality and level of *Sphaerocodium tortuosum*.

BENFRIKA & BULTYNCK (2001, 2003): Report on lower Emsian conodonts from the Dar-es-Smene Formation and of upper Emsian to Eifelian conodonts from the Kheneg-en-Nmer Formation.

JANSEN (2001): Brief comments on Lower Devonian brachiopods of the Oued Cherrat (CHALOUAN material).

KAISER et al. (2007): Comparison of the Upper Devonian of the Oulmes Region with other contemporaneous Meseta successions, including the Oued Cherrat.

ABOUSSALAM et al. (2012): Preliminary note on new conodont data for the Oued Cherrat Devonian.

EICHHOLT et al. (2013): Preliminary new data on reefal faunas and microfacies at Aïn Khira and Aïn-as-Seffah.

NAHRAOUI et al. (2012): Study on the quality of the reefal limestones of the Oued Cherrat as a new source for the regional cement industry.

ABOUSSALAM et al. (2013a): Refined lithostratigraphy and preliminary new conodont data for the isolated reefal olistolite at Aïn-as-Seffah.

ABOUSSALAM et al. (2013b): Dating the onset of Middle Devonian reef growth in the Oued Cherrat as lower Givetian.

NEQQAZI et al. (2014): Discovery of conodonts from the Viséan-Serpukhovian transition in two northern sections near Souk el Had and at Dhar Bou Ghazouani (= Dhar Bou Ghazwani).

SCHWERMANN (2014): Unpublished M.Sc. Thesis on Middle/Upper Devonian shark teeth from Morocco, including the description of *Phoebodus fastigatus, Ph. gothicus gothicus*, and *Ph. gothicus transitans* from Aïn-al-Aliliga and Aïn-as-Seffah.

HELLING, S. & BECKER, R. T. (2015): Preliminary data on a new Pragian trilobite

assemblage from the Aïn-al-Dakhla Formation of Aïn-al-Aliliga.

EICHHOLT & BECKER (2016): Detailed microfacies and reef development study in the Oued Cherrat Zone, with a revised regional lithostratigraphy and facies logs for Aïn Khira South and Aïn-as-Seffah.

BECKER & ABOUSSALAM (2019): Note on the development of Emsian/Eifelian global events in the Meseta, including remarks on the Daleje Event in the Oued Cherrat.

3. Summary of succession

In terms of palaeogeography and synsedimentary structural geology, the Cherrat River Subzone sensu PIQUE et al. (1980) belonged in the Devonian to a narrow and elongated elevation with shallow-water sedimentation and adjacent steep slopes that caused mass flow and turbidite re-deposition. Reworked Lower Devonian clasts show that both shallow and deeper-water facies existed at the same time. Givetian strata were strongly affected by syn- and post-sedimentary block tilting and partial uplift, which caused the closely-spaced interfingering of reef beds, intra-formational breccias and mass flows. Well-rounded pebbles and the deep erosion into Lower Palaeozoic strata suggest that the top of tilted blocks formed synsedimentary islands, at least in the middle/upper Famennian. These may have been a source of clastic detritus for the Ben Slimane and Sidi Bettache Basins in the W and E, respectively. However, the regional provenance of thick Famennian/Tournaisian silt- and sandstones requires further analyses. The main Variscan deformation occurred towards the end of the Lower Carboniferous, after an episode of upper Viséan to Serpukhovian carbonates with still open marine conodonts (NEQQAZI et al. 2014).

Refinements of the original lithological division of CHALOUAN & HOLLARD (1979) and CHALOUAN (1981) result in the following formation and member sequence:

3.1. Upper Silurian

The oldest Palaeozoic of the Oued Cherrat is represented by Ludlow graptolite shales and limestones (S_s), which have not yet received a formation name. They may reflect the post-Caledonian transgression, as in the Rabat-Tiflet Zone to the N (e.g., EL HASSANI et al. 1988).

CHALOUAN (1981) speculated that beds with scyphocrinitids, which are so characteristic for the Silurian-Devonian transition in other Meseta and Anti-Atlas regions, including the adjacent Ben Slimane region (ZAHRAOUI 1991), might have been cut off by faulting.

3.2. Lochkovian

CHALOUAN (1981) did not recognize Lochkovian beds, probably caused by the strong fault fragmentation of the region, not due to non-deposition. ZAHRAOUI (1991, 1994a) observed the Silurian-Devonian transition, with shallow-water shales and limestones of assumed Lochkovian age, in the Kaf Nzaha section in northern parts of the Oued Cherrat (S of Aïn Khira, see Fig. 2). The unit requires further investigations. *Uncinatograptus uniformis*, the defining graptolite for the Devonian base, has been recognized near Ben Slimane (DESTOMBES & JEANETTE 1996; ZAHRAOUI 1991).

An isolated pebble of black "*Orthoceras* Limestone" from Aïn Dakhla yielded unexpectedly a faunule with middle Lochkovian index conodonts (*Ancyrodelloides transitans*). It proves that a pelagic Lochkovian limestone setting was also developed in the region although it did not leave any known current outcrop. Middle Lochkovian conodonts are in general practically unknown so far from the Western Meseta (e.g., absent from the Rabat-Tiflet Zone, BENFRIKA et al. 2007).

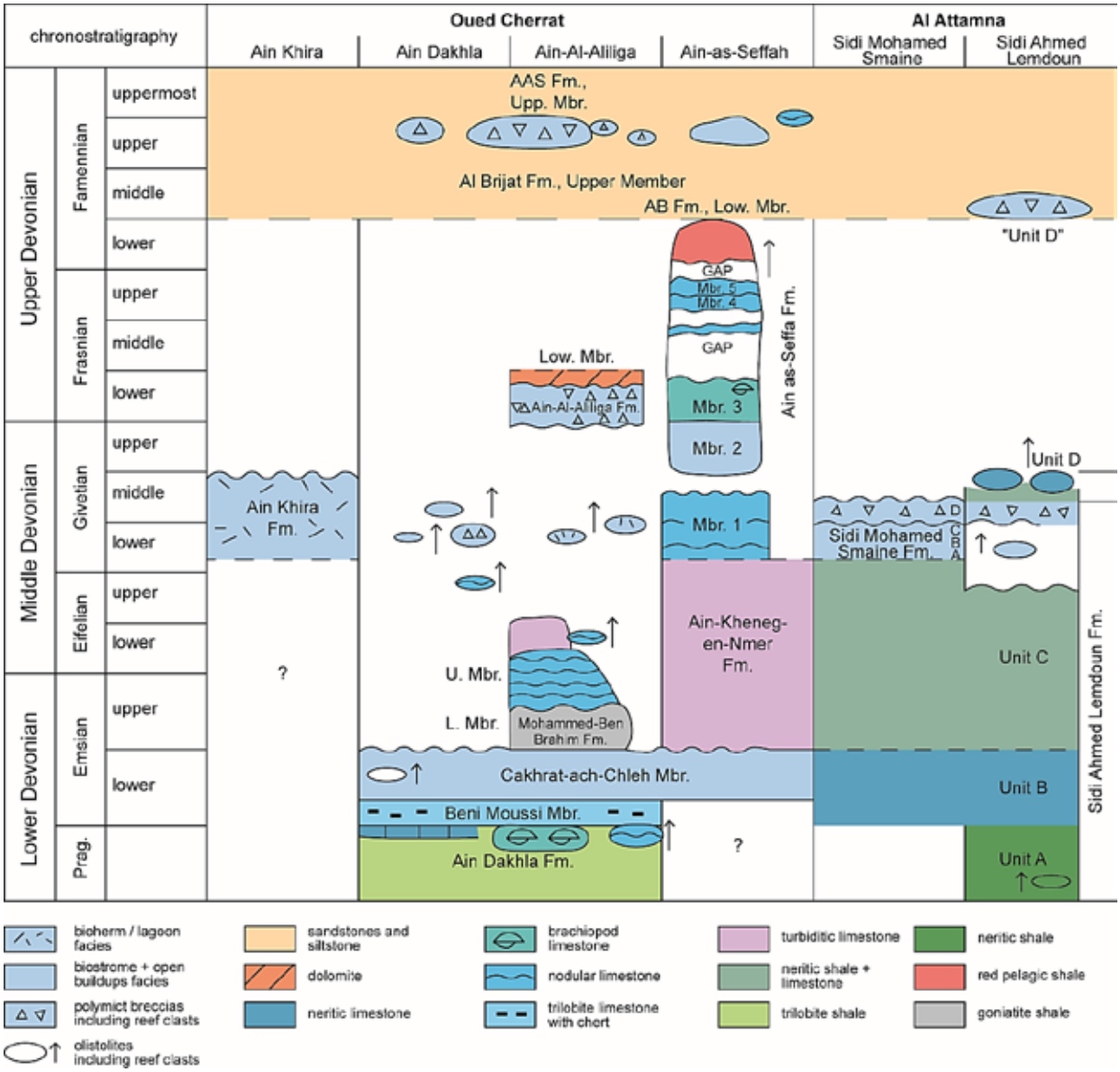

Fig. 3: Revised Devonian lithostratigraphy and correlation of the Oued Cherrat (four successions, from N to S) with the Al Attamna (two successions), the continuation of the reef belt to the S, for comparison (re-drawn from EICHHOLT & BECKER 2016, fig. 3).

3.3. Pragian

The **Aïn-ad-Dekhla Formation** (d_2) is a package of grey, greenish-grey or dark-grey silty shales with intercalated thin sandstones and a diverse, neritic Pragian fauna. Fossils are commonly coated by yellowish limonite, which indicates hypoxic conditions within the sediment – not at the sea floor. The rich brachiopod and trilobite fauna requires revision (e.g., RACHEBEUF 1980; JANSEN 2001; HELLING & BECKER 2015). The preliminary faunal list, with some updated brachiopod identifications by U. JANSEN (Frankfurt a. M.; marked by an *), gives an impression of a rich benthic ecosystem:

various bivalves
gastropods
Ctenochonetes ibericus (abundant, first recorded as "*Strophochonetes (Ctenochonetes)* cf. *aremoricensis*")
Rhenoschizophoria sp. (resembling *Rh. torkozensis*)*
Dalejodiscus aff. *subcomitans** (see Fig. 42.3)
Eucharitina oehlerti
Torosospirifer sp. (previously *Brachyspirifer crassicosta*)*

"Hysterolites nerei" (normally a spiriferid from Bohemia)
*Dixonella ayensis**
Filispirifer e.g. *merzakhsaiensis*. (previously recorded as *Acrospirifer fallax* Group)*
Oligoptycherhynchus cf. *daleidensis*
other rhynchonellids ("*Camarotoechia*")
Reedops cephalotes
possibly other phacopids ("*Phacops* sp.")
Metacanthina sp. (two species)
other asteropygids (previously listed as "*Pilletina* sp.", "?*Paracryphaeus* sp.", and "*Pseudocryphaeus*")
Odontochile sp.
Wenndorfia sp. (?= "*Parahomalonotus* sp.")
large benthic ostracods
solitary rugose corals
tabulate corals

The brachiopods suggest a correlation with the Pragian Assa Formation (Rich 1) of the Dra Valley in the western Anti-Atlas (compare JANSEN 2001 and JANSEN et al. 2007). In the upper part, lenticular and bioclastic limestones with a rich brachiopod fauna, including *Euryspirifer* sp. (not the quoted, younger *E. pellicoi*; see JANSEN 2001), give a transition towards the overlying carbonate formation. The dacryoconarid *Nowakia (Turkestanella) acuaria* provides a firm Pragian age for this upper part/member.

An isolated allochthonous block of micritic griotte limestone re-deposited in the Famennian of Aïn-al-Aliliga yielded unexpectedly upper Pragian icriodids (*Latericriodus steinachensis*). This block of deeper-water, non-siliceous, nodular facies suggests that there was originally a carbonate ramp dipping eastward. This palaeorelief was reversed by Eovariscan tectonic uplift of the eastern Oued Cherrat Zone, leading to reworking and westward shedding.

3.4. Emsian

The subsequent **Dhar-es-Smene Formation** (d_3) is revised and subdivided here. It includes all the thin-bedded and neritic to massive, biostromal, limestones exposed in cliffs and large quarries W and E of the Oued Cherrat (Fig. 1). 20-30 m of well-bedded, light- or dark-grey, sometimes dolomitized limestones with abundant chert nodules are assigned to the new **Beni Moussi Member** (d_{3-1}), named after the hill/area W of the type-section at the Aïn Dakhla spring. The rich shallow-water fauna consists of crinoid debris, brachiopods (various spiriferids, atrypids, rhynchonellids, chonetids), ostracods (beyrichiids), trilobites (phacopids, asteropygids), rugose corals, tabulate corals (*Thamnopora, Favosites*), receptaculitids, calcareous algae, bryozoans, dacryoconarids, and gastropods. The taxonomy of the fauna needs to be revised. The diagenetically mobilized chert derived probably from siliceous sponges. Based on the insufficiently known brachiopod fauna, the new member seems to range from the Pragian-Emsian transition to the lower Emsian. So far, there are no conodonts; several samples from the upper part were barren or included only non-diagnostic single cone genera.

CHALOUAN (1981) noted an up to 20 m thick upper intercalation of silty shales and yellowish, dolomitic limestone with neritic fauna (including "*Euryspirifer* sp. cf. *extensus"*, which, however, is an upper Emsian species of *Arduspirifer*, see JANSEN 2001). ZAHRAOUI et al. (2000, fig. 4) published a detailed section log showing several shallowing-upwards sequences, with two main regressive episodes in the lower/middle part, separated by more argillaceous deepening intervals. The formation and member base should be placed at the base of their massive Bed 8.

The main, upper part of the Dhar-es-Smene Formation provides the cliffs and active limestone quarries of Dhar-es-Smene, Aïn Dakhla (=Aïn-ed-Dekhla), and Aïn-al-Aliliga. ABOUSSALAM et al. (2012, 2013) showed that the thick, main reef belt E of the Cherrat river (Fig. 1) is also lower Emsian age, since the index conodont *Latericriodus bilatericrescens*

bilatericrescens occurs at its base at Cakhrat-ach-Chleh, as well as in typical d_3 limestones of Aïn Dakhla. Consequently, the type Cakhrat-ach-Chleh Formation sensu CHALOUAN & HOLLARD (1979) became a synonym of their Dhar-es-Smene Formation. However, the lithostratigraphic term could be kept as a member name (**Cakhrat-ach-Chleh Member** in EICHHOLT & BECKER 2016; d_{3-u}) for the main, up to 250 m thick reefal part of the Oued Cherrat Lower Devonian carbonate platform. Typical are grey to bluish-grey, partly dolomitized, medium- (20-30 cm) or thick-bedded (up to 2 m), biostromal to non-bedded (biohermal) bioclastic limestones with crinoid debris, stromatoporids, receptaculitids, colonial and solitary Rugosa, tabulate corals (thamnoporids, favositids, alveolitids), bryozoans, brachiopods (atrypids, schizophoriids), gastropods, rare trilobites (phacopids and asteropygids), and calcimicrobes, such as *Sphaerocodium tortuosum* MAMET, 1999. As in the Beni Moussi Member, there was considerable facies and thickness variability along strike.

Towards the S (Aïn-al-Qcob and beyond), the facies became more detrital, dark (organic-rich), or rose to violet in color, and somewhat siliceous. In this undivided Dhar-es-Smene Formation, BENFRIKA & BULTYNCK (2003, "Unit A") found *Caud. celtibericus*, which ranges in the Anti-Atlas from equivalents of the classical (Czech) upper Pragian (= basal Emsian sensu the current Zinzilban GSSP) ca. into the middle of the lower Emsian (ABOUSSALAM et al. 2015). Rich typical lower Emsian *Latericriodus* faunas occur in reworked crinoidal limestone olistolites at Aïn Dakhla. We assume that they derived from uplifted and eroded strata of the Cakhrat-ach-Chleh Member of the region.

The top of this member is often cut off by faulting (e.g., at its type locality and at Aïn Dakhla). Where the succession is complete (e.g., at Cakhrat Mohammed-Ben-Brahim), a gradual deepening is indicatated by the change to finer bioclastic and finally to micritic and nodular limestone. CHALOUAN (1981) reported apart from small brachiopods (*Plectospira*), ostracods, single corals, dacryoconarids, and *Caudicriodus* cf. *curvicauda*. However, typical *Caud. curvicauda* do not range above the basal Emsian and hardly overlap with *Lat. bilatericrescens bilatericrescens* (see ABOUSSALAM et al. 2015). Our new data prove that the initial deepening at the top of the Dhar-es-Smene Formation occurred within the range of *Criteriognathus steinhornensis*, which characterizes the upper half of the lower Emsian. This suggests a possibly correlation with the transgressive, global Upper Zlíchov Event sensu GARCÍA-ALCALDE (1997).

EL HASSANI & BENFRIKA (1995, 2000) emphasized facies and palaeobathymetric differentiation within the Dhar-es-Smene Formation along the Oued Cherrat resulting from synsedimentary tectonic instability. Therefore, it is difficult to follow individual beds/packages from one section to the next. This aspect recommends future more detailed microfacies and sequence stratigraphic analyses along a N-S transsect, combined with a revision of brachiopod taxonomy. As an example, a unique, isolated thick brachiopod coquina followed by detrital limestones occurs in our new "central section" at Aïn-al-Aliliga (see below).

The subsequent, argillaceous **Mohammed-Ben-Brahim Formation** (d_{4-1}) is restricted to its type region around Cakhrat Mohammed-Ben-Brahim in the ca. middle part of the Oued Cherrat. It is characterized by up to 100 m of dark-grey, calcareous and partly pyritic shale. It contains a pelagic assemblages of goniatites, orthocones, bivalves, small solitary rugose corals, and rare, relatively large phacopids. A squashed *Gyroceratites* Fauna (Fig. 4) from the base, typical for the basal upper Emsian (LD IV-A in the zonal scheme of BECKER & HOUSE 2000b), proved that its sharp base correlates

with the global Daleje Event (BECKER et al. 2019). E. A. HILALI found a specimen of "*Anarcestes lateseptatus*" in the shale (CHALOUAN 1981), which places higher parts of the formation in middle/upper parts of the upper Emsian (LD IV-D), even if the species identification requires confirmation. It should be noted that upper Emsian strata with anarcestids were placed for a long time (but wrongly) in the "Couvinian" or Eifelian (see KERGOMARD 1970, CHALOUAN 1981, and ZAHRAOUI 1994b). Records of the large-sized and spinose asteropygid *Psychopyge elegans* from Cakhrat Mohammed-Ben-Brahim are in full accord with an upper Emsian age (see MORZADEC 1988).

Fig. 4: Squashed *Gyroceratites* sp. from reddish-weathering pyritic (secondarily limonitic) shales in the basal part of the Mohammed-Ben-Brahim Formation at Cakhrat Mohammed-Ben-Brahim.

Due to its soft rheology, the Mohammed-Ben-Brahim Formation tends to be affected by tectonism. In our new "central section" at Aïn-al-Aliliga, it can be subdivided into two members. The **Lower Member** ($d_{4\text{-}1l}$) is shaly, the new **Upper Member** ($d_{4\text{-}1u}$) consists of ca. 6.5 m of nodular, micritic limestone with anarcestids and conodonts of the *Icriodus fusiformis* Zone (basal part of the upper Emsian, ABOUSSALAM et al. 2015).

Fig. 5: The Aïn-Kheneg-en-Nmer Formation at Aïn-as-Seffah in the southern Oued Cherrat, showing two limestone units to the right and left (Cherrat Valley slope) interrupted by a more shaly interval with poor outcrop.

3.5. Eifelian

The **Aïn-Kheneg-an-Nmer Formation** ($d_{4\text{-}2}$) is defined as a 20-150 m thick alternation of dark-grey shales and dark-grey to black, thin- to medium-bedded, detrital or turbiditic limestones. The thickness increases from Aïn-al-Aliliga to the S (Aïn-as-Seffah), where two limestone units are separated by a more shaly middle package (Fig. 5). The macrofauna is very sparse. Some tabulate corals, phacopids, small brachiopods, and deeper-water bivalves (*Panenka*) were noted by CHALOUAN (1981). Conodonts identified by P. BULTYNCK include a range of "middle" Eifelian (middle/upper *Po. costatus* Zone) polygnathids and icriodids, such as *Po. angusticostatus, Po. angustipennatus, Po. robusticostatus, Po. pseudofoliatus, Linguipolygnathus linguiformis, Icriodus regularicrescens, I. curvirostratus/introlevatus,* as well as *Tortodus intermedius*. Observed agoniatite cross-sections may refer to *Fidelites* or *Foordites*. BENFRIKA & BULTYNCK (2003), however, showed that the formation begins more to the S, at Aïn-al-Qcob, already in the upper Emsian *L. serotinus* to *Po. patulus* Zones. This is fully supported by data from our new "central section" at Aïn-al-Aliliga, where the formation base falls within the *L. serotinus*

Zone. Therefore, it starts within the ca. upper half of the upper Emsian. The lower Eifelian was recognized ca. 13 m above the base but the still crude sampling has not yet pinpointed the series boundary. The basal Eifelian Choteč Event is locally not distinctive. Upper Eifelian conodonts, including the index species *T. kockelianus*, are regionally known from the top of the formation (Aïn-as-Seffah) and from reworked blocks in Famennian olistolite units. The Eifelian/Givetian boundary is not preserved within the faulted sections that have been studied so far. As a result, and unlike as in the Rabat-Tiflet Zone to the NE, there is no regional record of the global Kačak Event(s).

3.6. Givetian

Thick (50-100 m) Givetian reef limestones form a narrow, third, eastern outcrop strip in northern parts of the Oued Cherrat (Fig. 2), which is intensively quarried. EICHHOLT & BECKER (2016) introduced for this economically important unit the term **Aïn Khira Formation** (d_5). The best outcrops from the research period between ZAHRAOUI (1991) and ZAHRAOUI et al. (2000), shown to an international audience during the SDS-IGCP 421 Morocco Field Meeting in spring 1999, have, unfortunately, disappeared in the meantime by quarrying. CATTANEO et al. (1993) recognized eight principle reef facies, which were arranged vertically into two major regressive cycles and several subcycles. Characteristic facies types are:

F1. Argillaceous dacryoconarid mud-wackestones (outer ramp or platform)
F2. Wacke-floatstones with some isolated reef corals, stromatoporids and crinoid debris (subtidal external platform with distal reef talus)
F3. Peloidal and crinoidal pack-grainstone with bryozoans (external platform with crinoid meadows)
F4. Stromatoporid and coral float-rudstone (proximal reef talus of the upper marginal slope or within the lagoon)
F5. Stromatoporid-coral frame-bindstone with massive reef builders (reef core)
F6. Amphiporid floatstone with parathuramminids and various bioclasts (deeper lagoonal)
F7. Amphiporid-parathuramminid mud-wackestone (deepest or most protected lagoonal parts)
F8. Peloidal birds-eye boundstones, peloidal micrites, and laminated bindstones (intertidal reef flat)

ZAHRAOUI (1991, 1994b) reconstructed a carbonate platform/ramp that deepened from the W to E. EICHHOLT & BECKER (2016) subdivided the inner platform/lagoonal facies set (F4 and F6-8) into eight microfacies types:

MF A1: Peloidal grainstone (lagoon parts with moderate water agitation and strongly restricted fauna).
MF A2: Detrital grain-rudstone or back reef breccias (= F4, coarse proximal talus on the inner side of the reef core or around patch reefs)
MF A3: *Stringocephalus-Amphipora* rudstone (storm layers within the lagoon)
MF A4: *Stachyodes-Thamnopora* float-rudstone (storm layers around patch reefs)
MF A5: Stromatoporiod float-rud-boundstone with up to 20 cm large bulbous stromatoporids (upper patch reef, part of F5)
MF A6: *Amphipora* float-rud-boundstone (= F6, protected deeper lagoon)
MF A7: Bioclastic mud-wackestone (= F7/8, protected and restricted, calm lagoon with occasional freshwater influx)
MF A8: *Stringocephalus* floatstone with bioturbation (protected wide lagoon with overall good living conditions)

Probably based on a third outcrop, CASIER et al. (1997) distinguished ten microfacies types. We did not observe their bioturbated siltstones (M1) and silty mud-wackestones (M2) in our section (see below), nor an abundance of (microbial) fenestrae, as in their M7 (ca. = MF A4), M8 (ca. = MF A6), and M10 (ca. our MF A7). The detailed analysis of the locally common foraminifers by VACHARD et al. (1994) resulted in the record of ten species of Parathuramminina and five species of Moravamminida (possible calcareous algae), including the new issinellid *Palachemonella maroccanica*.

The Givetian age of the Aïn Khira Formation is confirmed by the index brachiopod genus *Stringocephalus* and the colonial marker coral *Phillipsastrea*. Records of *Cyrtospirifer* show that the succession ranged at least locally into the upper Givetian. Among the diverse ostracods (50 taxa of the Eifelian shallow-water ecotype), *Polyzygia beckmanni beckmanni* and rare *Poly*. cf. *insculpta* confirm the Givetian age (CASIER et al. 1997).

Towards the S, at Aïn Dakhla, Givetian reef limestones are only known as reworked olistolites within the much younger Al Brijat Formation. Crinoidal limestone blocks with lower/middle Givetian conodonts show that originally an open, lower ramp/platform (with F2) was developed before tectonic uplift and erosion destroyed it completely.

Further to the S, at Aïn-al-Aliliga, an open neritic to biostromal carbonate ramp was subject to recurrent, strong synsedimentary seismic events. This led to a more than 50 m thick alternation of coarse breccia beds (mass and debris flow deposits), biostromal limestones with silicified stromatoporids and corals, and intercalated, well-bedded, conodont-bearing limestones (Flinz-type facies). All rock types yielded in several samples exclusively middle Givetian to basalmost Frasnian (*Ancyrodella rotundiloba pristina* Zone, MN 1 Zone) conodont assemblages. Therefore, we assign the part of the **Aïn-al-Aliliga Formation** of CHALOUAN & HOLLARD (1979) that lacks any volcanite or quartzite pebbles/blocks to a new **Lower Member** ($d_{7\text{-}1}$) It overlies N of the W-E running track with an angular unconformity the Dhar-es-Smene Formation. Basal beds are rich in icriodids, higher parts are in polygnathid biofacies.

GENDROT et al. (1969) suggested that the second, up to 200 m thick eastern reef limestone cliff at Cakhrat Mohammed-Ben-Brahim is of Givetian age, as it is also shown in the cross-section of CHALOUAN (1981). This would make it a preserved southern continuation of the Aïn Khira Formation but currently there is no biostratigraphic age control. Re-sampling is required, especially since there is a fault contact to the supposedly older beds (Mohammed-Ben-Brahim Formation; CHALOUAN 1981, ZAHRAOUI 1994b).

Fig. 6: Weathered *Manticoceras* specimen as seen on a bedding plane of the "*Manticoceras* Limestone" (Member 5) at Aïn-as-Seffah, southern Oued Cherrat.

The term **Aïn-as-Seffah Formation** (d_6) of CHALOUAN & HOLLARD (1979) has been revised by ABOUSSALAM et al. (2013b) to include all parts of the internally complex large limestone olistolites embedded at Aïn-as-Seffah within the Al Brijat Formation. Only the thin-bedded **Member 1** (d_{6a}) and the open biostromal **Member 2** (d_{6b}) fall in the Givetian. But their contact is disconformable and much of the middle Givetian is missing. This proves an intra-Givetian tectonic phase preserved within the big main allochthonous block.

3.7. Frasnian

There is only a poor previous record of Frasnian strata from the Oued Cherrat, which agrees with the general pattern of the Meseta Devonian. In the N, there is no section that display strata that overlie conformably the Aïn Khira Formation. Since the Lower Member of the Aïn-al-Aliliga Formation yielded basalmost Frasnian index conodonts, overlying thin-bedded dolomites are also of (lower)

Frasnian age. *Belodella*, the only conodont recovered, did not survive the end-Frasnian mass extinction.

The best Frasnian evidence comes from Aïn-as-Seffah, where it is strongly condensed and incomplete, with unconformities between **Member 3** (d_{6c}, lower Frasnian, massive brachiopod limestone) and **Member 4** (d_{6d}, top-middle to upper Frasnian flaserlimestone). The famous rose limestone with *Manticoceras* (**Member 5**, d_{6e}, Fig. 6) is just 65 cm thick. Based on MN 13a Zone (KLAPPER 1989; = *Pa. bogartensis* Zone) conodonts, it correlates in time with the latest Frasnian starting at the top of the Lower Kellwasser level. There is no regional evidence for the Upper Kellwasser Limestone; the Frasnian-Famennian transition falls in another hiatus.

3.8. Famennian

Evidence for lower Famennian strata is even weaker in the Oued Cherrat region. ABOUSSALAM et al. (2013b) emphasized at Aïn-as-Seffah a lenticular, up to 10 m thick unit of red shale, which was obviously attached to the main limestone olistolite prior to its re-deposition. It was assigned to a new **Lower Member** (d_{7-2}) of the Al Brijat Formation but it is so distinctive and regionally unique that it should receive its own lithostratigraphic name in future.

The typical or **Upper Member** (d_{7-3}) of the **Aïn-al-Aliliga Formation** sensu CHALOUAN & HOLLARD (1979) and CHALOUAN (1981) is an up to 70 m thick channel fill consisting of chaotically-bedded, strongly polymict and extremely coarse, massive breccia unit, best exposed at the Aïn-al-Aliliga spring. Apart from a wide array of up to 3 m large reworked limestone clasts, including many Givetian reefal blocks, there are (sub)rounded Lower Palaeozoic, dark-grey quartzite pebbles, and light-grey weathering volcanites. The matrix is calcareous, iron-rich (reddish) or siliceous. CHALOUAN (1981) noted irregularly interbedded sandstone and quartzite beds, which may refer to large, flat olistolite blocks. The age of the unit is difficult to assess. Individual clasts and a large bulk sample yielded to us only sparse to diverse middle/upper Givetian conodonts. This is in contrast with records from supposed breccia matrix of *Bispathodus costatus* (towards *B. spinulicostatus*) and *I. cornutus* in CHALOUAN (1981). Two upper Givetian species, *I. expansus* and *Po.* ex gr. *pennatus,* were allegedly associated, which suggests a mixed, reworked fauna. *Bispathodus costatus* is the index taxon of the *B. costatus* Subzone (of the *B. aculeatus aculeatus* Zone) in the upper half of the upper Famennian (see HARTENFELS 2011). There is some support from our Sample VFP, which yielded no Famennian conodonts but some middle/upper Famennian *Phoebodus* teeth (SCHWERMANN 2014: two subspecies of *Phoeb. gothicus*). The combined evidence suggests an upper Famennian re-deposition age. It was preceded by a long interval of non-deposition (main Frasnian to lower Famennian) and middle/upper Famennian block tilting causing uplift, deep erosion, and reworking, with some rounding in a coastal setting. Seismic events on steep elevated flanks induced gravitational mass flow transport down a steep ramp. Due to the large clast size and localized occurrences, the source areas must have been very close, right at the eastern margin of the Oued Cherrat Zone. Some of the mass flows seem to have ended in "shark-infested" open water or even killed them.

The **Al Brijat Formation** (dh) is an even more complex unit since is consists locally very variably of thick siliciclastics (grey to brownish or greenish silty shales, micaceous siltstones, and thin- or cross-bedded sandstones), intercalated mass flows, and isolated or accumulated olistolites of highly variable age and lithology. Compact packages of reworked limestones and breccias may be seen as local tongues of the Aïn-al-Aliliga

Formation (Fig. 7). However, there was repeated seismic activity all along the extended Oued Cherrat and not necessarily any continuity between individual mass flow units. The recognition of double reworking (olistolites consisting of cannibalized Givetian breccias) is of principle importance to understand the polyphase regional synsedimentary tectonics.

Fig. 7: Large corroded olistolite blocks of reworked Middle Devonian limestone breccias, re-deposited as mass flow in the Famennian Al Brijat Formation (tongue of Aïn-al-Aliliga Formation) at Aïn Dakhla (picture width 1 m).

CHALOUAN (1981) proposed a synthetic (combined from different localities) succession for the Al Brijat Formation, which extends widely into the adjacent southern Sidi Bettache Basin to the E. For example, their upper succession includes the distinctive Tournaisian and Viséan limestones of Sidi Jilali and Sidi Radi (IZART & VIESLET 1988). Concentrating on the Oued Cherrat area, our observations support the following succession:

Unit 1: Conglomerate/breccia with reworked reef limestone of Cakhrat Mohammed-Ben-Brahim. A supposed lower Famennian age (KERGOMARD 1970) is not based on published conodont data. A correlation with the Upper Member of the Aïn–al-Aliliga Formation (*B. costatus* Subzone) seems more likely but requires further sampling.

Unit 2: Thick package (150 m or more) of silty shales and siltstones, upwards with increasingly dominant sandstones.

Unit 3: 10-20 m thick, lenticular, polymict breccias, conglomerates and isolated olistolites with reworked Lower/Middle Devonian limestones, including many reefal blocks, cannibalized breccias, and sandstone/quartzite clasts. Our new samples from several localities provided no evidence for reworked Upper Devonian limestones. This is not really surprising since the youngest strata will have been eroded first and should have been re-deposited in Unit 1.

Unit 4: Ca. 300 m of alternating silty shales, siltstones and, increasing towards the top, sandstones.

Unit 5: Up to 30 m thick, relatively fine conglomerate/breccia with rounded limestone and angular quartzite clasts. This unit underlies in the S, at Ghar al Anz (in the SW of topographic sheet, 1 : 50 000, Sidi Bettach), a thin black shale with laminated limestone concretions and an overlying dolomitized carbonate unit. Unfortunately, the first did not yield any conodonts to us.

The age of the formation and especially the precise timing of Eovariscan reworking events is still poorly constrained. As stated by CHALOUAN (1981), there have been two peak intervals of Famennian re-deposition. Unless good palynological data become available, it will remain impossible to separate upper/uppermost Famennian and Tournaisian strata in the upper part of the formation. Some samples have been given to C. HARTKOPF-FRÖDER (Krefeld) but results are not yet available. So far, there is no record of black shales that might mark the onset of the global Hangenberg Crisis, as in the Oulmes region to the E (KAISER et al. 2007). As a hypothesis, the D/C boundary regression may be represented by the upper part of Unit 4 to Unit 5.

3.9. Lower Carboniferous

The thick, upper and eastern part of the Al Brijat Formation comprises the lower Tournaisian since it is overlain at Sidi Jilali, in the southern Sidi Bettache Basin, by a limestone with middle Tournaisian conodonts (IZART & VIESLET 1988; new samples). As

suggested in FADLI (1994a), the term Al Brijat Formation should be restricted to the siliciclastics below this Sidi Jilali Member and below the supposedly equivalent dolomitic limestones of Ghar al Anz in the S (Ghar al Anz Member). The middle Tournaisian to middle Viséan clastics and intercalated limestones (e.g., the Viséan Sidi Radi Member) of the southern Sidi Bettache Basin fall in the complex, flyschoid Khourifla Formation. In the Oued Cherrat, transgressive, upper Viséan limestones with index foraminifers have been named by CHALOUAN & HOLLARD (1979) as Mechra-al-Kraret (open shelf limestones and shales) and Kaf-Anzaha Formations (shallow-water limestones). NEQQAZI et al. (2014) showed that the Mechra-al-Kraret Formation ranges into the Viséan-Serpukhovian transition with *Lochriea cruciformis* and *Mestognathus bipluti*. Whilst the latter was widespread in the upper Viséan (e.g., ABOUSSALAM et al. 2017: Marrakech region), *L. cruciformis* enters above *L. ziegleri*, the proposed future Serpukhovian index species (e.g., BARHAM et al. 2015). However, this level is much older than the traditional Viséan-Namurian boundary of Central Europe (e.g., WANG et al. 2018). Therefore, the conodont evidence does not prove that the open marine Oued Cherrat Carboniferous includes Namurian equivalent strata.

Since we have not studied or re-sampled the Viséan, our detailed review and summary of Oued Cherrat stratigraphy ends with the Al Brijat Formation.

4. Key successions

4.1. Givetian reef at Aïn Khira South

Givetian reefs stretch as a narrow band from Aïn Khira, ca. 6 km E of Bouznika, for ca. ca. 3 km to the SSE. The successions described by ZAHRAOUI (1991), CATTANEO et al. (1993), and ZAHRAOUI et al. (2000) have been quarried away. This is unfortunate since former small quarries exposed reef facies types beautifully in sawed walls. As a consequence, EICHHOLT & BECKER (2016) published a section log (from 2012) and the facies history for an inner platform succession at the southern margin of the most southern quarry at that time (Fig. 8), here named as section Aïn Khira South. The evidence can be summarized as follows:

The local total thickness of the Aïn Khira Formation is almost 100 m. Conodont samples were barren but *Stringocephalus* cross-sections found at 12 and 59 m above base prove a lower to middle Givetian age (Fig. 9). At the base, there are middle- to dark-gray peloidal grainstones (MF A1) with gastropods and subordinate brachiopods. At 7 m there are up to 30 cm thick, late diagenetic dolomite boulders, followed by a re-onset of MF A1. At 9 m begins a short interval with bioclastic grainstone (MF A2, Fig. 10) containing fragmented stromatoporids, corals, and some crinoid debris.

Back-reef shedding of crinoid fragments in channels or during storms is also known from contemporaneous German reefs (e.g., KREBS 1974). An *Amphipora* Boundstone (MF A6**)** at 11 m documents the return to restricted, calm lagoonal conditions. It is overlain by storm beds consisting of *Stringocephalus-Amphipora* float-/rudstone (MF A3, 11.5-15 m, Fig. 11). At 16-20 m, more peloidal grainstones (MF A1) are overlain by *Stachyodes-Thamnopora* float-/rudstones (MF A4). Subsequent bioclastic mud-/wackestones indicate even more restricted conditions and a deepening interval from 23 m on (MF A7). The fossil content is poor (ostracodes, rare gastropods, parathuramminid foraminifers). Small-sized sparite fenestrae indicate a microbial content (Fig. 12). Between 33 and 35 m, peloidal grainstones (MF A1) are intercalated, as evidence for an interval of again increased turbidity. At 44-46 m a small patch reef episode with MF A6 (*Amphipora* float-bafflestone) is developed. A thicker patch reef

interval ranges from 48-59 m. *Stachyodes-Thamnopora* float-rudstones (MF A4) occur at the base, followed by MF A5 (Fig. 13). Such reefal structures within the inner platform are characterized by small bulbous or laminar stromatoporids, which interspaces were settled by solitary Rugosa, branching tabulates, and dendroid stromatoporids (*Stachyodes, Amphipora*). At 59 m, MF A8, *Stringocephalus* floatstones (Fig. 9), become characteristic. Despite their thick shells, this brachiopod group preferred protected lagoons (e.g., BECKER et al. 2016a). Wide-spread disarticulated valves show their sensivity to episodic major storm events.

At 64-65 m and 70-71 m, there are thin *Amphipora* rud-bafflestones (see Fig. 14), a typical back-reef facies that re-occurs at the top (95-97 m, Fig. 15). The main upper part of the succession is formed by the deeper lagoonal MF A7. This suggests a second deepening phase, as it was also shown in the more northern locality of CATTANEO et al. (1993). MF A4, *Stachyodes-Thamnopora* float-rudstone, occur at 75-76 and ca. 83 m. They are typical for lagoon parts adjacent to patch reefs; both forms are more robust and storm-resistant than *Amphipora*.

Characteristic for our section is the lack of cyclicity and the rarity of fenestral/microbial facies. It lacks the unit with laminites (F8 of CATTANEO et al. 1993) separating the two deeper lagoonal sequences. Instead, there are the solid patch reef boulders of 48-59 m. We did not reach the reef top. Therefore, we cannot asses at Aïn Khira South the reasons for the reef extinction. Further studies are required to solve this question.

Fig. 8: View on the logged Givetian inner platform reefal succession exposed in 2012 near the southern end of Aïn Khira. Beds are exposed in large, partly poorly stratified boulders (GPS coordinates N33°42'56,9'' W007°01'12,8'').

Fig. 9: Field photo from Aïn Khira South showing a typical, thick-shelled *Stringocephalus* cross-section with median septum, embedded in fine-grained bioclastic limestone.

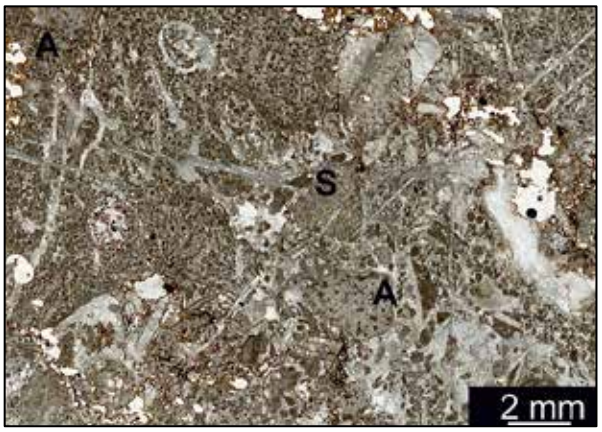

Fig. 10: MF A2, bioclastic peloidal grainstone with debris of blocky stromatoporoids (S), and *Amphipora* (A), Aïn Khira South at 10 m.

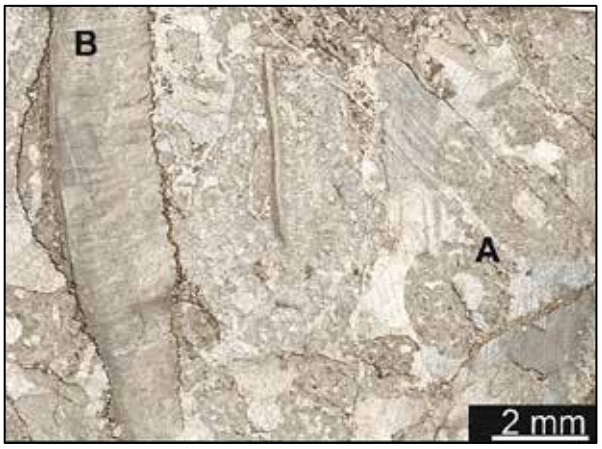

Fig. 11: MF A3, sparitic rudstone with *Amphipora* (A) and thick *Stringocephalus* shells (B), Aïn Khira South at ca. 12 m.

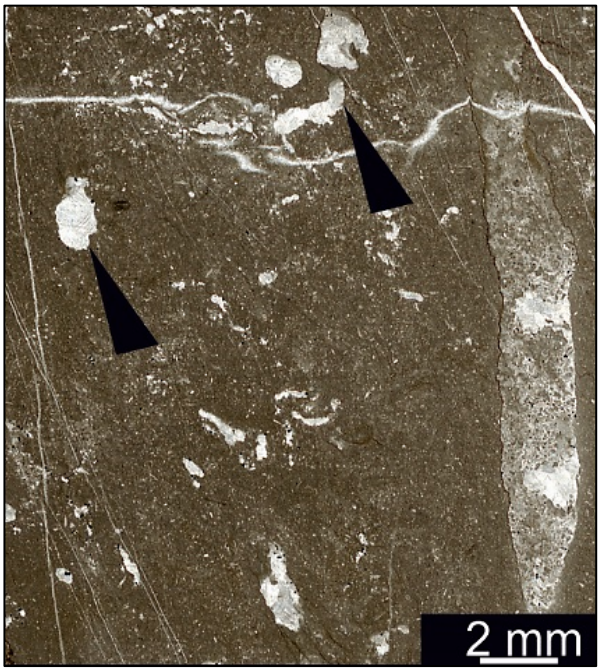

Fig. 12: MF A7, dense mudstone with fenestral (microbial) birdseyes (black arrows), AKS at 29 m.

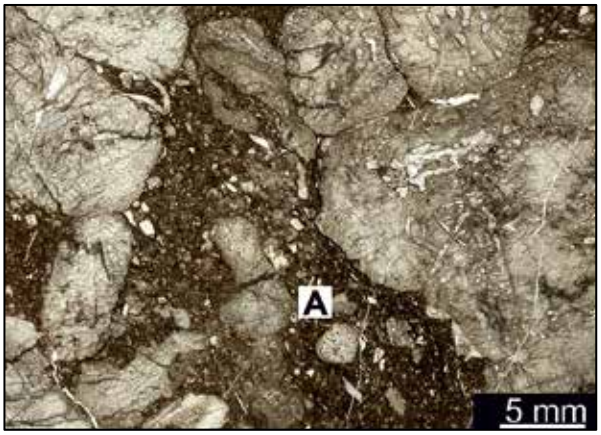

Fig. 13: MF A5, stromatoporoid float-rudstone: between bulbous stromatoporids lie delicate *Amphipora* (A)-rich mud seams. Irregular component contacts create a stylobreccioid structure, Aïn Khira South at 56 m.

Fig. 14: Field example of a weathered *Amphipora* rud-bafflestone (MF A6) from Aïn Khira South.

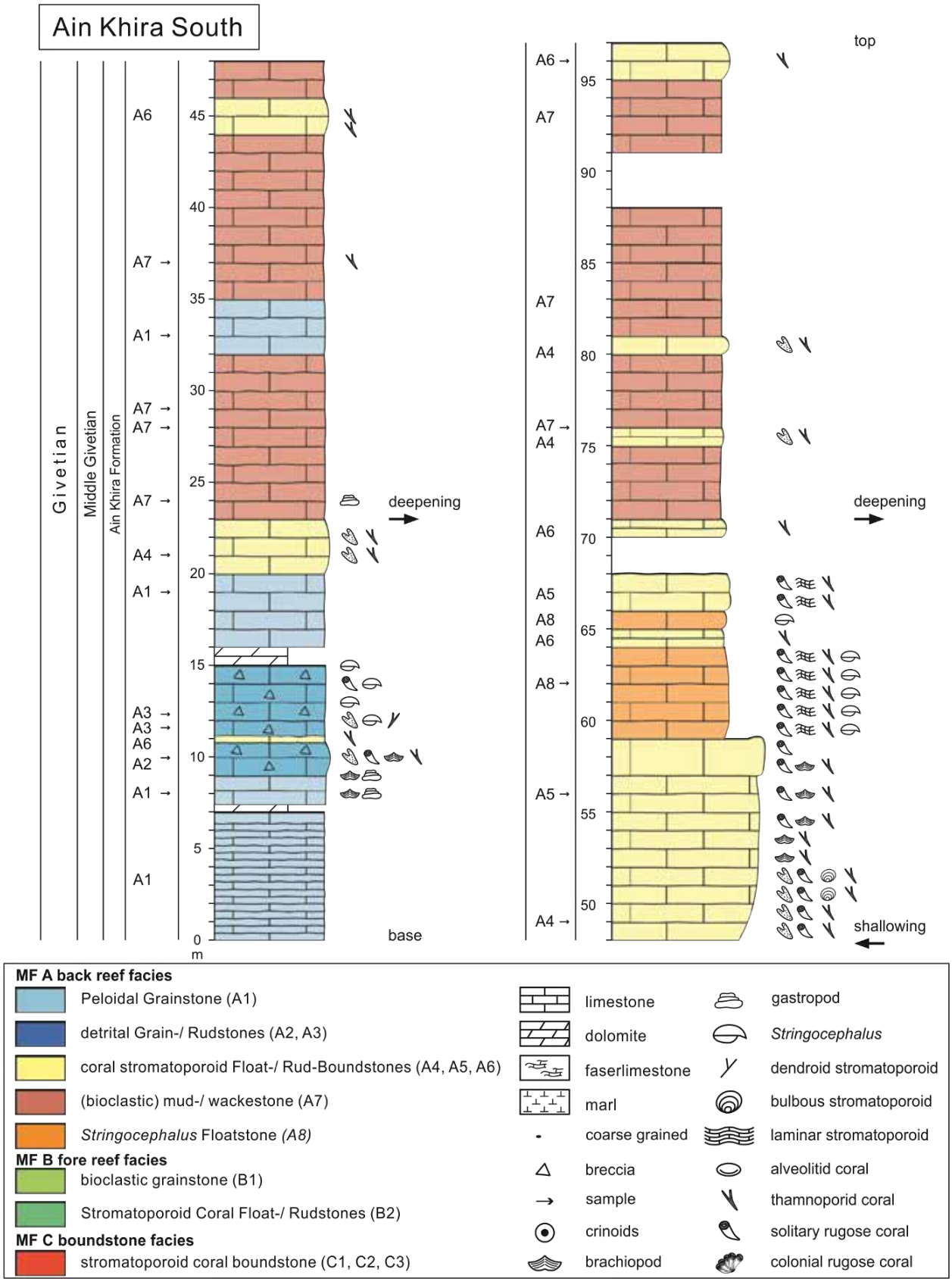

Fig. 15: Inner platform macro- and microfacies succession at Aïn Khira South, based on logging in 2012. Two transgressive episodes but no cyclicity are evident (EICHHOLT & BECKER 2016, fig. 9)

4.2. Pragian to Famennian at Aïn Dhakla

CHALOUAN & HOLLARD (1979) and CHALOUAN (1981) published a geological cross-section from the Beni Moussi/Aïn Dhakla area W of the Oued Cherrat (Fig. 17) to Cakhrat-ach-Chleh (Fig. 1) on the eastern side. This includes the type localities for the Pragian Aïn-ed-Dekhla, Emsian Dhar-es-Smene, and originally supposed Givetian (but also Emsian) Cakhrat-ach-Chleh Formations. Based on our re-sampling, the ca. W-E succession can be summarized as follows:

The shales of the Aïn-ed-Dekhla Formation at the western end are rather deeply weathered and often covered. ZAHRAOUI et al. (2000, fig. 4) illustrated a detailed section log for the increasingly calcareous Pragian/Emsian transition. Starting from the Aïn Dhakla spring at x = 349.2 and y = 340.85 (topographic sheet, 1 : 50 000, NI-29-XI-4b Benslimane), the new Beni Moussi Member consists of well-bedded, fossiliferous light- to medium-grey crinoidal and bioclastic limestones with many chert nodules. In the higher part there are frequent phacopid trilobites and some gastropods. Conodont samples from this part were, unfortunately, barren.

There is a gradual transition towards the massive, thick- or non-bedded, biostromal Cakhrat-ach-Chleh Member. A middle-grey, fine-grained crinoidal limestone from the base yielded a rich conodont fauna with *Caudicriodus celtibericus* (Figs. 18.12-13), *Lat. bilatericrescens multicostatus* (Figs. 18.14-15), and the single-cone species *Neopanderodus perlineatus* (Fig. 18.16). This assemblage is typical for shallow settings of the *Lat. bilatericrescens bilatericrescens* Zone in the ca. lower half of the lower Emsian (see ABOUSSALAM et al. 2015). The subsequent, light-grey, thick and massive reefal blocks are partly rich in stromatoporids and alveolitids. Gastropod limestones, beds with small brachiopods, and fine-grained bioclastic limestones to mudstones are intercalated. Towards the top there is a strong increase of dolomitization, which destroyed the fossil content.

The upper part of the lower Emsian reef is cut off by a normal fault. Many big dolomitized blocks lie on the slope of the plateau E of the fault (Fig. 16). Due to poor outcrop, it is not really clear if they only cover the slope or whether they are embedded in a shale matrix. CHALOUAN (1981) placed the subsequent, very thick, first brownish weathering, then green shales (Figs. 16, 19), which weather in small, narrow ravines, in his d_2 ("Siegenian argillites"). However, the shales are unfossiliferous, unlike the typical Aïn-ed-Dekhla Formation. Unlike as in the W, they grade on the next hill to the E into cross-bedded sandstones and reddish dolomite beds (Fig. 20).

A single slab of "Orthoceratid Limestone" from the base of the problematical shales yielded single Pa-elements of *Ancyrodelloides transitans* (Fig. 21) and *Wurmiella* sp. (possibly a new species with arched low carina and narrow, triangular basal cavity). The first is the index species for the *Anc. transitans* Zone in the lower half of the middle Lochkovian; it does not range above the middle Lochkovian (e.g., CORRADINI & CORRIGA 2012; VALENZUELA-RÍOS et al. 2015). Although the limestone block is alien to the thick green hales, it leads to the suspicion that at least large parts of the shale unit are of Lochkovian age. This has to be resolved by palynological data (Fig. 19).

Fig. 16: View on the blocky, reefal part (Cakhrat-ach-Chleh Member, d_{3u}) of the Dhar-es-Smene Formation (upper left) at Aïn Dakhla, followed after a fault contact by deeply weathered, brownish, possibly Lochkovian shales, which are partly covered by dolomitized reef blocks (to the upper right).

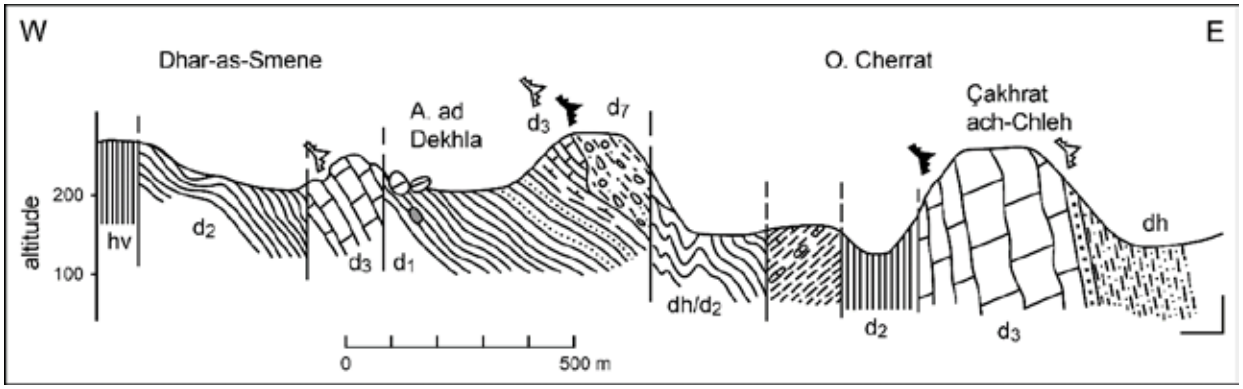

Fig. 17: Revised stratigraphy of the transsect from Beni Moussi and Dhar-es-Smene in the W to the eastern slope of the reef cliff at Cakhrat-ach-Chleh (middle Oued Cherrat region, updated from CHALOUAN & HOLLARD 1979).

The plateau with a quarry and small settlement between Dhar-es-Smene and the Cherrat valley to the E exposes banks of crinoidal to biostromal limestone (Fig. 22), which CHALOUAN & HOLLARD (1979) assigned to d_3. Two conodont samples were barren, which is typical for the upper Dhar-es-Smene Formation. Downslope and on the next hill E of the sandstones mentioned above, there is a thick succession of grey shales and siltstones (Al Brijat Formation, Fig. 22) with intercalated accumulations of isolated, up to 2 m large limestone olistolites and massive, compact limestone breccias (Figs. 7, 23). This 10-20 m thick unit, a tongue of the Aïn-al-Aliliga Formation, (d_{7-3}) can be followed downslope to the main road, where the number of reworked blocks decreases. Among the olistolites, middle to dark grey crinoidal limestones are dominant.

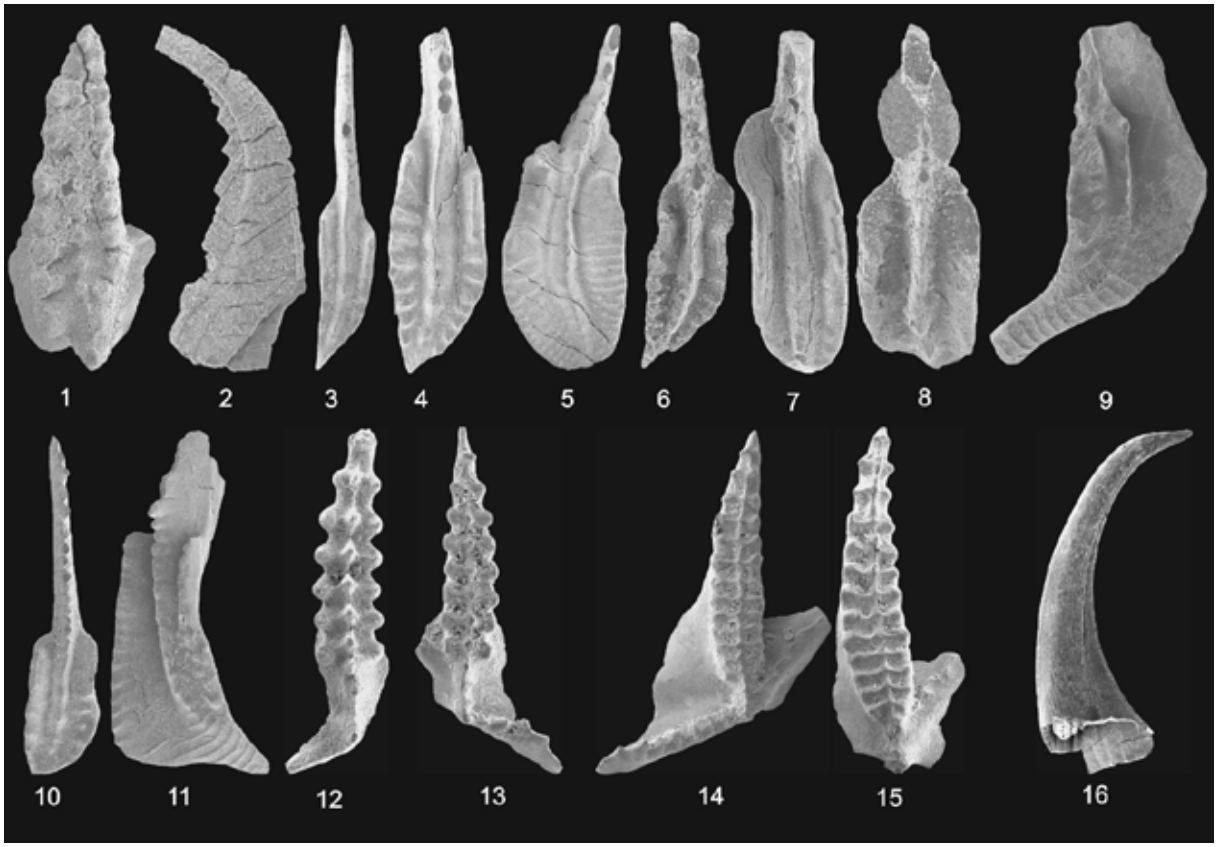

Fig. 18: Conodonts from a double reworked breccia (1-8) and from other olistolites (9-11) within the Al Brijat Formation (dh) at the eastern summit W of the Oued Cherrat, and from the basal Cakhrat-ach-Chleh Formation at Aïn Dakhla (12-16, d_{3u}) **1.** *Icriodus retrodepressus*, x 45; **2.** *Belodella resima*, x 80; **3.** *Polygnathus* aff. *xylus*, with narrowly angular posterior platform end, x 65; **4.** *Po. paradecorosus*, x 75; **5.** *Po. costatus*, x 30; **6-7.** *Po. timorensis*, x 50 and x 60; **8.** *Po. varcus*, x 50; **9.** *Linguipolygnathus klapperi*, x 30; **10.** *Po. ansatus*, x 40; **11.** *L. linguiformis*, x 35; **12-13.** *Caudicriodus celtibericus*, x 80 and x 50; **14-15.** *Lat. bilatericriodus multicostatus*, x 35 and 55; **16.** *Neopanderodus perlineatus*, x 55.

Sample S2 yielded lower Givetian conodonts (*Linguipolygnathus klapperi*, Fig. 18.9, and *L. linguiformis*, Fig. 18.11), Sample S3 *Po. ansatus* (Fig. 18.10), the index species of the *Po. ansatus* Zone in the upper half of the middle Givetian. A double reworked breccia block (Fig. 23.2) displayed the very heterogenous nature of a strongly unsorted and angular clast assemblage. There are reworked dark-grey mudstones, middle-grey bioclastic wackestones, partly with irregular, microbial fenestrae, peloidal grainstones, coarse, bioclastic crinoid rudstones, and isolated fragments of different species of tabulate corals (thamnoporids, *Roseoporella*). Most clasts are in diagenetic dissolution contacts with thin brownish, sideritic or goethitic seams. Such a breccia produced a mixed conodont fauna, consisting of Eifelian (*Po. costatus*, Fig. 18.5, *Icriodus retrodepressus*, Fig. 18.1) and lower/early middle Givetian taxa (*Po. timorensis*, Figs. 18.6-7, *Po. varcus*, Fig. 18.8, and *Po.* aff. *xylus*, Fig. 18.3), in association with the long-ranging *Belodella resima* (Fig. 18.2). One specimen is identified as the top-Givetian to lower Frasnian *Po. paradecorosus* (Fig. 18.4). Reefal blocks typically do not have conodonts. Rud- and boundstones contain up to 20 cm large components, such as abundant tabulate corals (alveolitids, favositids, thamnoporids), stromatoporids, receptaculitids, brachiopods, and rare trilobite remains. There is no evidence of middle Frasnian to Famennian clasts.

Fig. 19: Outcrop of monotonous green shales (?Pragian) exposed along the road and on the lower slope below (SE) of the Dhar-es-Smene reef; with C. HARTKOPF-Fröder (Krefeld) sampling for palynomorphs.

Fig. 20: View from the main road from Aïn Dakhla to the E, showing the slope occupied by Lochkovian/Pragian shales, followed high on the next hill (Hill E) by sandstones.

Fig. 21: Conodonts from the "Orthoceratid Limestone" clast embedded in lower parts of the shale unit, E of the fault that cuts off the Dhar-es-Smene reef (see Fig. 16). Left: *Ancyrodelloides transitans* (blade length = 1.2 mm); middle-right: *Wurmiella* sp. (blade length = 1.47 mm).

Fig. 22: Well-bedded, grey crinoidal limestones exposed at the southern shoulder of the plateau between Dhar-es-Smene and the Oued Cherrat, interpreted by CHALOUAN & HOLLARD (1979) as an eastward re-occurrence of the Dhar-es-Smene Formation (d_3).

1

2

Fig. 23: Tongue of Aïn-al-Aliliga Formation within the Al Brijat Formation at the hill E of Dhar-es-Smene. **1.** Field photo of large, compact, very solid breccia mass exposed on the SE slope; **2.** Thin-section of breccia: polymict intraclast rudstone with unsorted, angular clasts, often in dissolution contact, and with only a small amount of brownish, iron-rich, fine matrix.

Our incipient analysis of the clast spectrum proves that an Eifelian-Givetian carbonate ramp, both with biostromes and adjacent open and deeper marine settings (polygnathid biofacies), once extended to the Aïn Dakhla region. It was obviously completely eroded by uplift after the middle/upper Givetian and then further reworked and re-sedimented in the upper Famennian (considering the sparse conodont data from Aïn-al-Aliga). The following thick shales and siltstones occupying the main eastern slope towards the Oued Cherrat probably represent the upper Brijat Formation, not the Aïn-ed-Dakhla Formation, as shown in the cross-section of CHALOUAN & HOLLARD (1979; Fig. 9).

4.3. Cakhrat-ach-Chleh region

The Cakhrat-ach-Chleh Member extends from its type locality northwards to an active quarry at Kaf al Baroud and from there, across the winding piste coming from Aïn Dakhla, to the central elevation of Mechra al Kraker (Fig. 1). We sampled and measured the section along the northern slope of the road, just opposite to Mechra al Kraker, at x = 350.7, y = 342.1 (Fig. 24). The bedding is steep, vertical or slightly overturned.

Since CHALOUAN & HOLLARD (1979) assigned the Cakhrat-ach-Chleh Formation to the Givetian, we were surprised to find unequivocal lower Emsian conodonts at the formation base (ABOUSSALAM et al. 2012, 2013). The record of *Lat. bilatericrescens bilatericrescens* (Fig. 25.1.), associated with *Bel. resima* (Fig. 25.2), resembles the *Lat. bilatericrescens* assemblage found at the base of the biostromal upper part of the Dhar-es-Smene Formation W of the Cherrat river. There is also no principle difference in the macrofauna of both reef units: we did not encounter any stringocephalids or Givetian-type rugose corals at Kaf al Baroun.

The lower Cakhrat-ach-Chleh Member (previously formation) consist of different carbonate platform microfacies types (Fig. 26) which re-occur in distinctive episodes. There was no bioherm but a wide, storm- and current-influenced shallow platform with dominant crinoid forests in deeper and marginal parts and with low-relief coral-stromatoporid patch reefs, that sheltered areas dominated by branching forms (thamnoporids, *Stachyodes*). Recurrent large storms destroyed almost completely the in-situ record of reef builders. Typical lagoonal facies, such as *Amphipora* or microbial limestones, are rare or missing. Our comprehensive section logging (at meter scale) established the following succession characterized by minor sea-level change and lateral shifts of patch reef construction (with some identifications my A. MAY, Unna; compare MAY 1993, 2005).

Base (0-3 m): middle-grey, variably coarse (pack- to rudstone), detrital crinoidal limestones; typical microfacies (Fig. 26.1): strongly recrystallized, flaser-bedded, crinoid-intraclast rudstone; storm-swept, open neritic, marginal, deeper platform setting with crinoid forests and an influx of open marine organisms (conodonts).

4-5 m: level with phaceloid rugose corals; subtidal patch reef.

5 m-A: fine-grained, recrystallized, micritic to microsparitic, bioturbated dacryoconarid packstone with fine and large pyrite aggregates (Fig. 26.2); short-termed deepening causing an intercalation of pelagic or at least deep neritic facies.

5 m-B: biostromal limestone with blocky stromatoporids (*Stromatoporella* sp.), laminar alveolitids (*Squameoalveolites?*), chaetetids, brachiopod debris, and solitary Rugosa; microfacies: stromatoporid-coral rudstone with fragmented crinoids and dark, brownish micrite matrix (Fig. 26.3); storm-influenced biostrome core.

Fig. 24: Well-bedded crinoidal limestone at the base of the Cakrat-ach-Chleh Member on the northern slope of Kaf al Baroun, which yielded typical lower Emsian conodonts.

13 m: light-grey to reddish, thick-bedded storm beds; microfacies: partly dolomitized grain-rudstone with large brachiopod fragments, intraclasts, crinoid and stromatoporid debris (Fig. 26.4); tempestitic biostrome platform.
14 m: light-grey, detrital crinoid limestone; deeper platform influenced by storms.
20 m: light grey or reddish-grey crinoid-reefal debris with thamnoporids; minor shallowing of platform.

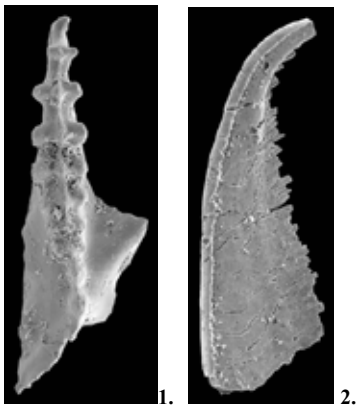

Fig. 25: Conodonts from the base of the Cachrat-ach-Chleh Member at Kaf al Baroun E of the Oued Cherrat. **1.** *Lat. bilatericrescens bilatericrescens*, **2.** *Bel. resima*.

22 m: light-grey reefal debris with crinoids, tabulate and solitary rugose corals; storm-ridden biostrome platform.
24 m: middle- to dark-grey stromatoporid and coral limestone; microfacies: *Stachyodes-Thamnopora* floatstone with some nodular stromatoporids; moderately protected reef patch on the platform.
30 m, increasingly coarse crinoid limestones; shallowing-upwards of deeper platform with crinoid forests.
50 m: laminar stromatoporids; biostrome core.
52 m: *Amphipora* floatstone with dense, micrite to microsparite matrix (Fig. 26.5); protected platform depression.
53-59 m: light-to middle grey crinoid limestone; deeper platform with storm-destructed crinoid forests.
60 m: middle-grey, detrital limestone with crinoids and alveolitids; microfacies: wacke-floatstone with fine shell debris, small, rounded tabulate coral clasts, very fine, reddish dolomite, and partly washed out micrite matrix (Fig. 26.6); storm-and current-influenced, moderately deep platform.
61-62 m: middle-grey, fine-grained crinoid limestone; deeper platform.
63-64 m: middle- to dark-grey Tabulata (*Scoliopora* sp.)-stromatoporid (*Stachyodes* sp.) limestones; microfacies: stromatoporid-coral floatstone with

subrounded reef builder clasts, shell filaments, and dark micrite to calcisiltite matrix (Fig. 26.7); moderately protected platform near a patch reef.
65-77 m: middle- to dark-grey crinoid limestones, occasionally with stromatoporids (69 m); longer-lasting episode of platform drowning with storm-ridden crinoid forests.
78 m: dolomitized *Stachyodes* baffle-rudstone; moderately protected platform near a patch reef.
80-84 m: middle grey, partly reddish-grey crinoid limestones; deeper platform.
84-85 m: reddish *Stachyodes* limestone; microfacies: *Stachyodes* rudstone with stylolithic clast contacts and fine, pyritic micrite matrix (Fig. 26.8); moderately protected reef patch.
86-88 m: reddish crinoid limestone; deeper platform.
89-91 m: middle- to dark-grey micritic limestone; platform drowning (?), but without influx of open water organisms.
92 m: detrital crinoid limestone; drowned/deeper platform.

At the eastern end, the limestones are sharply cut off by a fault; the biostrome extinction patterns cannot be studied. The following silty shales and laminated, micaceous siltstones belong to the Al Brijat Formation, possibly to higher parts since we did not observe any limestone olistolites.

Fig. 26: Heterogeneous microfacies of the Cachrat-ach-Chleh Emsian reef platform. **1.** Coarse, strongly recrystallized, flaser-bedded, crinoid-intraclast rudstone with oblique running, post-sedimentary calcite vein, at 3 m, x 2.8; **2.** Dark, fine-grained, recrystallized, micritic to microsparitic, bioturbated dacryoconarid packstone with fine and large pyrite aggregates, at ca. 5 m, x 2.4; **3.** Stromatoporid-coral rudstone with chaetetids, some fragmented crinoids and dark, brownish micrite matrix, at ca. 5 m, x 1.9; **4.** Coarse, partly dolomitized grain-rudstone with large brachiopod fragments, intraclasts, crinoid and stromatoporid debris, at 13 m, x 2.4; **5.** *Amphipora* floatstone with dense, micrite to microsparite matrix, at 52 m, x 2.7; **6.** Wacke-floatstone with fine shell debris, small, rounded coral clasts, very fine, reddish dolomite, and partly washed out micrite matrix, at 60 m, x 2.8; **7.** Stromatoporid-Tabulata floatstone with subrounded reef builder clasts, shell filaments, and black, micrite to calcisiltite matrix, at 64 m, x 1.7; **8.** *Stachyodes* rudstone with stylolithic clast contacts and fine, pyritic micrite matrix, at 85 m, x 2.

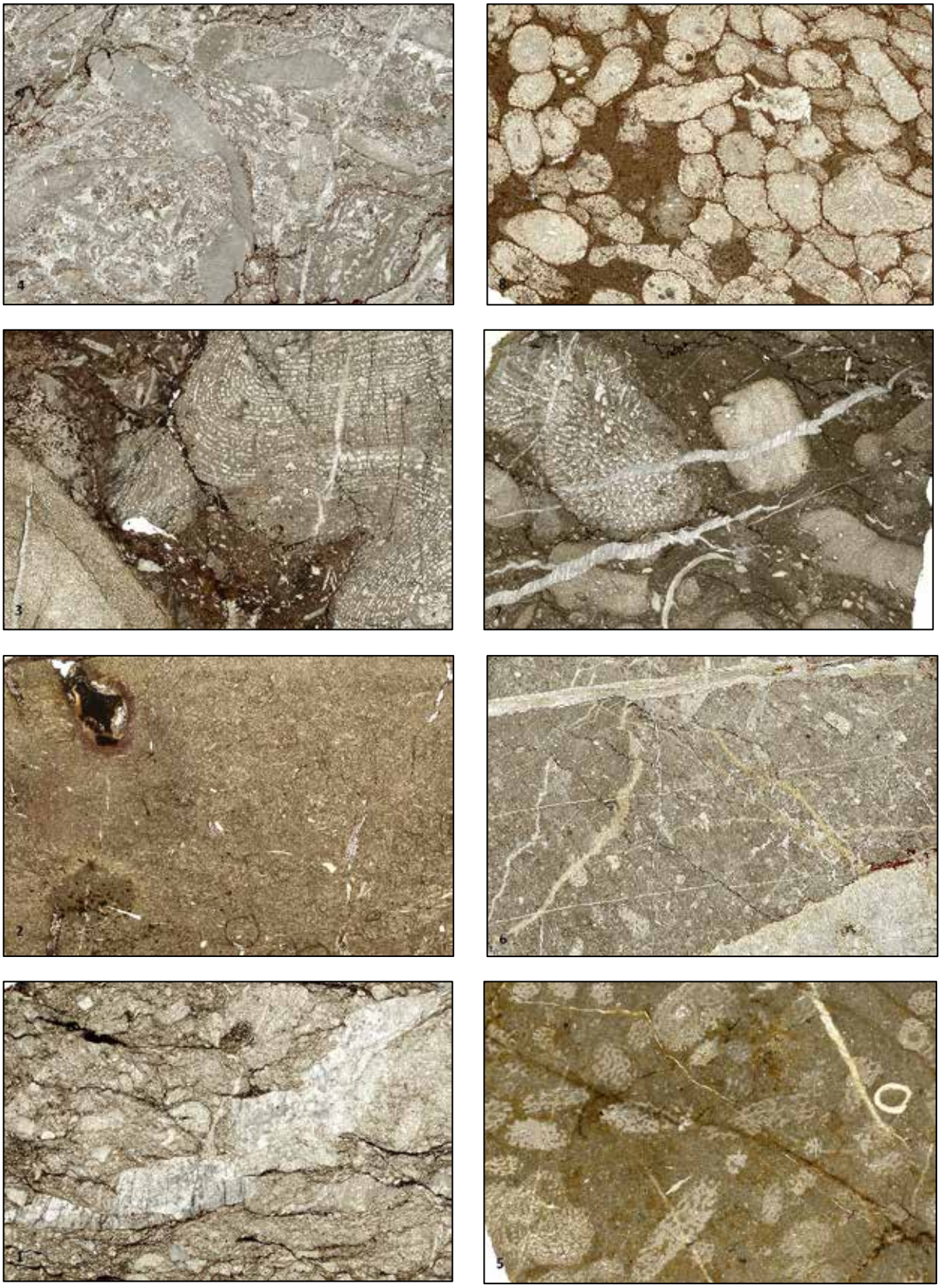

Fig. 26

Fig. 27: Thick-bedded alternation of basal Frasnian limestone breccias and biostromal limestone at the type locality of the Lower Member of the Aïn-al-Aliliga Formation.

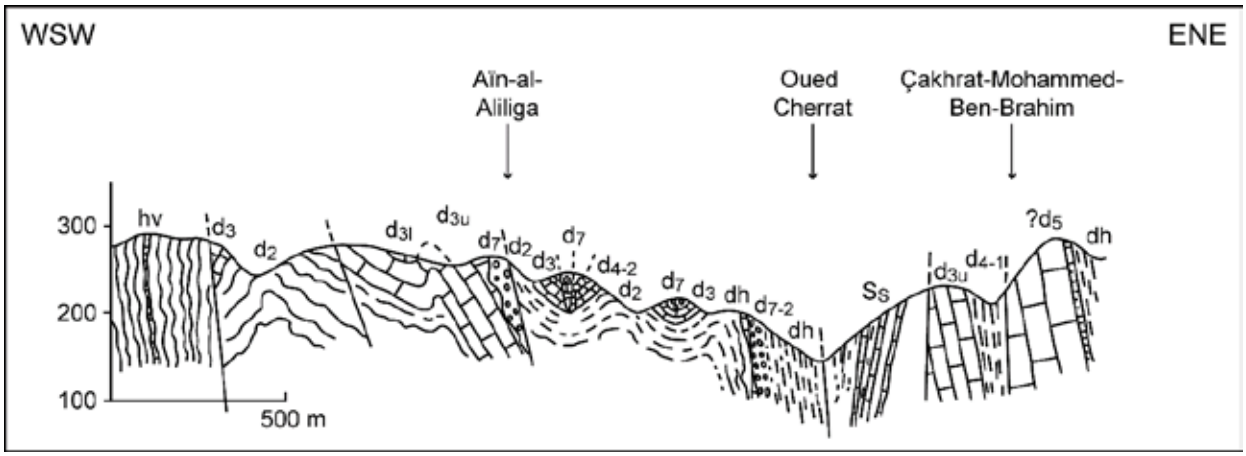

Fig. 28: Geological cross-section from the area W of Aïn-al-Aliliga to Cakhrat Mohammed-Ben-Brahim in the E; for detailed explanation see text (updated from CHALOUAN 1981, fig. 4); d_2 = Pragian, d_3 = lower Emsian, $d_{4\text{-}1}$ = upper Emsian, $d_{4\text{-}2}$ = Eifelian, d_5 = Givetian, d_7 = upper Famennian, dh = upper Famennian/Tournaisian, hv = Viséan).

4.4. Pragian to Famennian at Aïn-al-Aliliga to Cakhrat Mohammed-Ben-Brahim

The locality name Aïn-Al-Aliliga stands for a ca. W-E running secondary valley starting on topographic sheet Benslimane, 1 : 50 000, just E of the asphalt road coming from Beni Moussi in the N, or just N of Dayet ach Choum. Following the 'piste' eastwards, which has been much improved in 2015, there is the Aïn-Al-Aliliga spring at ca. x = 350.55, y = 337.05 (GPS N33°37'16.3'' W007°00'48.9''). From there, the track winds down to the Oued Cherrat, where it takes a sharp turn, reaching the bases of the two massive limestone units of

Cakhrat Mohammed-Ben-Brahim (the first at ca. x = 351.5, y = 337.75). Our detailed logging and re-sampling followed the cross-section of CHALOUAN (1981, fig. 4), resulting in stratigraphic revisions and improvements (Fig. 28). We did not study the Viséan and Pragian strata W of Aïn-Al-Aliliga (Fig. 28).

4.4.1. Beni Moussi Member

At the western end of the widely visible limestone outcrop (GPS N33°37'17.0'' W007°01'09.2''), there is a ca. 20 m thick succession of medium- to dark-grey, well-bedded, solid, neritic limestones with crinoid debris, poorly reserved phacopids, brachiopods, receptaculites (Fig. 28), and common chert nodules, the Beni Moussi Member of the Dhar-es-Smene Formation (d_{3u}). A typical microfacies are peloidal, bioclastic mud-wackestones (Fig. 30). Conodont samples were barren. Therefore, the position of the Pragian/Emsian boundary is locally unknown, especially with respect to the currently open stage boundary definition (current Zinzilban GSSP definition versus the proposed new level at the entry of *Eolinguipolygnathus excavatus* M114; see discussion in CARLS et al. 2008, 2009).

4.4.2. Cackrat-ach-Chleh Member and Lower Member of the Aïn-Al-Aliga Formation

There is a gradual transition into the massive boulders of the thick, poorly studied lower Emsian reef (Cakhrat-ach-Chleh Member, Fig. 31). It occupies as an anticline the top of the northern hill, where it is increasingly exploited by a new quarry. In the woody SE slope, it is sometimes difficult to locate precisely the boundary between the Emsian reef complex and the overlying Aïn-Al-Aliga Formation. Controlled by folding and faulting, the latter cuts down variably into the Beni Moussi or Cakhrat-ach-Chleh Members.

The Lower Member of the Aïn-Al-Aliga Formation begins with distinctive, thick, polymict limestone conglomerates and breccias (Figs. 32-33) that show neither sorting nor grading. Uplift and erosion of a local carbonate platform occurred after lithification; many clasts show cut off corals. There must have been a long period of erosion that reached down into different units, as represented by black (lagoonal) mudstones, middle-grey crinoid limestones, and middle-grey coral-stromatoporid float-rudstones (Fig. 33). At least partially, recurrent reworking in a nearshore high-energy setting led to clast rounding prior to re-deposition. The matrix is a brownish dolomite-siderite mud. It suggests that the unit originated in a nearshore setting with incipient evaporation and the accumulation of fine, iron-rich terrestrial mud. During the seismically triggered downslope transport, the mass flow picked up isolated tabulate corals and branching stromatoporids (*Stachyodes*). Their fragments lie free in the matrix, next to fragmented reefal limestone clasts (Fig. 33). These corals and sponges lived shortly before or at the time of the seismic event. Matrix lamination may be the result of current-induced winnowing after the main re-deposition event.

Fig. 29: Field photo of a limestone slab with a large, eroded *Receptaculites* (total diameter = 11 cm; problematical thallus of green algae), upper part of Beni Moussi Member at Aïn-Al-Aliliga.

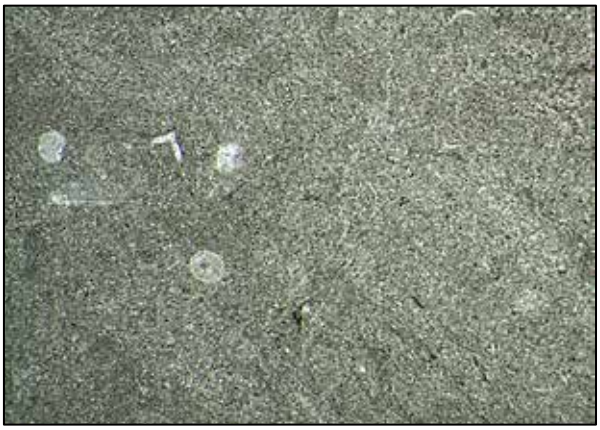

Fig. 30: Rather monotonous peloidal mudstone with some crinoid debris from the upper Beni Moussi Member at Aïn-Al-Aliliga.

Fig. 31: Massive reef boulders of the Emsian Cakhrat-ach-Chleh Member at Aïn-Al-Aliliga (slope NW of spring), view from the W-E track.

Fig. 32: Coarse, unsorted breccia (mass flow deposit) from near the base of the Lower Member of the Aïn-Al-Aliliga Formation (basal Frasnian). Clasts are angular to subrounded, light-grey weathering limestones embedded mostly without contact in a brownish, non-calcareous matrix (picture width = 13 cm).

Fig. 33: Polished section of the same slab as in Fig. 31, showing the heterogeneity of limestone clasts: dark-grey mudstones (lower part, partly rounded), medium-grey crinoid limestones (wacke-packstones, middle to upper part), coral-rich float-rudstones, and isolated tabulate corals (alveolitids, thamnoporids). The fine dolomite-siderite matrix is laminated in the upper part.

Fig. 34: Slab of bluish *Stachyodes* floatstone from the Lower Member, typical for a shallow lagoonal setting.

Fig. 35: Floatstone with isolated, silicified rugose and tabulate corals from the middle, non-brecciated biostromal limestone within the Lower Member of the Aïn-Al-Aliliga Formation.

Fig. 36: Medium-sized *Heliolites* colony from the Lower Member of the Aïn-Al-Aliliga Formation, typical for Givetian reefs (picture width ca. 10 cm).

Fig. 37: Silicified *Phillipsastrea* colony from the Lower Member of the Aïn-Al-Aliliga Formation, index rugose coral for the Givetian/Frasnian (picture widths 5 cm).

Fig. 38: Large, silicified alveolitid coral from the Lower Member, Aïn-Al-Aliliga Formation (picture width 15 cm).

The more than 50 m thick Lower Member consists of two boulder units with breccias and a bedded middle interval with silicified coral-brachiopod limestones (Fig. 35) and detrital, dark-grey, autochthonous limestones that resemble the inter-reefal Flinz limestones of the Rhenish Massif. We observed the following facies types:

a. well-sorted crinoidal grainstones with syntaxial cements (EICHHOLT & BECKER 2916, fig. 7a, MF B1a) – crinoid meadows
b. bioclastic crinoid grainstone with brachiopods and solitary Rugosa, often silicified – biostrome margin
c. brachiopod-solitary Rugosa floatstone, often silicified (EICHHOLT & BECKER 2016, fig. 7e, MF C1) – biostrome margin
d. coral floatstone with thamnoporids, alveolitids, laminar stromatoporids, and solitary Rugosa, often silicified (Fig. 34, MF C3) - biostrome
e. *Stachyodes-Thamnopora* floatstone (MF A7, Fig. 34) – protected inner biostrome or bioherm lagoon
f. gastropod floatstone – biostrome depression or lagoon
g. coral float-rudstone with tabulate (*Favosites, Thamnopora, Alveolites*) and rugose (*Phillipsastrea*) corals, sometimes silicified (Fig. 37) – storm affected biostrome to bioherm
h. coral-rich reef breccias (extraclast rudstones, Figs. 41.1-4) with Tabulata (MF B2b, *Heliolites*, Fig. 36, *Alveolites*, Fig. 38*, Thamnopora*, Fig. 41.3), bulbous or laminar stromatoporids (up to 20 cm large), and solitary Rugosa (Fig. 41.1) – seismically shocked biostrome (in-situ brecciass) and proximal mass flows on the upper slope of tilted block
i. crinoidal grainstones with reefal slump blocks – seismically shocked biostrome margin, receiving clasts from uplifted, tilted block
j. organic-rich mudstones - lagoon

The facies assemblage shows that there was a biostromal carbonate platform bordered by crinoid forests and brachiopod-rugose coral banks (see facies model of EICHHOLT & BECKER 2016, fig. 6). The bulbous stromatoporids and common rudstones combined with some back-reef facies types indicate that a small bioherm with steep slopes and a sheltered lagoon developed eventually. Since most samples yielded at least some conodonts, an influx of open-water organisms persisted. In the lower part, icriodid-rich shallow-water conodont faunas are typical. The platform was strongly affected by syn- and post-sedimentary seismic shocks (block tectonics), leading to internal brecciation and the shedding of mass and debris flows from uplifted and tilted near-by areas. The polymict nature of the breccias (Figs. 41.1-4) shows that they do not represent “normal” marginal slope

debris flows of a bioherm. At the top of the Lower Member, a reworked polygnathid-dominated assemblage shows that outer ramp limestones started to be uplifted and eroded.

The age of the destructed carbonate platform can be assessed by the dating of individual blocks and of mixed faunas from breccia units (Tab. 1). The oldest breccias should provide the youngest age, the age of carbonates which were eroded first. This approximates the onset of Eovariscan reworking. None of our samples from the Lower Member includes any Famennian conodonts. The stratigraphically youngest taxon, indicating the basalmost Frasnian (MN 1 Zone), is an *Ad. rotundiloba pristina* from the "lower conglomerate" (Fig. 39). It is associated with *Po. webbi* and *Po. paradecorosus*, two species that straddle the Givetian-Frasnian boundary (e.g., ABOUSSALAM & BECKER 2007). Typical lower/middle Givetian *Linguipolygnathus* (*L. linguiformis* and *L. mucronatus*) show that some of the clasts derived from much older parts of the carbonate platform that pre-dated the global Taghanic Crisis (ABOUSSALAM 2003). This is supported by reworked *L. linguiformis* in younger conglomerates (Fig. 40.7). A second sample from the basal part of the Lower Member ("basal breccia") may be upper Givetian in age but all taxa found range into the basal Frasnian. Sample AAA is dominated by *Icriodus expansus* (56 %), followed by two morphotypes of *I. subterminus* (47.5 %, Fig. 40.1-2); *I. tafilaltensis* is present, too. The assemblage falls in the *I. subterminus* Zone sensu NARKIEWICZ & BULTYNCK (2010) but it is not possible to specify a subzone.

A sample from the main part of the conglomerate/breccias is rather species-rich, heterogeneous and heterochronous in nature. There are single cone taxa typical for very shallow reefal settings (*Belodella resima, Neopanderodus perlineatus*), a small amount of lower/middle Givetian forms (*L. linguiformis*, Fig. 40.7), middle/upper Givetian icriodids (*I. brevis*, 40.3, *I. difficilis*, Fig. 40.4, *I. expansus*,

Fig. 39: *Ancyrodella rotundiloba pristina* from the "lower conglomerate" near the base of the Lower Member of the Aïn-Al-Aliliga Formation (max. width = 0.43 mm)

Fig. 40.5, *I. tafilaltensis*, Fig. 40.6), long-ranging lower-upper Givetian polygnathids (*Po. xylus*, Fig. 40.11, *Po. varcus*, Fig. 40.10), and upper Givetian index polygnathids, such as *Po. ordinatus* (Fig. 40.12, *Po. paradecorosus, Po.* cf. *paradecorosus* (Fig. 40.9: approaching the platform size and ornament of *Avignathus decorosus*), and *Po. dengleri dengleri.* One specimen (Fig. 40.8) represents a still un-named new genus and species, which ABOUSSALAM (2003) illustrated as *?Skeletognathus* n. sp. from the top-Givetian *Skel. norrisi* Zone of the Montagne Noire. According to NARKIEWICZ & BULTYNCK (2010), the presence of *I. symmetricus* indicates that basal Frasnian clasts are present. Associated are agglutinating foraminifers (*Hyperammina, Thurammina, Tolypammina*), indicative for clasts from condensed sedimentation, intertidal ooids with polished surface, and pyritized juvenile bivalves, evidence for hypoxia – each representing completely different biofacies.

	Ain-Al-Aliliga Formation, Lower Member						Upper Mbr.		Al Brijat Fm.	
Conodont zones	**?MN 1**	**MN 1**	***subt.***	**MN 1**	**MN 1**	**Frasn.**	**Frasn.**	**(Fam.)**	***steinach.***	**L.Giv.**
Sample no.	**base breccia**	**lower cgl.**	**AAA**	**main cgl.**	**top reef**	**top dom.**	**Klotz**	**VFP**	**griotte**	**block**
Belodella resima	2			11	22	**6**		3		
Prionodina sp.	1									
Po. xylus	7	1		4			3	3		
Po. varcus	1			6	34					
Po. ovatinodosus	1									
Po. paradecorosus	**2**	3	1	17	82			623		
I. tafilaltensis	3		2	4	1?			94		
I. expansus	1		114	9				35		
Ling. linguiformis M δ1b		1		4			2			2
Ling. mucronatus		1								
Ad. rotundiloba pristina		**1**								
Po. webbi		1					?2	25		
I. subterminus Morph alpha			67					9		
I. subterminus Morph beta			30					23		
Neopand. perlineatus				7						
I. symmetricus				**3**			**1**	3		
I. difficilis				3						
I. brevis				2			2			
Po. cf. *paradecorosus*				3						
Po. dengleri dengleri				1						
Po. ordinatus				1				1		
N. Gen. n. sp.				**1**						
Po. aff. *xylus*					17					
I. n. sp. aff. *symmetricus*					9					
Po. aff. *paradecorosus*					1					
Po. timorensis							3			
Po. alatus								42		
Po. aff. *dubius*								16		
Po. pollocki								2		
Polygnathus sp. (pathol.)								1		
T. variabilis								6		
T. aff. *caelatus*								3		
Phoebodus gothicus								**x**		
T. aff. *weddigei*								2		
Caud. steinachensis									**3**	
Panderodus sp.									9	

Tab. 1: Range of conodonts and sharks in samples from the type Aïn-Al-Aliliga and olistolites within the Al Brijat Formation.

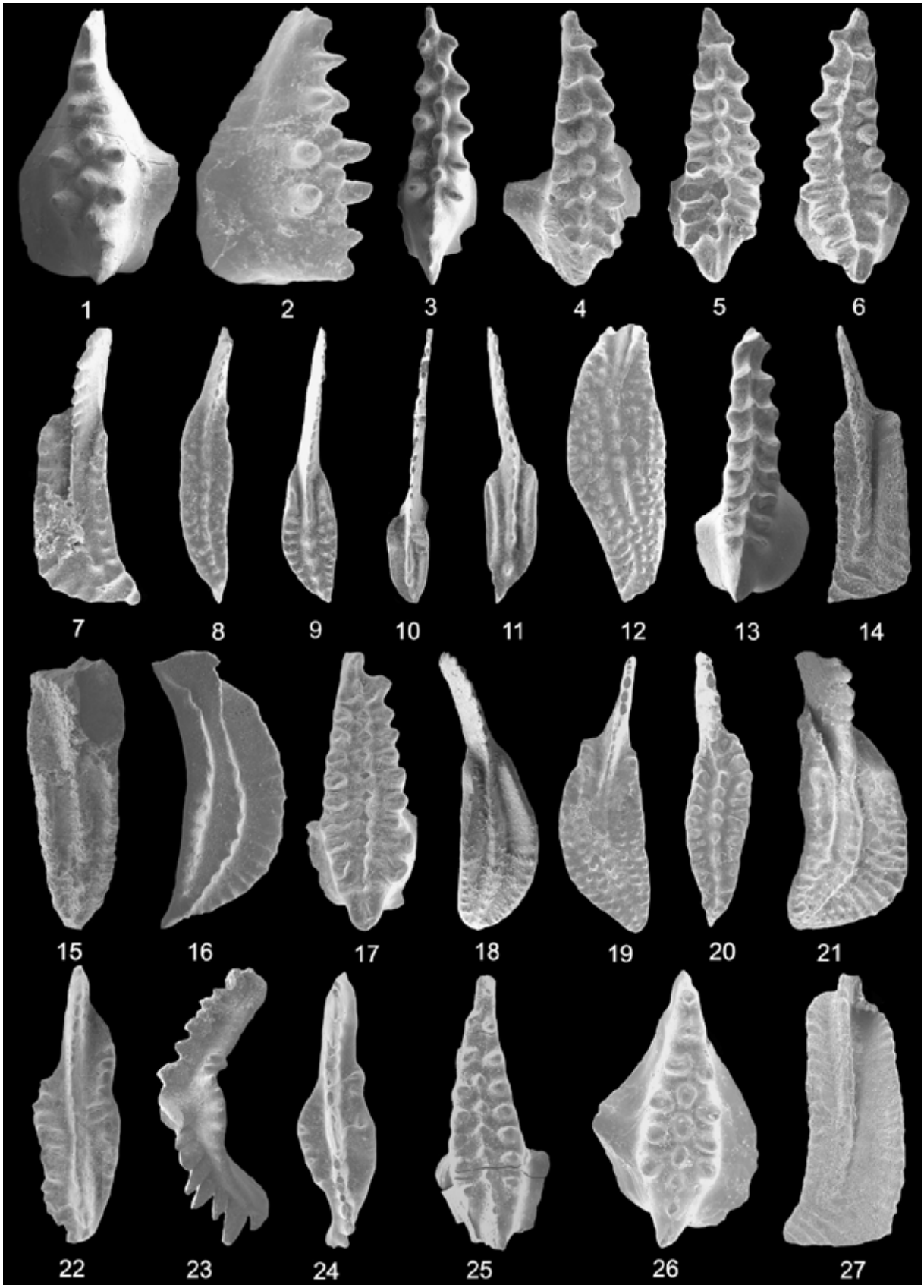

Fig. 40: Conodonts from Aïn-Al-Aliga, samples AAA (1-2), main conglomerate (3-12), "Klotz" (13-16), VFP (17-26), and Al Brijat (sample "block", 27). **1-2.** *I. subterminus*, x 90; **3.** *I. brevis*, x 85; **4.** *I. difficilis*, x 65; **5.** *I. expansus*, x 70; **6.** *I. tafilensis*, x 60; **7.** *L. linguiformis*, x 70; **8.** N. Gen. n. sp., x 60; **9.** *Po. paradecorosus*, with long free blade, transitional towards the Pa element of *Avignathus decorosus*, x 60; **10.** *Po. varcus*, x 55; **11.** *Po. xylus*, x 80; **12.** *Po. ordinatus*, x 45; **13.** *I. symmetricus*, x 60; **14.** *L. linguiformis*, x 70; **15.** *Po. timorensis*, x 85; **16.** *Po. webbi*, x 50; **17.**

I. tafilaltensis, x 55; **18.** *Po. alatus*, x 35; **19.** *Po. ordinatus*, x 40; **20.** *Po. pollocki*, distorted, x 45; **21.** *Po. webbi*, x 40; **22.** *T.* aff. *caelatus*, with partially free blade, x 35; **23.** *T.* aff. *weddigei*, x 40; **24.** *T. variabilis*, x 40; **25.** *I. expansus*, x 60; **26.** *I. subterminus*, x 85; **27.** *L. linguiformis*, x 50.

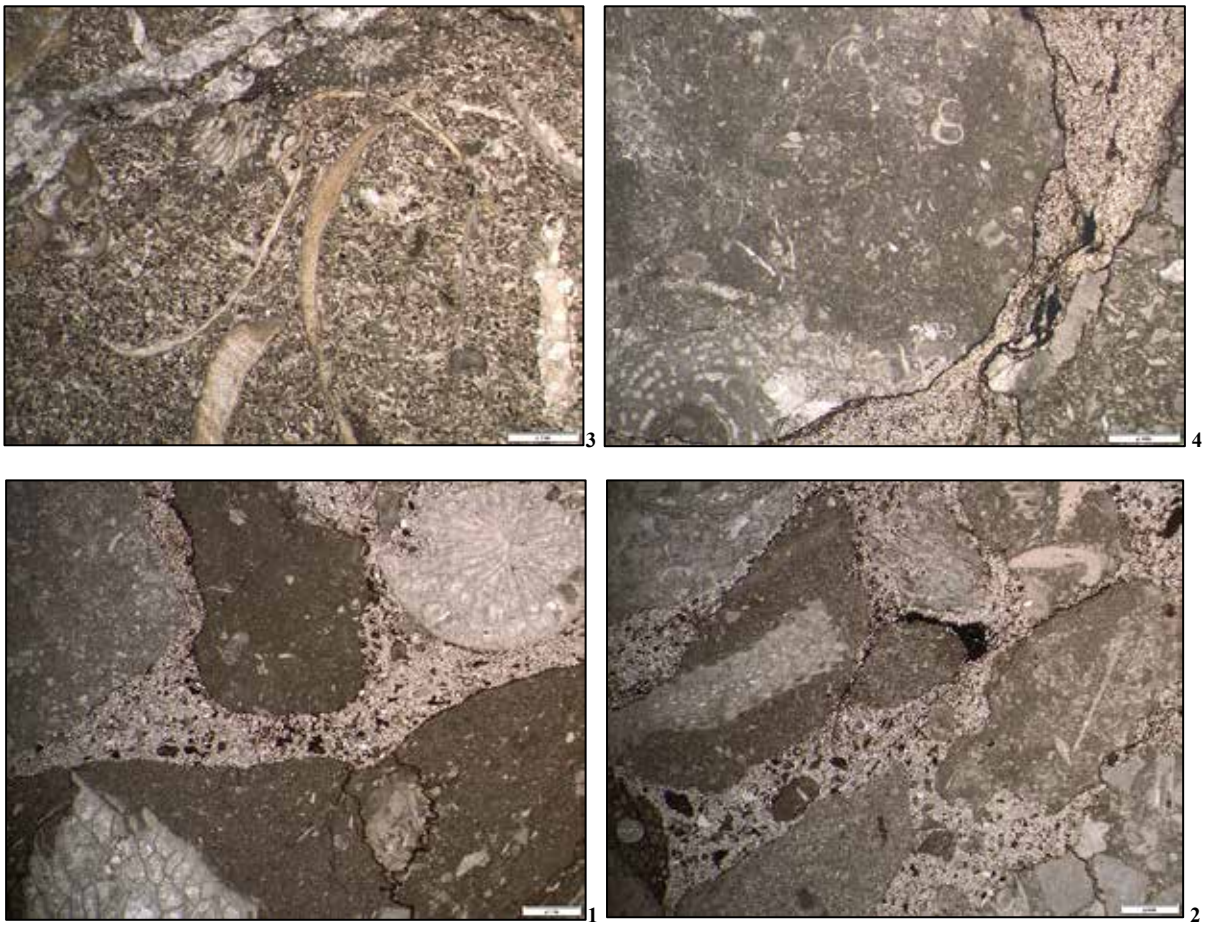

Fig. 41: Microfacies of breccia samples from the Lower Member of the Aïn-Al-Aliliga Formation; scale bar = 2 mm. **1.** Extraclastic rudstone with subrounded clasts of dark-grey bioclastic wackestone with gastropod (upper center), middle-grey bioclastic wackestone with crinoid debris (upper left), bioclastic coral floatstone with favositids (lower part), and an isolated solitary rugose coral, all sitting in a dense, unsorted, bioclastic packstone matrix, "Lower conglomerate" (MN 1 Zone); **2.** Extraclastic rudstone showing additional, mostly angular clast types, such as coarse crinoidal packstone (lower right), dark-grey intraclast pack-rudstone with a parathuramminid foraminifer (lower left, *Cribrosphaeroides (Parphia) robusta*), middle-grey bioclastic floatstone with a thamnoporid branch (middle left), and an isolated fragment of tabulate coral (upper center), "Lower conglomerate" (MN 1 Zone); **3.** Sparitic brachiopod-coral grain-rudstone with variably recrystallized, thin to thick brachiopod shells, thamnoporids, and other tabulate corals in a fine intraclast matrix, "main breccia" (basal Frasnian); **4.** Coarse extraclastic rudstone with clasts of middle-grey bioclastic wackestones rich in fine crinoid debris, small gastropods, and tabulate coral (perhaps *Coenites*, lower left), "basal breccia" (top-Givetian).

From the top of the middle, non-brecciated interval of the Lower Member comes a sample ("top reef") with some scolecodonts (typical for neritic limestones) and spherical "conodont pearls" (see LINDSKOG et al. 2017 for a recent discussion). Among the conodonts, *Po. paradecorosus* and *Po. varcus* are dominant. Associated are *I.* n. sp. aff. *symmetricus* sensu SCHUMACHER (1971), *Po.* aff. *xylus* (with *Po. varcus*-type anterior basal pit), and *Po.* aff. *paradecorosus* (even more transitional towards *Av. decorosus*; with a long free blade and wider, flatter small platform than in typical *paradecorosus*). This fauna indicates a top-Givetian age for the clasts.

The combined evidence dates the first main episode of Eovarican uplift and reworking as top-Givetian to basal Frasnian. It is remarkable that there are no pre-Givetian clasts/conodonts. Erosion had not yet penetrated the Givetian carbonate platform. A younger age should have resulted in the presence of typical Frasnian or Famennian conodont assemblages. At the eastern end of the main Aïn-Al-Aliliga hill, the Lower Member is overlain by yellowish, thin-bedded dolomites without macrofauna that dip gently to the E. They yielded only belodellids (Tab. 1). This suggests a post-reefal calm, very condensed, and very shallow to slightly evaporitic sedimentation that was no younger than the Frasnian.

4.4.3. Upper Member of Aïn-al-Aliliga Formation

The typical Aïn-al-Aliliga Formation is exposed around the spring and characterized by up to 3 m large, rounded or angular clasts, abundant dark-grey weathering quartzites, light-grey volcanites, and mixed limestones (Fig. 42). The clast size decreases upwards, whilst dolomitization increases. One block ("Klotz") yielded a mixed conodont fauna with lower/middle Givetian (*L. linguiformis*, Fig. 40.14, *Po. timorensis*, Fig. 40.15, *Po. xylus, I. brevis*) and basal Frasnian species (*I. symmetricus*, Fig. 40.13, and *Po. webbi*, Fig. 40.16). A very rich and diverse conodont assemblage came from Sample VFP (Tab.1), collected just N of the track. It is by far dominated by *Po. paradecorosus* (70 %), followed by common (10.5 %) *I. tafilaltensis* (Fig. 40.17). There are various polygnathids of the Givetian-Frasnian transition: *Po. ordinatus* (Fig. 40.19), *Po. alatus* (Fig. 40.18), *Po. webbi* (Fig. 40.21), *Po.* aff. *dubius*, and *Po. pollocki* (Fig. 40.20). Lower/middle Givetian index species or even older taxa are absent. A minor content of tortodids (*T.* aff. *caelatus*, Fig. 40.22, *T.* aff. *weddigei*, Fig. 40.23, *T. variabilis*, Fig. 40.24) resembles the bloom of the genus in the Taghanic Crisis Interval at the middle/upper Givetian boundary (ABOUSSALAM 2003; ABOUSSALAM & BECKER, 2011). Three *I. symmetricus* indicate the basal Frasnian (NARKIEWICZ & BULTYNCK 2010).

The mixture of (only) upper Givetian/basal Frasnian and Lower Palaeozoic clasts is intriguing. It could be explained by the original transgression of an upper Givetian carbonate platform directly on an uplifted Lower Paleozoic block - prior to the second Eovariscan uplift. This aspect requires confirmation by further sampling: the search for clasts of other time intervals. We could not confirm the upper Famennian conodonts reported in CHALOUAN (1981). However, we found in Sample VFP five teeth of *Phoebodus gothicus gothicus* and four teeth of *Ph. gothicus transitans* (SCHWERMANN 2014). The first subspecies ranges in the Anti-Atlas from high in the lower Famennian (*Pa. glabra pectinata* Zone) to the upper Famennian (*B. costatus* Subzone). In Poland, it ranges even higher, until the global Hangenberg Event (e.g., GINTER & IVANOV 2000). The second subspecies was so far only known from the supposed middle/upper Famennian of Algeria (GINTER et al. 2002). The combined data show that the second regional Eovariscan reworking event occurred high in the upper Famennian.

4.4.4. Aïn-ad-Dekhla Formation

Down towards the Oued Cherrat, the western slope of the winding track exposes, after an obvious fault, Pragian fossiliferous silty shales (Fig. 44). There are very common trilobites, especially asteropygids (two species of *Metacanthina*, Fig. 43.2), homalonotids (*Wenndorfia,* Fig. 43.1), and *Odontochile*, as well as spiriferids, strophomenids (*Dalejodiscus* aff. *subcomitans*, det. U. JANSEN, Frankfurt a. M., Fig. 43.3), large ostracods (zygobeyrichiid, det. H. GROOS-UFFENORDE, Göttingen, Fig. 43.4), and solitary

rugose corals (HELLING & BECKER 2015; HELLING in BECKER 2015). As typical for the formation, fossils are stained by limonite. The neritic siliciclastic facies is in contrast with the subsequent shallow-water limestones. There must have been a change in the weathering regime and in the discharge of fine detritus, perhaps induced by a change from humid to arid conditions.

Fig. 42: Upper Member of the Aïn-Al-Aliliga Formation in outcrop (type locality), with unsorted, subrounded, polymict clasts.

4.4.5. "Central Section"

Around the next corner to the E, another fault delimits the Pragian shales and the dip changes, with beds becoming younger from E to W. This was not evident in the cross-section of CHALOUAN (1981), who suggested, instead, a syncline structure. Along the track lies our "central section", which ranges from the upper Pragian (Fig. 45) into the Eifelian (Figs. 48, 50). The basal, greenish-grey shale (Bed 1) belongs to the upper part of the Aïn-ad-Dekhla Formation. This is supported by some trilobites found in a shale package below (to the E). Bed 2 is a peculiar, 70 cm thick, dark-grey, massive but lenticular brachiopod floatstone (Figs. 45, 46). Apart from a few scolecodonts, it yielded a monotypic conodont fauna with *Caud*. cf. *curvicauda*. Typical representatives of the species and similar cf. specimens (without curved posterior end) range in the Anti-Atlas from the upper Pragian *Lat. steinachensis* Zone into the basal Emsian. Therefore, we place the brachiopod limestone close to the Pragian-Emsian transition. Since there is no change of bedding (Fig. 45), the contact to the overlying shale appears to be conformable (Beds 3 and 5, with limestone lenses = Bed 4). However, the overlying limestone (Bed 6, bioclastic wackestone, Fig. 50.1) yielded much younger conodonts from the lower-upper Emsian transition (Tab. 2). Where is the thick Dhar-es-Smene Formation? In the field we did not observe a fault (Fig. 45) but the lenticular nature of the brachiopod limestone is suspicious and indicates tectonic contacts. The fauna of Bed 6 includes common *Bel. resima,*

1

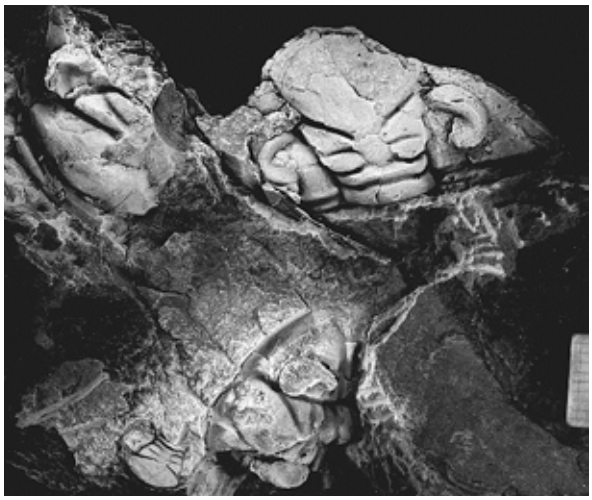

2

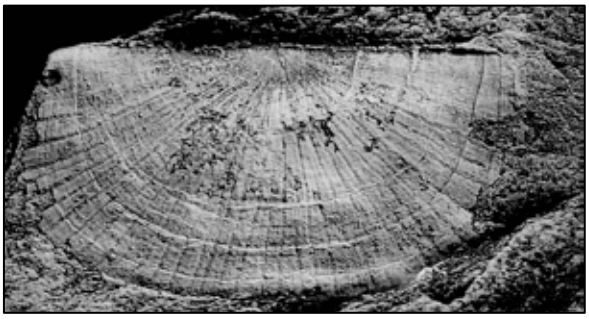

3

4

Fig. 43: Trilobites and brachiopods from the Aïn-ad-Dekhla Formation at Aïn-al-Aliliga. **1.** *Wenndorfia* sp., cephalon, length = 10.4 mm; **2.** Four cephala of *Metacanthina* n. sp.; **3.** Small strophomenid *Dalejodiscus* aff. *subcomitans* (Plectambonitoidea; det. U. JANSEN), width 12 mm; **4.** Large zygobeyrichiid (width = 6 mm).

Fig. 44: Trilobite-rich shales of the Aïn-ad-Dekhla Formation on the eastern slope at Aïn-al-Aliliga.

Fig. 45: Upper Pragian brachiopod limestone, followed conformably (?) by a shale unit (base of measuring stick), limestones with basal upper Emsian conodonts, and (above the stick) supposed Daleje Shale equivalents (Lower Member of Mohammed-Ben-Brahim Formation).

Fig. 46: Upper Pragian brachiopod limestone (floatstone), Bed 2 of "central section" at Aïn-al-Aliliga.

Neop. perlineatus, acrotetrids (minute, phosphatic, cone-shaped inarticulate brachiopods), and acanthodian dermal scales. Age diagnostic is *Latericriodus beckmanni sinuatus*, which enters in the Anti-Atlas in the *Lat. latus* Zone (upper part of lower Emsian), but it ranges into the upper Emsian (ABOUSSALAM et al. 2015). *Icriodus homorectus* first occurs in the basal upper Emsian *I. fusiformis* Zone.

The shales of Beds 3 and 5 and the 1.3 m thick greenish shale of Bed 5 are tentatively correlated with the Daleje Shales at the base of the upper Emsian. At the top is an up to 2 m large slump block (Bed 10) and evidence of faulting. It is followed by ca. 6.5 m (Beds 11-27a) of thin-bedded, bioturbated, macrofauna-poor nodular limestone and flaserlimestone. This unit, which has no other described exposure in the Oued Cherrat, is assigned to a new, local Upper Member of the Mohammed-Ben-Brahim Formation (Figs. 47, 49). Bed 13b is a trilobite floatstone (Fig. 50.2) with anarcestid cross-sections (Fig. 48). It also contains *Bel. resima* and *Caudicriodus culicellus culicellus* (Tab. 2). The latter is an alternative index species for the basal upper Emsian *I. fusiformis* Zone (GOUWY & BULTYNCK 2003; ABOUSSALAM et al. 2015).

Beds 27b–57b represent fine crystalline, macrofauna-poor calcisiltites that alternate with dark-grey shales. They are assigned to the Aïn Kheneg-en-Nmer Formation. Typical are dark-grey, detrital, weakly bioturbated mudstones with trilobite debris (Fig. 50.3), small shell filaments, or parathuramminids (Fig. 49.4). The latter are normally typical for Givetian lagoons (VACHARD et al. 1994; EICHHOLT & BECKER 2016) but may range into hypoxic open marine settings (see BECKER et al. 2016b for a Famennian example), As an exception, we collected a large *Favosites* colony in Bed 33. This tabulate coral genus is also known to range from reefal into deeper-water, muddy settings (e.g., POTTHAST & OEKENTORP 1987).

In the lower part, Bed 31 yielded *L. bultyncki*, an alternative index species for the upper Emsian *L. serotinus* Zone. It is more common in Morocco than the zonal name-giving species (ABOUSSALAM et al. 2015). In the middle and upper part (top Bed 31, Beds 45/46, Bed 55b) there is evidence for slumping and synsedimenary seismic instability but this is overprinted by the post-sedimentary tectonics. Bed 41 is rich in trilobite debris. The *L. serotinus* Zone ranges at least until Bed 50-3. Due to the still too crude sampling, the Emsian-Eifelian boundary cannot be fixed. There is no sedimentary expression of the global Choteč Event in the basal Eifelian. Bed 57b yielded a typical lower Eifelian conodont assemblage (*Po. costatus* Zone) with dominant single cones (*Bel. resima*, Fig. 51.1, *Neop. perlineatus*, Fig. 51.2), rare *Po. costatus* (Fig. 51.3) and *Po. zieglerianus* (Fig. 51.4). The conodont biofacies indicates a neritic setting but associated planktonic ostracods (entomozoids, Fig. 52) are more typical for a pelagic environment. A small shale/marl cliff (Bed 59) follows.

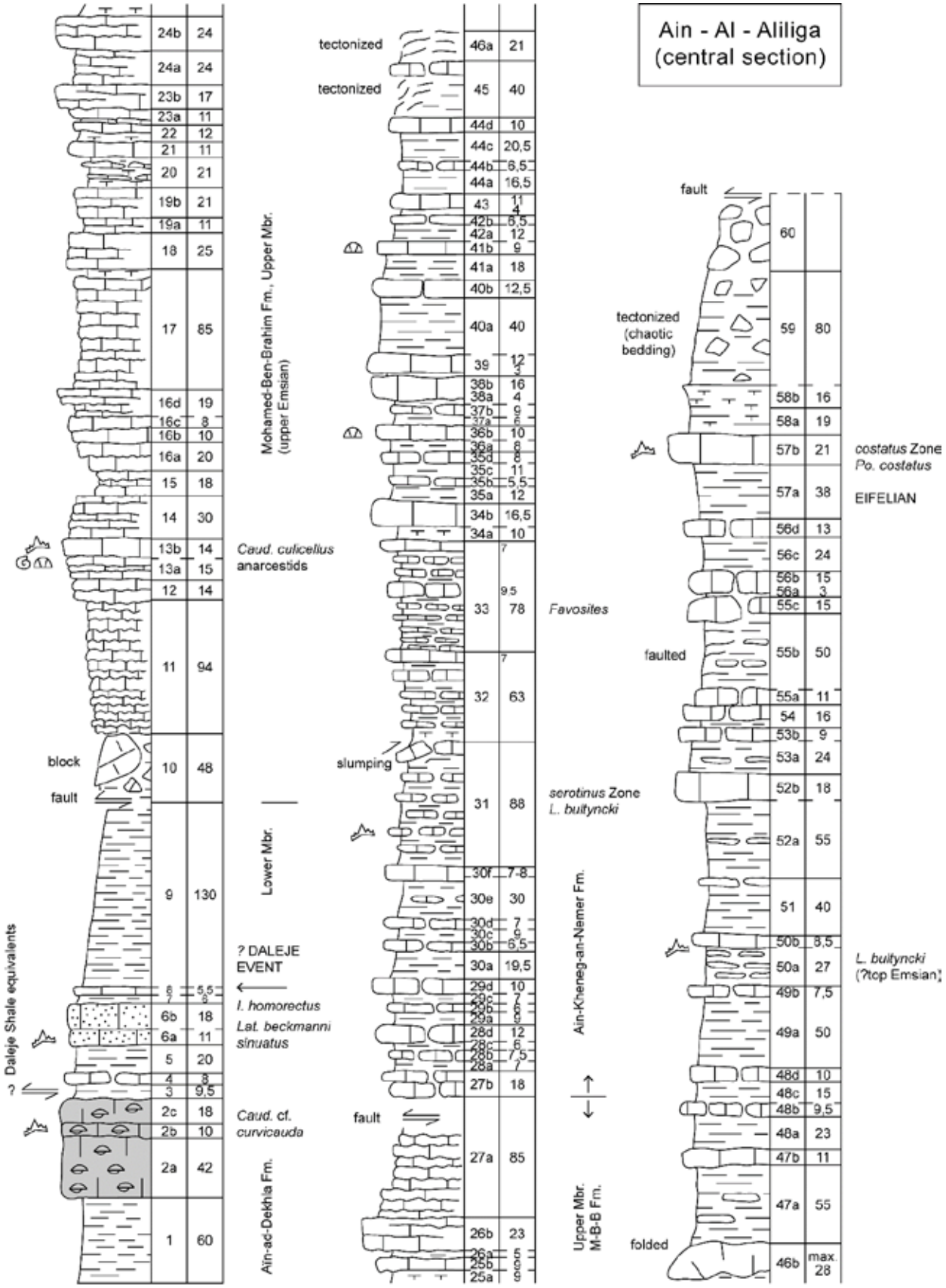

Fig. 47: Section log for the Emsian/Eifelian "central section" at Aïn-al-Aliliga showing the lithostratigraphy, slumping intervals, position and age of conodont samples, and the sparse macrofauna record.

Aïn-al-Aliliga, central section						
Conodonts zones	***steinachensis***	***fusiformis***		***serotinus***		***costatus***
Sample no.	**brachiopod lst.**	**base "Eif. lst."**	**Em 13**	**Em 31-2**	**Em 50-3**	**top D3**
bed no.	**2a**	**6a**	**13b**	**31-2**	**50-3**	**57-b**
Caud. cf. *curvicauda*	**32**					
Lat. beckmanni sinuatus		**5**				
I. homorectus		**5**				
Bel. resima		27	7	*	1	17
Neopand. perlineatus		10	*	1	*	9
Caud. culicellus culicellus			**15**			
Ling. bultyncki				**1**	1	
Po. costatus						**1**
Po. zieglerianus						1
total conodonts	**32**	**47**	**22**	**2**	**2**	**28**

Tab. 2: Conodonts from the "central section" at Aïn-al-Aliliga, illustrating the mysterious gap between top-Pragian and top lower Emsian limestones.

Fig. 48: Cross-sections of phacopids and an anarcestid in the Upper Member of the Mohammed-Ben-Brahim Formation at Aïn-al-Alilig (Bed 13b, picture width 7 cm).

The western end of the "central section" is characterized by irregular bedding and slumping (Fig. 53). Limestone beds disintegrated to bands of limestone blocks. This interval ranges to the fault zone that separates the Aïn-ad-Dekhla Formation (d_2) in the W.

4.4.6. Al Brijat Formation (dh)

CHALOUAN (1981) showed a second small syncline with limestones of the Dhar-es-Smene Formation (d_3) in his cross-section (Fig. 28). Limestones do not crop out along the track that winds down towards the Oued Cherrat. A fault zone separates greenish shales of the Aïn-ad-Dekhla Formation (d_2) from unfossiliferous, grey silty shales of the Al Brijat Formation (dh). On the gentle slope above the main curve to the E, close to the Cherrat river, the shales are deeply weathered and include numerous isolated olistolites. Dominant are reef limestone blocks with solitary Rugosa, *Thamnopora* and stromatoporids, crinoid limestones, and cannibalized (secondarily reworked) breccia clasts. One of the conglomerate block yielded two specimens of *L. linguiformis* (Fig. 40.27).

Fig. 49: New Upper Member of the Mohammed-Ben-Brahim Formation at Aïn-al-Aliliga, consisting of micritic, pelagic flaserlimestone.

This proves that parts of a lower/middle Givetian carbonate ramp were excavated and double reworked. In addition, there are laminated limestone concretions without conodonts. A single clast of light-grey griotte limestone (bioturbated bioclastic wackestone, Fig. 54) contained, surprisingly, three specimens of the upper Pragian index icriodid *Lat. steinachensis*. Associated are more common *Panderodus* and acrotetrid brachiopods. This deeper neritic, calcareous litho- and biofacies is in strong contrast to the ca. contemporaneous, siliciclastic Aïn-ad-Dekhla Formation to the W. Most likely, the clasts derived from a deeper neritic upper Pragian carbonate ramp that once existed E of the clastic shelf area. It may have been equivalent to the transitional limestones reported from Aïn Dakhla (CHALOUAN 1981; see 3.4.) but the biofacies is clearly different. It is unlikely that the "griotte" block was transported over a large distance.

4.4.7. Cakhrat Mohammed-Ben-Brahim

The main track follows the NW side of the Oued Cherrat. According to CHALOUAN (1981) the shales in this part are Silurian in age, which implies a steep fault separating them from the shales and siltstones of the Al Brijat Formation. The following area named as Cakhrat Mohammed-Ben-Brahim is marked by two steep cliffs with reef limestone, the first of which is in fault contact with the shales at its western end (Fig. 55). The general succession and geological structure of the area has first been documented by GENDROT et al. (1969).

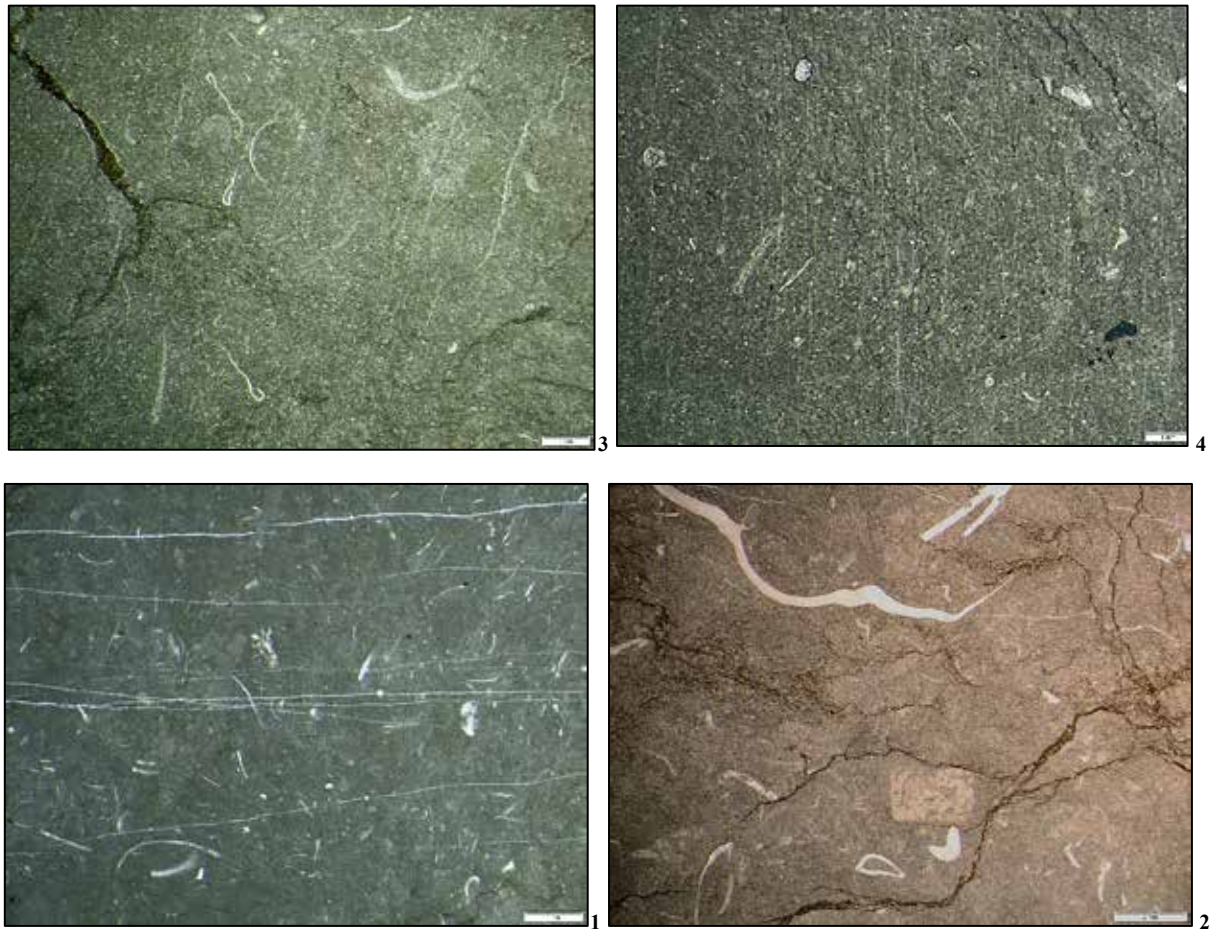

Fig. 50: Mikrofacies of carbonates from the "central section" at Aïn-al-Aliliga; scale bar = 2 mm. **1.** Bioclastic wackestone with dense, fine, bioturbated micrite matrix, shell filaments and rare trilobite fragment,s Bed 6a, *I. fusiformis* Zone, basal upper Emsian; **2.** Bioturbated, nodular trilobite floatstone with partly microsparitic matrix and many dissolution seams, Bed 13b, *I. fusiformis* Zone, basal upper Emsian, Upper Member of Mohammed-Ben-Brahim Formation; **3.** Detrital, bioclastic mud-wackestone (calcisiltite) with trilobite debris and shell filaments, Bed 31-3, *L. serotinus* Zone, upper Emsian, basal Kheneg-an-Nmer Formation); **4.** Detrital, dark-grey mudstone (calcisiltite) with parathuramminid foraminifers (*Moravammina*, *Bisphaera*), Bed 57b, *Po. costatus* Zone, lower Eifelian, Kheneg-an-Nmer Formation.

Fig. 51: Conodonts from the lower Eifelian of the "central section" of Aïn-al-Aliliga (Bed 57b). **1.** *Bel. resima*, x 75; **2.** *Neop. perlineatus*, x 80; **3.** *Po. costatus*, x 80; **4.** *Po. zieglerianus*, x 85.

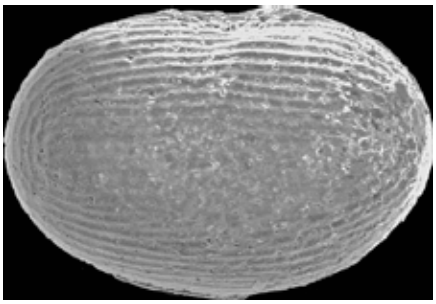

Fig. 52: Entomozoid ostracod from Bed 57b (lower Eifelian) of Aïn-al-Aliliga, "central section".

Fig. 53: Top part of the "central section" at Aïn-al-Aliliga showing poor bedding due to strong slumping, overprinted by the main Variscan tectonics.

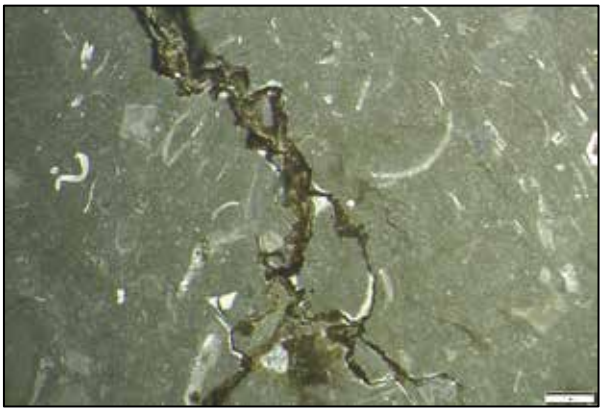

Fig. 54: Microfacies of the upper Pragian "griotte clast" found in the Al Brijat Formation at Aïn-al-Aliliga, a light-grey, bioclastic wackestone with trilobite, crinoid, and mollusk debris.

The Emsian "ensemble récifal inférieur" sensu GENDROT et al. consist of an anticlinal structure, complicated by faulting and secondary folding. Along the track, medium- to thick-bedded limestones of the Cakhrat-ach-Chleh Member stand near-vertical or dip variably steeply (with 80°) to the W and E (in the eastern part). Dominant are light- to middle-gray crinoidal limestones with only subordinate reefal organisms. The typical microfacies are bioclastic wacke-floatstones and calcisiltites (Fig. 56). GENDROT et al. (1969) separated a fore-reef slope setting in the W from dominant off-reef bank carbonates in the E. Two samples from the western and main part of the up to 130 m thick sequence yielded, in accord with the shallow litho- and biofacies, only single cone taxa (Sample R2 with six *Bel. resima* and acrotetrids, Sample S7 with six *Bel. resima* and six *Neop. perlineatus*).

Towards the eastern end, the track slope exposes an isolated giant stromatoporid with ca. 1 m diameter. It is overlain by well-bedded, bioclastic to increasingly nodular limestones. A sample from this interval yielded *Caud. celtibericus* (12 specimens), *Criteriognathus steinhornensis* (12 specimens), *Lat. beckmanni beckmanni* (two specimens), *Lat. bilatericrescens bilatericrescens* (four specimens), *Neop. perlineatus* (13 specimens), and, by far dominant, *Bel. resima* (90 specimens, 63 %). This assemblage is typical for the upper part of the lower Emsian (*Crit. steinhornensis* Zone or *Lat. latus* Zone of the icriodid zonation, ABOUSSALAM et al. 2015). The absence of polygnathids and the *Belodella* enrichment confirm a neritic environment.

The well-bedded top of the Dhar-es-Smene Formation is sharply overlain by reddish shales of the (main) Mohammed-Ben-Brahim Formation. This facies break represents regionally the global Daleje Event and transgression, which suddenly drowned the extensive lower Emsian carbonate platform. The squashed fauna consists of common goniatites (*Gyroceratites* sp., Fig. 57), orthoconic cephalopods, rare phacopids, and up to 8 cm large bivalves (*Panenka*). This assemblage is typical for a basal upper Emsian (LD IV-A) pelagic setting, as it is widespread in the eastern Anti-Atlas (Tafilalt, e.g., BECKER et al. 2018a, 2018b) or in the classical Daleje Shale region of Bohemia (e.g., CHLUPÁČ & KUKAL 1988; CHLUPÁČ & LUKEŠ 1999).

Separated by a fault zone (Fig. 27) follows the second, near vertically bedded, up to 200 m thick reefal unit ("barre calcaire supérieur" of GENDROT et al. 1969). It has been assigned to the Givetian/Frasnian but we do not have new biostratigraphic data that could confirm or reject this dating. GENDROT et al. (1969) showed the presence of for-reef breccias W and

E of a wide, central part with bank facies and a thinner back-reef interval. At the eastern end, the reef was shown to have been eroded by another tongue of the calcareous, conglomeratic Aïn-al-Aliliga Formation, locally with a siliciclastic matrix (GENDROT et al. 1969, pl. 3, fig. 6).

Fig. 55: View from the track next to the Cherrat river on the steep and faulted first (western) reefal limestone cliff at Cakhrat Mohammed-Ben-Brahim, here assigned to the Cakhrat-ach-Chleh Member (lower Emsian).

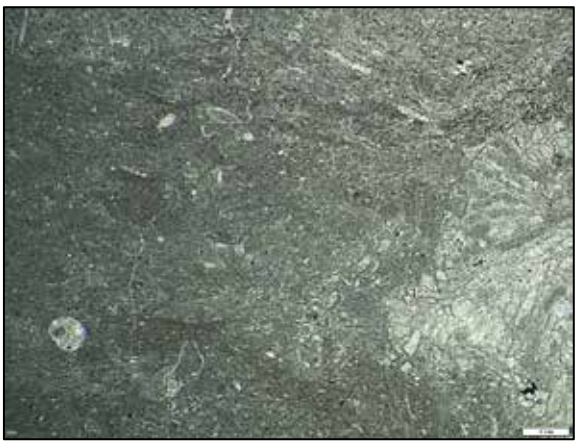

Fig. 56: Example for the dominant microfacies of the Cakhrat-ach-Chleh Member of the Dhar-es-Smene Formation at Cakhrat Mohammed-Ben-Brahim, a bioturbated, bioclastic (detrital) wacke-floatstone with shell filaments, trilobite remains, gastropods, and an isolated favositid coral, grading into calcisiltite in the upper part.

Fig. 57: Limonitic, flattened *Gyroceratites* sp. with typical concave flank lirae from the basal Mohammed-Ben-Brahim Formation at its type locality (max. diameter = 27 mm.).

Fig. 58: The isolated olistolite complex of Aïn-as-Seffah on the upper eastern slope towards the Oued Cherrat, recognizable from the distance by its marker tree, and surrounded by middle/upper Famennian siliciclastics of the Al Brijat Formation. The limestones in the front left represent the top of the Eifelian (*Po. eiflius* Zone) Aïn Kheneg-an-Nmer Formation, which is cut off by a fault.

4.4. Middle/Upper Devonian at Aïn-as-Seffah

The Emsian reef band of the Oued Cherrat (Fig. 2) is not well exposed in the area of Aïn-as-Seffah (or Aïn-as-Safah, topographic sheet, 1 : 50 000, Benslimane, x = 351.45, y = 334.9, GPS N33°34'30.8'' W006°59'18.7''). However, this locality is peculiar because of an isolated, allochthonous, ca. 40 m thick, internally structured slump unit of Givetian reef limestone and adjacent strata (Fig. 58). It has been named by CHALOUAN & HOLLARD (1979) as Aïn-as-Seffah Formation. ABOUSSALAM et al. (2013) introduced a member subdivision (Fig. 59) and provided preliminary conodont data, which enable a precise dating of unconformities, changes in facies and sea-level, the reef extinction, and for under- and overlying pelagic units (members). EICHHOLT & BECKER (2016) studied the microfacies succession of the biostrome (Members 2-3). The olistolite ends in the S by a fault but grades on the northern slope into a level of many smaller olistolites.

4.4.1. Aïn Kheneg-an-Nmer Formation.

Between the N-S running road and the main olistolite lies the plateau of Dhar al Qlaqez. It is occupied by an upper Emsian to upper Eifelian succession, the Aïn Kheneg-an-Nmer Formation. Beds dip mostly to the E with a variably inclination of ca. 45-90° (average ca. 60°). In the W, there are ca. 30 m of platy, marly, detrital to crinoidal, thin-bedded (up to 10 cm thick), dark-grey limestones alternating with calcareous shales. The microfacies is monotonous (silty, dark-grey calcisiltites, Fig. 58). Conodont sampling was without success.

After a ca. 45 m wide outcrop gap, probably occupied by weathered shales, follows to the E a second, limestone-dominated part of the formation (ca. 80 m).

Fig. 59: The monotonous microfacies of the lower Aïn Kheneg-an-Nmer Formation: unfossiliferous, silty, poorly bioturbated mudstones (calcisiltites; scale bar = 1 mm).

This upper part tends to form small cliffs in the upper slope towards the Oued Cherrat (Figs. 5, 58). The basal alternation of dark-grey, poorly fossiliferous (some small brachiopods, crinoid debris) limestones and shale exposed in a fenced area did not yield conodonts (Sample 1). Further ca. 150 m to the E, solid limestones (10-20 cm thick) were exploited in a small quarry, where (?overturned) beds fall steeply to the E. Laminated beds suggest a tempestitic or turbiditic origin. Sample 2 from the eastern quarry margin falls in the top-Eifelian *Po. eiflius* Zone (NARKIEWICZ & BULTYNCK 2018), an upper subdivision of the former *Tortodus kockelianus* Zone. Apart from both index species (1 and 3 specimens), we found *Po. angustipennatus* (3 specimens), *Po. parawebbi* (3 specimens), *L. linguiformis* (3 specimens), and two questionable *I. hollardi*. There is no evidence for the global Kacak Event Interval before the limestones are cut off by a fault; the Eifelian-Givetian transition is not preserved.

4.4.2. Member 1 of Aïn-as-Seffah Formation

Unlike the Eifelian succession, beds within the main olistolite fall with 50-70° to the SW (202°/50° to 220°/69°). ABOUSSALAM et al. (2013) assigned the more than 20 m thick alternation of light- to middle-grey, unfossiliferous, thin- to medium-bedded (2-20 cm) and often lenticular flaserlimestones and calcareous shales to Member 1 of the Aïn-as-Seffah Formation. It underlies the reef sequence but continues on the southern side in parallel (laterally) to the reef boulders, with a strictly disconformable contact of both members. In the lower part (Unit A, Fig. 60) there are only isolated limestone lenses in shale, which increase in number in the top 2 m.

The ca. 4 m thick Unit B consists of many isolated, thin limestones in calcareous shale matrix. Conodont Sample 3 from its main part was barren. Sample 4 from the top yielded *I. difficilis* (Fig. 61.1) and *I. obliquimarginatus*. (Fig. 62.1). In the zonal scheme of BULTYNCK (1987), both taxa should not overlap but a late morphotype ranges in the Montagne Noire (southern France) until the Taghanic Crisis (WALLISER 1990; ABOUSSALAM 2003). *Icriodus difficilis* is the index species of the shallow-water *I. difficilis* Zone, which base has been correlated with the ca. middle part of the *Po. varcus-rhenanus* Zone (GOUWY & BULTYNCK 2002). Therefore, Unit B is assigned to the lower part of the middle Givetian, while the underlying, thicker Unit A probably includes parts of the lower Givetian.

Just a little bit higher, the base of Unit C (Sample 5) produced *I. difficilis* (Figs. 61.2-3) in association with *L. linguiformis* (Fig. 61.5) and *L. klapperi* (Fig. 61.4). The latter two taxa are long-ranging in the top Eifelian to middle Givetian (e.g., WALLISER & BULTYNCK 2011). Sample 6a with *I. difficilis* (Fig. 62.2), *Po. xylus* (Fig. 62.4), and *L. linguiformis* (Fig. 62.3) from the top of Unit C, and the laterally equivalent Sample 6b (= C+14m; collected 14 m above a solid limestone within Unit A) with *L. linguiformis* and *Bel. triangularis* (Fig. 62.5) still fall in the same conodont zone (Tab. 3). The neritic microfacies of Sample 6b (Fig. 72.1) is a middle-grey to brownish, flaser-bedded, bioturbated, bioclastic wacke-

packstone with brachiopods, tabulate corals, shell filaments, crinoid debris, micrite to calcisiltite matrix, and iron-stained, dark pressure solution seams.

conodont zones	***difficilis***						***cristatus ectypus***		***norr.***	**MN 1**	**MN 1**
sample no.	**4**	**5**	**6a**	**6b**	**7a**	**7b**	**8**	**9**	**L**	**10**	**11**
unit and field no.	**top B bel. C**	**base C**	**C top**	**top C +14m**	**base D b. reef**	**AAS 2 loose**	**low. D 1.5m**	**50cm ab. C**	**AAS 1 loose**	**top reef**	**top D 1.4m**
L. linguiformis	*	2	8	1							
I. difficilis	**1**	5	9	*	5	*	1	*	*	*	*
I. obliquimarginatus	2	*	*	*	3						
L. klapperi		1									
Po. xylus			1	*	*	4	*	2	4		
Bel. triangularis				1							
Prioniodina sp.					1						
Po. pseudofoliatus					4						
I. brevis brevis						1					
I. expansus							3	*	1		
Po. cristatus ectypus							**3**				
Po. dubius							**3**	*	*	8	3
Po. pennatus								1	*	*	1
Po. paradecorosus									**9**	2	19
S. pietzneri									7		
I. tafilaltensis									2	14	
Po. webbi									3	*	5
Po. alatus									**1**	*	1
I. subterminus										2	
Po. cf. *lanei*										1	*
Po. pollocki										3	*
I. symmetricus										**24**	23
Ancyrodella sp.										**1**	*
Bel. resima											1
Ad. rotund. pristina											42
Po. cristatus cristatus											2

Tab. 3: Ranges of conodonts in Member 1 to the lower part of Member 3 of the Aïn-as-Seffah Formation.

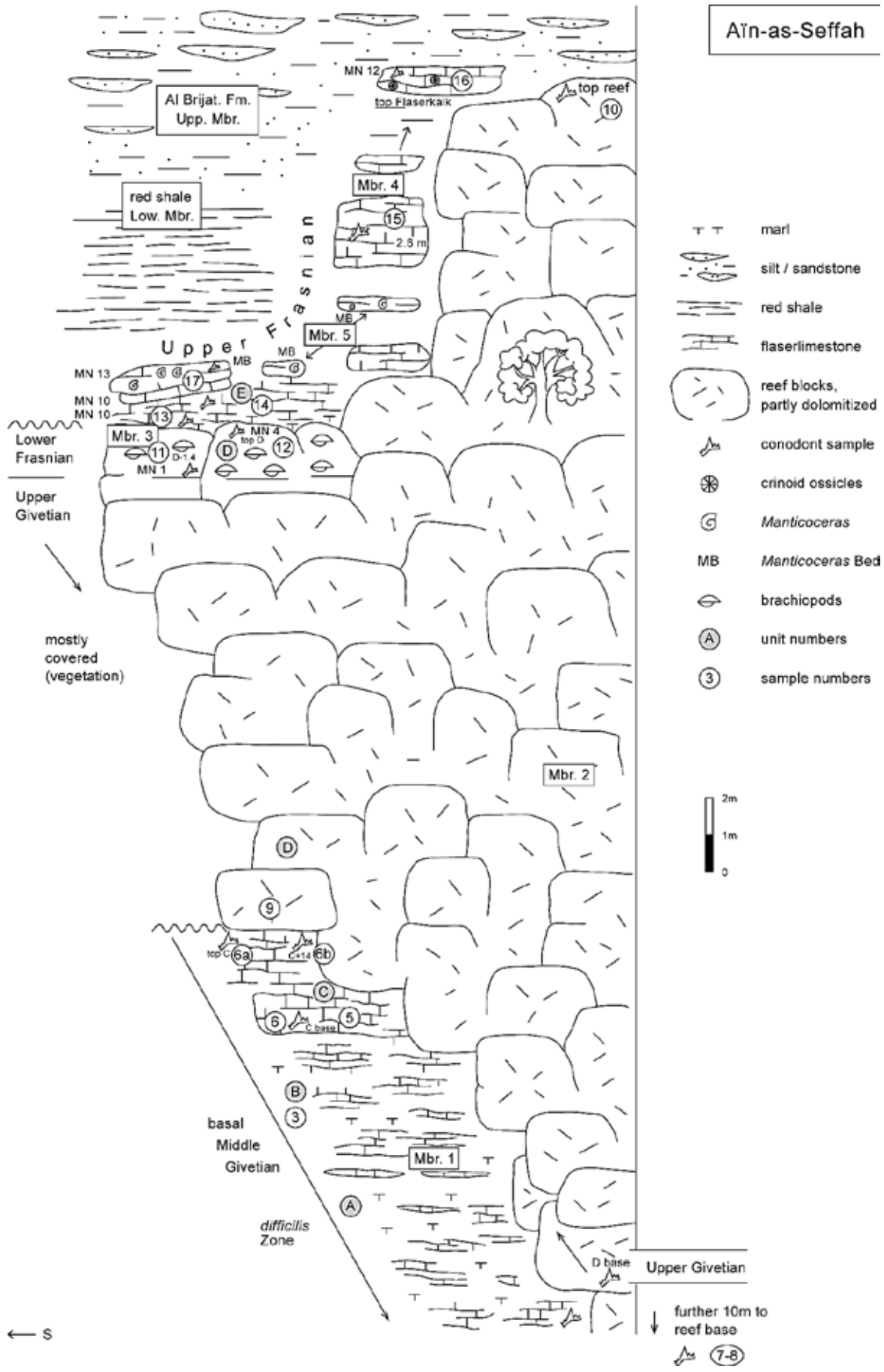

Fig. 60: Sketch showing the spatial relationship of units/members and conodont samples for the southern part of the Aïn-as-Seffah Formation, with the marker tree providing orientation in the field.

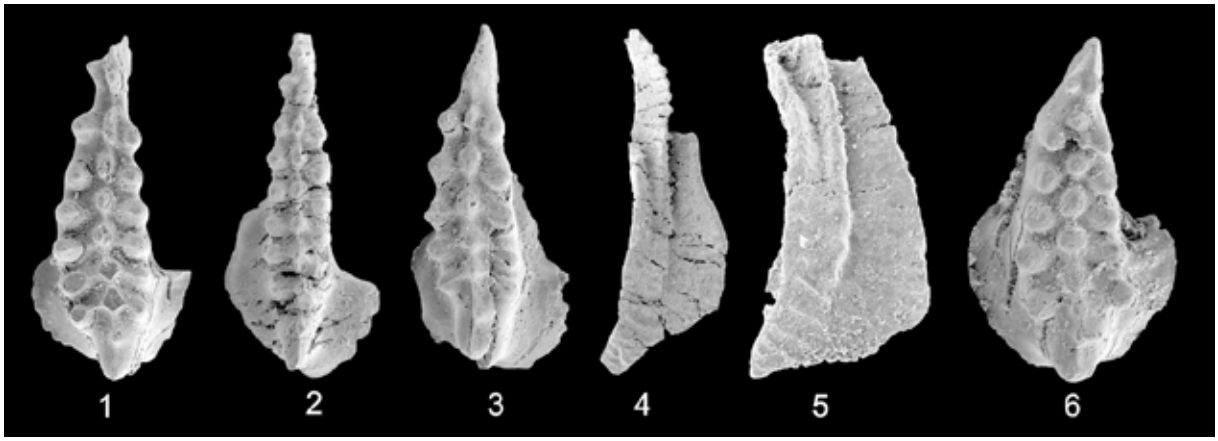

Fig. 61: Conodonts from Units B/C within Member 1 of the Aïn-as-Seffah Formation, showing the variability in icriodids. **1.** *Icriodus difficilis*, typical morphptype, top of Unit B (Sample 4), x 60; **2.** *I. difficilis*, narrow and straight morphotype, base of Unit C (Sample 5), x 60; **3.** *I. difficilis*, morphotype with low number of node rows, base of Unit C (Sample 5), x 60; **4.** *L. klapperi*, base of Unit C (Sample 5), x 30; **5.** *L. linguiformis*, base of Unit C (Sample 5), x 55; **6.** *I difficilis*, robust and curved morphotype with strongly alternating nodes, trending towards *I. expansus*, top of Unit C (Sample 6a), x 65.

4.4.2. Reefal Member 2 of Aïn-as-Seffah Formation

Member 2 consists of up to 3 m large, massive limestone boulders (Fig. 63), which made the section logging difficult. Therefore, Fig. 60 is a simplified sketch using a rough meter scale. Within the member, three regressive episodes can be recognized following changes in macro- and microfacies (EICHHOLT & BECKER 2016, fig. 10).

The Aïn-as-Seffah "reef" was originally a small, isolated patch reef that developed on the neritic, muddy carbonate platform of Member 1. A distinctive zonation with fore reef, reef core, and back reef never developed. The initial phase of Member 2 consists of crinoid grainstone (MF B1a), representing a subtidal crinoid bank. Subordinate biostrome organisms, such as stromatoporoids and *Alveolites*, were fragmented and scattered by storms. One meter above base, fragments become larger and more divers. This suggests initial biostrome growth (a "parabiostrome" sensu ÁLVARO et al. 2007) but there are only few in-situ reef builders (Fig. 65). There are now coral-intraclast rudstones with washed out, peloidal grainstone matrix and solitary Rugosa (Sample 7a, Figs. 67, 72.2) or detrital coral-stromatoporoid float-rudstones (MF B2a, Fig. 66.2). Both formed probably by high-energy storm events but we cannot exclude some slumping due to synsedimentary tectonism. Between 8 and 16 m above base, floatstones with fragments of *Thamnopora*, *Alveolites* and solitary Rugosa prevail. Laminar stromatoporoids dominate at 4 and 8 m (Fig. 66.1).

In situ laminar stromatoporoids are preserved at 17 to 18 m. They stabilized detritus-rich float-/rudstones in the transition towards coral-stromatoporoid boundstones (MF C2a and MF C2b, 19-22 m). *Phillipsastrea* boundstones appear 19 m above the base (Fig. 64). This interval marks the first of the three shallowing upwards cycles. It is overlain by detrital coral-stromatoporoid float-rudstones at 22-28 m (MF B2a). Intercalated is a crinoid grainstone at 24-26 m, which deposited during relative deepening. At 28 m, coral-stromatoporoid boundstones reappear, either with *Phillipsastrea* (MF C2a) or as *Thamnopora* or *Stachyodes* rud-bafflestones (MF C2b, Fig. 66.3).

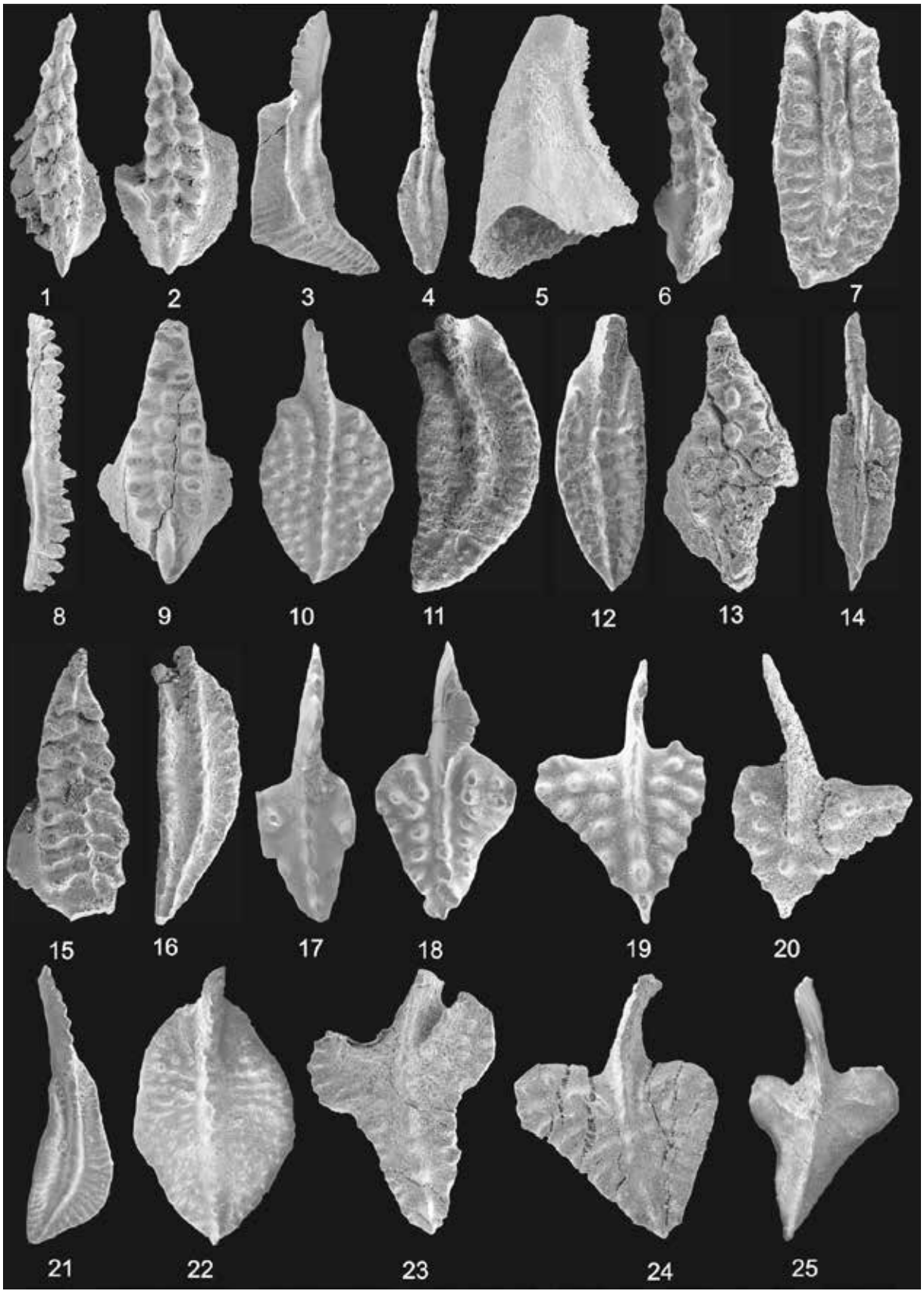

Fig. 62: Conodonts from Member 1 (Units B/C) to the lower part of Member 3 (Samples 11-12) of the Aïn-as-Seffah Formation. **1.** *I. obliquimarginatus*, top Unit B (directly below Unit C; Sample 4), x 55; **2.** *I. difficilis*, top Unit C (Sample 6a), x 60; **3.** *Ling. linguiformis*, top Unit C (Sample 6a), x 30; **4.** *Po. xylus*, top Unit C (Sample 6a), x 30; **5**

Bel. triangularis, top Unit C (Sample C+14m = 6b), x 65, **6.** *I. obliquimarginatus*, base Unit D (Sample 7a), x 80; **7.** *Po. pseudofoliatus*, base Unit D (Sample 7a), x 90; **8.** *Prioniodina* sp., base Unit D (Sample 7a), x 40; **9.** *I. expansus*, 1.5 m above base Unit D (Sample 8), x 65; **10.** *Po. cristatus ectypus*, 1.5 m above base Unit D (Sample 8), x 40; **11.** *Po. pennatus*, middle Unit D, 50 cm above top Unit C (Sample 9), x 50; **12.** *Po.* cf. *tafilensis*, middle Unit D, 50 cm above top Unit C (Sample 9), x 70; **13.** *I. subterminus*, top reef, top Unit D (Sample 10), x 80; **14.** *Po.* cf. *lanei*, top reef, top Unit D (Sample 10), x 45; **15.** *I. tafilaltensis*, top reef, top Unit D (Sample 10), x 60; **16.** *Po. pollocki*, top reef, top Unit D (Sample 10), x 50; **17.** *Ad. rotundiloba pristina*, early morphotype, Member 3, upper 1.4 m of Unit D (Sample 11), x 50; **18.** *Ad. rotundiloba pristina*, larger, therefore more advanced morphotype, Member 3, upper 1.4 m of Unit D (Sample 11), 30; **19-20.** *Ad. africana*, top Unit D, top Member 3 (Sample 12), both x 65; **21.** *Po. webbi*, Member 3, upper 1.4 m of Unit D (Sample 11), x 35; **22.** *Po. cristatus cristatus*, Member 3, upper 1.4 m of Unit D (Sample 11), x 40; **23.** *Ad. hamata* (= *gigas* M2), top Unit D, top Member 3 (Sample 12), x 50; **24-25.** *Ad. pramosica*, top Unit D, top Member 3 (Sample 12), x 54 and x 40.

Fig. 63: Massive (up to 3m thick) reef boulders of Member 2 on the logged southern side at Aïn-as-Seffah.

Fig. 64: Field photo of a *Phillipastrea* from the lower half of Member 2 at Aïn-as-Seffah (picture width ca. 4 cm).

Laterally to a dolomitized part of the second and rather massive biostrome unit, at the southern margin (left in Fig. 60), Sample 9 (Fig. 68) is a recrystallized coral-crinoid pack-rudstone with fragmentary favositids, other tabulate corals, and coarse, angular crinoid debris. It represents a shallow platform storm facies but the tectonic and diagenetic overprint is very strong.

Fig. 65: Field photo of silicified alveolitids encrusting in situ a solitary rugose coral at Aïn-as-Seffah (picture width ca. 10 cm).

A strongly brecciated coral-stromatoporoid float-rudstone (MF B2a) at 37 m signals the deepening above the second biostrome phase. Above, dolomitization obscures the facies trend at 40-42 m: this interval forms the top reef on the southern side (Fig. 60). Subsequent (higher) reef boulders with breccias and rudstones can be found around and just above the marker tree. The brecciated interval ends at ca. 46 m, slightly higher than the tree level. It is overlain up to the top by the third regressive, biostromal phase with *Phillipsastrea* Boundstones (MF C2a, Fig. 69). These contain crinoid debris, alveolitids, and laminar stromatoporids.

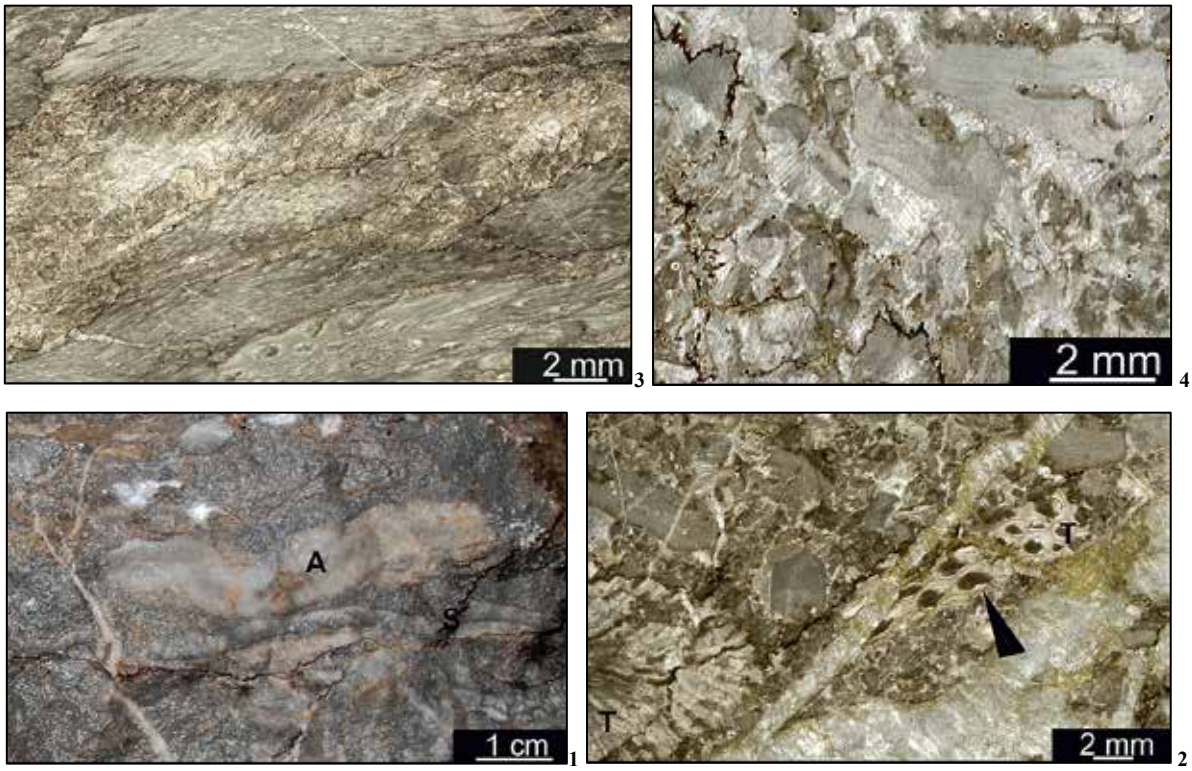

Fig. 66: Examples of reef facies from Unit D of the Aïn-as-Seffah Formation. **1.** MF B2a, open marine reef breccia with laminar stromatoporoids (S) and alveolitids (A) as clasts within a crinoidal grainstone matrix, lower part of Member 2; **2.** MF B2a (Aïn-as-Seffah type), tempestitic rudstone with thamnoporid branches (T, with geopetal fillings marked by arrow), other tabulate corals (lower left), and coarse crinoid debris, within a sparitic, crinoidal grainstone matrix, lower part of Member 2; **3.** Tectonically elongated MF C2b, *Thamnopora* rud-bafflestone with a sparitic matrix, Member 2, 29 m above base; **4.** MF B1b, coarse, recrystallized crinoid-brachiopod grainstone, top of Unit D (Member 3, Sample 12).

The age of the Aïn-as-Seffah reef is fairly well constrained by conodont data. The presence of conodonts within reef breccias and crinoid limestones proves a recurrent influx of open water biota, unlike as in Devonian bioherms. A conodont sample from near the base of Member 2 provides the same early middle Givetian age (*I. difficilis* Zone) as Member 1. Sample 7a yielded the same association of *I. difficilis* and late forms of *I. obliquimarginatus* (Fig. 62.6). The presence of *Po. pseudofoliatus* (Fig. 62.7) and *Prioniodina* (Fig. 62.8) indicate a slightly deeper neritic setting. A different fauna with *I. brevis brevis* and *Po. xylus* was obtained from a loose block (Sample AAS 2). These conodont data suggest that the initial biostrome was established in the middle Givetian when the mud supply stopped. This resembles the Givetian reef initiation in the Rhenish Massif (BECKER et al. 2016a).

Sample 8 from ca. 1.5 m above the member base is markedly younger. There are three typical upper Givetian species, *I. expansus* (Fig. 62.9), *Po. dubius*, and *Po. cristatus ectypus* (Fig. 62.10), the index species of the *Po. cristatus ectypus* Zone (ABOUSSALAM 2003). Combined with the irregular lateral contact to Member 1, we suspect that the main part of Member 2 is an allochthonous slump mass that glided onto Member 1 in the upper Givetian. Accordingly, at the lateral end of the outcrop (left in Fig. 60), the same age gap exists between the top of Member 1 (Unit C, Sample 6b) and Sample 9 from the light-grey, massive, detrital limestones (Fig. 68) just 50 cm above. The latter yielded with *Po. pennatus* (Fig. 62.11) and *Po.* cf. *tafilensis* (Fig. 62.12)

two further upper Givetian species. They are typical for deeper-water settings, for example of the eastern Anti-Atlas (ABOUSSALAM & BECKER 2007). An even younger, top-Givetian age (*Skel. norrisi* Zone) applies to the conodont assemblage from a block of reef breccia collected loose at the base of the outcrop (Sample AAS 1). Age diagnostic are the most common polygnathid, *Po. paradecorosus*, as well as *Po. alatus* (see lowest range established by ABOUSSALAM & BECKER 2007), The sample yielded also the only local *Schmidtognathus pietzneri*, a species that does not range above the *Skel. norrisi* Zone.

Fig. 67: Microfacies near the base of Unit D (Member 2, Sample 7a, middle Givetian): biostrome breccia (MF B2a), coral-intraclast rudstone with solitary rugose corals and a peloidal grainstone matrix (picture width = 4.2 cm).

The detrital limestone at the top of Member 2 (Sample 10) falls in the basal Frasnian, based on a fragmentary *Ancyrodella* sp. (Fig. 70.1) and frequent (ca. 45 % of the fauna) *I. symmetricus* (Fig. 68.2). Other typical forms for this level are *I. subterminus* (Fig. 62.13), *Po.* cf. *lanei* (Fig. 62.14; with a different platform shape than in the types of *lanei*; compare ABOUSSALAM & BECKER 2007, figs. 6L-M), *Po. paradecorosus, I. tafilaltensis* (Fig. 62.15), and *Po. pollocki* (Fig. 62.16). The relatively diverse conodont sample indicates a deeper neritic, non-reefal environment. This suggests that the reef drowning occurred in the course of the second (MN 1 Zone) phase of the global, transgressive Frasnes Events.

Fig. 68: Strongly recrystallized coral-crinoid pack-rudstone with tabulate corals, diffuse crinoid debris, dolomite crystals, and iron-stained dissolution seams (Sample 9, Member 2, upper Givetian, scale bar = 2 cm).

Fig. 69: Vertically cut, tectonically distorted *Phillipsastrea* colony from the biostromal upper part of Member 2 at Aïn-as-Seffah (picture width = 3 cm).

4.4.3. Brachiopod limestone, Member 3

At the southern margin (Fig. 60), thick, dolomitized reef limestone boulders with bulbous, laminar and branching (*Stachyodes*) stromatoporids turn without a bed boundary rapidly into ca. 2 m of light-grey, brachiopod-rich detrital limestones, Member 3 sensu ABOUSSALAM et al. (2013). There are coarse, recrystallized crinoid-brachiopod grain-floatstones (MF B1b, EICHOLT & BECKER 2016). The brachiopods are thick-shelled but not well preserved and difficult to extract.

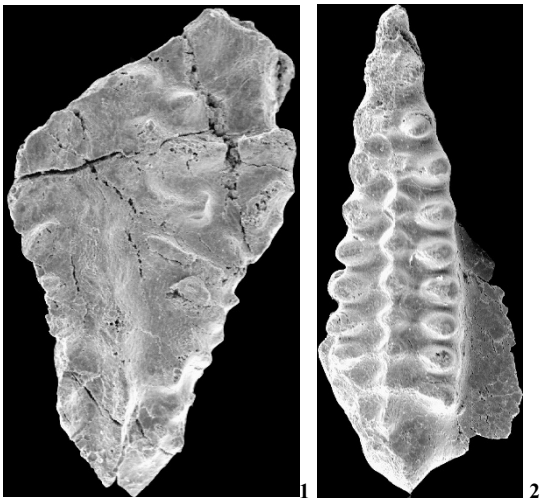

Fig. 70: Basal Frasnian index conodonts from Sample 10, collected from the last solid limestone at the top of Member 2 of the Aïn-as-Seffah Formation, ca. 8 m above the marker tree. **1.** Fragmentary *Ancyrodella* sp. (possibly an advanced *Ad. rotundiloba pristina*); **2.** *I. symmetricus*.

Conodonts from the lower 1.4 m (Sample 11) gave the same basal Frasnian age as the top of Member 2, despite the lateral height difference of 9-10 m of reef limestone (Fig. 60). Early (Fig. 62.17) and larger, more advanced (Fig. 62.18) morphotypes of *Ad. rotundiloba pristina*, the MN 1 Zone index species, are common (43 % of the fauna). They are followed in terms of abundance by *I. symmetricus* (24 %) and *Po. paradecorosus* (ca. 20 %). Apart from some usual lower Frasnian polygnathids (*Po. webbi, Po. alatus, Po. pennatus*), there are two specimens of the much rarer *Po. cristatus cristatus* (Fig. 62.22). The rather sudden change from reefal boundstones to conodont-rich (ancyrodellid-icriodid-polygnathid biofacies), deeper neritic brachiopod limestones underlines the role of reef drowning as the main extinction agent and the local significance of the Frasnes Events (see BECKER & ABOUSSALAM 2004).

Member 3 is a strongly condensed and probably stratigraphically incomplete unit, since Sample 12, a crinoid-brachiopod grainstone (Fig. 66.4), yielded already rich conodonts from the top of the lower Frasnian (top MN 4 or *Ad. nodosa* Zone; ABOUSSALAM & BECKER in PIZARZOWSKA et al. in press; Tab. 4). Typical for a post-reefal, current- and storm-influenced neritic facies are the dominant ancyrodellids (see VANDELAER et al. 1989). The most common form is *Ad. nodosa* (= *gigas* M1), whose early to middle stages may resemble closely the older *Ad. rotundiloba soluta* (Fig. 71.1.). Associated are almost equally common *Ad. africana* (Figs. 62.19-20), rarer *Ad. pramosica* (Figs. 62.24-25), and a constricted form with marginal ribbing (Fig. 62.23) that we include in *Ad. hamata* (= *gigas* M2, *Ad. symmetrica* or *Ad. buckeyensis*). However, that species occurs normally higher, in the late middle Frasnian (KLAPPER & KIRCHGASSER 2016). Among the polygnathids, there are *Po. webbi* (Fig. 62.21), more common *Po. paradecorusus* (Fig. 71.14), *Po. alatus*, and "*Po.* aff. *angustidiscus*" sensu HUDDLE (1981) (Fig. 71.13). Among the icriodids, we found *I. symmetricus*, unusually young *I. difficilis* (Fig. 71.2), and a form with large basal cavity, tentatively assigned to *I. pupus*. The palmatolepids (s.l.) are represented by *Mesotaxis guanwushanensis* M3 (sensu ABOUSSALAM & BECKER in PIZARZOWSKA et al. in press; Figs. 71.6-7), with a slight widening of the elongated basal pit, *Mes. asymmetrica* (Figs. 69.4-5), slender *Mes. bogoslovskyi*, different morphotypes of *Zieglerina unilabius* (Figs. 71.8-10), and an unusually narrow morphotype of *Pa. transitans* (Fig. 71.12, transitional towards *Pa. keyserlingi*), the MN 4 Zone index species. The presence of *Nothognathella ziegleri* (Fig. 71.11), its assumed Pb element, supports our *Palmatolepis* identification.

The long interval of the MN 2 to main part of MN 4 Zone is either missing or extremely condensed within the less than 50 cm between Samples 11 and 12. On the originally exposed central reef top, there was a much longer period of non-deposition. Member 3 is lacking and the top of Member 2 is laterally bordered by upper Frasnian flaserlimestone (Fig. 60).

Conodonts zones	**MN 4**	**MN 10**		**?MN 10**	**MN 12**	**MN 13**
sample no.	**12**	**13**	**14**	**15**	**16**	**17**
unit and field no.	**top D (Mbr. 3)**	**base E (Mbr. 4)**	**below *Mant.* Bed**	**2.8m above tree**	**top flaserlst.**	***Mant.* Bed (Mbr. 5)**
I. difficilis	6					
Po. paradecorosus	19	14	22	24 def		
Po. webbi	2	*	*	*	6 + 1 def.	7
Po. alatus	1					1
Po. cf. *lanei*	1					
Po. pollocki	*	*	*	6 def		
I. symmetricus	3	20	50	59 def	23	
Ad. africana	90					
Ad. nodosa (*gigas* M1)	**100**	5				
Ad. hamata (*gigas* M2)	10					
A. pramosica	13					
I. pupus	2					
Z. unilabius	8					
Pa. transitans	2					
M. guanwushanensis M3	4					
M. asymmetrica	6					
M. bogoslovskyi	5					
Po. "aff. *angustidiscus*"	3					
Nothognathella sp.	1	2	*	4	*	2
Pa. plana		**1**	**1**	*	*	2
I. curvatus			9			
Ad. curvata early morph			38	2		
Ag. coeni			7	*	1	
Ag. leonis			2			
Ag. triangularis					12	1 + 1 cf.
Pa. hassi					1?	16
Pa. winchelli					**1**	
Pa. wildungensis					2	
I. alternatus alternatus					5	
Ad. curvata late morph					14	52
Pa. "ljaschenkoae"						21
Ag. asymmetricus						**10**
Po. amana						5
Pa. "proversa"						2
Palmatolepis sp. (def.)						3
Po. imparilis						7
Po. aff. *incompletus*						3
Pa. bogartensis morph B						**4**

Tab. 4: Stratigraphic ranges of conodonts in the top of Unit D (upper Member 3) to Member 5 (*Manticoceras* Limestone) at Aïn-as-Seffah.

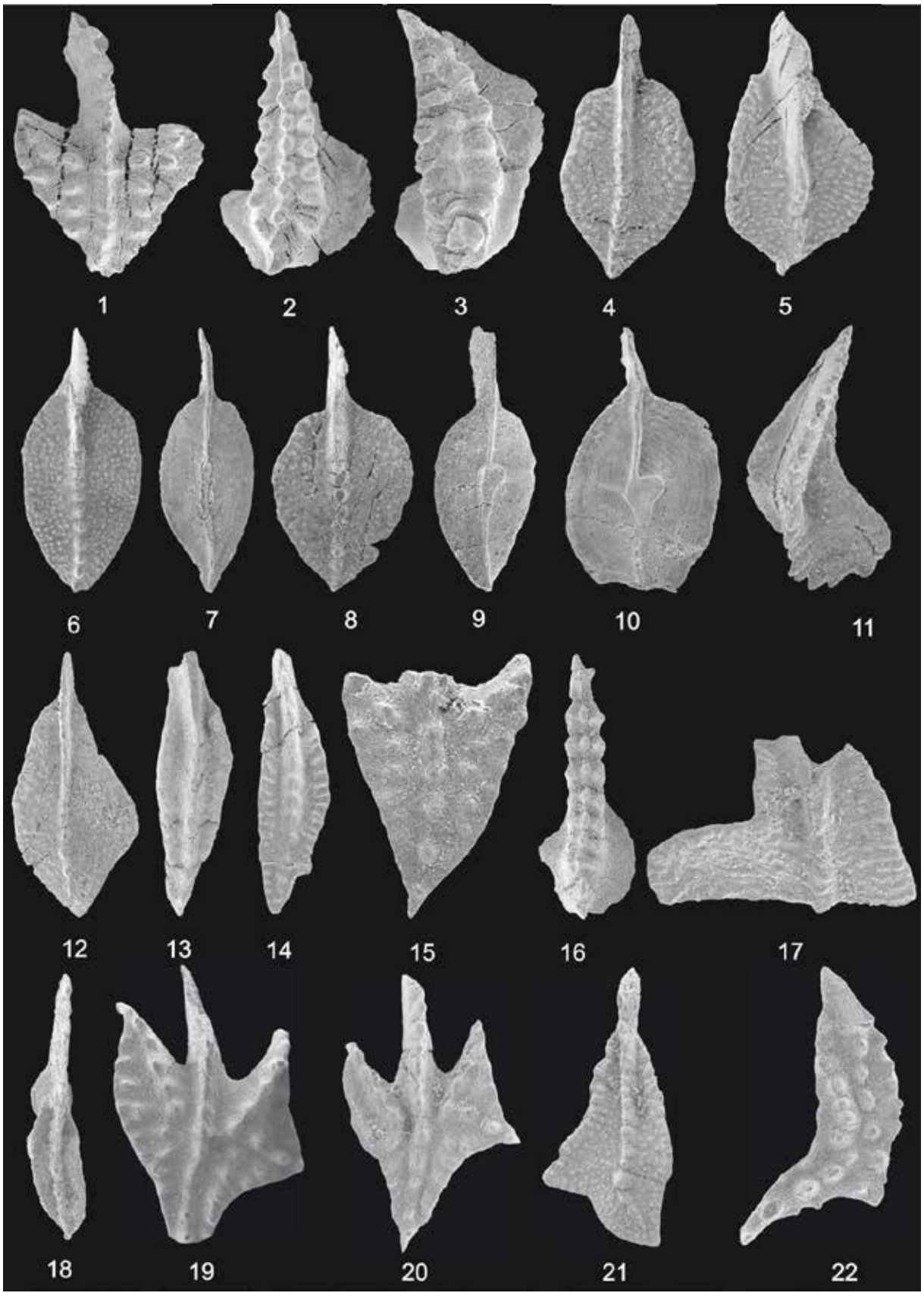
1
2
3
4
5
6
7
8
9
10
11
12
13
14
15
16
17
18
19
20
21
22

Fig. 71: Conodonts from the top Member 3 to top Member 4 of the Aïn-as-Seffah Formation; Sample 12 (top Unit D, 1-14), Sample 13 (base Unit E, 15-16, 18), Sample 14 (top Member 4, 17, 19), and Sample 16 (20-22). **1.** *Ad. nodosa* (resembling *Ad. rotundiloba soluta*), x 40; **2.** *I. difficilis,* x 55; **3.** *I. pupus*, x 65; **4-5.** *Mes. asymmetrica*, two different morphotypes, x 40 and x 45; **6-7.** *M. guanwushanensis* M3, slightly transitional towards *Z. ovalis*, both x 40; **8.** *Z. unilabius*, nodose morphotype, x 40; **9.** *Z. unilabius*, narrow morphotype, x 45; **10.** *Z. unilabius*, wide morphotype, x 50; **11.** *Nothognathella ziegleri*, x 60; **12.** *Pa. transitans*, narrow form, transitional towards *Pa, keyserlingi*, x 35; **13.** *Po.* aff. *angustidiscus* sensu HUDDLE (1981), x 40; **14.** *Po. paradecorosus*, x 40; **15.** *Ad. nodosa* (= *gigas* M1), posterior fragment, x 75; **16.** *I. symmetricus*, narrow form, x 50; **17.** *Pa. plana*, fragment showing the rectangular anterior margin of the outer lobe, x 45; **18.** *Po. xylus*, x 80; **19.** *Ad. curvata* early morph, x 55; **20.** *Ad. curvata* late morph, x 60; **21.** *Pa. winchelli*, tectonically elongated, x 30; **22.** *Ag. coeni*, fragmentary, x 80.

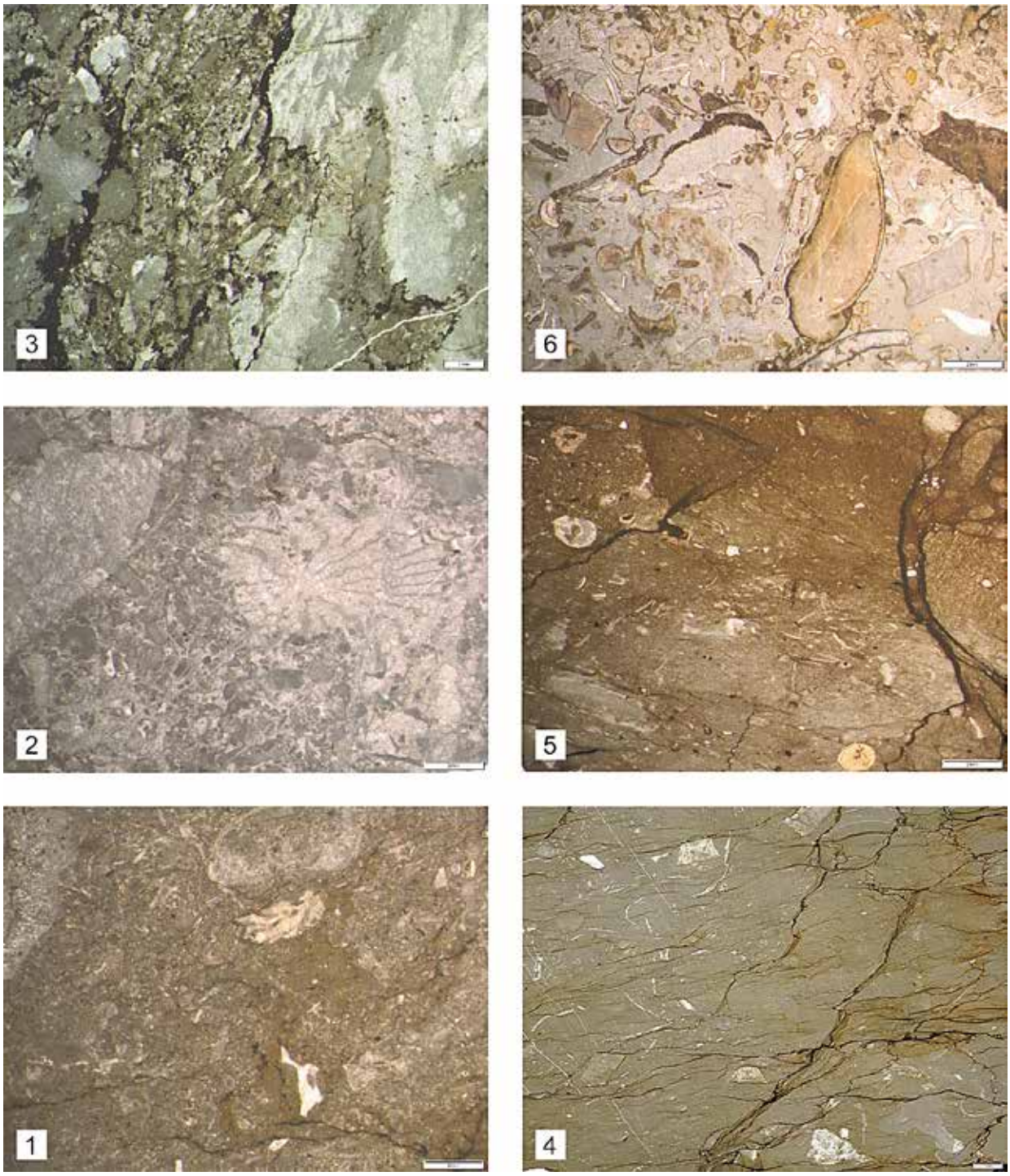

Fig. 72: Microfacies of non-reefal carbonates at Aïn-as-Seffah (Members 3-5, scale bar = 2 mm). **1.** Bioturbated, flaser-bedded bioclastic wackestone with shell filaments, crinoid debris, fragmentary tabulate corals and variably micritic or calcisiltite matrix, Sample 6b (top Unit C, Member 1, *I. difficilis* Zone); **2.** Details of Fig. 65: intraclast-coral float-rudstone with peloidal grainstone matrix, rich in crinoid debris and with eroded solitary Rugosa, Sample 7a (Member 2, base Unit D, *I. difficilis* Zone); **3.** Strongly unsorted, heterogeneous flaser-bedded intraclast pack-rudstone with angular crinoid fragments, tabulate corals, and a peloidal matrix, Sample 13 (base Member 4, top middle Frasnian, MN 10 Zone); **4.** Flaser-bedded mud-floatstone with dense, weekly bioturbate micrite matrix, isolated crinoid fragments, shell filaments, and a *Sphaeromanticoceras* cross-section (lower right), Sample 15 (upper Member 4, 2.8 m above marker tree, middle Frasnian); **5.** Nodular, bioturbated, bioclastic mud-wackestone with crinoid debris, shell filaments, and iron-coated dissolution seams, Sample 16 (top Member 4, upper Frasnian, MN 12 Zone); **6.** Cephalopod-extraclast floatstone with dense, fine micrite matrix, many coated, unsorted grains, juvenile goniatites, phosphate clasts, and shell filaments, Sample 17 (*Manticoceras* Bed, Member 5).

4.4.4. Member 4 of Aïn-as-Seffah Formation.

The outcrop distribution of Member 4 is highly irregular, curving backwards around the upper margin of the reef boulders in the SW and re-appearing, after an interruption by a Member 5 block, adjacent to the top of Member 2 (left in Fig. 60). The strike and dip do not follow this outcrop pattern, which suggests an array of individual, slumped blocks. The main macroscopic lithology is grey, thin-bedded, platy, flaser- and nodular limestone. Above the sharp and marly base, there are still some clasts of reefal organisms. Sample 13 (Fig. 72.3) is a heterogeneous, flaser-bedded intraclast pack-rudstone without any sorting, strongly fragmented crinoid debris, some thamnoporid branches, hematite enrichments, especially along dissolution seams, and with a washed out, sparitic peloid-intraclast grainstone matrix. It represents a proximal debris flow originating from the flank of the drowned reef, which was exposed for a long time to erosion and submarine carstification. This interpretation is supported by the neritic conodont biofacies (Tab. 4: dominance of *I. symmetricus*, Fig. 71.16, and *Po. paradecorosus*, rare *Ad. nodosa*, Fig. 71.15, and *Po. xylus*, Fig. 71.18), and a fragmentary *Pa. plana*, (Fig. 71.17), the index species of MN 10 Zone (top middle Frasnian). The main middle Frasnian, MN 5-9 Zones, falls in a long period of non-deposition and erosion. Just slightly higher, Sample 14 represents a deeper neritic setting, characterized by a mixed icriodid-ancyrodellid-polygnathid facies (with 33 % *I. symmetricus*, 25.5 % *Ad. curvata*, Fig. 71.19, and 15 % *Po. paradecorosus*). A single *Pa. plana, Ancyrognathus coeni* (Fig. 71.22) and *Ag. leonis* suggest that the sample still falls in the MN 10 Zone (= *Pa. plana* Zone). The thin section (Fig. 73) shows a strongly nodular mudstone with some crinoid and shell debris, deposited during increasing sea-level rise and under calm conditions. As a contrast to the base of the member (Sample 13), there are now a few dacryoconarids, a typical pelagic (planktonic) organism group. The abundance of minute iron oxide grains indicates hypoxic conditions.

Fig. 73: Microfacies of the main part of Member 4 (Unit E, Sample 14), a nodular, hypoxic mudstone with dacryoconarids, rare crinoids, other bioclasts, and a dense matrix rich in small iron oxide grains (scale bar = 2 mm).

Fig. 74: SW corner of the Aïn-as-Seffah outcrop, with massive, dolomitized boulders to the right, overlain by flaserlimestone (Members 4 and 5) in the foreground, and with a few higher isolated blocks in the midground, followed by bushy outcrop of the Al Brijat Formation.

Sample 15 from a flaserlimestone succession lateral to the last reef boulders (Figs. 60, 74) continues the calm mudstone facies (Fig. 72.4). Pelagic biota are here represented by shark teeth (*Phoebodus fastigatus*, SCHWERMANN 2014) and the cross-section of a goniatite (*Sphaeromanticoceras*). This genus ranges from the lower middle (UD I-F_3) to the top-Frasnin (BECKER et al. 1993). Conodonts belong to a similar biofacies as below, but with only rare ancyrodellids. The majority of specimens is affected by tectonic deformation. Although we did not find a single *Palmatolepis*, we assume the same age as for the similar samples below: MN 10 Zone.

The youngest part of Member 4 (Sample 16) lies as isolated blocks adjacent to the southern corner of the last reef boulders (Figs. 60, 74), well above the block with Sample 15. In thin-section, the microfacies (Fig. 72.5) is a brownish, bioturbated, nodular, bioclastic mud-wackestone with crinoid debris and shell filaments. No planktonic or nektonic groups are present. Most conodonts are less deformed than below. Apart from abundant *I. symmetricus* (35 % of the fauna), there are ca. equally frequent *Ancyrognathus* (20 %, mostly *Ag. triangularis*) and *Ancyrodella* (22 % *Ad. curvata*). An upper Frasnian age is based on the joint occurrence of *Ag. triangularis* and *I. alternatus alternatus*. A single, tectonically elongated *Pa. winchelli* (= *Pa. subrecta*, Fig. 71.21, with some resemblance of the platform shape to *Pa. khaensis* from Thailand; SAVAGE 2013) dates the fauna as MN 12 Zone (= *Pa. winchelli* Zone). Currently we have no local record of the basal upper Frasnian (MN 11 Zone) but there is an un-sampled interval between Samples 15 and 16.

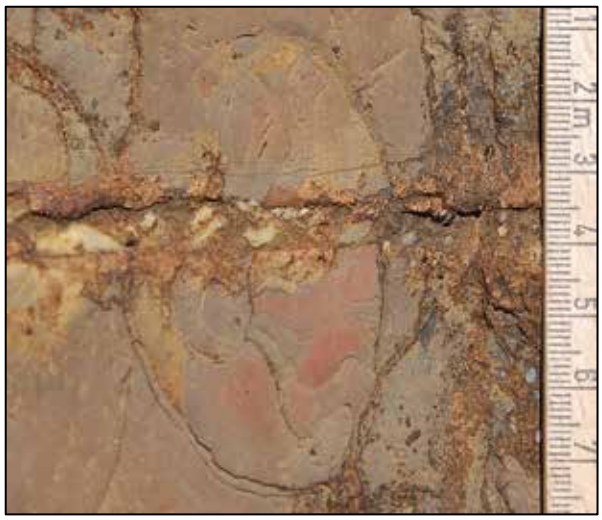

Fig. 75: Fully septate, eroded *Manticoceras* sp., cut by a healed fracture, as seen in the field (Member 5 of Aïn-as-Seffah Formation).

4.4.5. Manticoceras Limestone, Member 5

Because of its exceptional nature for the Moroccan Meseta, the grey to reddish goniatite limestone of Member 5 has been frequently mentioned in the literature (e.g., CHALOUAN & HOLLARD 1979; EL HASSANI & BENFRIKA 1995; ZAHRAOUI et al. 2000). However, there was no data base for the assumed early Frasnian age. The up to 8 cm large manticoceratids are too poorly preserved to provide a specific age. One cross-section belongs to the strongly compressed, long-ranging *M. lamed* Group; others have somewhat wider whorls. Associated are breviconic oncoceratids, longi-orthocones, small, solitary, deep-water Rugosa, and crinoid debris. The microfacies is rather unusual (Fig. 72.6), a cephalopod-extraclast floatstone with

many coated grains, crinoid pieces, juvenile goniatites, phosphate clasts, and shell filaments floating in a very dense, reddish, fine micrite matrix. The dark micrite or phosphatic envelopes of the coated particles show that these were reworked prior to re-deposition. There is no grading or sorting and the up to 6 mm large allochems/extraclasts stand in a remarkable contrast to the very fine matrix that indicates a calm sedimentary regime. The depositional mechanism is currently obscure but shedding from the drowned reef after a phase of non-deposition and reworking is evident. This interpretation fits the conodont age. Almost all conodonts are distorted or twisted by tectonism (Fig. 76). This severely hampers a precise identification, especially of palmatolepids, in which the platform shape is the most diagnostic feature. Despite this complication, we could identify *Ag. asymmetricus* (Fig. 76.3) and *Pa. bogartensis* (Fig. 76.5), the index species of the MN 13a Zone (*Pa. bogartensis* Zone). In some specimens of *Ag. triangularis* (Fig. 76.1), the outer lobe has been bent backwards, as in *Ag. barbus*. The same deformation may explain specimens with *Pa. proversa*-type anterior lobe (Fig. 76.4) and a platform shape and ornament as in *Pa. nasuta* or *Pa. ultima*. Tectonically elongated forms (Fig. 76.2) resemble *Pa. ljaschenkoae* or *Pa. khaensis* but cannot be identified reliably. Polygnathids are often easier to name (*Po. amana*, Fig. 76.6, *Po. imparilis*, *Po. webbi, Po. alatus, Po.* aff. *incompletus*).

The MN 13a Zone age means a correlation with the interval from the top of the Lower Kellwasser to the intra-Kellwasser levels (e.g., KLAPPER 1997; HOUSE et al. 2000; BECKER et al. 2016c). The mixed ancyrodellid (37.5 %)-palmatolepid (35 %) facies indicates a deeper carbonate ramp setting. There are no dark Kellwasser beds; the Frasnian-Famennian boundary is not preserved.

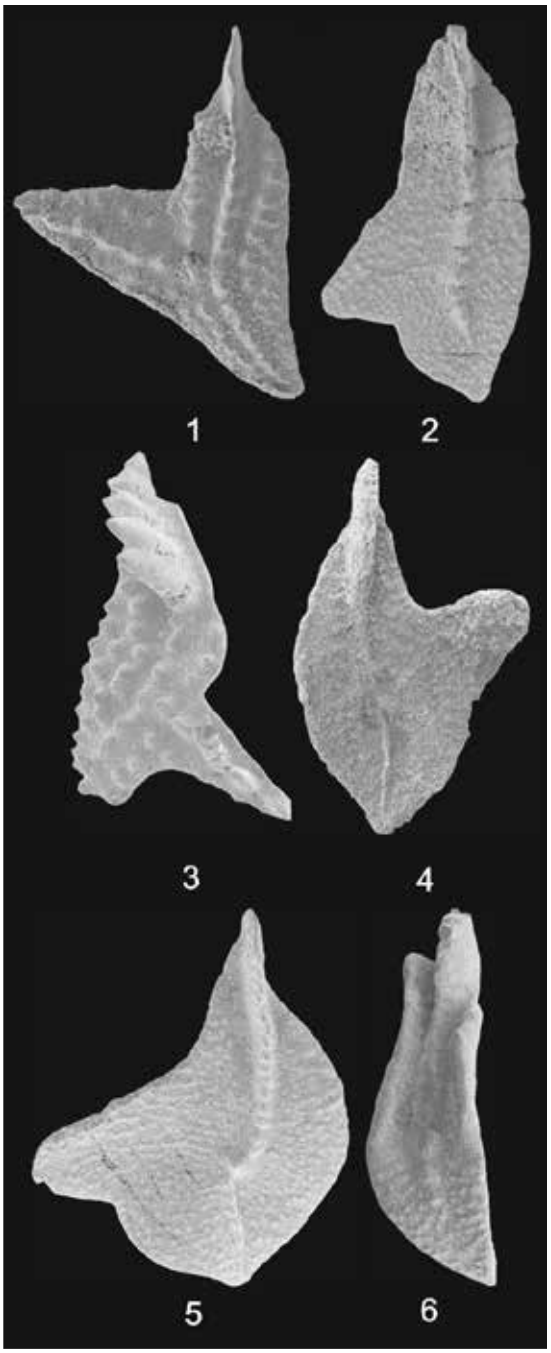

Fig. 76: Tectonically distorted upper Frasnian conodonts from Member 5 of the Aïn-as-Seffah Formation (Sample 17). **1.** *Ag. triangularis* with anterior direction of the side lobe due to distortion, x 45; **2.** Specimen resembling "*Pa. ljaschenkoae*", x 30; **3.** Folded *Ag. asymmetricus*, x 50; **4.** "*Pa. proversa,* with anterior orientation of side lobe due to distortion (otherwise resembling *Pa. nasuta*), x 50; **5.** *Pa. bogartensis* morph B, x 45; **6.** *Po. amana*, x 45.

4.4.6. Al Brijat Formation

Restricted to the SE corner of the outcrop (upper left in Fig. 60) is a distinctive,

unfossiliferous, 4-10 m thick package of red shale, the **Lower Member** of the Al Brijat Form sensu ABOUSSALAM et al. (2013). Its palaeotopographically constrained distribution laterally to the last reef boulders, indicates that it was originally attached to the main olistolite prior to redeposition. The red shale resembles the red, basal middle Famennian, basinal (deep pelagic) "Cypridinenschiefer" (lower Hemberg Formation) of the Rhenish Massif (e.g., DENCKMANN 1905; KREBS 1979; BECKER 1992). However, this lithofacies similarity does not necessarily mean an identical age. So far, there are no fossils that date the Lower Member. The fully oxygenated, strongly oligotrophic, C_{org}-poor lithology prevents any palynological analysis.

The **Upper Member** lies above a sharp lower contact (basal unconformity). It begins with ca. 30 m of deeply weathered shales, siltstones, and lenticular sandstones that exhibit common slump folding. As evident from the olistolites, there was recurrent seismic activity. A higher, ca. 20 m thick unit consists of fine or silty shales, reddish at the base and then olive-colored, with siltstone nodules. The latter have prospects for palynological data. By comparison with Aïn-Al-Aliliga, we assume preliminarily an upper Famennian age. We did not observe limestone clasts above the main olistolite level.

Devonian and basal Carboniferous of the allochthonous nappes at Mrirt (eastern part of Western Meseta) – review and new data

Ralph Thomas Becker, Zhor Sarah Aboussalam, Ahmed El Hassani, Sven Hartenfels & Heiko Hüneke

Fig. 1: The Eifelian (left minor cliff) to top-Frasnian (bent limestone in the middle ground) at Anjadam S of Mrirt, with Sarah Aboussalam (white cap) and Lahssem Baidder (red cap) for scale.

1. Introduction

The Mrirt region lies in the eastern part of the Western Meseta or of the Variscan Central Massif, close to the northwestern margin of the Middle Atlas. A locally dominant geographic feature is the Gara de Mrirt mountain (Fig. 2: Al Gara, 1534 m) ca. 6 km ESE of the Mrirt town, which is formed by tabular Miocene carbonates that overlie a strongly folded and faulted Devonian to Lower Carboniferous succession. The Palaeozoic of the Azrou-Mrirt-Khenifra region belongs to a system of nappes that originated from the East. These were thrusted during the main Variscan deformation phase onto the autochthonous Tanadra-Bou Tazert Unit (or Kasba Tadla-Azrou Anticline, autochthonous part of the Azrou-Khenifra Basin), which consists of contemporaneous strata (e.g., Huvelin 1970; Allary et al. 1972; Ribeyrolles 1976; Faik 1988; Bouabdelli 1989). The Ziar-Mrirt Nappe overlies the southern margin of the Azrou Nappe and ranges from the NW of Mrirt to the Ziar (= Ziyyar) region in the SW. South of Mrirt, it is overlain by the northern margin of the Khenifra Nappe (Fig. 3). The largest areas of the Ziar-Mrirt Nappe are occupied by Ordovician strata and Quaternary cover. Close to Mrirt, the folded Devonian is best exposed at

the SW foot of the Gara de Mrirt and at Anajdam to the SW (Figs. 2, 4). Viséan carbonates form a narrow strip of exposure at the Jebel Aouam (= Jbel Awam). An important Upper Viséan wildflysch outcrop is situated NW of Mrirt at the Jebel Tanoualt (Fig. 4). Ca. 20 km SW of Mrirt, near El Krad, lies the Devonian of the Akellal (or Brouha Ahallal) Plateau, which forms a steep eastern slope towards the main road from Mrirt to Khenifra.

Fig. 2: Geographic position of the Tibouda/Bou Ounebdou OuN) area at the SW slope of the Gara de Mrirt ("Al Gara"), of the Anjadam section SSW of Mrirt town (Anaj), and of the Jebel Aouma (= Jbel Awan) W of Mrirt (extract from topographic map 1 : 50 000, sheet NI-30-VII-1b Mrirt).

2. Research history

The Mrirt region became famous for Devonian fossils and strata since descriptions in the monograph by H. TERMIER (1936) on the geology of Central Morocco and the western Middle Atlas. Our summary concentrates on the allochthonous nappe succession, excluding the more western Devonian exposed in the Tighza (= Tirza) to Agarad-n-Azdaït (= Dechra Aït Abdallah) belt. The Devonian of the Jebel Bouchot shown in Fig. 4 belongs to the southern part of the Dechra Aït Abdallah zone. Especially famous for the allochthonous Mrirt Devonian are Famennian brachiopod limestones with the peculiar, relatively large-sized rhynchonellid genus *Dzieduszyckia.* These are supposed to represent "cold vent" (deeper marine methane seap) ecosystems (e.g., SANDY 1995; BALINSKI & BIERNAT 2003). Equally famous are good exposures of the two Kellwasser Limestones near the Frasnian-Famennian boundary (e.g., LAZREQ 1992a, 1999; RIQUIER et al. 2005, 2007). The Famennian provides text-book examples for re-sedimentation events related to Eovarican block faulting (e.g., WALLISER et al. 2000; HÜNEKE 2006, 2007).

The regional research history can be summarized as follows:

TERMIER (1927a, 1927b): First reference to the Gara de Mrirt area as a Devonian fossil locality based on the record of "*Gephyroceras intumescens*" (which may refer to any species of *Manticoceras*).

TERMIER (1936): Pioneer study of Hercynian Morocco with a description of Bou Ounebdou (= Bou Nebedou). Faunas include Frasnian *Manticoceras*, middle Famennian (Upper Devonian III) *Sporadoceras*, and upper Famennian (UD IV/V) goniatites ("cf. *Aganides sulcatus* = *Prionoceras* sp.) and clymeniids (*Laevigites hoevelensis* = *Clymenia laevigata* Group; *Gonioclymenia speciosa*), as well as nautiloids, bivalves, and brachiopods.

TERMIER (1936, 1938a) and TERMIER & TERMIER (1948, 1949, 1950a): Taxonomy and phylogeny of *Dzieduszyckia* species, then assigned to the genus *Halorella*; Bou Ounebdou as the type locality of *H. crassicostata*, *H. tenuicostata,* and *H. intermedia* (with three subspecies).

TERMIER & TERMIER (1950): Illustration of the suture of a *Gonioclymenia speciosa* from Bou Ounebdou (Bou Nebedou; Upper Devonian V-B).

ROCH (1950, p. 161): Reference to the occurrence of supposed *Manticoceras carinatum* and *M. intumescens* at Bou Ounebdou, reaching partly giant size (> 30 cm diameter).

AGARD et al. (1955): Recognition of uppermost Famennian ("Strunian") strata overlying Frasnian-Famennian cephalopod limestones on the Akellal Plateau.

AGARD et al. (1958): Silurian-Devonian transition and Middle/Upper Devonian succession of the Akellal Plateau, and Upper Viséan beds of the Jebel Aouam.

WILLEFERT (1963): Description of graptolites from around the Silurian-Devonian boundary of the Touchchent section (Akellal Plateau).

BIERNAT (1967): Re-assignment of the Bou Ounebdou *Halorella* species to the Polish genus *Dzieduszyckia*.

HOLLARD (1967): Brief summary of the Bou Nebedou succession (in fig. 4).

HOLLARD et al. (1970): Stratigraphic position of the *Dzieduszyckia* limestones, giving details for the Famennian of the Touchhent section (Akellal Plateau).

HUVELIN (1970, 1973): Structural geology and synsedimentary tectonics in the Mrirt region.

HOLLARD & MORIN (1973): New details for *Dzieduszyckia* occurrences in the Mrirt region, re-illustrating a cross-section for Bou Ounebdou from 1936, which (wrongly) suggests a synclinal structure at the top.

TERMIER et al. (1975): Brief reference to the Bou Ounebdou Upper Devonian and its faunas.

RIBEYROLLES (1976): Tectonics of the Aguelmous to Mrirt region.

BENSAID (1979): Reference to the Mrirt Devonien succession.

FRANCOIS et al. (1986): Silurian-Devonian transition at the Jebel Aouam.

FAIK (1988): Unpublished Ph.D. Thesis on the general stratigraphy and structural geology of the Mrirt region, with a subdivision of the regional Devonian into 10 units.

BOUABDELLI (1989): Unpublished Ph.D. Thesis on the structural geology of the Azrou-Mrirt-Khenifra region.

LAZREQ (1992a, 1992b, 1999): Upper Devonian lithostratigraphy, conodont stratigraphy, and biofacies of sections at Bou Ounebdou and Anajdam, with a focus on the Frasnian-Famennian boundary.

BECKER (1993a): Brief summary of Upper Devonian goniatite occurrences in the Mrirt region, mentioning a new record of paratornoceratids.

ZAHRAOUI (1994): Schematic lithostratigraphic column for the Emsian to Famennian assigned to the Bou Ounabdou Formation (sensu FAIK 1988).

FADLI (1994): Reference to the Frasnian of Anajdam and the Famennian and Tournaisian of Touchchent.

BOUBDELLI (1994): Tectonics of the Azrou-Khenifra region, showing a geological cross-section, including Anajdam.

BECKER (1993b, 1994), BECKER et al. (1997), and BECKER & HOUSE (2000): Upper Frasnian to middle Famennian nappe reconstruction, litho- and goniatite stratigraphy at Gara de Mrirt (= Bou Ounebdou), including the two Kellwasser Events, emphasizing similarities with the Montagne Noire succession of southern France.

WALLISER et al. (1995, 2000): Detailed litho- and conodont stratigraphy of the Tibouda-Bou Ouenebdou (sections Mrirt I-III) area and precise dating of Eovariscan xenosediments and reworking phases.

SANDY (1995): Re-interpretation of the *Dzieduszyckia* mass occurrences of the Mrirt area as examples for Mid-Palaeozoic cold seep chemosymbionthic habitats.

GIRARD & ALBARÈDE (1996): Investigation of trace element geochemistry of F-F boundary conodonts, comparing trends in sections of southern France and at Mrirt (Bou Ounebdou).

HÜNEKE (2001, 2006, 2007, 2013): Detailed description, conodont biostratigraphy, and microfacies of three Tibouda-Bou Ounebdou sections (MT, MG, and M), with a focus on synsedimentary (Famennian) tectonic instability, reworking, and on bottom current patterns.

FEIST (2002): Description of trilobites from the level between the two Kellwasser Limestones; Bou Ounebdou as type locality of the youngest known odontopleurid, *Gondwanaspis mrirtensis*, and of the proetid *Pteroparia ziegleri maroccanica*.

CHAKIRI (2002): Unpublished Ph.D. Thesis on the sedimentology of Devonian successions of the Meseta, including the Mrirt region and its Frasnian-Famennian boundary interval.

BALINSKI & BIERNAT (2003): Taxonomy and stable isotope geochemistry of Mrirt region *Dzieduszyckia*, including specimens from Touchchent and Bou Ounebdou (= Bou Nebedou).

FEIST (2003): Re-assignment of the proetid trilobite *Pteroparia ziegleri maroccensis* from Mrirt to the new genus *Chlupaciparia*.

DOPIERALSKA (2003, 2009) and DOPIERALSKA et al. (2015): Use of 17 Frasnian/Famennian samples from Gara de Mrirt for the analysis of neodymium isotopes in conodont phosphate, as a tool to reconstruct palaeoceanographic changes.

CRONIER et al. (2004): Use of *Acuticryphops* (Phacopida) material from Bou Ounebdou in a comparative morphometric study of trilobite eye ontogeny and variability.

GIRARD et al. (2005): First record of *Palmatolepis linguiformis*, index-species of MN 13b Zone (*Pa. linguiformis* Zone), at Mrirt (Bou Ounebdou).

RIQUIER et al. (2005, 2007): Isotope and trace metal geochemistry and magnetic susceptibility of the Frasnian-Famennian boundary beds at Bou Ounebdou and Anajdam.

AVERBUCH et al. (2005): Whole rock geochemistry across the F-F boundary.

GIRARD & RENAUD (2007): Use of conodonts from the Kellwasser Beds at Gara de Mrirt in a quantitative study of morphometry, abundance, and generic distribution patterns as the base for correlations at the Frasnian-Famennian boundary.

BAMOUMEN et al. (2008): Sedimentary, magmatic and tectonic history of the Upper Viséan of the Azrou-Khenifra Basin, with a geological cross-section at the Jebel Tanoualt (= Tanwalt) ca. 7 km NE of Mrirt.

GIRARD & RENAUD (2008): Use of Mrirt populations of the common conodont *Ancyrodella curvata* in a study of growth allometry and extinction patterns at the Frasnian-Famennian boundary.

RAJI & BENFRIKA (2009): Conodont alteration index variability of the Mrirt Devonian suggesting overprints by hydrothermalism.

GIRARD et al. (2010): Inclusion of *Palmatolepis* assemblages from the Kellwasser Beds at Bou Ounebdou in a statistical study on uppermost Frasnian relationships between morphometry and palaeobiogeography.
TAHIRI et al. (2011): Summary of the Gara de Mrirt geology as Stop 29 of an excursion guide through the northwestern Meseta.

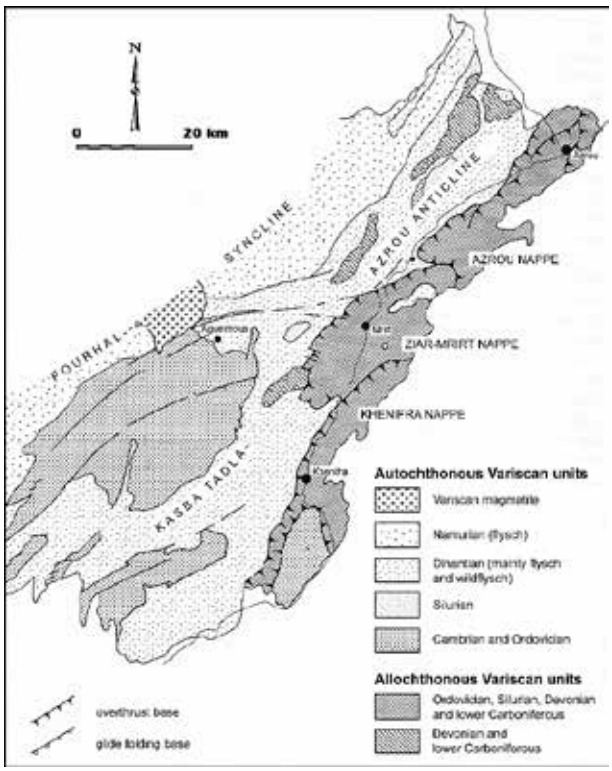

Fig. 3: Overview of the tectono-sedimentary units in the eastern part of the Central Massif, showing the position and outline of the Ziar-Mrirt Nappe (HÜNEKE 2001, fig. 41).

LE HOUEDEC et al. (2013): Oxygen isotopes and Sr/Ca ratios in conodonts across the F-F boundary, comparing trends at Coumiac (southern France) and Mrirt.
BALTER et al. (2019): Use of Upper Devonian conodonts from Mrirt in a calcium isotope study that addresses the general question of the trophic position of conodonts in Palaeozoic ecosystems.
FEIST (2019): Description of the basal Famennian phacopid *Nephranops* from Bou Ounebdou.

3. Palaeogeographic setting

The distance of post-sedimentary westward transport of the Azrou-Mrirt-Khenifra nappes is currently unclear but it is assumed that Devonian deposition took place in the eastern part of a joint Azrou-Khenifra Basin. Synsedimentary block faulting occurred throughout the basin in the middle Givetian to lower Frasnian, middle/upper Famennian, and in the Tournaisian to Middle Viséan but the nappe movement post-dated these Eovariscan events and occurred during the main Variscan tectophase at the end of the Lower Carboniferous. Within the Ziar-Mrirt Nappe, all Devonian to Tournaisian sediments are characteristic of an outer shelf hemipelagic to pelagic setting, with condensed limestones alternating during eustatically driven deepening episodes with grey-green shales, marls, or black shales. Neritic carbonates and biostromes/reefal buildups are restricted to the Dechra Aït Abdalla region, which formed the western part of the Azrou-Khenifra Basin.

4. General succession (Fig. 5)

The Ziar-Mrirt Nappe does not represent a homogenous sedimentary unit. There are both similarities and differences between the Ziar, Anajdam, and Bou Ounebdou successions, and the latter consists of a stack of smaller-scale nappes (e.g., BECKER & HOUSE 2000). The Anajdam section lacks thick conglomerate/breccia units, which probably led to the assignment as a parautochthonous unit in FADLI (1994). All of the Ziar-Mrirt Nappe is characterized by significant episodes of non-deposition, with a main interval in the lower/middle Givetian.

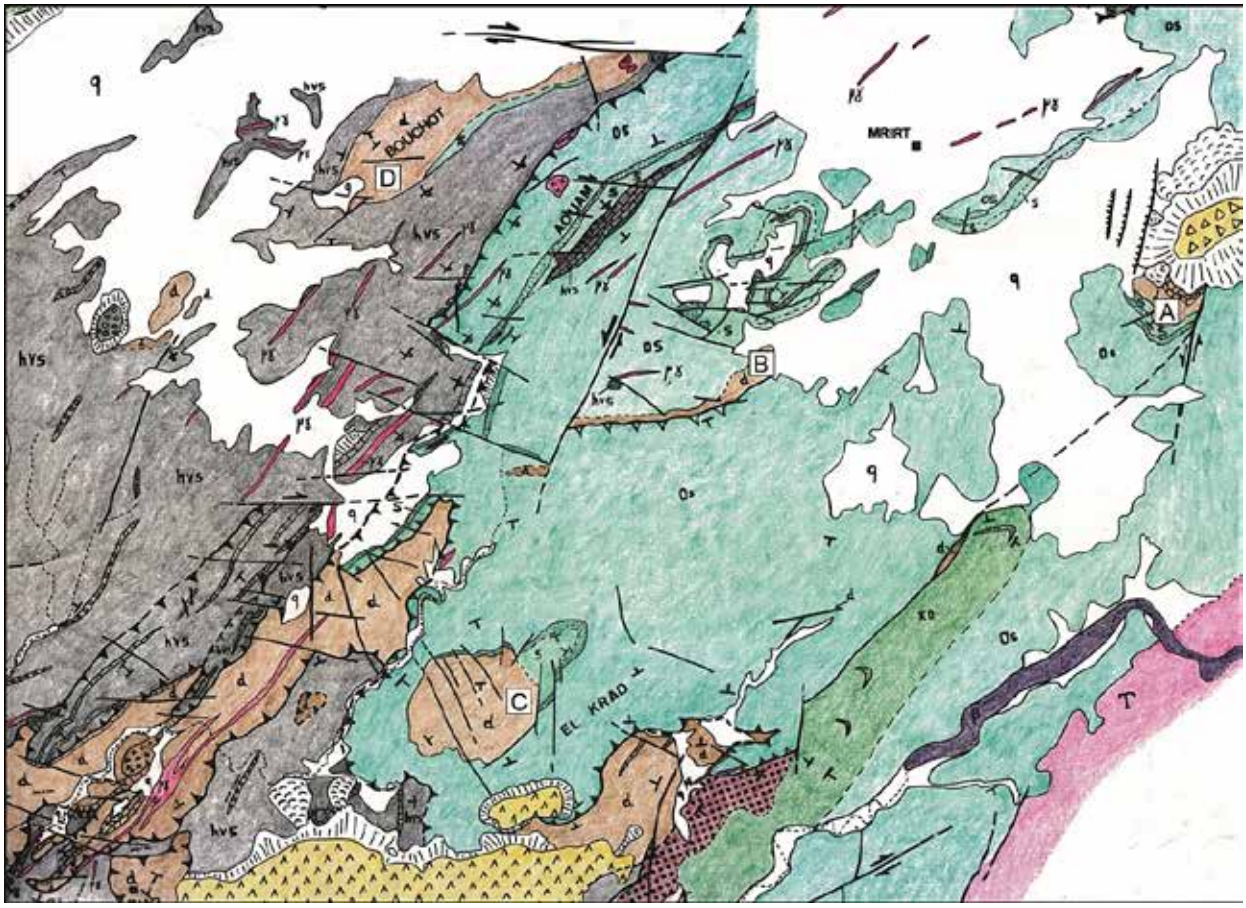

Fig. 4: Geological map of the Mrirt region based on surveys of M. RIBEYROLLES and A. LAVENU (see RIBEYROLLES 1976), showing the position of Devonian outcrops of the Gara de Mrirt (A), Anajdam (B), of the Akellal Plateau (C) around El Krad, and the Jebel Bouechot (D; Dechra Aït Abdallah Devonian outside the Ziar-Mrirt Nappe). KO = Cambro-Ordovician, Os = Upper Ordovician, S = Silurian, d = Devonian, hvS = Upper Viséan, red areas (μγ) = Hercynian rhyolites, microgranites, and granites, red area with black dots = Permian (Autunian), T = Triassic, yellow top of the Gara de Mrirt = Miocene, yellow Λ = Tertiary volcanics, ß = Quaternary basalts, q = Quaternary.

Upper Givetian and Frasnian condensed pelagic limestones and calcareous contourites are associated with further hiatuses. Both erosional and depositonal features are caused by bottom-current induced reworking and redepositon during times of overall regression. Widespread occurrence of Famennian density-flow and rock-fall deposits probably reflect uplift by block faulting, leading to increased slope instability and gravity-induced resedimentation Typical lithofacies and faunas of the Ziar-Mrirt Nappe, for example the *Dzieduszyckia* limestones, griotte blocks, and Kellwasser limestones, compose many olistolites in the Upper Viséan of the Khenifra area, for example at the Jebel Tabainout (e.g., see MULLIN et al. 1976 and AGER et al. 1976). This suggests close palaeogeographic relationships within the Azrou-Khenifra Basin, prior to nappe emplacements. All sediments were subject to significant diagenesis but the illite crystallinity data and conodont colors (CAI) suggest that the regional burial temperature did not exceed 250° (DOPIERALSKA 2003; RIQUIER et al. 2007).

The upper Silurian-lower Lochkovian transition of the Ziar-Mrirt Nappe is charackterized by fissile, graptolite-rich black shales and local *Scyphocrinites* Limestone (e.g., AGARD et al. 1958; FRANCOIS et al. 1986). Apart from monograptids and lobolites, phyllocarid shields, orthocones, and pelagic bivalves have been reported from this interval.

The higher Lochkovian and Pragian consists of grey calcareous shales and thin-bedded nodular limestones. TERMIER et al. (1975) introduced the term **Bou Nebedou Formation** (= Bou Ounabdou Formation in FAIK 1988) for the pelagic strata of the Mrirt region, which is here subdivided into a new lower (Lochkovian to Eifelian/middle Givetian; pre-unconformity) **Anajdam Member** and a younger (top-Givetian to upper Famennian, post-unconformity) Mrirt Member. Both include numbered new submembers. Whilst the Lochkovian is difficult to recognize by faunas, a Pragian age (in the classical sense) for upper parts of the predominantly argillaceous **Submember A** (Lochkovian to Pragian) is proven by the index dacryoconarid *Nowakia (Turkestanella) acuaria* (FRANCOIS et al. 1986) and by the conodont *Caudicriodus* aff. *curvicauda* (WALLISER et al. 2000) from interbedded thin limestone. Locally (Jebel Aouam region), there is a typical Pragian trilobite fauna with the phacopid *Reedops*, the cheirurid *Crotalocephalus*, odontopleurids, harpids, and proetids. Such assemblages, however, also could be of basal Emsian age. For example, *Odontochile*, which was recorded from Sidi Bou Ignousen (AGARD et al. 1958), and which may refer to a species of the related genus *Zlichovaspis*, is characteristic for the Pragian-Emsian transition of the Anti-Atlas (e.g., HOLLARD 1978; BECKER et al. 2004; DE BAETS et al. 2010).

As noted above, the Pragian/Emsian boundary is difficult to place in the region, especially since there are so far no reports of lower Emsian marker conodonts. A locally developed silty/sandy interval (Unit B of WALLISER et al. 2000, **Submember B**) may reflect one of the lower Emsian eustatically controlled regressions. More typical, and following above, are thin bedded, poorly fossiliferous (almost no conodonts) alternations of light-grey calcareous shale and flaserlimestone (Unit C of WALLISER et al. 2000, **Submember C**).

Submember D of the Anajdam Member is a thick dark shale unit, which has been correlated by WALLISER et al. (2000) with the Bohemian Daleje Shale of the basal upper Emsian. Equivalent is a very distinctive, green to dark-grey shale unit with (primary) pyritic pelagic faunas in the Tafilalt (Unit K of the Amerboh Formation, see BECKER et al. 2013, 2018a). Sedimentary similarities between the eastern Anti-Atlas, Tinejdad allochthon (WARD et al. 2013), Skoura region (see below), and the Mrirt area support the concept of a continuous sedimentary basin stretching from the cratonic Anti-Atlas to the central Meseta during the Emsian.

Submember E of the Anajdam Member consists of the next higher alternation of grey shales, nodular shales, and thin flaser limestones. The report of juvenile *Icriodus angustus* and *Now. (Now.) richteri* (WALLISER et al. 2000) and a reference to the occurrence of anarcestids at Touchchent (HOLLARD & MORIN 1973) give an upper Emsian age. **Submember F** begins with more solid flaserlimestones, which yielded upper Eifelian conodonts in higher parts, at the transition towards alternating shales, nodular shales, silty shales, and nodular limestones. Locally there are dark shales that are rich in dacryoconarids (HOLLARD & MORIN 1973: Touchchent).

So far, there are no index conodonts or other fauna of the lower to main middle Givetian for all of the Ziar-Mrirt Nappe. WALLISER et al. (2000) mention a single conodont fauna with *Linguipolygnathus linguiformis*, the *Po. varcus* Group, and "*Polygnathus* sp. aff. *Po. bryanti*". The latter taxon may refer to a relative of *L. transversus* that is typical for higher parts of the middle Givetian.

The new **Mrirt Member** (= "Calcaires à *Manticoceras*" in FAIK 1988 and ZAHRAOUI 1994) begins with the upper part of the upper Givetian (*Po. cristatus ectypus* to

Skeetognathus norrisi Zones). There are either condensed grey micrites or dark-grey shales with lenticular, dark limestones, which represent the **Lower Frasnes Event** Interval (**Submember 1**; BECKER 1993b). Extreme condensation and sedimentary gaps are the rule and continue in the lower/middle Frasnian (MN 3-9 Zones). Bigradational micro-sequences of calcilutites, calcisitites and calcarenites represent calcareous contourite deposits. Most indicative are cross-laminated styliolinid grainstones. These contourites, together with repeated periods of non-deposition and even erosion, reflect variably strong influences of deep-marine bottom currents (HÜNEKE 2006, 2007).

Submember 2 is characterized by solid, light-grey flaserlimestones with abundant goniatites (manticoceratids, beloceratids) that range from the *Palmatolepis plana* Zone (MN 10 Zone) to the *Pa. winchelli* Zone (upper MN 12 Zone; see LAZREQ 1992a, 1999). The interval from the base of the dark-grey, organic-rich Lower Kellwasser Limestone (LKW, top MN 12 Zone with *Ancyrognathus asymmetricus*) to the top of the dark Upper Kellwasser Limestone (UKW, top-Frasnian) forms the new **Submember 3**, which can be subdivided into the LKW, intra-KW, and UKW beds. The LKW is developed as a solid, rather prominent marker bed whilst the UKW is more recessive and less solid, just as on the outer shelf carbonate platform of the Mt. Peyroux Nappe of the southern Montagne Noire (BECKER et al. 1989; BECKER 1993a, 1993b; BECKER & HOUSE 1994, 2000a).

Submember 4 includes basal Famennian solid, light-grey thin-bedded limestones, followed by a thick package of nodular shales and limestones, in the upper part with abundant cheiloceratids. This succession represents pelagic accumulation. It is a clear equivalent, both in terms of lithology and biofacies, of the "vrai griotte" of the Montagne Noire (see FEIST 1985; "Calcaire griotte" in FAIK 1988 and in the summary log of ZAHRAOUI 1994, fig. 13).

Synsedimentary block faulting led to local uplift, reworking of Frasnian to lower Famennian limestones, and the gravity-induced re-deposition of dm- to m-sized clasts within laterally restricted mass and debris flow deposits (griotte conglomerates, Fig. 6, and polymict breccias with chaotic bedding). WALLISER et al. (2000) distinguished transported, early lithified xeno-sediments, which are not part of the normal succession. Examples are reworked dark Kellwasser limestones or *Dzieduszyckia* coquinas. HOLLARD et al. (1970) and HOLLARD & MORIN (1973) suggested that the latter may be normally embedded within the higher part of the lower Famennian but we did not encounter autochthonous occurrences in the studied sections (see WALLISER et al. 1995). The first main reworking phase related to Eovariscan block movements started in the Ziar-Mrirt Nappe at the end of the lower Famennian (Upper *rhomboidea = Pa. gracilis gracilis* Zone sensu SPALLETTA et al. 2017; locally with *Pa. quadrantinodosa inflexa, Pa. minuta schleizia*, and *Pa. stoppeli*). It lasted into the lower part of the middle Famennian (*Pa. marginifera marginifera* Zone; WALLISER et al. 2000; HÜNEKE 2001).

The base of **Submember 5** is marked in undisturbed sections by a sudden change from nodular griotte to more solid, light grey micrites with ammonoids (e.g., *Maeneceras*; HOLLARD et al. 1970), as at the base of the "supragriotte" (Upper Member of the Griotte Formation) in the Montagne Noire. It is highly unlikely that this similarity is a coincidence; it reflects deposition in a wide, single, continental shelf basin that stretched from the source region of the Ziar-Mrirt Nappe to southern Europe (BECKER & HOUSE 2000a), without interruption by a true oceanic area. The strong similarity of the Mrirt and Montagne Noire Upper Devonian clearly rejects ideas that the

Meseta had a synsedimentary plate tectonic position to the West of Iberia or far to the East of the European Variscides.

Based on typical goniatites and clymeniids, the flaserlimestone deposition lasted at least until high in Famennian IV (*Po. styriacus* to *Pa. gracilis expansa* Zones). Isolated records of index clymeniids of Famennian V (Dasbergian; TERMIER 1936: *Gonioclymenia* and *Clymenia*), a thin detrital limestone with conodonts of the upper Famennian *Bispathodus costatus* (Sub)Zone (LAZREQ 1992a, 1999), and reworked conodonts of the uppermost Famennian *B. ultimus ultimus* Zone (HÜNEKE 2001) suggest that the pelagic carbonate platform (or the Mrirt Member) continued originally ca. until the Hangenberg Crisis (HÜNEKE 2006). However, its upper part has widely been cut off by the second major episode of Eovariscan erosion and re-sedimentation.

The subsequent, variably thick succession of pebble rudstones/conglomerates, coarse, polymict breccias, and isolated olistolites, which often alternates with fossil-poor, olive-green shales, is here named after the main mountain E of Mrirt, as the new **Al Gara Formation**. Since it includes individual clasts that consist internally of conglomerates/breccias, there was clearly a second generation of reworking, which cannibalized the older, Famennian reworking units. Rock fall and various types of density flows have caused the resedimentation. The type locality is Section M of HÜNEKE (2001). There, the formation reaches a thickness of ca. 30 m. On the Akellal Plateau to the S, a comparable conglomerate/breccia lies with an angular unconformity on the Famennian succession (AGARD et al. 1955; HOLLARD & MORIN 1973). This proves a significant synsedimentary block tilting in the nappe source area. While it is possible to date precisely the age of individual clasts/olistolites (top-Givetian to uppermost Famennian), the precise (second) re-deposition age is less clear. A single, autochthonous solitary rugose coral recovered from the green shale matrix at Bou Ounebdou suggests a Lower Carboniferous age. This is supported by sparse miospore evidence (MARSHALL in BECKER et al. 1997: Viséan).

Conglomerates of the Dechra Aït Abdallah allochthon W of Mrirt yielded "Strunian" brachiopods, especially *Syringothyris*, a marker genus of the post-Hangenberg Extinction interval (e.g., ZONG et al. 2015). The co-occuring trilobite *Pudoproetus* enters at the same level (transgressive Upper Hangenberg Crisis Interval) in the Tafilalt (HAHN et al. 2016) and elsewhere. However, it is unclear whether the very different Mrirt conglomerates/breccias and olistolites have the same re-deposition age (see brief discussion in AGARD et al. 1958). At the Bou Khedra between Mrirt and Azrou (BOUABDELLI 1994), a lithologically similar package of green shales overlies with a strong angular unconformity a thick Lower Devonian succession. At the base, it contains clasts of reworked Givetian limestone. This un-named green shale is overlain by conglomerates, quartzites, and sandstones, the Bou Khadra-Afoud Formation, which yielded Upper Tournaisian brachiopods in higher parts (BOUABDELLI 1989; ZAHRAOUI 1994). Much younger are the breccias and large olistolites that include the same Upper Devonian lithofacies and faunas as at the Bou Ounebdou, again with reworked conglomerates, in the SE of the Jebel Tabainout W of Khenifra (LAVENU 1976; MULLIN et al. 1976). These klippen are part of a wildflysch that deposited above Upper Viséan shallow-water limestones with corals (ARETZ & HERBIG 2010).

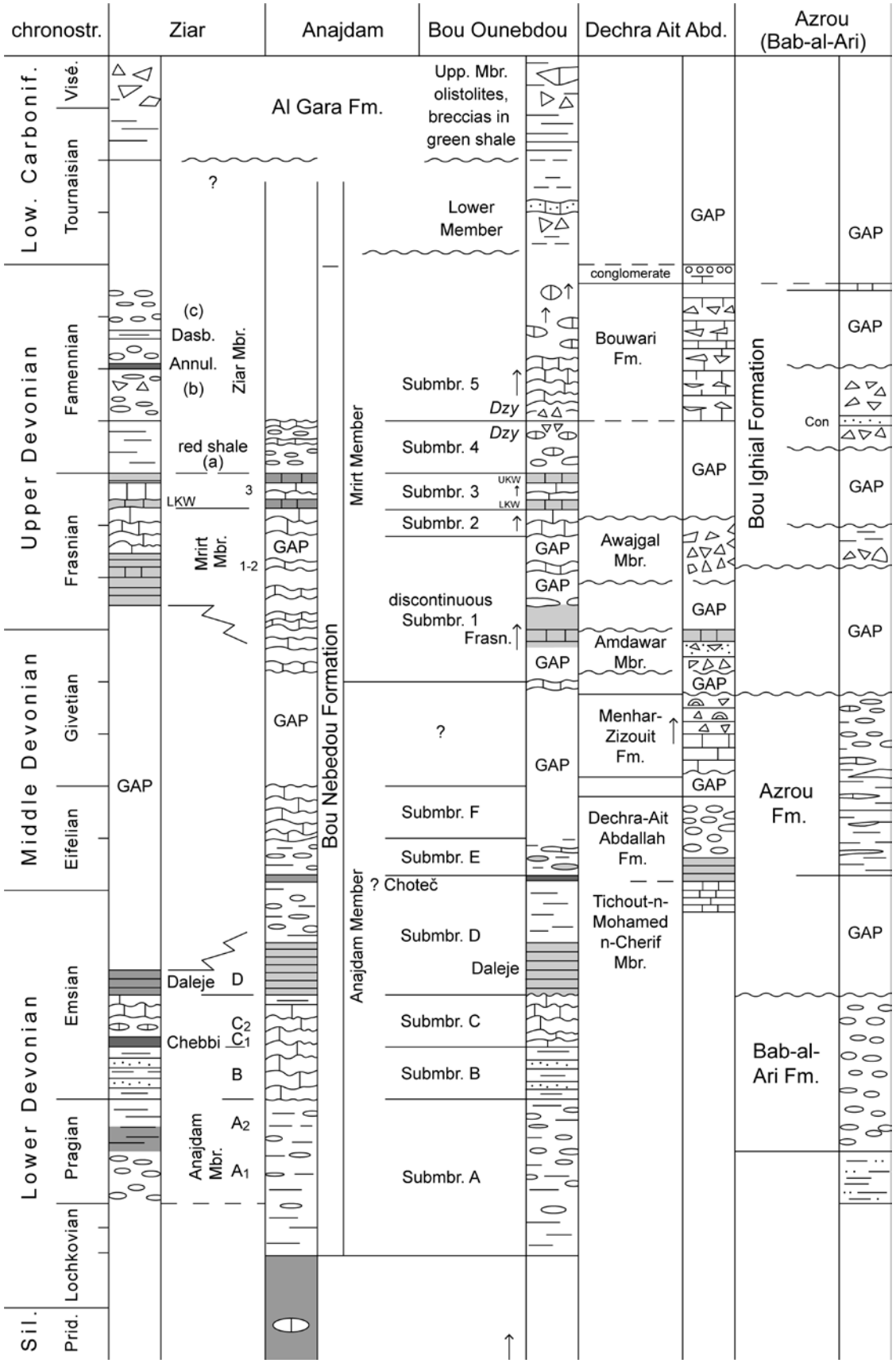

Fig. 5: Comparison of the general Devonian succession of the Ziar-Azrou Nappe (seperate for Ziar, Anajdam, and the Bou Ounebdou) with the Devonian of the Dechra Aït Abdallah W of Mrirt. *Dzy* = *Dzieduszyckia*, Frasn. = Frasne Event, LKW/UKW = Lower and Upper Kellwasser levels, Con = Condroz Events, Annul. = *Annulata* Event, Dasb = Dasberg Event.

Fig. 6: Massive lower Famennian "griotte conglomerate" (lobe-shaped deposit of a gravity flow/non-cohesive debris flow) overlying greenish-grey calcareous shales with flat limestones nodules at Bou Ounebdou, eastern end of Hill A, lower section (ca. section MG of HÜNEKE 2001).

Fig. 7: View from the Anajdam section towards the NW, showing top-Silurian black shales with abundant graptolites in a small gully in the midground to the left, a gentle slope formed by poorly exposed Lochkovian/Pragian calcareous shales and thin limestones (Bou Nebedou Formation, Anajdam Member, Submember A), and the base of the supposedly basal Emsian minor limestone cliff to the right (Submember B).

Regional comparisons suggest that different parts of the original Azrou-Khenifra Basin were affected by individual block movements. This happened repeatedly and partly at different times in the long Famennian to Viséan interval. This led to facies differentiation of adjacent tectonic units.

5. Anajdam

5.1. Location

The Anajdam section lies on topographic sheet Mrirt, NI-30-VII-1b, 1 : 50 000, along a minor hill and settlement at the coordinates x = 481.25, y = 281.58, ca. 5 km SE of Mrirt. So far, only the Upper Devonian succession has been published in detail (e.g., LAZREQ 1992a, 1999; RIQUIER et al. 2005, 2007). It is the type-section of the Anajdam Member of the Bou Nebedou Formation. Our new logging started with the first more solid nodular limestones (Figs. 7-8) and ended in the basal Famennian.

5.2. Lower Devonian

A small gully NW of the measured section exposes graptolite-rich, fissile black shales with large pyrite nodules of the upper Silurian to basal Devonian (Fig. 7). The local graptolite fauna has not yet been analysed. The shaly to silty **Submembers A/B** at the base of the **Anajdam Member** are poorly exposed. The detailed section log of Fig. 10 begins with thin-bedded shales and dacryoconarid-rich (Fig. 9), relatively dark, yellowish weathering nodular limestones (bioclastic wackestones) of **Submember C**, which form a small cliff within the northern hill slope (Fig. 8). The lack of dacryoconarid orientation (e.g., in Beds 1b and 5) and their abundance prove a eutrophic, quiet outer ramp setting with low sedimentation rate. Slumping as indicator of synsedimentary tectonics occurs in Bed 2. Conodont samples were barren (Bed 1b) or yielded only rare icriodid fragments (Bed 5), which are too poor to confirm the assumed lower Emsian age. Bed 5 is a partly microsparitic, bioturbated styliolinid wacke- to packstone with some ostracods. Above lie ca. 1.5 m of greenish-grey silty shales (Bed 6).

The transition to darker shales marks the base of **Submember D**, the assumed local Daleje Shale Equivalent. It contains numerous slump blocks consisting of fine crystalline, dark to middle grey limestone, which are partly laminated (e.g., at the top of Bed 10).

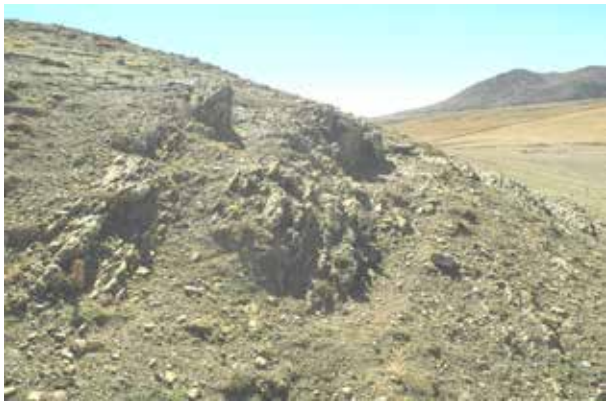

Fig. 8: Supposed lower Emsian cliff (Anajdam Member, Submember C, Beds 1-5, ca. 6.3 m thick) consisting of thin-bedded, nodular, unfossiliferous limestone with some slumping as evidence of tectonic instability.

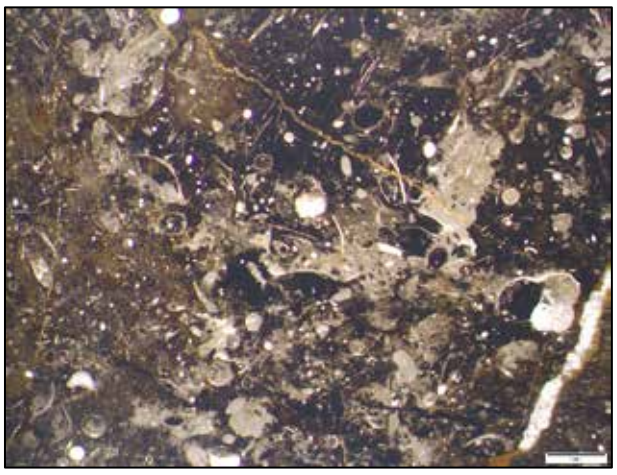

Fig. 9: Microfacies of Bed 1b, a bioturbated bioclastic wackestone to floatstone with abundant dacryoconarids, shell filaments, crinoid remains, and gastropods, floating in a rather dark, variably C_{org}-rich micrite matrix (scale bar = 1 mm).

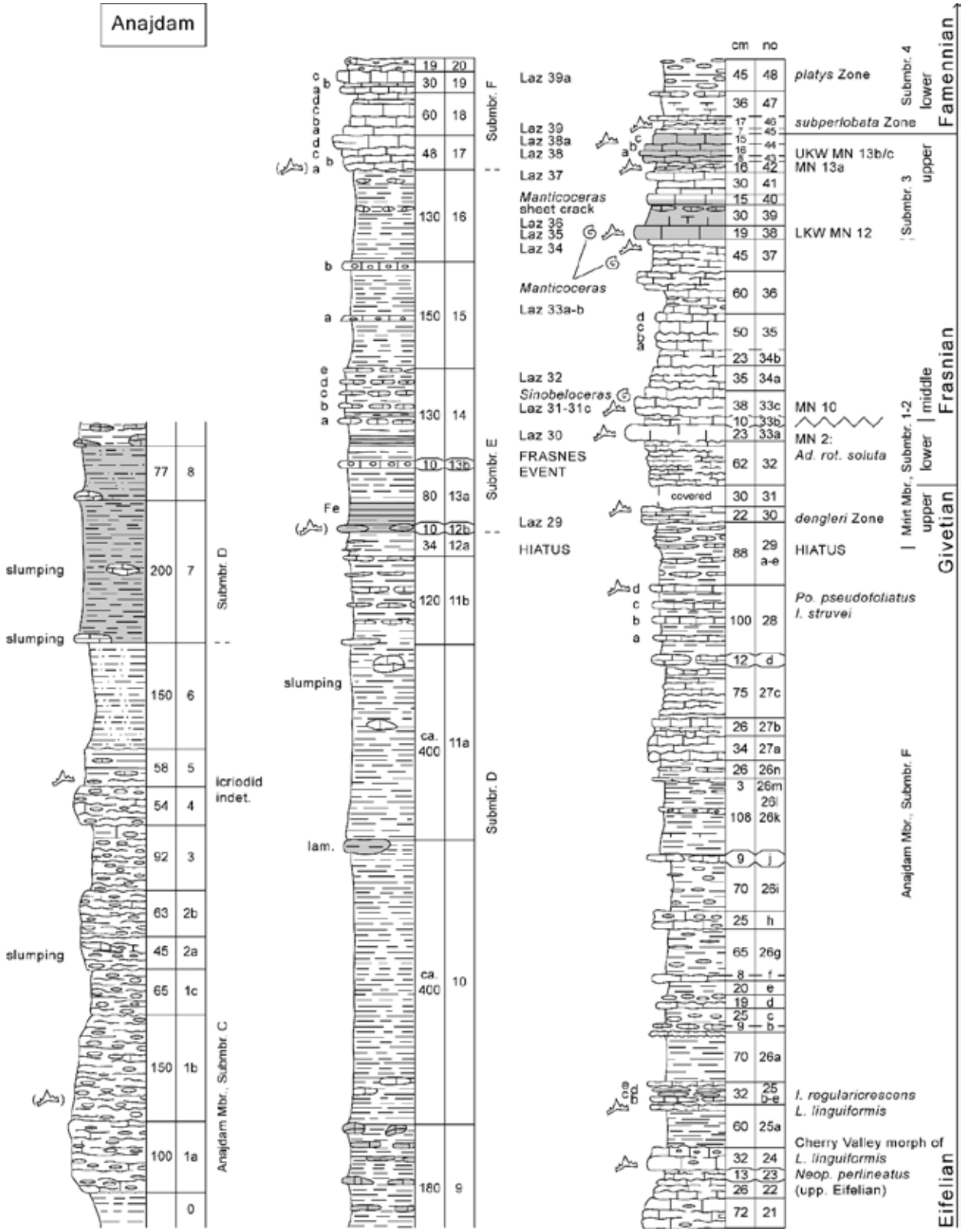

Fig. 10: Emsian to basal Famennian litho-, chrono-, conodont and event stratigraphy at Anajdam, showing the position of barren (in brackets) and productive conodont samples, identified conodonts or conodont zones, and the correlation with the samples of LAZREQ (1992a, 1999).

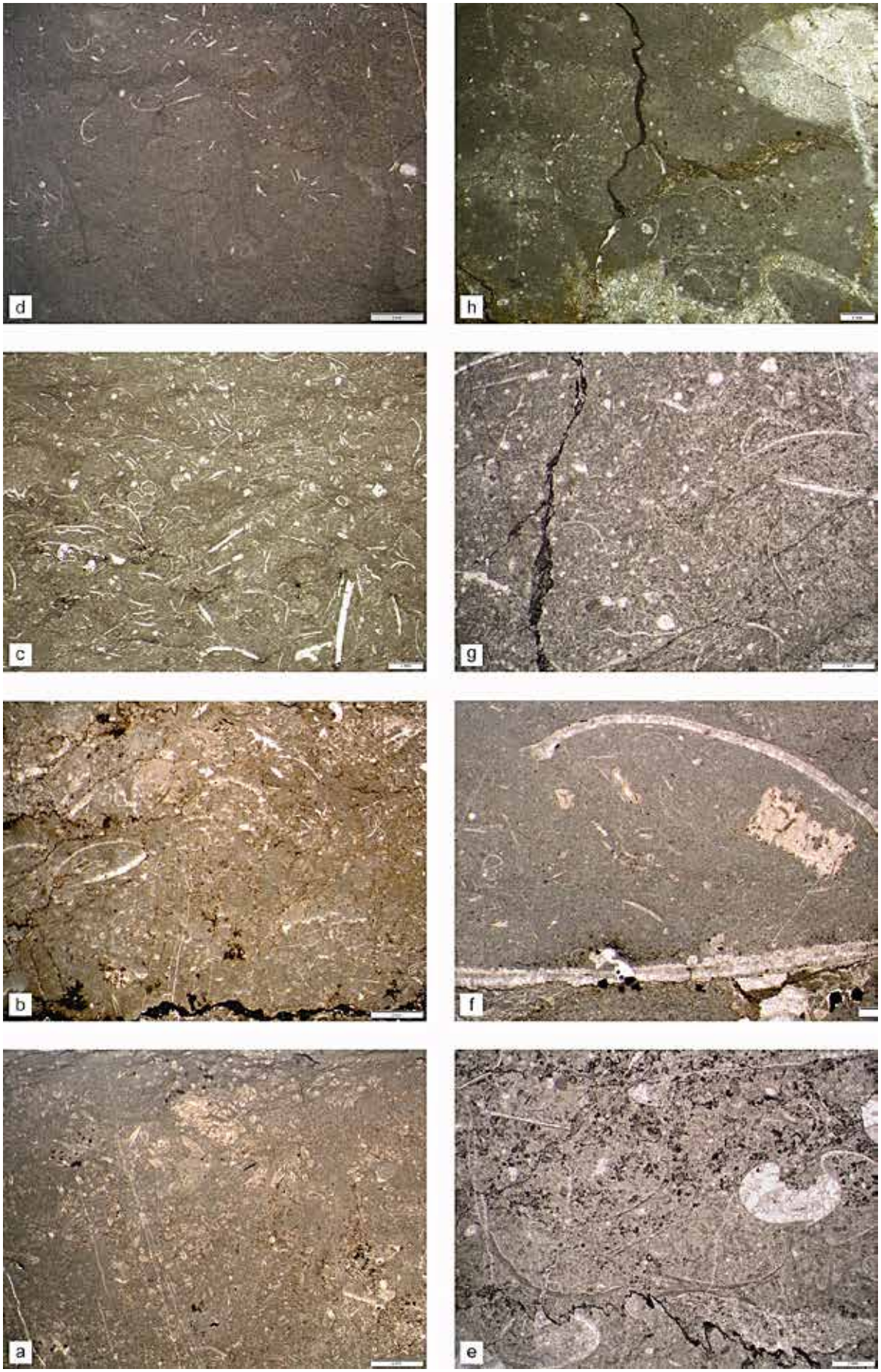

Fig. 11

Fig. 11: Thin-sections showing characteristic microfacies of the Mrirt Member at Anajdam. **a.** Styliolinid packstone, Bed 30, top-Givetian (*Po. dengleri dengleri* Zone); **b.** Recrystallized styliolinid wackestone with mollusk debris, Bed 33a, lower Frasnian (MN 2a Zone, *Ad. rotundiloba soluta* Subzone); **c.** Bioturbated styliolinid wackestone with gastropods, ostracods, mollusk, and trilobite debris, Bed 33c, top-middle Frasnian (MN 10 Zone, *Pa. plana* Zone); **d.** Mudstone with some shell debris, Bed 45, upper Frasnian (immediately below LKW, MN 12 Zone, *Pa. winchelli* Zone); **e.** Strongly recrystallized, sparitic wackestone with goniatites and mollusk debris, showing a stylolithic dissolution seam in the lower part LKW, Bed 38 (top MN 12 Zone with *Ag. asymmetricus*); **f.** Mud-wackestone with large, crushed cephalopod shells (with a basal dissolution seam of the lower shell), crinoid pieces, and dispersed, fine hematite, Intra-KW limestone, Bed 42, top-Frasnian (MN 13a Zone, *Pa. bogartensis* Zone); **g.** Recrystallized wackestone (microsparite) with tentaculitoids, ostracods, and large mollusk debris, upper part of UKW, topmost Frasnian, Bed 44c (MN 13b/c Zone, *Pa. linguiformis* Zone); **h.** Strongly bioturbated mud-wackestone, partly with washed out micrite matrix, basal Famennian, Bed 45 (*Pa. subperlobata* Zone). Scale bar = 2 mm, except for d and h (1 mm); for further explanations see text.

5.2. Middle Devonian (Eifelian)

Submember E begins with a thin, distinctive interval of black shale with limestone (Bed 12b: a strongly recrystallized microsparite with some crinoid ossicles) and limonite concretions (lower Bed 13a). In the absence of fauna (barren conodont sample), it can only be speculated whether this level represents the global Choteč Event. Above, there are alternating lighter grey shales and thin nodular limestones (Beds 14-16). **Submember F** starts with more solid limestones (Beds 17-24). At the base, Bed 17 lacks conodonts and is a poorly fossiliferous mud-wackestone with styliolinids, rare ostracods, crinoid, and trilobite debris. It was deposited on a deep outer shelf ramp. At the top of this interval, Bed 24 yielded the Cherry Valley Morphotype of *L. linguiformis*. The Cherry Valley Limestone of New York State falls in the upper Eifelian. This supports the assumption that Submembers E and F represent the lower part of the Middle Devonian. Records of *L. linguiformis* and *I. regularicrescens* from the top of Bed 25a agree with this interpretation. The second species enters ca. in the middle part of the *Po. costatus* Zone with *Po. pseudofoliatus* and ranges into the Givetian. The change from solid to more thin-bedded limestones and an increase of shales/marls above Bed 24 reflect a slight deepening but the thin limestones continue the microfacies from below. Accordingly, Bed 25a is a bioturbated, styliolinid-rich bioclastic wackestone with a partly microsparitic matrix. Until there are better biostratigraphic data, we hesitate to correlate the local minor deepening with one of the upper Eifelian eustatic signals. A small conodont fauna from the top of Submember F (Bed 28d) still consists of typical Eifelian polygnathids (*Po. pseudofoliatus*) and icriodids (*I. struvei*) while normally common Givetian members of both genera are lacking. Therefore, we assume that all of the lower/middle Givetian is locally missing in a disconformity due to non-deposition (long-lasting, strong bottom current activities). The microfacies of Bed 28d is characterized by an increase of the styliolinid content, which supports the interpretation of increasing condensation and a reduced deposition and washing out of fine micrite.

5.3. Top-Givetian/Famennian (Mrirt Member)

Although there is no evidence for any faulting or unconformity, Bed 30, the base of the **Mrirt Member** (**Submember 1**), shows a significant stratigraphic jump from the top-Eifelian (of Bed 28d) to the top-Givetian, either within Bed 29 or at the base of Bed 30 (Fig. 10). The microfacies (Fig. 11A), a styliolinid packstone with only minor micrite matrix, provides support for a strongly reduced

sedimentation rate. The conodont assemblage of Bed 30 is rich and diverse:

Linguipolygnathuis linguiformis Morph A* (rare)
*Linguipolygnathus weddigei** (rare)
Polygnathus varcus (rare)
Polygnathus dubius (moderately common)
Polygnathus ordinatus (rare)
Polygnathus cristatus ectypus (rare)
Polygnathus dengleri dengleri
Polygnathus paradecorosus (common)
Polygnathus pollocki (rare)
Polygnathus webbi
Polygnathus pennatus
Polygnathus "collieri Morph 2" (moderately common)
Ctenopolygnathus angustidiscus (moderately common)
Klapperina disparilis (common)
Schmidtognathus peracutus
Schmidtognathus gracilis (rare)
"Ozarkodina" proxima (rare)
"Ozarkodina" sannemanni (moderately common)
N. Gen. n. sp.
Icriodus difficilis
Icriodus expansus
Icriodus aff. *obliquimarginatus*

The fauna falls clearly in the *dengleri dengleri* Subzone of ABOUSSALAM & BECKER (2007). The rare linguipolygnathids are regarded as having been reworked. They indicate that lower/middle Givetian strata once deposited in the area, but these were eroded during subsequently increasing bottom-current intensity, which also caused the strong condensation. The listed new genus is the same unusual form as described in ABOUSSALAM (2003) as *?Skeletognathus* n. sp. Two fragmens of middle Frasnian conodonts suggest a minor stratigraphic leak from above. LAZREQ (1992a, 1999) placed her corresponding Samples 29 and 29a in the old *Schmidtognathus hermanni-cristatus* (now *cristatus ectypus*) and *Klapperina disparilis* Zones. This suggests that slightly older upper Givetian strata are preserved laterally within the extremely condensed succession. She also reported *Linguipolygnathus* and a few other polygnathids, such as *Po. xylus* and *Po. ovatinodosus*. The latter two species are known to range into the upper Givetian and lower Frasnian.

Whilst there is so far no record of the terminal Givetian *Skel. norrisi* Zone, the basal Frasnian has been found by LAZREQ (1992a, 1999) in her Samples 30/ 30a. The MN 1 Zone was proven by the index taxon *Ad. rotundiloba pristina* and by supposed *Ad. rotundiloba binodosa* (?juvenile *pristina* specimens). An unusually early *Mesotaxis asymmetrica* record refers to a strongly ornamented form that is somewhat transitional towards *Po. cristatus cristatus* (see LAZREQ 1999, pl. 3, figs. 1-2). Our Bed 33a yielded *Ad. rotundiloba soluta*, the index species for the lower part of the MN 2 Zone. (*Ad. rotundiloba soluta* Subzone), in association with *Po. alatus* and other polygnathids that continue from below. The bed is a microsparitic styliolinid wackestone with mollusk debris, dispersed hematite, and partly washed out micrite matrix (Fig. 11b). This suggests condensed, slightly dysoxic deposition on a subphotic outer shelf ramp.

A significant gap, extending from the higher part of MN 2 Zone (*Ad. rotundiloba rotundiloba* Subzone) to MN 9 Zone (*Pa. proversa* Zone) follows in our section. LAZREQ (1992a, 1999), however, found a thin development of the *Pa. transitans* (MN 4 Zone), *Pa. punctata* (MN 5/6 Zones), and *Pa. hassi* Zones (ca. MN 7-9 Zones) in her lateral Samples 30b-f. **Submember 2**, the Calcaires à *Manticoceras* of FAIK (1988), includes the thin Beds 33b-37. Some light grey, bioturbated micrite beds are very rich in corroded gephuroceratids (Fig. 13). Loose material include a new relative of *M. intermedium* with relatively wide and deep umbilicus (Fig. 14B). Near the base, Bed 33c is a fossiliferous wackestone (Fig. 11C) with styliolinids, gastropods, other mollusk debris, trilobite remains, and subordinate ostracods.

Fig. 12: The somewhat disconformable contact (angular bedding or slumping) between the topmost Givetian (Bed 30 with hammer, *Po. dengleri dengleri* Zone) and the basal Frasnian (MN 2a or *Ad. rotundiloba soluta* Zone recognized in the thick Bed 33a). The overhanging Bed 33c falls already in the top middle Frasnian (MN 10 Zone), indicating a long interval of non-deposition (late lower Frasnian to main middle Frasnian). The same applies to the succession below Bed 30, where there is no evidence for the lower/middle and early upper Givetian.

Fig. 13: Strong condensation leading to mass accumulations of eroded, median-sized manticoceratids at the top of an upper Frasnian bedding surface exposed laterally to the main section.

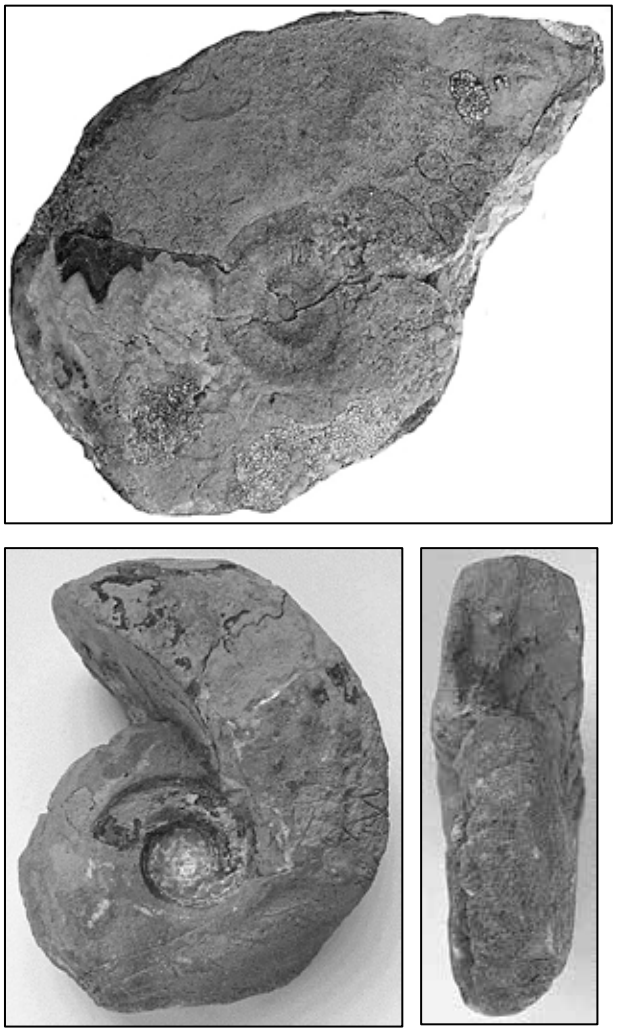

Fig. 14: Two Frasnian goniatites from Anajdam. Upper picture: *Sinobeloceras* aff. *acutum* (CHAO, 1956), Bed 33, with five E- and outer U-lobes (max dm = 84 mm); lower two pictures: *Manticoceras* n. sp. aff. *intermedium* (WEDEKIND, 1913a), loose, with moderately thick, flat whorls, wider, deeper umbilicus than in typical *M. intermedium* (max. dm 72 mm).

Fig. 15: *Mantiococeras* Bed of Fig. 13 overlain by dark-grey (organic-rich) Kellwasser Limestone.

Fig. 16: The dark-grey Lower Kellwasser Limestones (Beds 38-40) in the foreground, light-grey intra-Kellwasser Beds (Beds 41-42), the thin Upper Kellwasser Limestone (Bed 43-44c above the hammer blade), followed by thin-bedded basal Famennian limestones (above the hammer, Beds 45-48).

Fig. 17: Adult *Phonixites frechi* (WEDEKIND, 1918), loose from light grey micrites of the lower Famennian (dm = ca. 64 mm).

It yielded several convolute specimens of *Sinobeloceras* (Fig. 14), which is characterized by five external lobes (four in *Mesobeloceras*, six to eight in the descendent and more involute true *Beloceras*). The associated rich conodont fauna is dominated by *Po. paradecorosus* (Fig. 18.11), *Pa. hassi* (Fig. 18.5), and *I. symmetricus* (Fig. 18.10). Associated are ancyrodellids (*Ad. lobata,* Fig. 18.3, *Ad. curvata* early form, *Ad. nodosa*, Fig. 18.1), ancyrognathids (*Ag. coeni,* Fig. 18.4, *Ag. barbus*, Fig. 18.2), and one *I. brevis* (Fig. 18.6-7). Subordinate *Pa. plana* (Fig. 18.9) and a transitional form towards *Pa. feisti* (Fig. 18.8) give an upper MN 10 Zone (*Pa. plana* Zone) age, near the top of the middle Frasnian.

The thin nodular to flaserlimestones of Beds 34-37 record a deepening interval related to the eustatic ***semichatovae*** **Transgression**, which was emphasized by SANDBERG et al. (1992). Increased sedimentation rates are documented by high amounts of micrite in the mudstone facies of Bed 37 (Fig. 11D). LAZREQ (1992a, 1999) found *Pa. subrecta*, the index species of MN 12 Zone (*Pa. winchelli* Zone) at the top of Submember 2 (in her Sample 34). Our corresponding sample from Bed 37 is rich in *Ad. curvata* early form (Fig. 19.12), *Ag. triangularis* (Fig. 19.14), *Po. webbi* (Fig. 19.17), *Pa. hassi, I. praealternatus* (Fig. 19.15), and *I. symmetricus*. More subordinate are *Ad. ioides* (Fig. 19.13), *Ad. gigas, Pa. kireevae* (Fig. 19.18), *Palmatolepis* ?n. sp. (Fig. 19.19 and a second un-figured taxon), *I. vitabilis* (Fig. 19.16), and early representatives of *I. alternatus*.

Submember 3 embraces the **two Kellwasser units** and ranges from Beds 38 to 44c (Figs. 10, 11, 16). The main **LKW** (Bed 38, see Sample 35 of LAZREQ 1999) is a solid limestone that is moderately rich in dark organic matter, buchiolid bivalves, tentaculitoids, and goniatites (*Manticoceras*). The thin section (Fig. 11E) shows goniatites and crushed mollusk shells, and a strong recrystallization, which is typical for KW beds in many regions (e.g., BUGGISCH 1972; WENDT & BELKA 1991).

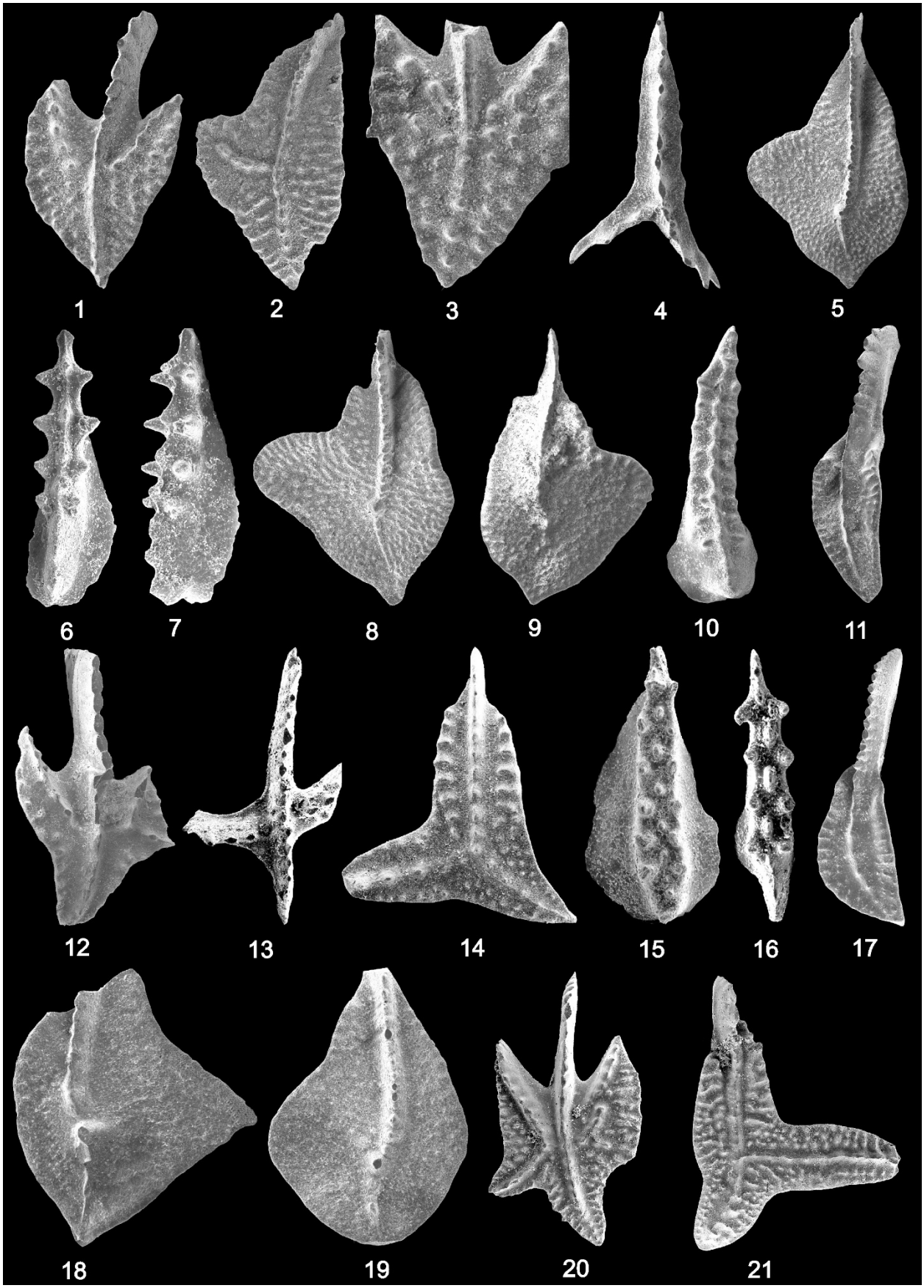

Fig. 18

Fig. 18: Conodonts from Beds 33C (1-11), 37 (12-19), and 38 (20-21). **1.** *Ad. nodosa*, x 40; **2.** *Ag. barbus*, x 40; **3.** *Ad. lobata*, x 60; **4.** *Ag. coeni*, x 65; **5.** *Pa. hassi*, x 35; **6-7.** *I. brevis*, x 110; **8.** *Pa.* aff. *plana*, x 45; **9.** *Pa. plana*, x 40; **10.** *I. symmetricus*, x 50; **11.** *Po. paradecorosus*, x 35; **12.** *Ad. curvata* early form., x 70; **13.** *Ad. ioides*, x 55; **14.** *Ag. triangularis*, x 50; **15.** *I. praealternatus*, x 6; **16.** *I. vitabilis*, x 110; **17.** *Po. webbi*, x 45; **18.** *Pa. kireevae*, x 60; **19.** *Palmatolepis.* ?n. sp.*,* x 55; **20.** *Ad. curvata* late form, x 35; **21.** *Ag. amana*, x 40.

The increase of organic matter created closed diagenetic systems with reduced pore water circulation. Palaeoproductivity indicators among trace elements (e.g., Ba/Al, Cu/Al, Ni/Al, Zn/Al; RIQUIER et al. 2005), the C_{org} content, and the blooming pelagic fauna indicate eutrophic conditions. Redox sensitive trace element ratios suggest dysoxic conditions, resulting from oxygen consumption required for the increased biogradation of the enhanced supply of organic matter. A minimum of magnetic susceptibility supports the prevailing interpretation of the LKW to have accumulated during an episode of maximum transgression (RIQUIER et al. 2007).

In the LKW conodont assemblage, *Ag. amana* (Fig. 18.21) is a newcomer, which signals higher parts of the MN 12 Zone (*Pa. winchelli* Zone; see KLAPPER & KIRCHGASSER 2016). Ancyrodellids, such as *Ad. gigas* (s.str., Fig. 19.1) and *Ad. curvata* late form (Fig. 18.20) co-occur. LAZREQ (1999, fig. 18) noted an icriodid spike in her conodont biofacies analysis, which expresses the palaeoecological change.

The top of the LKW shows bioturbation. The overlying argillaceous to concretionary Bed 39 forms a middle part of the LKW (= Sample 36 of LAZREQ 1999). The more solid Bed 40 is the top part of the LKW, still with manticoceratids, in which the amount of dark C_{org} decreases upwards. This suggests a gradual trend towards better oxygenated, normal and mesotrophic pelagic conditions. LAZREQ (1992a, 1999) recorded from her corresponding Sample 37 *Pa. rotunda*, the index species of MN 13a Zone (*Pa. bogartensis* Zone), *Ag. asymmetricus*, as well as a new, rather slender ancyrognathid (n. sp. B).

The **intra-KW beds** (Beds 41-42) are thin-bedded and nodular towards the top. Magnetic susceptibility data, a positive double spike, suggest a regressive peak in the upper half of this interval (AVERBUCH et al. 2005; RIQUIER et al. 2007). Near the top, Bed 42 is a mud- to wackestone with isolated crinoid pieces, conodonts, rare tentaculitoids, large cephalopod fragments, and small amounts of dispersed hematite (Fig. 11F). Bioturbation was weak, indicating dysoxic conditions. The conodont fauna includes a flood of small palmatolepids, abundant *Pa. bogartensis* (four different morphotypes, Fig. 19.5-8)*, Pa. hassi,* some *Pa. winchelli* (cf. Fig. 19.9), *Ag. asymmetricus* (Fig. 19.2), *Ad. curvata* late form, moderately common *I. alternatus alternatus* (Fig. 19.4), and subordinate *I. alternatus mawsonae*. The assemblage is typical for MN 13a Zone (*Pa. bogartensis* Zone). But since *Pa. linguiformis* is extremely rare both in the Montagne Noire and Mrirt region (GIRARD et al. 2005), a basal MN 13b Zone age (lower *Pa. linguiformis* Zone) cannot be excluded. The directly overlying, recrystallized, dark-grey, organic-rich **UKW** can be subdivided into four thin subunits (Beds 43 to 44c) that were not separated in previous section logs. The unit correlates with Samples 38 and 38a of LAZREQ (1999). Sheet cracks indicate minor interruption of sedimentation (Fig. 15), as in the eastern Anti-Atlas (see WENDT & BELKA 1991). The microfacies (Fig. 11G) is a microsparitic bioclastic wacke-packstone with tentaculitoids, some ostracods, and mollusk debris. Trace element ratios prove increased trophic and dysoxic to even anoxic conditions, as for the LKW (RIQUIER et al. 2005).

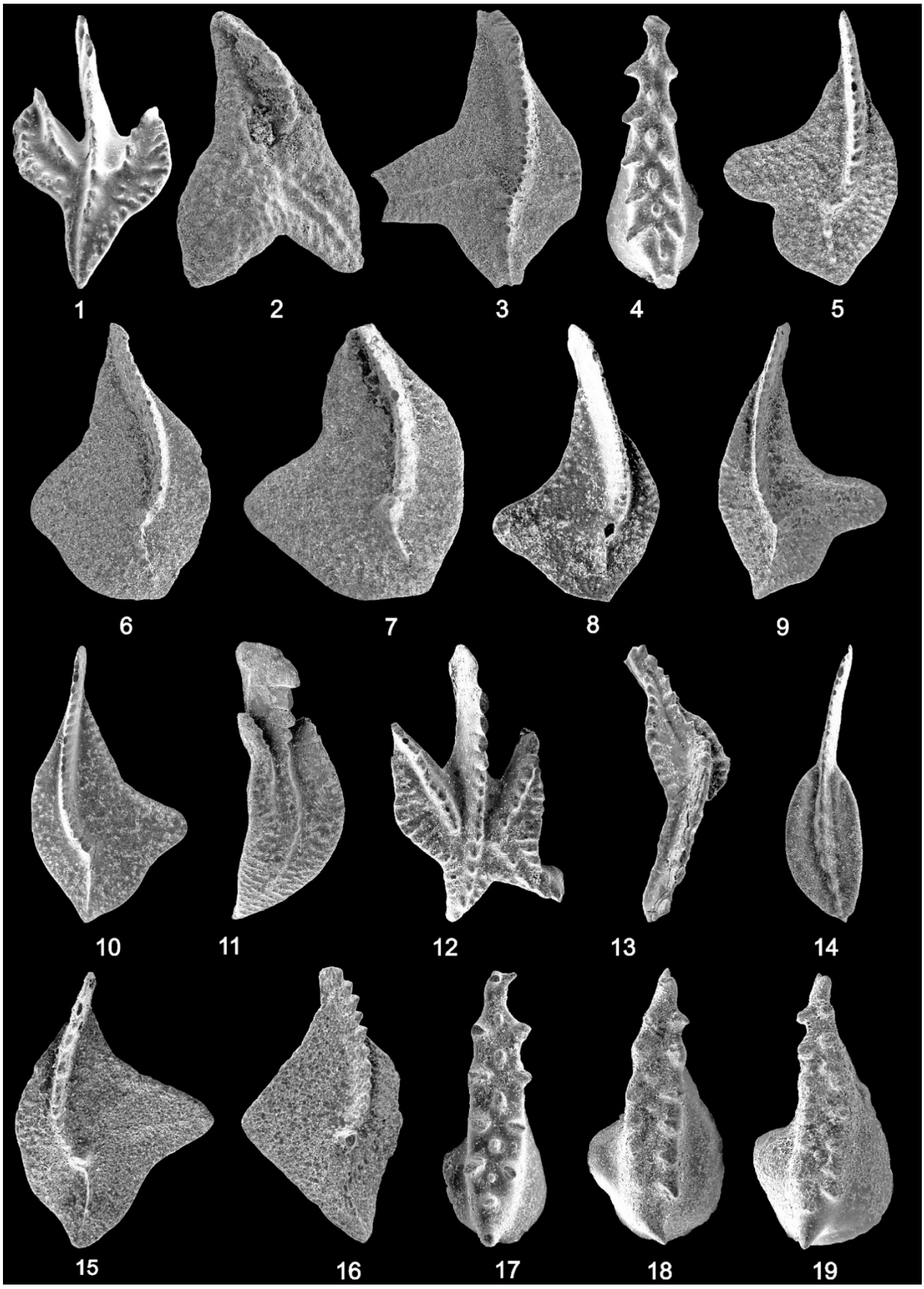

Fig. 19

Fig. 19: Conodonts from Beds 38 (1, MN 11), 42 (2-8, MN 13a/b), 44C (9-13, MN 13c), and 45 (14-19, *subperlobata* Zone). **1.** *Ad. gigas*, x 45; **2.** *Ag. asymmetricus*, x 30; **3.** *Pa.* cf. *nasuta*, x 40; **4.** *I. alt. alternatus*, x 80; **5.** *Pa. bogartensis* M-A, x 60; **6.** *Pa. bogartensis* M-B, x 65; **7.** *Pa. bogartensis* M-C, x 75; **8.** *Pa. bogartensis* M-D, x 65; **9.** *Pa*. cf. *winchelli*, x 35; **10.** *Pa*. aff. *bogartensis*, x 45; **11.** *Po. imparilis*, x 35; **12.** *Ad. curvata* l.f., x 50; **13.** *Nothognathella* sp., x 50; **14.** *Neo.* aff. *communis*, x 65; **15.** *Pa. ultima*, x 65; **16.** *Pa. del. delicatula*, x 125; **17.** *I. alt. alternatus*, x 85; **18.** *I. alt. mawsonae*, x 60; **19.** *I. alt. helmsi*, x 60.

This explains the lack of any endobenthos and of oxygen-sensitive epibenthos. Magnetic susceptibility and maximum $CaCO_3$ contents signal, as for the LKW, deposition during a time of very high sea level, when the carbonate ramp setting became increasingly distal (RIQUIER et al. 2007). Sample 38 included specimens of *Pa. semichatovae* (LAZREQ 1999, pl. 10, figs. 1-3), which should normally not occur so high in the Frasnian. In relation to the underlying light grey limestones, polygnathids are slightly enriched (ca. 20 % of the total fauna, LAZREQ 1999, fig. 27). The top of the UKW (Sample 38a) yielded *Ag. ubiquitus* and *Pa. ultima* (= *praetriangularis*), the two index species of the terminal Frasnian MN 13c Zone (*Ag. ubiquitus* Zone/Subzone). Our new sample from Bed 44c also produced several *Ag. ubiquitus*, a large variety of *Pa. bogartensis*, many specimens with a lappet-like side lobes as in *Pa. amplificata* (*Pa*. cf. *winchelli*, Fig. 19.9), narrow forms identified as *Pa*. aff. *bogartensis* (Fig. 19.10), *Pa. hassi,* rare *Pa.* cf. *brevis*, common *Po. webbi* and *Ad. curvata* late form (Fig. 19.12), *Po. imparilis* (Fig. 17.11), nothognathellids (Fig. 19.13), all three subspecies of *I. alternatus*, and the perhaps youngest known *Enantiognathus*. Locally, there is little evidence for a palmatolepid extinction within the upper UKW, as a supposed marker of the MN 13b/13c Zone boundary.

The **Frasnian-Famennian** stage **boundary** is locally marked by a sudden return to organic-poor, light grey micritic limestones. Bed 45, the base of **Submember 4**, is a strongly bioturbated bioclastic wackestone with a surprising high amount of possibly reworked tentaculitoids and mollusk debris. Sharp changes of the matrix and its color give the impression of reworked mudclasts, as described from the basal Famennian bed of Rhenish sections (Schmidt Quarry, SCHINDLER 1990; Beringhauser Tunnel, HARTENFELS et al. 2016). Geochemical data support a gradual but strong return to fully oxic and less nutrient-rich palaeoceanographic conditions (RIQUIER et al. 2005, 2007). Rising magnetic susceptibility shows a regressive trend, which, however, is less pronounced than the pre-UKW Regression. *Phoenixites frechi*, the only F-F boundary survivor goniatite, occurs as large, loose specimens (Fig. 17). The conodont fauna of Bed 45 is restricted and typical for the basal Famennian *Pa. subperlobata* Zone. Despite the presence of mudclasts and tentaculitoids, there is no evidence of reworking of conodonts from Frasnian strata. There are abundant *Pa. ultima* (Fig. 19.15), subordinate *Pa. subperlobata,* some small *Pa. delicatula delicatula* (Fig. 19.16), *I. alternatus alternatus* (Fig. 19.17), *I. alternatus helmsi* (Fig. 19.19), *I. alternatus mawsonae* (Fig. 19.18), *Po. procerus,* and a possibly new polygnathid, which is probably the ancestor of *Neopolygnathus communis communis* (Fig. 19.14). Typical *Neo. communis communis* enter higher in the lower Famennian, within the *Pa. crepida* Zone (see discussion in WANG et al. 2016). Some simple ozarkodinids from Bed 45 fall in the genus *Walliserodina* SCHÜLKE, 1999. One *Palmatolepis* is transitional between *Pa. ultima* and *Pa. triangularis*. LAZREQ (1999) noted an increase of relative icriodid abundance, which is an extinction-related opportunistic biofacies feature, not necessarily a consequence of sea level change.

The subsequent Famennian sedimentary and faunal succession has been described by LAZREQ (1992a, 1999). She found all lower Famennian (Submember 4) conodont zones up to the Upper *rhomboidea* Zone (now *Pa. gracilis gracilis* Zone, SPALLETTA et al. 2017). The lithology fluctuates between nodular shale and nodular limestone. The two levels of the regressive Lower and Upper Condroz Events are weakly marked by two levels of more solid limestone in the (Lower) *Pa. rhomboidea* and *Pa. gracilis gracilis* Zones, separated by a shale unit. Peak abundances of palmatolepids, as probable indicators of transgression, are recorded high in the *Pa. termini* Zone (Middle *crepida* Zone) and in the *Pa. glabra pectinata* Zone (Uppermost *crepida* Zone). This reflects the two phases of maximum deepening of the so-called, prolonged "**Nehden Event**", which is not a true event but an interval of strong radiation when the shelf had reached its widest extension. Cheiloceratids, that record this radiation in outer shelf settings, have not yet been collected at Anajdam.

6. Bou Ounebdou (Gara de Mrirt)

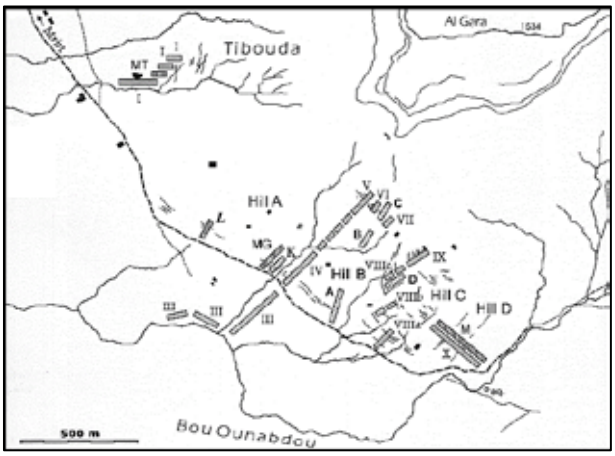

Fig. 20: Position of the numerous numbered sections distinguished at Bou Ounebdou (Bou Nebedou or Bou Ounabdou) SE of Mrirt. E/NE-W/SW running gullies separate the Tibouda sections in the NW, Hill A (with Section MG), Hill B (with Sections A-C), Hill C (with Section D), and Hill D (with Sections X and M; updated from HÜNEKE 2001, fig. 42).

6.1. Location and overview

The Bou Ounebdou area at the SW/S slope of the Gara de Mrirt (or Al Gara, Fig. 2) mountain exposes the Devonian in numerous lateral sections (Fig. 20) and in cliffs of two small-scale nappes that overlie each other directly (see BECKER & HOUSE 2000a, fig. 2), exemplified by the repetitive sections A and B/D (Fig. 19). The erosion at the base of the overlying, Lower Carboniferous Al Gara Formation has truncated the Famennian of both nappes but laterally to a variable extent. Shales with embedded conglomerates, breccias and large olistolites under- and overlie the incomplete Upper Devonian of both nappe successions. Below, there is no undisturbed contact to the Lower/Middle Devonian that can be best studied at Tibouda (Fig. 18; x = 282.97, y = 488.66) and in Section III of WALLISER et al. (2000). Our investigations concentrated on the Upper Devonian and, therefore, we have to refer to the latter publication. It included Pragian index species (e.g., *Nowakia (Turkestanella) acuaria*) for Submember A of the Anajdam Member, a silty/sandy Submember B, and some upper Emsian conodonts and dacryoconarids, such as *Now. (Now.) richteri*. The so far only reliable evidence for (top) middle Givetian strata is based on a conodont sample with "*Polygnathus* sp. aff. *bryanti*". The Middle Devonian requires further studies.

The following summary combines for the Upper Devonian a brief review of the many previous publications with detailed new data. Around the Frasnian-Famennian boundary, there are many similarities with the Anajdam succession.

6.2. Frasnian

Unit/Bed A in the slope below the lower cliff/nappe consist of dark-grey shales with numerous, partly meter-sized and internally folded slump blocks, including laminated black limestone (clasts of Bed B, see below), light-grey Frasnian micrites, and Famennian *Dzieduszyckia* Limestone. The latter prove that Unit A is a post-Famennian tectonic melange formed during nappe emplacement, not a Givetian unit. Bed B is a lenticular, solid, laminated, pyritic black marker limestone (10-20 cm thick). It forms the base of the **Mrirt Member** of the Bou Nebedou Formation. Locally, the lithofacies of **Submember 1** differs strongly from the contemporaneous oxic limestones of Anajdam (see Fig. 5). At Bou Ounebdou, the first pulse of the global Frasnes Events is well-developed as an anoxic interval (BECKER 1993b). The absence of macrofauna and bioturbation suggests hostile conditions on the sea floor. Sample 30 of LAZREQ (1999) yielded *M. falsiovalis* (s.l.), which refers possibly to a morphotype of the closely related *M. guanwushanensis* (see new taxonomic notes by ABOUSSALAM & BECKER in PIZARZOWSKA et al. 2020 in press). In any case, this forms provides a topmost Givetian age (*norrisi* = basal *falsiovalis* Zone).

Bed C is an up to 3 m thick (Section A), laminated, black shale unit, locally with partly irregularly embed (slumped), lenticular, middle

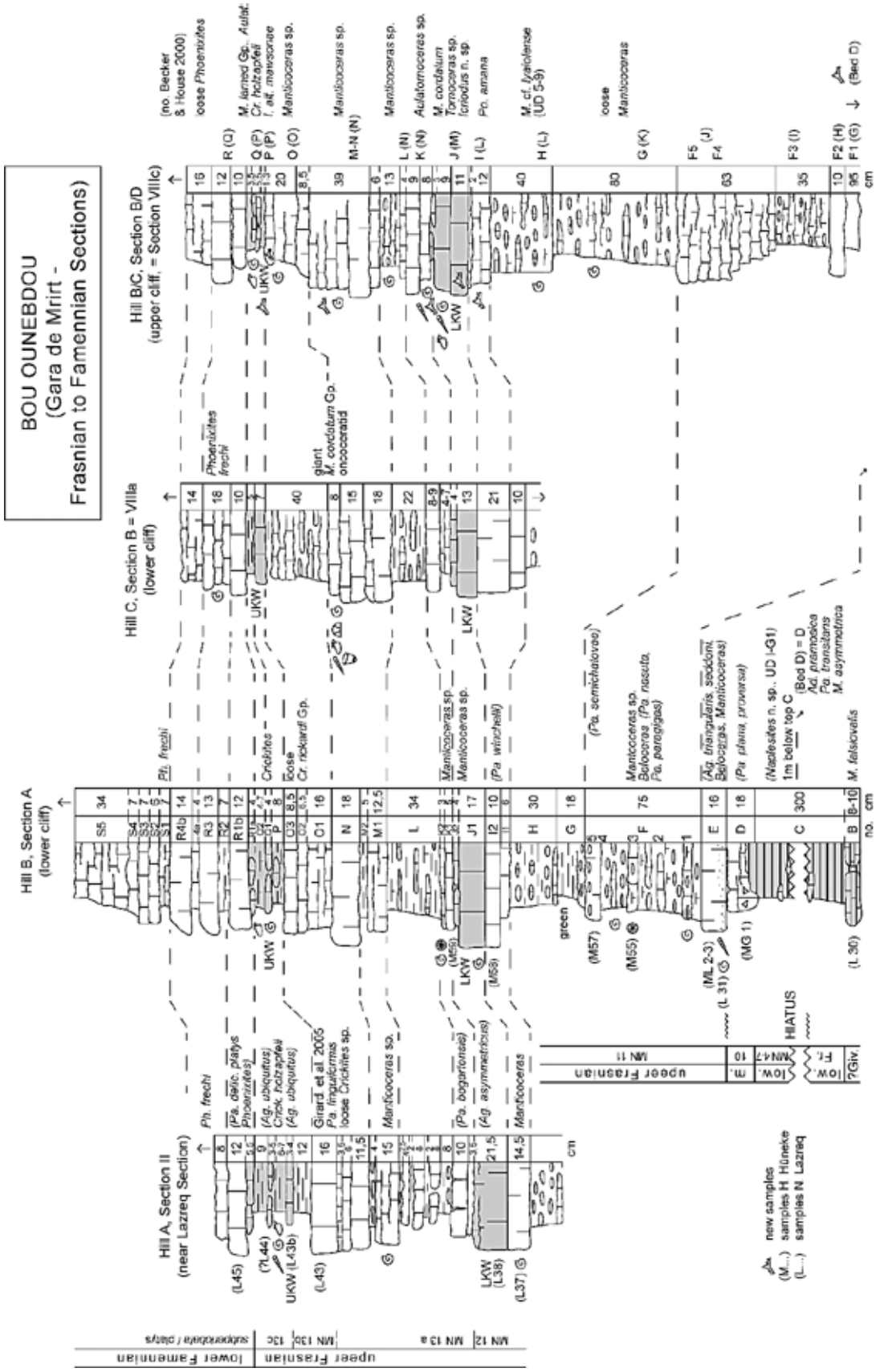

Fig. 21: Correlation of four lateral Frasnian successions at Bou Ounebdou: Hill A, lower cliff, slightly W of main section of LAZREQ (1992a, 1999), Hill B, lower cliff, Section A, Hill C, lower cliff, Section ß (= Section VIIIa), and Hill B/C, continuous outcrop between Section B/D (= Section VIIIc). The bed numbering was harmonized, leading to changes in Section B/D (numbers of BECKER & HOUSE 2000a given in brackets). Numbers in brackets in Sections II and A refer to sample numbers in LAZREQ (1999: L-numbers) and HÜNEKE (2001: M-numbers).

Fig. 22: *Naplesites* n. sp. (with three E- and three outer U-lobes), loose from Bou Ounebdou (max. dm = 86 mm).

to dark grey limestones. Records of *Pa. transitans, M. asymmetrica, Zieglerodina unilabia*, and *Ad. pramosica* from a limestone in the higher part give a top lower Frasnian age (MN 4 Zone, *Pa. transitans* Zone). Associated are *I. symmetricus*, *Po. dengleri dengleri*, and *Po. varcus*. So far, there is no record of MN 1-3 Zones but the anoxic interval may represent the complete interval from the upper pulse of the Frasnes Event (MN 2a Zone, *Ad. rotundiloba soluta* Subzone; see ABOUSSALAM & BECKER 2007) to the top lower Frasnian Timan Event sensu HOUSE et al. (2000b).

The middle Frasnian (upper part of Submember 1) is locally almost missing (Fig. 21). The only evidence is a loose specimen of *Naplesites* (Fig. 22), which is the index genus of Upper Devonian (UD) G_1, correlating with the upper part of MN 6 to lower MN 7 Zone in eastern North America (KLAPPER & KIRCHGASSER 2016), in the Anti-Atlas (BECKER et al. 2018b), or Western Australia (BECKER & HOUSE 2009). The fully grown specimen belongs to the new species with three external U-lobes that occurs in the Tafilalt.

As at Anajdam, **Submember 2** is characterized by a strongly condensed but more or less complete succession of outer shelf, light-grey well-oxygenated limestones with goniatites and other pelagic fauna. Coarsening-to-finning-upward micro-sequences comprise calcarenites (styliolinid grain- to packstones with locally preserved horizontal and cross-lamination), laminated calcisiltites (rich in conodonts and phosphate clasts), and bioturbationally mottled calcisiltites and calcilutites – analogous to contourite formations in modern oceans (HÜNEKE 2007, 2013). While calcarenites and calcisiltites result from vigorous bottom-current activity, calcilutites are formed under conditions of weak current influence or pelagic rain.

Bed D is detrital, irregularly developed, up to 20 cm thick, and contains intraclasts that prove some reworking high in the middle Frasnian. Records of *Pa. plana* and *Pa. proversa* (Sample MG1 of HÜNEKE 2001) place the unit in MN 10 Zone (*Pa. plana* Zone). The thickness of the overlying, solid marker limestone (Bed E = Bed F in BECKER & HOUSE 2000a) varies laterally between 16 and 47 cm. There are more intraclasts at the base and large orthocones and ammonoids (*Beloceras, Manticoceras, ?Maternoceras*). Conodonts from Samples 31 of LAZREQ (1999) and Sample MG 2/3 of HÜNEKE (2001) include *Ag. triangularis* and *Ag. seddoni*, as markers of the MN 11 Zone (*Pa. feisti* Zone). The sudden change to a sequence of thin-bedded nodular shales and limestones (Unit/Bed F = Beds G-J in BECKER & HOUSE 2000a) reflects an overall deepening, the ***semichatovae* Transgression** just above the base of the MN 11 Zone. This is parallelled by a major change of seawater geochemistry, as manifested in a gradual, strong positive excursion of neodymium isotopes, with a maximum at the base of Bed F (Sample 98 of DOPIERALSKA 2003; DOPIERALSKA et al. 2015). The same influx of supposed open Prototethys water masses has been recorded in the Tafilalt. *Thalassinoides* burrows are an indicator of fully oxic conditions. There are manticoceratids and beloceratids. At the top lies a more solid flaserlimestone. The main part (Sample M55 of

HÜNEKE 2001) yielded *Pa. nasuta* and *Pa. paragigas*, which provide a correlation with the Early *rhenana* Zone sensu ZIEGLER & SANDBERG (1990). Sample M57 from the top of Unit/Bed F contained *Pa. semichatovae*, the iconic species for the major eustatic, transgressive phase that shall define the base of the upper Frasnian.

Beds G/H are a couplet of up to 120 cm thick (= Beds K to middle L in BECKER & HOUSE 2000a) more argillaceous or more calcareous nodular units. This level yielded in section B/D a first Moroccan relative of the involute, slender, and fast expanding *M. lyaiolense* (Fig. 23), which differs from the types in a somewhat wider and narrower flank lobe. The Russian *M. lyaiolense* occurs also in higher parts of MN Zone 11 (*feisti* Zone; e.g., BECKER et al. 2000). There are other loose manticoceratids, such as *M.* aff. *lenticulare* (Fig. 24), related to an insufficiently known Chinese (Hunan) species with flattened but strongly converging flanks, and a large, compressed fragment of *M. evolutum* (Fig. 25). The latter was previously only known from slightly smaller specimens of the Saoura Valley, Algeria (PETTER 1959). The closely related, also large-sized *M. latisellatum* occurs typically in the early upper Frasnian of northern Russia (BOGOSLOVSKIY 1969; BECKER et al. 2000). One specimen (Fig. 26) is very close or identical with *M. simulator*, the New York State type-species of the genus, in which the subumbilical L-lobe stays rounded during ontogeny. Finally, there is a new species, *M. inflatum* n. sp. (Fig. 27), which is closest to the Northern Russian *M. solnzevi*. The admixture at Bou Ounebdou of manticoceratids with very different palaeogeographic relationships emphasizes the kosmopolitan nature of upper Frasnian pelagic faunas during times of maximum transgression.

Bed I (Bed L in BECKER & HOUSE 2000a) is a thin (up to 30 cm thick), solid marker limestone with some *Manticoceras* (at Hill A) and *Pa. subrecta* (= *winchelli*; Sample M58 of HÜNEKE 2001), the index species of the MN 12 Zone. A new restricted sample yielded *Ad. curvata* late form, *Po. amana, Po. aequalis, I. symmetricus*, and others. Bed I forms the lower part of the minor cliff, which is mostly built by the sharply overlying, dark-grey **LKW Limestone** (Bed J1, up to 25 cm thick, Bed M in BECKER & HOUSE 2000a) at the base of **Submember 3**. LKW fossils include *M. lamed*, *Aulatornoceras* sp., *Tornoceras* sp., *Buchiola*, orthocones, and homoctenids. A rich conodont fauna of LAZREQ (1999, Sample L38) and a new sample yielded *Ag. triangularis*, the late morphotype of *Ad. curvata, Ag. asymmetricus*, the marker for the top of MN 12 Zone, and a new species of *Icriodus* with a few nodes on the upper surface of the basal cavity, outside the platform (spindle). As at Anjadam, there is a bloom of icriodids (LAZREQ 1999). A thin upper subdivion (Bed J2) forms a recessive top.

RIQIER et al. (2005, 2007) proved similar geochemical conditions for Bou Ounebdou as at Anjadam. The outer shelf carbonate ramp deepened and became eutrophic (with a peak of Ba/Al and V/Cr values, AVERBUCH et al. 2005) and dysoxic. JOACHIMSKI et al. (2002) and RIQUIER et al. (2005) documented the associated positive carbon isotope excursion known from many other sections on a global scale (e.g., JOACHIMSKI & BUGGISCH 1993; JOACHIMSKI et al. 2001; BUGGISCH & JOACHIMSKI 2006). It indicates increased bureal of organic carbon and a maximum of oceanic organic productivity. A pronounced positive excursion of $\delta^{18}O$ in LKW conodonts means that this occurred in parallel with rapidly falling sea surface temperatures, in the scale of 4-7°C. However, congruent transgression and major cooling represent opposite trends that are not easy compatible. A coincident sharp decrease of Sr/Ca ratios has been linked by LE HOUDEC et al. (2013) with an increasing erosion of calcite-dominated reef bodies. However, the LKW transgression drowned the carbonate shelfs, for example of the Ardennes (e.g.,

Fig. 23: *Manticoceras* aff. *lyaiolense* BOGOSLOVSKIY, 1969, loose specimen, upper nappe, Section B/D, showing the slender, fast expanding (WER = 2.9) whorl form and narrow umbilicus of the typical species but with a different flank saddle (max. dm = 82.8 mm).

Fig. 24: *Manticoceras* aff. *lenticulare* XU, 1977 loose specimen showing characteristic, flattened, strongly converging flanks and a steep, narrow umbilicus (max. dm = 66 mm).

Fig. 25: Large, loose fragment (whorl height at last septum = 67 mm) of a *Manticoceras evolutum* PETTER, 1959 from Gara de Mrirt, showing the widely arched flank saddle (saddle width/height = ca. 1.7) as typical for the *M. latisellatum* Group.

Fig. 26: Gara de Mrirt *Manticoceras simulator* (HALL, 1874) a species that was previously only known from eastern New York (e.g., HOUSE & KIRCHGASSER 1993, 2009), showing the compressed, discoidal whorl form and typical, rather wide and rounded L-lobes at 30 mm diameter (max. dm = 46 mm).

Fig. 27: *Manticoceras inflatum* n. sp., holotype (Geomuseum Münster), loose from the upper Frasnian of Section II (Hill A, max. dm = 38 mm).

Fig. 28: *Manticoceras* aff. *guppyi* GLENISTER, 1958, loose at Gara de Mrirt, upper nappe, Hill B, Section B (max. dm = 107 mm; thicker than the *guppyi* holotype and with higher whorl expansion rate at ca. 2.8).

HOUSE et al. 2000a; MOTTEQUIN & POTY 2016), and did not erode them. A higher content of Ca in the marine limestones at Bou Ounebdou, whilst the Sr influx remained stable, may be explained alternatively by blooms of calcite-producing and photosynthetic cyanobacteria that probable also make up the present, amorphous C_{org}.

The up to 50 cm thick Beds K/L (**Intra-KW Limestone**, lower part of Bed N in BECKER & HOUSE 2000a) reflect a gradual post-LKW deepening with a change from thin-bedded, light grey flaserlimestone with goniatites (*Manticoceras, Aulatornoceras*) to more deeply weathered nodular shales, marls, and green calcareous shales. There was a gradual return to fully oxic and oligotrophic conditions with low carbon isotope and moderately high Sr/Ca values. Sample M59 (HÜNEKE 2001) from the base yielded *Pa. rotunda* (= *bogartensis*), the index species of MN 13a Zone (*Pa. bogartensis* Zone. FEIST (2002, 2003) found in Bed K (his level 1A) the trilobites *"Harpes" neogracilis*, *Chlupaciparia maroccanica*, *Acuticryphops acuticeps*, and *Otarion stigmatophthalmus*. These are of highest importance for the understanding of trilobite extinctions associated with the global Kellwasser Crisis. A subsequent minor shallowing episode is represented by the up to 45 cm thick Beds M/N (middle to upper parts of Bed N in BECKER & HOUSE 2000a), a succession of light-grey, bioturbated, platy, solid cephalopod limestone that form a minor cliff. The regressive trend is not prominent in the magnetic susceptibility curve (RIQUIER et al. 2007). Beds M/N yielded the upper trilobite assemblage of FEIST (2002, 1B) with *Gondwanaspis mrirtensis*, *"Harpes",*

Palpebralia brecciae, *Otarion*, and *Acuticryphops.* Among the conodonts, *Ag. triangularis* and *Ad. curvata* late form are common (new sample).

The overlying limestones are, again, more thin-bedded and recessive (Bed O, up to 40 cm thick). *Manticoceras* are rather common in Beds M-O and can reach giant size (25 cm diameter or more, e.g. in Section ß). Such large representatives of the *M. cordatum* Group probably belong to a new species. One well-preserved, loose specimen (Fig. 28) is very similar to the top-Frasnian *M. guppyi* GLENISTER, 1958 of Western Australia, where it occurs in UD I-L and the *Pa. linguiformis* Zone (MN 13b Zone; see BECKER & HOUSE 2009). This agrees well with the discovery of rare *Pa. linguiformis* by GIRARD et al. (2005) in beds just below the UKW. We found at the top of Bed O (in Section B/D) only *Ag. asymmetricus, Ad. curvata* late form*, Pa. bogartensis, Pa. hassi, I. alternatus alternatus,* and *I. alternatus mawsonae*. Another important faunal element at this level are oncoceratids. The Bou Ounebdou fossil record underlines the survival of several important faunal groups right until the base of the Upper Kellwasser Event, as first described from the F-F boundary stratotype at Coumiac, southern France (BECKER et al. 1989; HOUSE et al. 2000a).

The dark-grey, organic-rich **UKW Limestone** (Beds P to R1a, Bed P in BECKER & HOUSE 2000a) is more argillaceous and more deeply weathered than the LKW. However, this is only partly evident in the detrital trace element proxies, magnetic susceptibility values, and carbonate content curves of AVERBUCH et al. (2005) and RIQUIER et al. (2005, 2007). The UKW seems to have been locally less anoxic than the LKW. There are at least two marl-limestone cycles (Fig. 21). Common fossils are goniatites (*M. lamed* Group, *Crickites holzapfeli*, the UKW index species of UD I-L_2, *Aulatornoceras* sp.), orthocones, homoctenids, buchiolids, and other bivalves. LAZREQ (1999) documented *Ag. ubiquitus*, the marker for MN 13c Zone (upper *linguiformis* Zone or *Ag. ubiquitus* Zone) in Samples L43a/44. The peak positive carbon isotope values, and, therefore, of oceanic productivity lies at the top of our Bed 44c (JOACHIMSKI et al. 2002; RIQUIER et al. 2005). C_{org} biodegradation caused probably an oxygen minimum at the top of the UKW. But since redox-sensitive elements are more enriched in the LKW, it is difficult to relate the sudden extinction of pelagic biota at the UKW top simply to a peak of open water anoxia. Extreme climatic fluctuations may also have been an important environmental factor. LE HOUEDEC et al. (2013) documented peak temperature for the lower part of the UKW, reverting suddenly to cooler values in the upper part. However, the cooling was much less drastic than within the LKW (see discussion in HARTENFELS et al. 2016). The Ca/Sr values were slightly more negative than in the LKW, which suggests a higher influx of biogenic calcite.

6.3. Famennian

According to LAZREQ (1992a, 1999), there is an unconformity right at the F-F boundary at Bou Ounebdou. The first Famennian bed (Bed R1b, Samples L45/46, base of **Submember 4**) contained already *Pa. delicatula platys*, the index species of the (now) third Famennian conodont zone (revised Middle *triangularis* Zone of ZIEGLER & SANDBERG 1990; *Pa. delicatula platys* Zone of SPALLETTA et al. 2017). Geochemical values prove a return to normal, oxic to slightly dysoxic and oligotrophic conditions (RIQUIER et al. 2007) but there are inconsistent carbon isotope data in JOACHIMSKI et al. (2002: marked negative shift) and RIQUIER et al. (2005: continuing high $\delta^{13}C$ values). A basal Famennian regression is supported by rising magnetic susceptibility values (AVERBUCH et al. 2005) and an increase of icriodid numbers (up to ca. 20 % of the fauna, LAZREQ 1999).

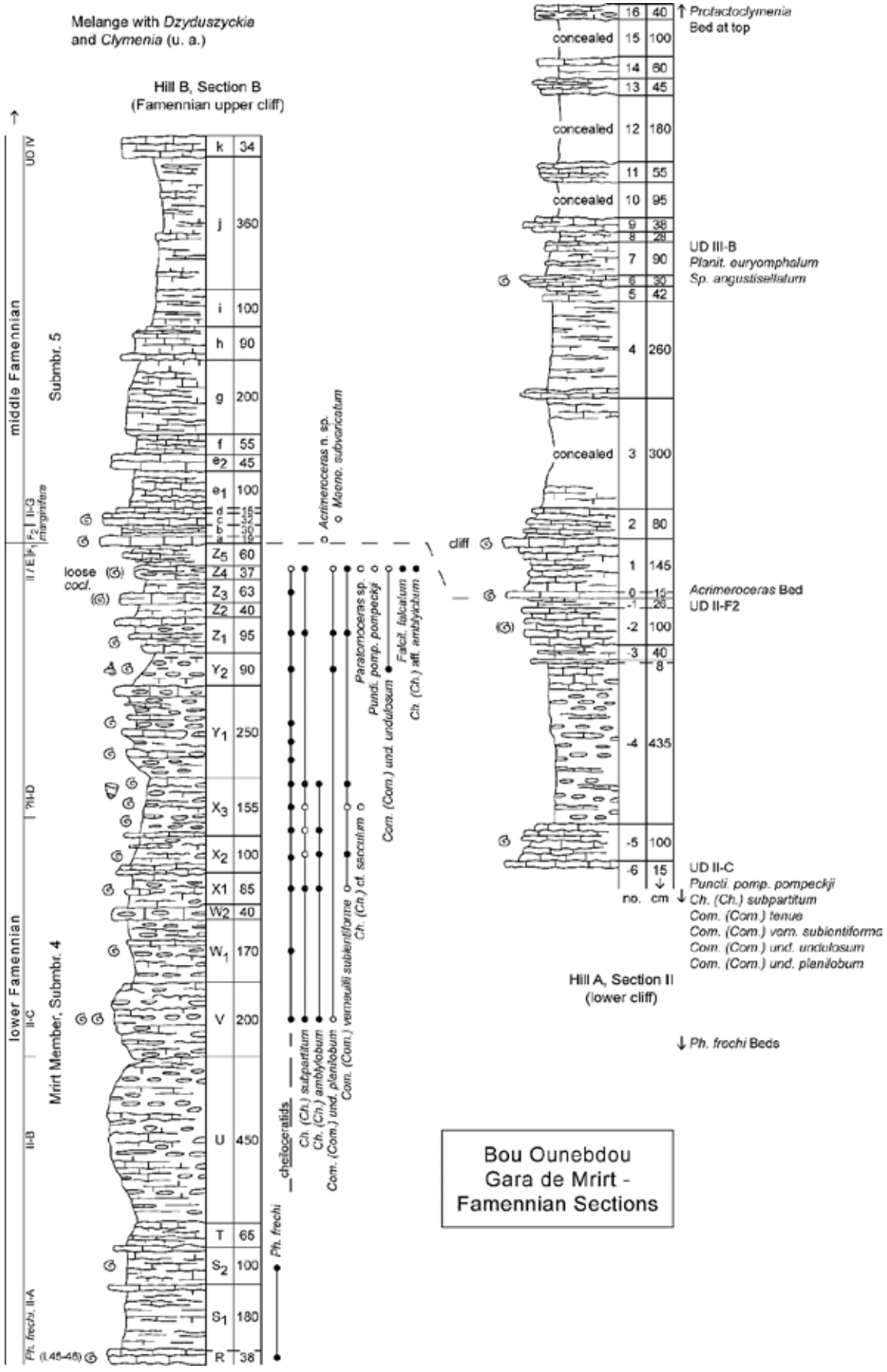

Fig. 29: Correlation of two Famennian sections at Gara de Mrirt, with ranges of ammonoids and their zonation.

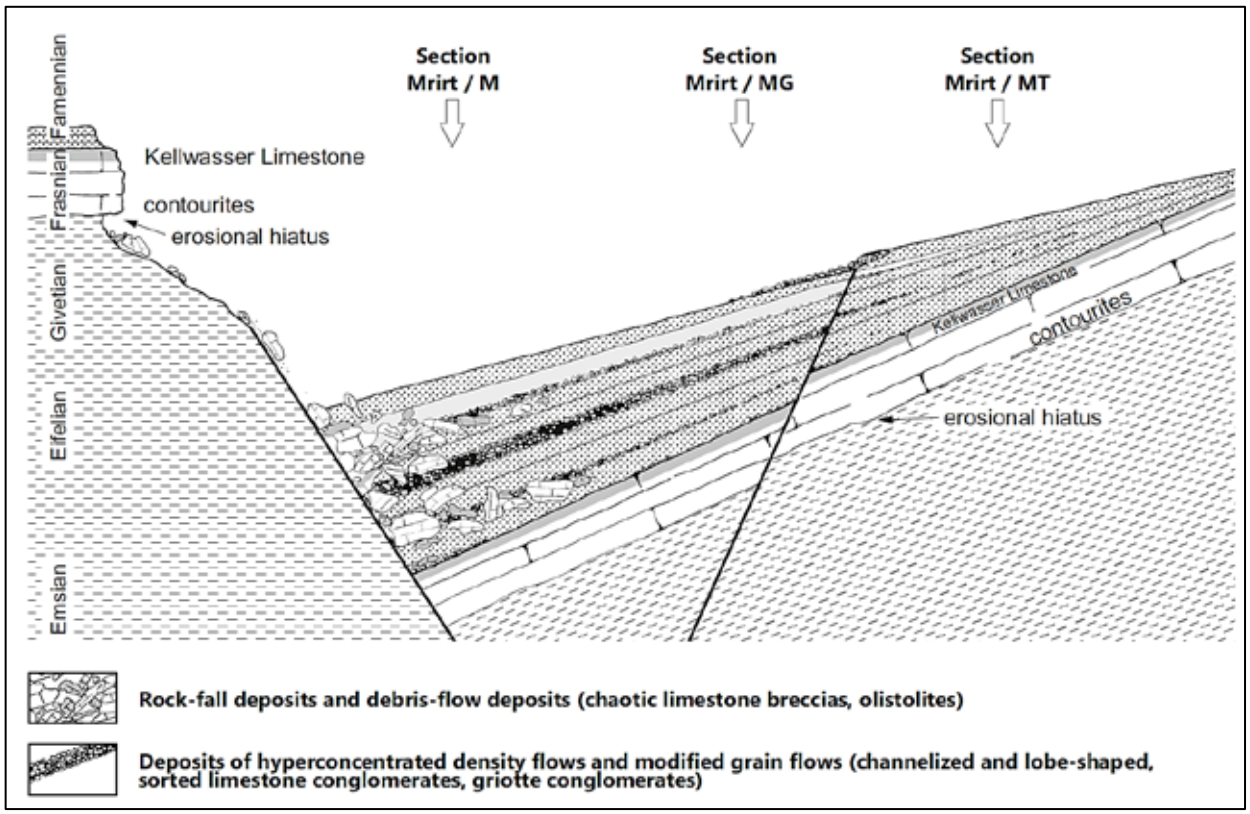

Fig. 30: Facies model for the laterally variable origin of Eovariscan resediments of Gara de Mrirt prior to and during the nappe displacement (HÜNEKE 2001, fig. 54). For location of sections Mrirt M, MG, and MT see Fig. 20.

It is also in accord with peak positive (cool) oxygen isotope values from conodont phosphate (LE HOUEDEC et al. 2013). The local F-F boundary hiatus is correlated with the basal Famennian reworking event recognized at Anajdam and elsewhere (BECKER et al. 2018). The boundary level should be re-sampled at the highest resolution for conodonts and microfacies in the sections with the thickest UKW development (Sections II and A, Fig. 21).

Our up to 50 cm thick, basal Famennian Bed R (Bed Q in BECKER & HOUSE 2000a) contains up to three solid flaserlimestones alternating with more argillaceous beds. There are common *Phoenixites frechi*, the opportunistic basal Famennian index goniatite (BECKER 1993a). The small-eyed pacopid *Nephranops (N.)* aff. *incisus* occurs in the first 20 cm of the Famennian. It records the earliest Famennian trilobite radiation after the drastic extinction at the UKW base (FEIST 2019). This initial recovery occurred just before the onset of *Pa. minuta minuta*, the index species of the *Pa. minuta minuta* Zone (= former Upper *triangularis* Zone, Sample L46a).

The overlying Beds S-Z (of Section B, ca. 21.5 m), yellowish weathering nodular shales and limestones, resemble strictly the "vrai griotte" of the southern Montagne Noire (BECKER 1993a, 1993b; BECKER & HOUSE 2000a). LAZREQ (1992a, 1999) recognized all lower Famennian conodont zones in Submember 4. Especially similar are the abundant cheiloceratid faunas, which range from UD II-C to II-F1. The Bou Ounebdou is one of the globally few successions, where the post-KW conodont and goniatite radiations can be correlated. However, the search for the oldest Cheiloceratidae within the thick Bed U requires further collecting. The oldest fauna from Bed V includes typical taxa of the second cheiloceratid zone (*Ch. (Ch.) subpartitum* Zone, UD II-C). Index taxa for UD II-D are locally surprisingly rare. Only *Armatites*

planidorsatus has been noted (BECKER & HOUSE 2000a), but as a locally rare form. At the top there are large-sized, rather unusual relatives of *Ch. (Ch.) amblylobum, Ch. (Ch.) sacculum,* and a loose *Paratornoceras*, which suggest that the level of UD II-E/F1 has been reached. This interval correlates with the *Pa. rhomboidea* and *Pa. gracilis gracilis* Zones (previous Lower and Upper *rhomboidea* Zones). The latter has been identified by LAZREQ (1999) based on records of *Po. triphyllatus* (see lower range in SPALLETTA et al. 2017). As in the Montagne Noire, the preservation of goniatites as isolated, corroded nodules is poor. However, the following taxa have ben identified so far (Figs. 29, 31):

Cheiloceras (Ch.) subpartitum subpartitum (Figs. 31c-d, m-n, partly unusually large, up to 67 mm dm)
Cheiloceras (Ch.) subpartitum crassum
Cheiloceras (Ch.) amblylobum
Cheiloceras (Ch.) aff. *amblylobum* (Fig. 31i-j)
Cheiloceras (Ch.) cf. *sacculum* (Fig. 31-g-h)
Compactoceras (Com.) verneulii sublentiforme (Figs. 31o-p)
Compactoceras (Com.) tenue
Compactoceras (Com.) undulosum undulosum (Figs. 31e-f)
Compactoceras (Com.) undulosum planilobum
Puncticeras pompeckji pompeckji (Figs. 31a-b)
Falcitornoceras falcatum (Fig. 31k-l)
Armatites sp. indet.
Paratornoceras sp.

WALLISER et al. (1999), LAZREQ (1999), and HÜNEKE (2001) emphasized the synsedimentary Eovariscan reworking and re-sedimentation at Gara de Mrirt. This is manifested, with strong variation in lateral sections, by monomict, "griotte conglomerates", polymict breccias, and many, often wildly displaced olistolites and slump blocks. Hyperconcentrated density flows (depositing sorted conglomerates) have been caused by slope instability on tilted blocks, while rock fall deposits (breccias, olistolites) originated at active fault scarps with variably steep slopes (HÜNEKE 2001; Fig. 30). In Section VIII (Hill C) of WALLISER et al. (2000), the re-sedimentation of "xeno-blocks" straddled the lower-middle Famennian boundary. This is supported by conodont data for Section MG (Hill A) in HÜNEKE (2001), where several pebbly rudstone beds range from the *Pa. gracilis gracilis* (= Upper *rhomboidea*, Sample MG89) to *Pa. marginifera marginifera* (= Lower *marginifera*) Zones (up to Sample MG140). Corresponding Eovariscan tectonic movements are wide-spread in the Moroccan Meseta. In Section B (Fig. 29), slumping, occurs in the lowest Famennian (Bed S2, higher *frechi* Zone).

Submember 5 equals the Montagne Noire "supragriotte" (e.g., FEIST 1985; BECKER 1993a). Its base is best observed in sections without massive reworking. Typical are thin-bedded, micritic, light-grey to rose-grey solid flaserlimestones with some ammonoids and other macrofauna (Beds a-k of Section B, Beds 0-16 of Section II, Fig. 29). At the base is a marker bed with thinly oxyconic *Acrimeroceras* that are mostly seen as cross-sections on the outcrop. *Armatites* cross-sections and orthocones are associated. A loose slab from Section D (Fig. 32) shows how large the local *Acrimeroceras* species may grow and that it lacks the typical varices of Tafilalt species (see BECKER 1993a and EBBIGHAUSEN et al. 2000). There are more similarities with the un-named large form that occurs in the Rhenish Massif (e.g., at Beringhauser Tunnel, HARTENFELS et al. 2016). The intriguing *Acrimeroceras* Bed represents a short-termed bioevent (faunal bloom interval) across the Variscan oceans/seas, from the Gara de Mrirt to the Pyrenees, Montagne Noire, Saxothuringian Zone, and Rhenish Massif. It falls in the basal middle Famennian (basal *Pa. marginifera marginifera* Zone; Sample 64 of LAZREQ 1999), as in the other regions. Just slightly above, in Bed c of Section B (Fig. 29), the first sporadoceratids enter. Apart from typical cross-sections, there are *Maeneceras subvaricatum*

nuntio, the index species for the base of UD II-G, and some loose, larger *M.* cf. *subvaricatum.* In Section II (Fig. 29), ca. 8 to 8.5 m above the *Acrimeroceras* Bed, a different goniatite fauna, typical for the higher middle Famennian (UD III-B, lower Hembergian of German terminology), was collected. It includes the two zonal index species *Planitornoceras euryomphalum* and *Sporadoceras angustisellatum* (Fig. 33). The absence of *Pseudoclymenia* faunas and the dominance of *Planitornoceras* and of *Sp. angustisellatum* strongly resemble the Tafilalt faunal succession (e.g., BECKER et al. 2002, 2018a). LAZREQ (1992a, 1999) recognized at this level the *Sc. velifer velifer* Zone, which agrees with conodont-ammonoid correlations elsewhere (e.g., BECKER & HOUSE 2009).

Fig. 31: Goniatites from the lower Famennian of Bou Ounebdou (Mrirt Member, Submember 5); **a-b.** *Puncticeras pompeckji pompeckji* (WEDEKIND, 1918), Section A, loose, x 1.3; **c-d.** *Cheiloceras (Ch.) subpartitum subpartitum* (MÜNSTER, 1839), Section B/D, Bed Y2, x 1.5; **e-f.** *Compactoceras (Com.) undulosum undulosum* (MÜNSTER, 1832), Section II, loose, x 1.3; **g-h.** *Ch. (Ch.)* aff. *sacculum* (SANDBERGER & SANDBERGER, 1850), Section B/D, Bed X3, x 1.2; **i-j.** *Ch. (Ch.)* aff. *amblylobum* (SANDBERGER & SANDBERGER, 1850), Section B/D, loose, x 1.2; **k-l.** *Falcitornoceras falcatum* (FRECH, 1887), Section B/D, loose, x 1; **m-n.** *Cheiloceras (Ch.) subpartitum subpartitum* (MÜNSTER, 1839), Section B/D, loose, x 1.5; **o-p.** *Compactoceras (Com.) verneuilii sublentiforme* (SOBOLEV, 1914), Section B/D, above Bed W, x 1.

Depending on the degree of erosion/reworking, the cephalopod limestone succession of Submember 5 ranges laterally variably to higher parts of the middle Famennian (*Sc. velifer velifer* Zone in the LAZREQ section) or into the upper Famennian. In Section A (Hill B) the slope on the back side of the lower cliff is formed by light-grey nodular limestone with unusually abundant goniatites and clymeniids that whether out freely:

Protactoclymenia stenomphala (common, Figs. 34a-b)
Protactoclymenia sp. indet. (common)
Stenoclymenia cf. *rectangula* (rare, relatively large specimen with suture and ventrolateral edges)
Platyclymenia (Pl.) cf. *pattisoni* (rare)
Platyclymenia (Pl.) subnautilina (Figs. 34e-f)
Platyclymenia (Pl.) sp. indet. (moderately common)
Prionoceras aff. *frechi* (moderately common, Figs. 34c-d)
Sporadoceras n. sp. (extremely compressed, rare)

The fauna falls in the basal upper Famennian UD IV-A (*Prionoceras* Genozone). The extremely thin new sporadoceratid is too poorly preserved to establish a new taxon. A correlation of the local *Protactoclymenia* Bed with *Annulata* Event beds or the overlying, usually very fossiliferous, so-called Wagnerbank (see HARTENFELS 2011; HARTENFELS & BECKER 2016) is possible. By contrast, the last limestone at the top of the upper cliff yielded beside shark teeth an older conodont fauna:

Branmehla ampla
Palmatolepis gracilis gracilis
Palmatolepis minuta schleizia
Palmatolepis perlobata helmsi
Palmatolepis rugosa trachytera
Polygnathus doulingshanensis
Polygnathus perplexus
Scaphignathus velifer velifer

This assemblage falls in the *Pa. rugosa trachytera* to *Pseudopolygnathus granulosus* Zones and pre-dates the *Annulata* Events. The regionally first recognition of faunas with *Pa. rugosa trachytera* is remarkable since they cannot be identified in the Anti-Atlas (HARTENFELS 2011, p. 39). Therefore, the Gara de Mrirt ammonoid and conodont record is a mixture of Tafilalt and southern Europe faunal elements, as it can be expected from an intermediate terrain.

Fig. 32: Extremely thinly oxyconic *Acrimeroceras* n. sp., loose from the basal Submember 5 of the upper cliff at Hill C (Section D, whorl width < 10 mm at ca. 140 mm dm).

Fig. 33: Strongly compressed (ww/wh = 0.28), typical *Sporadoceras angustisellatum* WEDEKIND, 1908 without varices and with high whorl expansion rate, Hill A, Section ß, Bed 6, *Pl. euryomphalum* Zone, UD III-B, max. dm = 54 mm.

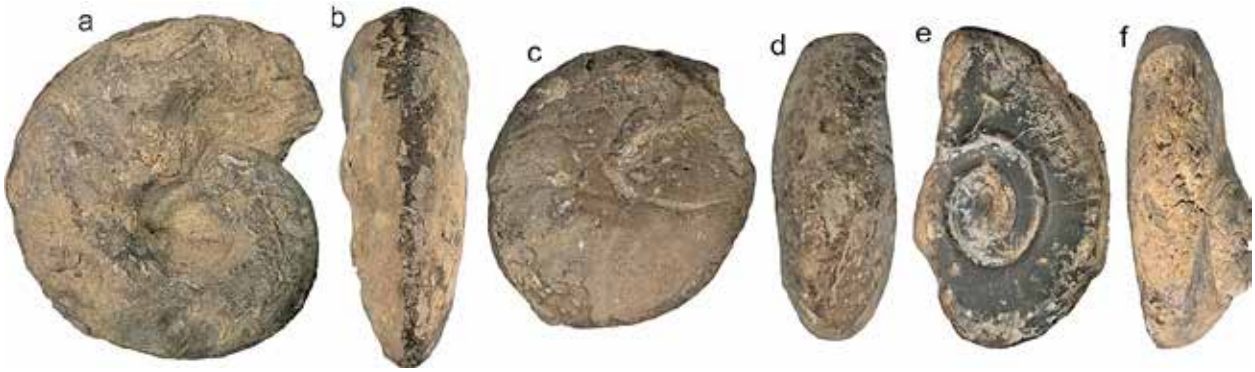

Fig. 34: Ammonoids from the *Protactoclymenia* Bed at the back side of the lower cliff at Hill B (Section A); **a-b.** *Protactoclymenia stenomphala* (PETTER, 1959), max. dm = 48 mm; **c-d.** *Prionoceras* aff. *frechi* (WEDEKIND, 1913b), max. dm = 28.5 mm; **e-f.** *Platyclymenia (Pl.) subautilina subnautilina* (SANDBERGER,1855), max. dm = 36 mm.

In Section M (Hill D) of HÜNEKE (2001), large slump blocks appear above nodular limestones with conodonts of the *Pa. minuta minuta /crepida* Zones (based on the presence of *Pa. minuta minuta* and *Pa. minuta loba* in Sample M72). The overlying thick succession of slump blocks, breccias, conglomerates and nodular limestone may represent a completely reworked unit or may consist of autochthonous middle/upper Famennian beds alternating with synsedimentary re-sediments. Conodonts from the last conglomerate above the lower cliff succession (top Section A, Hill B) represent an admixture of lower to upper Famennian taxa:

Bispathodus spinulicostatus M1
Bispathodus stabilis stabilis
Bispathodus stabilis vulgaris
Bispathodus stabilis zizensis
Branmehla ampla
Icriodus sp.
Palmatolepis glabra lepta late morphotype
Palmatolepis glabra pectinata M1
Palmatolepis glabra prima M3 or M1
Palmatolepis gracilis gracilis
Palmatolepis perlobata schindewolfi
Palmatolepis perlobata sigmoidea
Palmatolepis tenuipunctata (fragmentary)
Palmatolepis termini
Palmatolepis triangularis M2
Pseudopolygnathus primus primus M3

Fig. 35: *Clymenia laevigata* (MÜNSTER, 1831), large-sized incomplete specimen found loose as an olistolite within the conglomerate/mass flow above Section B (Hill B, upper cliff, max. wh = 35 mm).

The youngest species, *B. spinulicostatus*, indicates at least the *B. aculeatus aculeatus* Zone. Combined with records of *B. costatus* in LAZREQ (1999, Sample L70) and of *B. ultimus* in HÜNEKE (2001, Sample M75), there is no doubt that the pelagic carbonate ramp existed originally through all or most of the upper/uppermost Famennian. However, there is so far no evidence for synsedimentary reworking in that time interval; all current age data come from re-deposited clasts, not from autochthonous limestone.

6.4. Lower Carboniferous (Al Gara Formation)

The northern slope of the lower cliff (e.g., at Section A, Hill B) and the plain below the second or upper cliff are occupied by poorly exposed shales, in the higher part with slump blocks, followed by interbedded, coarse, polymict conglomerates, which are, again, overlain by a brownish, fine conglomeratic crinoidal limestone. Unfortunately, the latter yielded no conodonts. It is unclear whether this distinctive bed correlates with the crystalline, crinoidal limestone of LAZREQ (Sample L70) that yielded a mixture of re-deposited upper Famennian and Lower Tournaisian conodonts, such as *Po. purus subplanus* and *Ps.* cf. *brevilaminus*. WALLISER et al. (2000) assigned the succession of Section VIII (Hill C) that lies above typical Submember 5 limestones, our **Lower Member** of the Al Gara Formation, provisionally to the "Etroeungt". The latter term, however, should be restricted to uppermost Famennian strata of the western Rhenish Massif/Ardennes (e.g., AMLER & HERBIG 2006). Accepting the sparse conodont data by LAZREQ (1999), and in accord with reworked upper Famennian conodonts in our new sample from the last polymict conglomerate of Section A, we assume a second Eovariscan reworking phase in the lower/middle Tournaisian. It may correlate with lower/middle Tournaisian tectonic and seismic events in the Oulmes region (BECKER et al. 2015), Tafilalt (KAISER et al. 2011; TAHIRI et al. 2013), and in the Tinerhir region to the SW (RYTINA et al. 2013), which is the Eo-Variscan 2 Event of MICHARD et al. (2008). It is also likely that the angular unconformities at the Bouechot W of Mrirt (FAIK 1988; BOUABDELLI et al. 1989) and at Bou Khedra N of Mrirt (e.g., BOUABDELLI 1989) formed during the same block faulting episode.

Olistolites within the reworking unit at the top of the lower nappe consist mostly of Upper Devonian cephalopod limestones, partly with cheiloceratids, but there are also *Dzieduszyckia* Limestones (Fig. 36). The coarse conglomerates near the top are distinctively polymict and poorly sorted. Isolated olistolite blocks may consist themselves of conglomerates. This proves a second reworking of Famennian re-sediments (presence of cannibalized reworking beds).

Fig. 36: Specimen of *Dzieduszyckia intermedia* (TERMIER, 1936), pedicle valve above, brachial valve below, extracted from an isolated *Dzieduszyckia* Coquina from the melange above the lower cliff (Hill B, Section A; max. incomplete width = 51 mm).

The lower slope of the upper cliff is assigned to a distinctive **Upper Member**, formed by green, silty shales. In higher parts, the latter turn into a melange of shale and Upper Devonian olistolites, which were obviously detached from the upper nappe during its emplacement. There are mostly black laminated or crinoidal limestones and concretions as well as micrites

with *Manticoceras* and *Beloceras*, all Frasnian in age (derived from just above). The shale unit appears to be identical with the green shales and siltstones that overlie the Bou Nebedou Formation in the upper cliff. A survey of isolated clasts from above Sections B/D (top of upper cliff) yielded the following array of lithologies:

upper Famennian, middle grey cephalopod limestone with large-sized clymeniids (*Clymenia laevigata*, Fig. 35, *Cyrtoclymenia* sp. with 180 mm dm)
lower Famennian griotte with cheiloceratids
brown encrinites with spiriferids (?Tournaisian)
rose colored, unfossiliferous micrites (probably middle Famennian)
reworked conglomerate (top lower/middle Famennian)
Dzieduszyckia Limestone (basal middle Famennian, based on a conodont fauna with *Pa. marginifera marginifera, Pa. glabra lepta* late morphotype, *Pa. perlobata schindewolfi, Pa. minuta schleizia, B. stabilis vulgaris*, and *Po. fallax*)
dark-grey limestone (?KW beds)
vein calcite
quartzite

The Viséan age of the Upper Member is constrained by palynomorphs from the green shale. There is a vague support from a single solitary rugose coral embedded in the shale matrix identified by D. WEYER (Berlin) as Gen. nov. aff. *Sochkineophyllum* n. sp. (see taxonomic notes below). The third regional reworking of Devonian strata and re-deposition of olistolites may have occurred before or during the nappe formation and transport process. Olistolites represent the detached "smaller-sized" fraction of the large, internally intact glide masses. The age of the nappe movements is still poorly constrained in the Mrirt region (compare the discussion in HUVELIN & MAPET 1997). Possibly, it occurred within the Upper Viséan, correlating with the thick wildflysch overlying the Jebel Tabainout SW of Khenifra. The latter includes very similar reworked Devonian strata, ranging from Frasnian flaserlimestone and Kellwasser beds to blocks of cheiloceratid-rich griotte, *Dzieduszyckia* Limestone and encrinites. However, in the Eastern Meseta to the NE (Debdou-Mekam Massif), the "D1 folding" of a thick flysch succession precedes unconformably overlying Upper Viséan strata (e.g., ACOTTO et al. 2019).

7. Taxonomic Notes

7.1. Ammonoids

Suborder Gephuroceratina
Superfamilie Gephuroceratoidea
Family Gephuroceratidae

***Manticoceras inflatum* BECKER n. sp.**
Figs. 27, 37

Type: The original of Figs. 27 and 37, currently the only known specimen (Geomuseum Münster).
Derivation of name: After the characteristic shell inflation.
Diagnosis: Medium-sized, whorls depressed throughout ontogeny, with strongly converging, rounded flanks and narrowly rounded venter, fast expanding (WER = ca. 3.0), involute (uw/dm = ca. 0.17), umbilical wall steep, deeply rounded, no distinctive ornament. Sutures with moderately high median saddle (< 50 % of flank saddle at medium size), wide and subsymmetric flank saddle (width/height = ca. 1.7), small pointed L-lobe and short, low saddle lateral outside the umbilical wall.
Description: The holotype is sufficiently preserved to justify the introduction of a new species. Shell parameters are as follows: dm = 38 mm, umbilical width = 6.3 mm (uw/dm = 0.17), whorl height = 20.4 mm (wh/dm = 0.54), whorl width = 22.2 mm (ww/dm = 0.58), apertural height = 16 mm (ah/dm = 0.42), ww/wh = 1.09, WER = 3.0. Most characteristic are the deep umbilicus and the whorl cross-

section, in combination with a wide and proportionally low flank saddle.

Discussion: The wide flank saddle places the new species in the *M. latisellatum* Group, which also includes, as the most similar species, the Russian *M. solnzevi*. The latter is more compressed at comparable size (see data in BOGOSLOVSKIY 1969) and its subumbilical saddle is slightly wider. All known other species of the *latisellatum* Group have compressed, discoidal conches. Similar whorl forms are developed in some species of *Crickites*, *Gephyroceras*, and in the *M. cordatum* Group. However, all these forms are characterized by higher and narrower, strongly asymmetric flank saddles. *Manticoceras bullatum* is less inflated at the same size (see WEDEKIND 1913), which is also true for *M. crassum* that, in addition, displays flattened flanks (see re-illustration of holotype in HOUSE & ZIEGLER 1977, pl. 6, fig. 2). *Gephyroceras rhynchostomum* has a different cross-section (see HOUSE & KIRCHGASSER 2009, pl. 22, figs. 6 and 9), and in *Cr. holzapfeli* (? = *rickardi*) the flanks do not converge strongly (WEDEKIND 1913). The Siberian *?Cr. altaicus* is characterized by extremely narrow flank saddles and a wider umbilicus, whilst in the associated *?Cr. neverovi*, the flank saddle and E-lobe are strongly asymmetric; the latter is dorsally incurved (see BOGOSLOVSKIY 1969). The new species is not placed in *Sphaeromanticoceras*, which has to be restricted to small-sized forms around the type-species (*Sph. affine*) that possess a ventral band in early stages (see CLAUSEN 1969).

Geographic and stratigraphic range: Restricted to the upper Frasnian of the eastern Central Meseta.

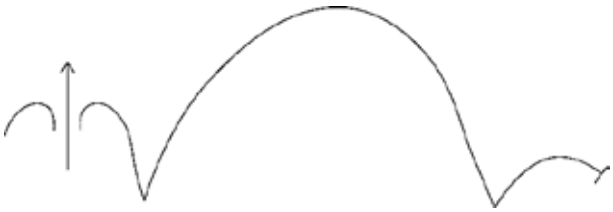

Fig. 37: Outer suture of the holotype of *M. inflatum* n. sp. at 11 mm whorl height, showing the wide, subsymmetric flank saddle as typical for the *M. latisellatum* Group.

7.2. Corals (by Dieter WEYER)

Gen. nov. aff. *Sochkineophyllum* n. sp.
Figs. 38.1-4

Material: Only a single specimen from the green shale matrix above the upper cliff at Bou Ounebdou, Hill C, Section D (Fig. 38).

Discussion: The new ahermatypic taxon is similar to *Sochkineophyllum* (elongated counter septum, initial tachylasmatoid trend sensu HUDSON 1936), but differs in the development of dissepiments at maturity. Hitherto, such a morphology has never been described. The precise stratigraphic age remains unknown. *Sochkineophyllum* occurred from the basal Lower Carboniferous [Lower Tournaisian: *Sochkineophyllum* n. sp. (SCHINDEWOLF 1942) and *Sochk. internectum* FEDOROWSKI, 1973] to the Middle Permian [Guadalupian: *Sochk. turgidiseptatum* (TIDTEN, 1972)]. Probably, the Gara de Mrirt specimen is of Viséan age, but our knowledge of Tournaisian ahermatypic Rugosa faunas is rather incomplete.

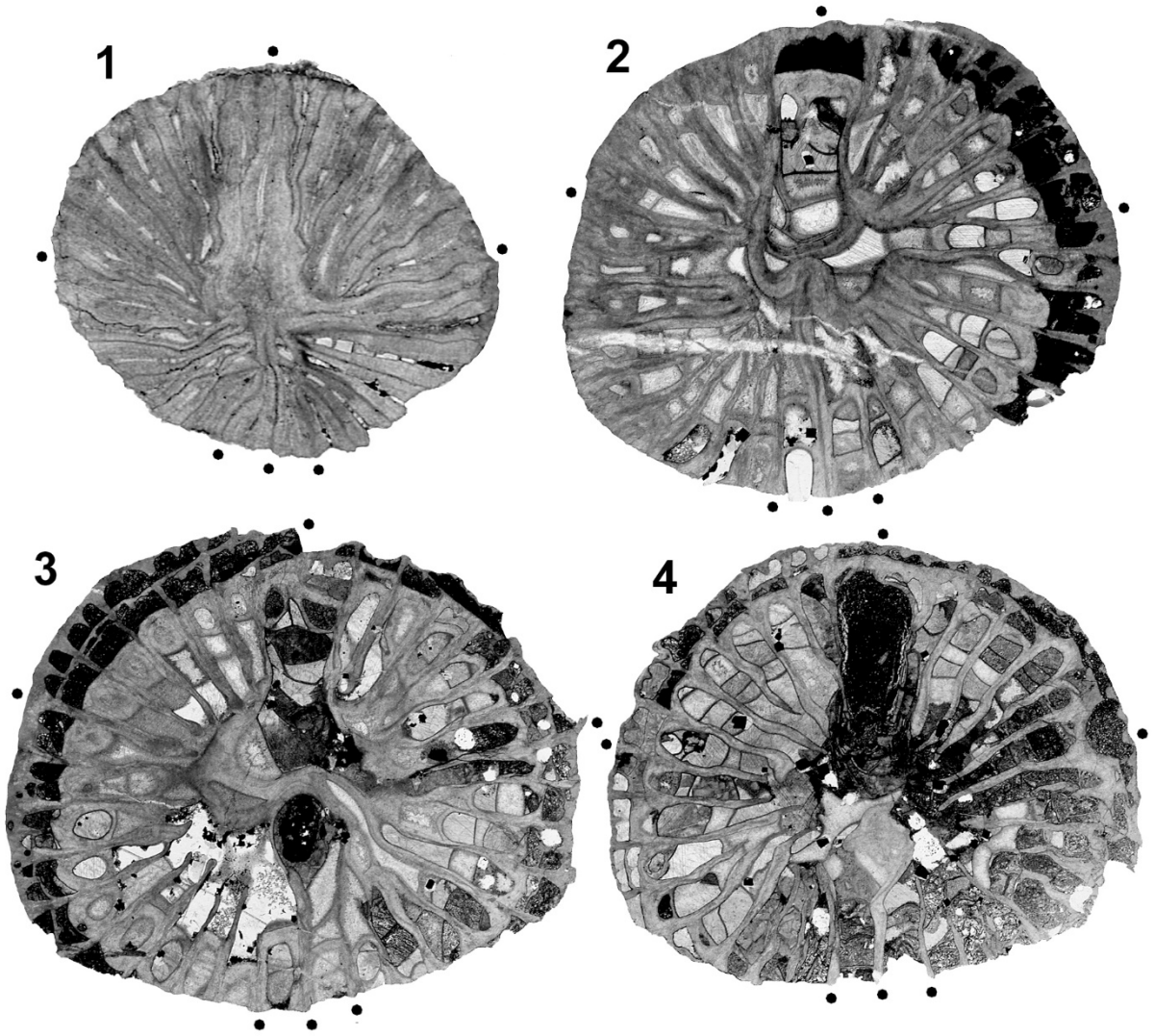

Fig. 38: Four thin sections of Gen. nov. aff. *Sochkineophyllum* n. sp. from the Lower Carboniferous of Gara de Mrirt, Bou Ounebdou, green shales at the top of the upper cliff, Hill C, Section D; x 8 (38.1) or x 4 (38.2-4); type collection of the Geomuseum Münster (thin sections and photos by D. WEYER).

The unique Devonian of Immouzer-du-Kandar (Middle Atlas basement) – biostratigraphy, faunas, and facies development

Zhor Sarah Aboussalam, Ralph Thomas Becker, Julia Richter, Sven Hartenfels, Ahmed El Hassani & Stephan Eichholt

Fig. 1: View (from the hill at Douar Ahmed-ben-Mellouk) on Devonian exposures of Immouzer-du-Kandar (hill rising from Chabat el Jenanet, Sections C2 and C3 of Cygan et al. 1990), our Section C4, with outcrop of the lower Emsian conglomerate (Chabat Jenanet Formation) along and above the track, faulted upper Emsian to lower Givetian limestones in the lower slope (new Ahmed-ben-Mellouk Formation), the reef breccia forming a small terrace ca. 2/3 upwards, and the Famennian upper slope (new Chabat el Hallouf Formation, Section C5) towards the top. The slope to the left (NNE) is occupied by Triassic red beds. Section numbers are marked in circles.

1. Introduction

The Middle Atlas divides the Moroccan Meseta into the Western and Eastern Meseta, which differ strongly in the Devonian in terms of facies and synsedimentary structural geology (e.g., overviews of El Hassani & Benfrika 1995, 2000). There is restricted knowledge of the Palaeozoic basement of the Mesozoic Middle Atlas, with the best and most important outcrops in the tectonic window ("boutonnière") at Immouzer-du-Kandar, ca. 40 km S of Fès. The wooded Jebel Kandar to the SW is a more than 1600 m high mountain built of Jurassic strata (Fig. 2). Fossiliferous Ordovician to Lower Carboniferous formations crop out to the NW, from Dour Rouda towards the SE, the Chabat el Jenanet,

and then towards the Chabat al Sitout (Fig. 4) The Devonian litho- and biostratigraphy of the area has been established by the CHARRIÈRE & RÉNAULT (1989) and CYGAN et al. (1990; Fig. 3). Comparisons with other Meseta regions showed from the beginning that the succession includes many unique sedimentological units, faunas and floras (FAIRON-DEMARET & REGNAULT 1986), which isolate it both from the closest Devonian of the East-Central Meseta (e.g., PIQUE & MICHARD 1981; Azrou-Khenifra nappes) and from the predominantly siliciclastic Eastern Meseta e.g., at Tazekka, which is separated by the Tazekka-Bsabis-Bekrit Fault Zone (see HOEPPFNER et al. 2005, 2006 for overview)). There are coarse conglomerates and slump masses with "alien" (e.g., TAHIRI et al. 2017) magmatic rocks, which must have been derived from a proximal Neoproterozoic to Lower Palaeozoic source. This differs considerably from the basement of other Meseta regions. Therefore, any new stratigraphical, sedimentological, palaeontological, and geochemical data add to the knowledge of a crucial segment of Meseta palaeogeography and tectonics. However, the Immouzer-du-Kandar Devonian may represent a transported, allochthonous unit, as the nappes of the Azrou to Khenifra region.

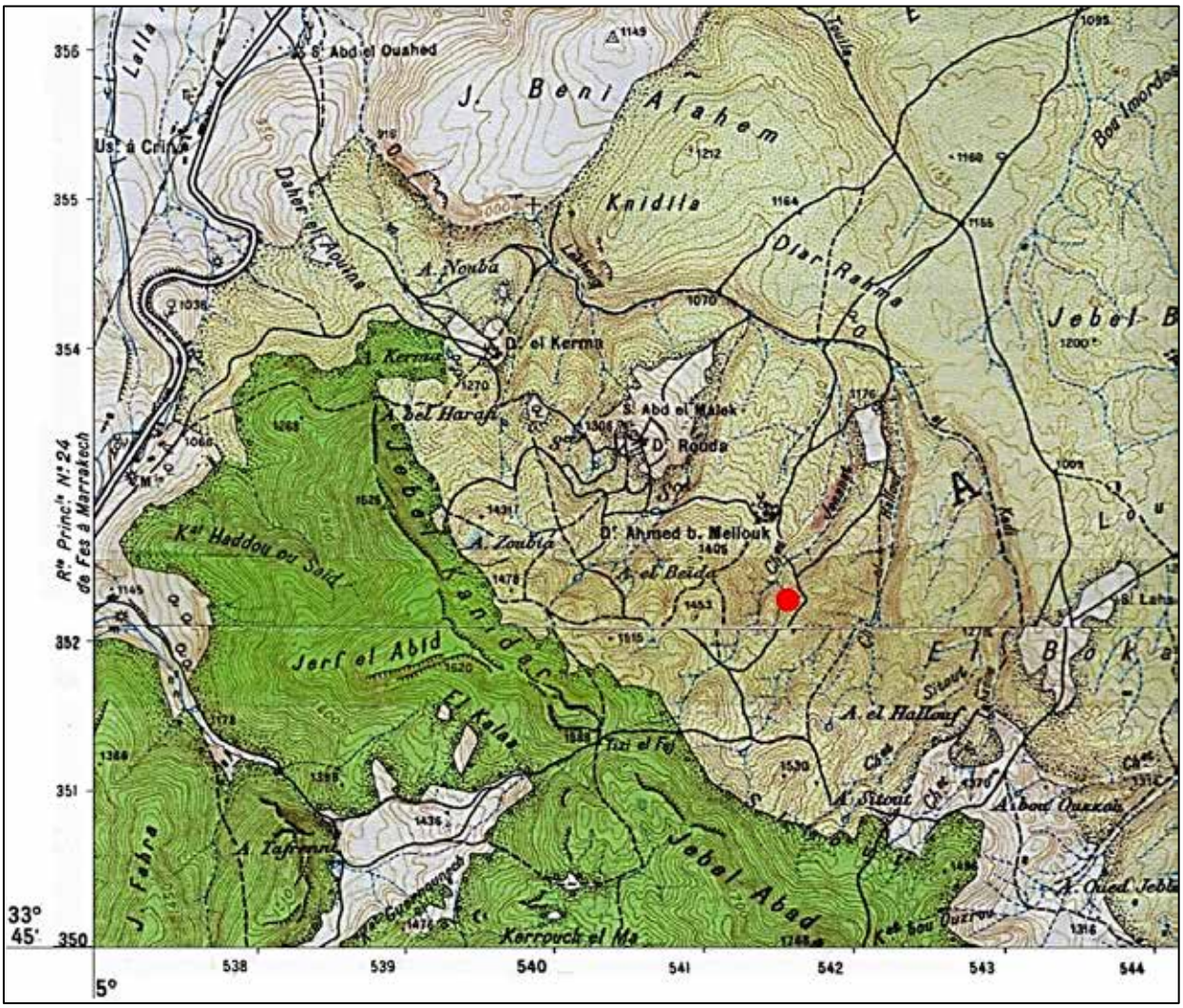

Fig. 2: Position of the Jurassic Jebel Kandar and the Jenanet succession (red dot for Fig. 1) in the SW corner of topographic sheet, 1: 50 000, NI-30-VIII-3c, Sefrout.

By detailed section logging, conodont and macrofauna sampling, as well as microfacies analyses in the last ca. 10 years, we can significantly refine the local litho- and biostratigraphy and provide a more precise reconstruction of facies changes, sea-level, and local influences of global events, for example around the Emsian-Eifelian, middle-upper Givetian, and Frasnian-Famennian boundaries. The studied sections begin in the branching valley of Chabet el Jenanat and ascend the western slope of the hill just to SE, reaching up to the crest (Figs. 1, 2, 4; at x = 541.8, y = 352.3; GPS N33°45′58.4′′, W4°56′50.9′′). There are numerous normal faults, which offset especially the upper Emsian to Givetian succession at close distance (Fig. 1). These had to be respected in order to avoid mistakes in the small-scale lateral correlations.

2. Research History

HORON (1954): First (unpublished) report on fossiliferous Silurian (with graptolites) to Lower Devonian (with brachiopods) strata at Immouzer-du-Kandar, followed by a Viséan transgression.

CHARRIÈRE & RÉGNAULT (1983) and CHARRIÈRE et al. (1984): Preliminary notes on the Immouzer-du-Kandar Devonian litho- and biostratigraphy.

BRICE et al. (1984): Description and biostratigraphic dating of Emsian, supposed Frasnian, and upper Famennian brachiopods.

FAIRON-DEMARET & RÉGNAULT (1986): Description of Lower and Middle Devonian plant remains, with implications for stratigraphy (Fig. 3) and palaeobiogeography.

RÉGNAULT & CHAUVEL (1987): Description of the first Lower Devonian carpoid of Morocco from the Aïn el Beida Formation, representing probably a new (un-named) genus of the Anomalocystitida (Mitrata).

OUARHACHE (1987): Unpublished thesis on the Palaeozoic to Triassic at the NW margin of the Middle Atlas S of Fés.

CHARRIÈRE (1989) and CHARRIÈRE & RÉGNAULT (1989): Principles of Devonian and Carboniferous litho- and biostratigraphy of Immouzer-du-Kandar.

CHARRIÈRE (1990): Unpublished Ph.D. Thesis on the Hercynian evolution of the Middle Atlas basement, with detailed data for Immouzer-du-Kandar.

WILLEFERT & CHARRIÈRE (1990): Detailed description of Ordovician and Silurian litho- and graptolite biostratigraphy.

CYGAN et al. (1990): Conodont biostratigraphy of Emsian to lower Frasnian units at Immouzer-du-Kandar and their significance for the understanding of the sedimentary evolution and palaeogeography of the region.

RACHEBEUF (1990a, 1990b): Record of the chonetids *Ctenochonetes robardeti* and *Plicanoplica carlsi* from lower Emsian grey shales of Immouzer-du-Kandar.

OUARHACHE et al. (1991): Records of Upper Viséan foraminifers, calcareous algae (*Koninckopora*), and "pseudo-algae", such as *Palaeoberesella, Kamaena, Stacheia,* and *Aoujgalia*.

EL HASSANI & BENFRIKA (1995, 2000): Overviews of the Devonian of the Moroccan Meseta, including a summary for the Middle Atlas basement.

BERKHLI (1999): Discussion of the foraminifer age of Viséan limestones at Immouzer-du-Kandar.

BERKHLI et al. (2000): Brief discussion of the microfacies of Upper Viséan limestones of Immouzer-du-Kandar in the frame of a general discussion of Lower Carboniferous sedimentologie and geodynamics of the NE Meseta.

SARTENAER (2000): Re-assignment of supposed *Planovatirostrum* sp. described by

BRICE et al. (1984) to the new genus *Phacoiderhynchus*.

JANSEN (2001): Brief comments on some of the Pragian brachiopods (*Euryspirifer*) described by BRICE et al. (1984).

MICHARD et al. (2008): Reference to the Chabat Jenanat conglomerate with reworked granites, ignimbrites, Ordovician quartzites, and Silurian slates.

GERRIENE et al. (2010): Reference to the possible occurrence of the aneurophytalean genus *Rellimia* in the "plant shale" at Immouzer-du-Kandar.

BECKER (2012): Illustration of the Eovariscan breccia at Immouzer-du-Kandar, as an example for double reworking.

BECKER & ABOUSSALAM (2014): Brief reference to the distinctive upper Givetian to middle Frasnian facies at Immouzer-du-Kandar.

SCHWERMANN (2014): Unspecified record of shark teeth in Frasnian samples from Immouzer-du-Kandar.

RICHTER et al. (2016): Preliminary new conodont data for the Emsian/Eifelian and upper Famennian at Immouzer-du-Kandar.

BECKER et al. (2016): Brief reference to the discovery of upper Givetian goniatites at Immouzer-du-Kandar.

RICHTER (2017): Unpublished M.Sc. Thesis on the upper Emsian to Eifelian and upper Famennian carbonate succession.

TAHIRI et al. (2017): Geochronological dating of granite clasts within the Chabat Jenanet Conglomerate as Ediacarian and Cambrian.

COZAR et al. (2019): Discussion of Immouzer-du-Kandar Viséan foraminifers in the context of survival and/or reworking of Lower/Middle Viséan forms into the Upper Viséan.

3. Facies setting and synsedimentary tectonics

The Immouzer-du-Kandar facies setting was very complex, with a close superposition of sediments with a terrestrial, coastal, siliciclastic inner shelf, carbonate platform, seamount, and deep pelagic origin (compare CHARRIÈRE & RÉGNAULT 1989, tab. 1). The presence of several coarse reworking units proves significant synsedimentary tectonic movements and active, steep fault scarps in the source region of material, from where mass flows moved downwards. The deep erosion into Neoproterozoic basement and the perfect rounding of pebbles show that an adjacent island must have existed, where material was constantly moved in fluviatile or coastal environments, prior to transport and downslope re-deposition. Parts of the topographic high were deeply drowned leading to condensed cephalopod limestone accumulation on a former seamount. But during highstands, pelagic anoxic to euxinic conditions developed. Upslope, along the island shoals, a top Middle to basal Upper Devonian reef existed, which was later uplifted and completely eroded. These strong contrasts indicate in total a tectonically highly active shelf basin slope near to one or more islands. After the complex Eovariscan period, the Viséan strata can be better placed in the palaeogeographic context of adjacent successions (e.g., BERKHLI et al. 2000).

4. Litho- and biostratigraphy

Our new studies concentrated on the Emsian to Famennian interval (Fig. 4), but for the sake of completeness, earlier and later intervals are included and briefly reviewed based on literature data.

4.1. Silurian-Devonian transition

A thick succession of Pridoli graptolite shales, previously without a formation name (proposal: Douar Rouda Formation), occurs around the Douar Rouda village (WILLEFERT et al. 1990, figs. 3-4). At the top, records of *Pristiograptus transgrediens* and *Linograptus posthumus* and scyphocrinitid debris give an

upper Pridoli age. CHARRIÈRE & RÉGNAULT (1989) recorded the Lochkovian index species *Uncinatograptus uniformis* from several samples but this was not upheld in the more detailed study of WILLEFERT et al. (1990). The same applies to a record of "*Monograptus hercynicus*" (Sample IK 92), which was changed to "*M.*" *prognatus*.

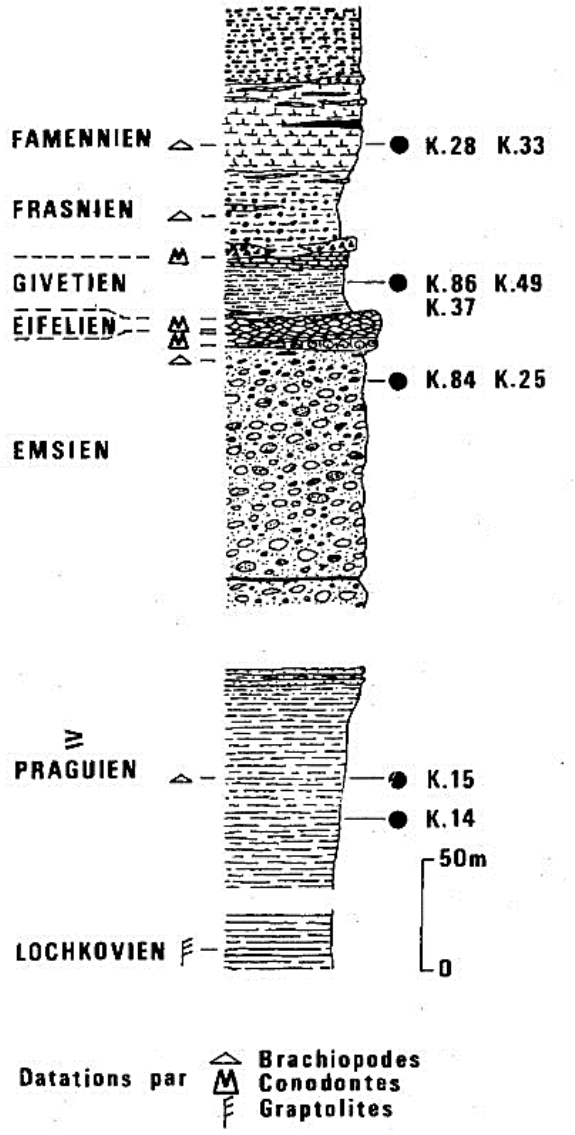

Fig. 3: Devonian lithological succession at Immouzer-du-Kandar by FAIRON-DEMARET & RÉGNAULT (1986, fig. 2), with proportions of unit thicknesses and the position of biostratigraphically relevant samples.

The graptolite-rich unit is conformably followed by a thick succession of nodular limestone ("barre noduleuse") with orthoconic cephalopods, nuculid bivalves, and fragmented crinoids. This un-named formation may correlate at least partly with the widespread *Scyphocrinites* Limestone of the Anti-Atlas (HAUDE et al. 2014) and many other regions (e.g., RÉGNAULT 1985), which straddles the Silurian-Devonian boundary (e.g., CORRIGA et al. 2013). However, there are no local conodont data so far. Therefore, a lower Lochkovian age still needs to be proven.

4.2. Aïn el Beida Formation (Pragian)

WILLEFERT et al. (1990) illustrated only a faulted lower contact of the thick, fine, rather monotonous, dark-grey, micaceous shales of the Aïn el Beida Formation. It forms a 250 m wide outcrop belt at the SE end of Douar Rouda (BRICE et al. 1984; Fig. 5). The laminated or slightly bioturbated shales yielded, apart from bivalves, gastropods, ostracods, bryozoans, and orthocones, abundant trilobites, including asteropygids, phacopids, and *Odontochile* (s.l.). The traditional Odontochilinae are most typical for the Pragian and extend into the basal Emsian (e.g., BUDIL et al. 2008). The known brachiopods, crinoids (*Asperocrinus*), plants (*Taeniocrada*), acritarchs, and poorly preserved spores (*Camptozonotriletes caperatus*) are not in conflict with a Pragian age (FAIRON-DEMARET & RÉGNAULT 1987). RÉGNAULT & CHAUVEL (1983) discovered a rare stylophorid echinoderm in this formation. The environment was a subtidal, moderately shallow shelf with a constant supply of fine siliciclastics from a hinterland that could have been at some distance. In comparison with the preceding pelagic nodular limestones, the Pragian was locally regressive. But there is currently no record for the middle/upper Lochkovian at Immouzer-du-Kandar (Fig. 3).

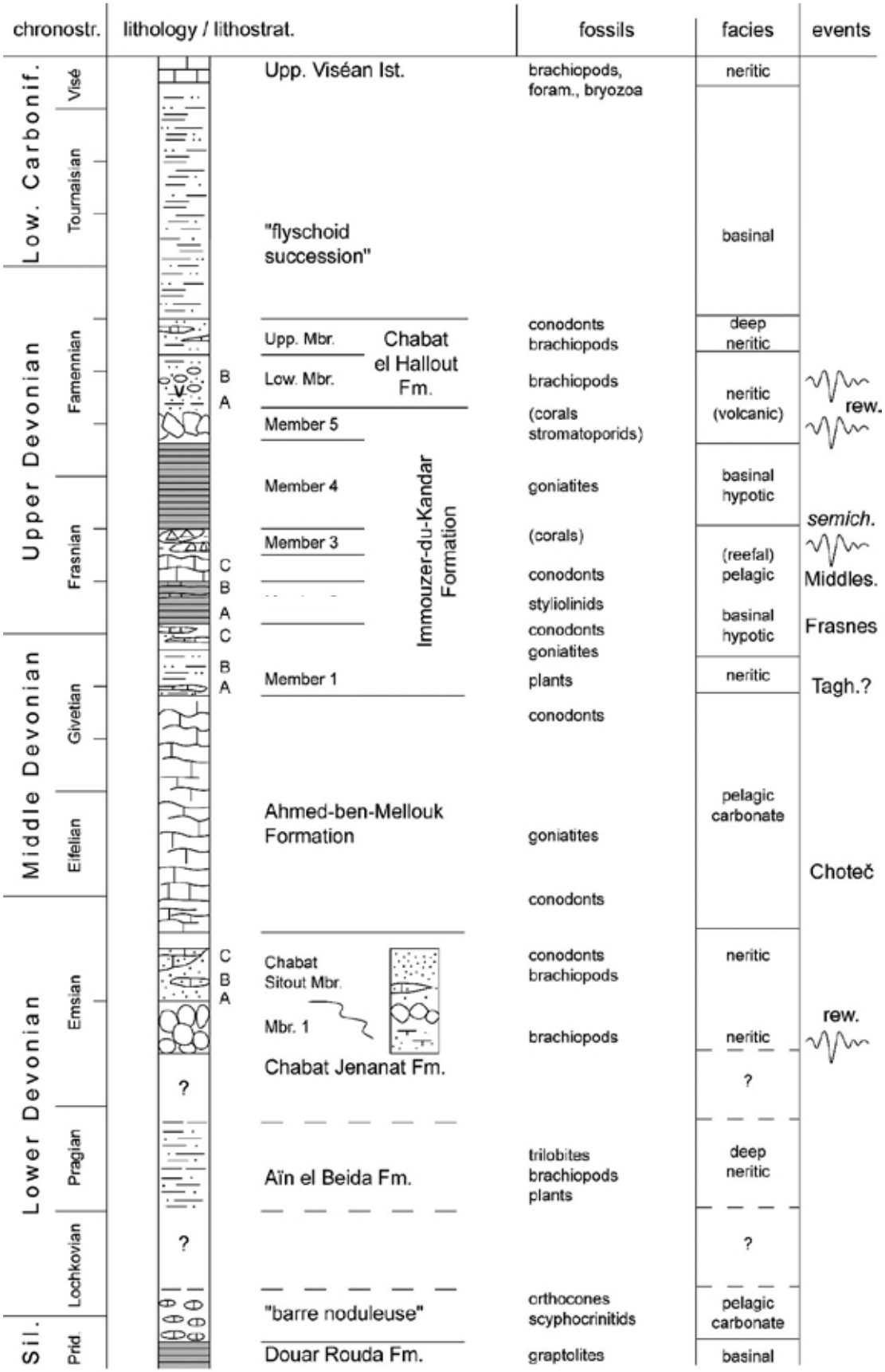

Fig. 4: Revised top-Silurian to Lower Carboniferous lithology and lithostratigraphy at Immouzer-du-Kandar. showing the succession of characteristic fossil groups, facies, seismically triggered reworking episodes, and locally expressed bioevents.

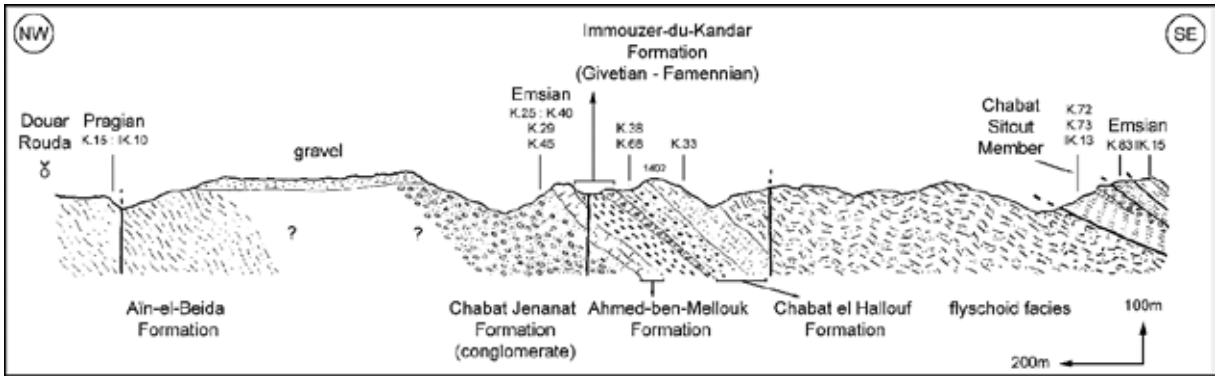

Fig. 5: Simplified geological cross-section through the Immouzer-du-Kandar Devonian (updated from BRICE et al. 1984, fig. 2, showing their sample numbers = K.-no.; compare more expanded NW-SE cross-section of CHARRIÈRE 1989, fig. 6), using the new lithostratigraphic units.

4.3. Chabat Jenanat Formation (lower Emsian)

The "Poudingue de la Chabat Jenanat" of BRICE et al. (1984) and CHARRIÈRE & RÉGNAULT (1989) is here re-named as Chabat Jenanat Formation but restricted to its main lithology, up to 100 m thick, coarse, strictly unsorted and polymict conglomerate with well-rounded pebbles (Figs. 5-6; Chabat Jenanat Conglomerate). The main lithologies are grey Ordovician quartzites, dark cherts (perhaps Silurian), slates, Neoproterozoic to Cambrian granites of unclear regional provenance (TAHIRI et al. 2017), and various acidic volcanites (Figs. 7-8). CHARRIÈRE & RÉGNAULT (1989) described various tuffs and ignimbrites. There is no evidence for any sorting or grading within thick beds. Therefore, sedimentation must have occurred as violent mass flows in channels along a significant slope. The source for the top-Precambrian to Lower Palaeozoic pebbles must have been at close distance (within a few km). Deep excavation and rounding occurred over considerable time in a fluviatile to coastal setting of an uplifted tectonic block forming an island. This enabled the excavation and mixing of very heterogeneous and heterochronous rocks. Marine re-sedimentation occurred due to a second phase of seismic activity (see also the sedimentary model of CHARRIÈRE & RÉGNAULT 1989), which caused gravitational gliding down from the original shallow-water setting. Therefore, the local change from subtidal shales and siltstones with neritic fauna to coarse conglomerate and high-turbulence does not necessarily mean a shallowing of the environment. It rather reflects a second interval of block faulting, which created an instable slope.

The timing of synsedimentary tectonism can be deduced from the age of the youngest observed clast and of the oldest overlying sediment. Limestone pebbles are very rare but we extracted one directly from the solid bed that was large enough for microfacies analysis and conodont dating. It represents a unique, hypoxic, ostracod wackestone (Fig. 9.1) with calcisiltite matrix, a facies type that does not occur in the overlying limestone succession. The single obtained, fragmentary *Polygnathus* s. str. is too incomplete for species identification but its small basal pit is a morphological feature that did not develop until the upper half of the lower Emsian (*Po. inversus* Zone; e.g., BULTYNCK 1987). Top-lower to basal upper Emsian conodonts occur in crinoidal limestones overlying the conglomerate (CYGAN et al. 1990; see below). In consequence, one block tilting phase must have occurred within the late lower Emsian, a time interval of ca. 3 ma duration (BECKER et al. 2020 in press). It was capable to uplift

sediment from subtidal, deeper neritic facies to a coastal level, leading there to rounding and pebble formation. Just slightly later, the pebble was picked up by a seismically triggered mass flow that brought with it much older pebbles that may have been around for a much longer time.

Strong lower Emsian block faulting and reworking is not common in other Meseta regions. BECKER et al. (2015) used the phrase "Eovariscan prelude" for the Lochkovian to Eifelian interval. The closest other evidence for a contemporaneous formation of breccias and olistolite emplacement comes from the Jebel ben Arab between Azrou and Meknes (LAZREQ 1990 and new data). As already noted by CYGAN et al. (1990), it is also no coincidence that the even closer Devonian of Bab-el Ari just NE of Azrou shows a peculiar unconformity high in the lower Emsian, with a subsequent gap encompassing all of the upper Emsian (BOHRMANN & FISCHER 1985). It seems that late lower Emsian tectonism and uplift is a distinctive feature at the NE end of the Western Meseta.

4.4. (new) **Chabat Sitout Member** (Emsian)

The type area of the new member is at the Chabet el Sitout valley (BRICE et al. 1984; Fig. 5), ca. 1.5 km SE of the conodont-bearing Section 1 of CYGAN et al. (1990; compare cross-section in CHARRIÈRE 1989). Unfortunately, faults complicate the succession. Calcareous shales with brachiopods underly lenticular limestones and conglomerates. This suggests that the shaly type unit (**Submember A**) is at least partially older than the Chabat Jenanat Conglomerate. Restricted support comes from the presence of the brachiopod *Bifida* aff. *dahlia*; typical *Bif. dahlia* occur in the lower Emsian Zlíchov Limestone of Bohemia (HAVLÍČEK 1956). The same brachiopod occurs in coquina sandstones at the top, adding to the local stratigraphic complexity.

Fig. 6: The coarse, polymict conglomerate (Chabet Jenanat) Formation as exposed at the base of the Jenanat hill.

Fig. 7: Details of the Chabet Jenanat Conglomerate, showing unsorted, well-rounded Lower Palaeozoic (probably Ordovician), light- to middle-grey quartzites and Ediacarian/Cambrian granite (center).

Fig. 8: Large clasts of grainy, yellowish-weathering volcanite in the Chabat Jenanat Conglomerate.


4


8


3

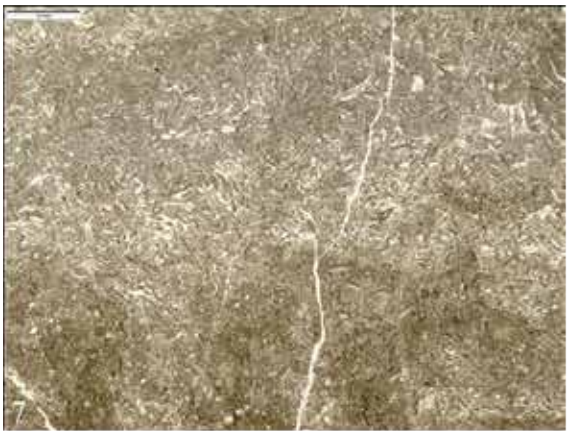
7


2


6

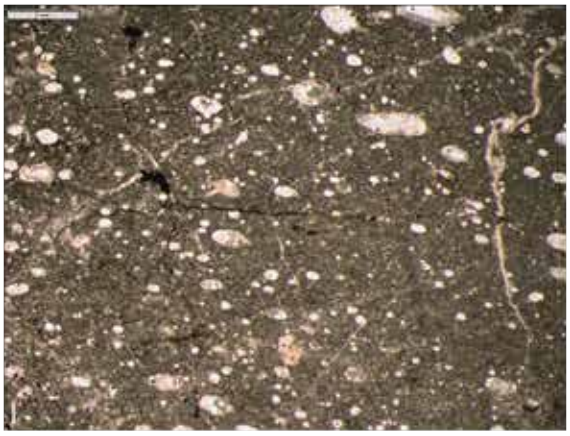
1


5

Fig. 9: Microfacies of a limestone pebble found within the Chabat Jenanat Formation (1) and of Emsian-Eifelian beds (new Ahmed-ben-Mellouk Formation) of Section C3 sensu CYGAN et al. (1990) (2-8); scale bar = 2 mm. **1.** Ostracod wackestone with grainy calcisiltite matrix and many fine pyrite grains; **2.** Bioturbated, flaser-bedded wackestone with trilobites, shell filaments, ostracods, rare dacryoconarids, micritic matrix and dark, clay and pyrite-enriched dissolution seams, Bed C3/1, *Po. serotinus* Zone/Subzone; **3.** Bioturbated, flaser-bedded, bioclastic wackestone with gastropods, mollusk debris, crinoid ossicles, and dense micrite matrix, Bed C3/2, *L. cooperi* Subzone; **4.** Bioturbated, flaser-bedded, bioclastic wacke-floatstone with trilobite cephala, fragmented, finely ribbed, large bivalves, and dense micrite matrix, Bed C3/4, *Po. partitus* Zone; **5.** Bioturbated, flaser-bedded, bioclastic wackestone with many dacryoconarids, trilobite and mollusk debris, and micritic matrix, Bed C3/6c, basal *Po. costatus* Zone; **6.** Bioturbated, flaser-bedded, bioclastic wackestone with some dacryoconarids, trilobite and mollusk debris, and dense micrite matrix, Bed C3/8a, higher *Po. costatus* Zone; **7.** Unsorted, bioturbated, bioclastic pack- and grainstone with abundant, small ostracods, dacryoconarids, masses of fine shell hash, micritic matrix in the lower and washed out, microsparitic matrix in the upper part, Bed C3/10b, *T. kockelianus* Zone; **8.** Bioturbated, flaser-bedded mud-wackestone with dacryoconarids (styliolinids), rare shell debris, and microsparitic to calcisiltitic matrix, middle part of Bed C3/27, *Po. varcus-rhenanus* Zone.

In the Chabat el Jenanat ravine, the conglomerate grades upwards into a thin unit of sandstones, locally again with a rich neritic brachiopod fauna (BRICE et al. 1984; Fig. 5). The facies was shallower and more proximal than in the Pragian Aïn el Beida Formation. Plant remains were descrined by FAIRON-DEMARET & RÉGNAULT (1986) as cf. *Haskinsia* and their abundance fits a nearshore environment. In Section C1 of CYGAN et al. (1990; Unit 3a), there are intercalated, lenticular detrital (sandy) limestones that lack conodonts. This ca. 3 m sequence forms a local **Submember B** (of the Chabat Sitout Member). The brachiopod assemblage (Samples K.25, K.29, K.40 and K.45) with *Leptostrophiella, Sicorhyncha, "Zdimir", "Uncinulus"* (s.l.), *Oligoptycherhynchus, Arduspirifer, Euryspirifer* (genus identification confirmed by JANSEN 2001, p. 194), and atrypids has been placed in the basal upper Emsian. This led to a correlation with the top of the Mdâouer-el-Kbîr Formation (Rich 3), which marks the lower-upper Emsian transition of the western Dra Valley (see JANSEN 2007 and ABOUSSALAM et al. 2015). Although the brachiopod fauna requires further work, it indicates that the level of the global Daleje Event post-dated the regional "Eovariscan prelude" of tectonic movements.

A local upper **Submember C** is formed in Section C1 (CYGAN et al. 1990) by up to 4 m of detrital, sandy to crinoidal limestones with conodonts. They deposited on a shallow open shelf after the clastic supply decreased strongly. There are no polygnathid faunas, as typical for such a palaeogeographic setting. The presence of *Latericriodus bilatericrescens* suggests a lower Emsian age, in contrast to the brachiopod age from just below. However, this species ranges just into the basal Dalejan (ABOUSSALAM et al. 2015, *I. fusiformis* Zone), a level which is, perhaps, supported by the associated "*Icriodus* sp." (if it represents an *Icriodus* s.str.). *Latericriodus beckmanni beckmanni*, another species straddling the lower-upper Emsian boundary (e.g. BERKYOVÁ 2009), was found in the middle part. *Icriodus* cf. *corniger* indicates that the next younger *I. corniger* Zone of the icriodid succession is reached at the top of Submember C. This conodont zone begins still low in the upper Emsian in upper parts of the extended Daleje Event Interval.

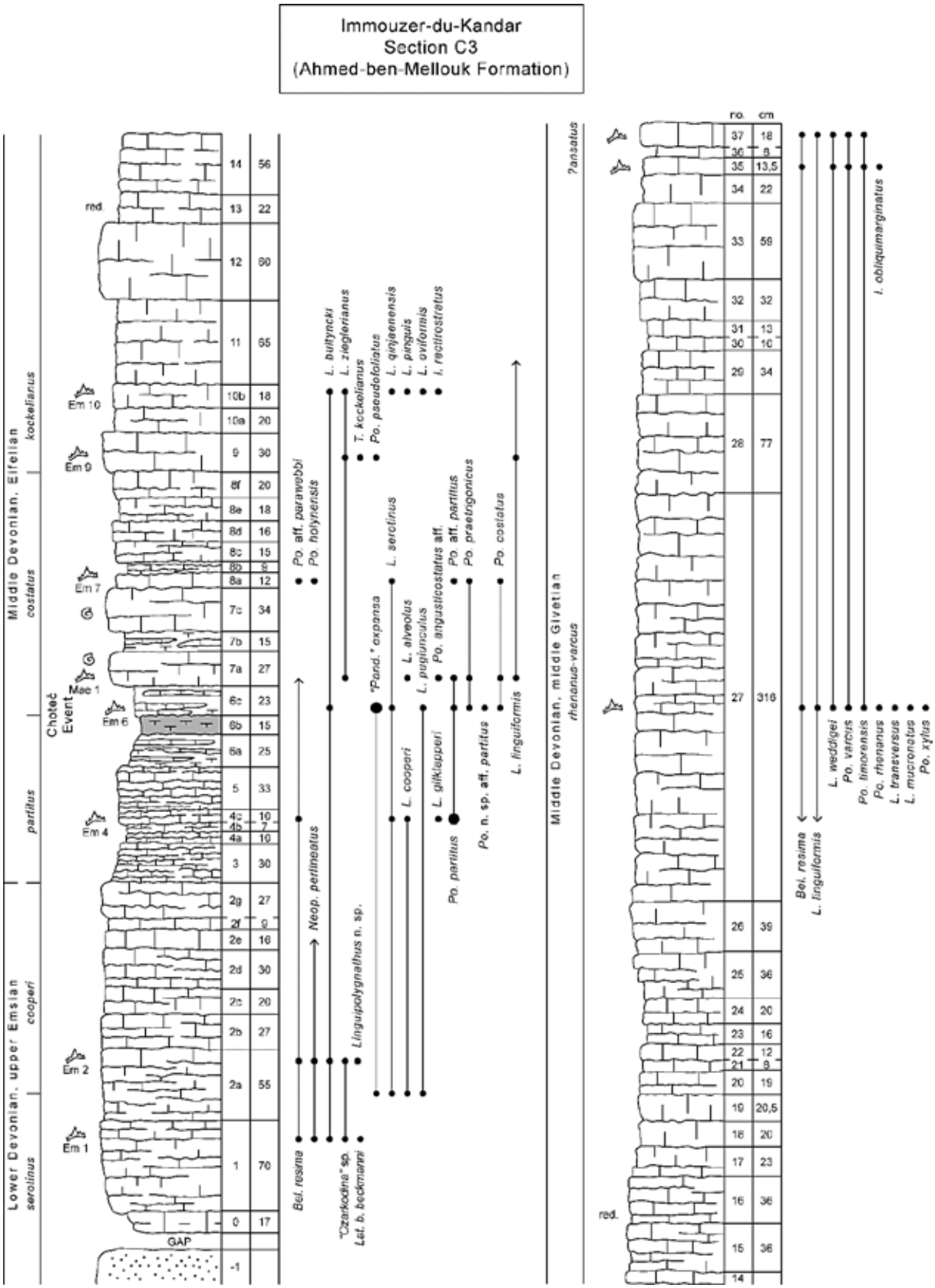

Fig. 10: Lithostratigraphy and conodont ranges in the type locality of the Ahmed-ben-Mellouk Formation (Section C3 of CYGAN et al. 1990) above the Chabat el Jenanat valley.

sample no.	**Em1**	**Em2**	**Em4**	**Em6**	**Mae 1**	**Em7**	**Em9**	**Em10**	**4m b. t.**	**top gr.**	**last bed**
bed no.	**top 1**	**2a**	**4c**	**6c**	**7a**	**8a**	**9**	**10b**	**27**	**36**	**37**
conodont zones	*serot.*	*coop.*	*partitus*	*costatus*			*kockelianus*		*rhenanus-varcus*		
Bel. resima	5	1	1	*	*	*	*	*	14	*	1
Neopand. perlineatus	5	3	*	*	*	*	*	*	1		
L. bultyncki	**11**	4	*	2 juv.	*	*	*	27			
"Ozarkodina" sp.	2	1									
Lat. beck. beckmanni	1										
L. undulatus n. sp.		2									
"Pand." expansa		1	`*	157							
L. serotinus		16	65	4	*	85					
L. cooperi		**1**	62?								
L. pugiunculus		5	*	1							
L. gilklapperi			>50								
Po. partitus			**>100**	15	*	4 aff.					
Po. praetrigonicus				15	4	8					
Po. n. sp. aff. *partitus*				1							
Po. costatus				**3**	1	5					
L. linguiformis					18	*	>10	*	8	63	14
L. cf. *linguiformis*					5						
Po. angusticostatus					2						
L. alveolus					1						
L. zieglerianus					16	*	21	8			
Po. holynensis						10					
L. aff. *parawebbi*						1					
T. kockelianus							**2 juv.**				
Po. pseudofoliatus							1				
L. qinjiaensis								8			
L. pinguis								2			
L. oviformis								2			
I. rectirostratus								1			
L. weddigei									4	8	3
L. transversus									**1**		
L. mucronatus									1		
Po. xylus									1		
Po. timorensis									8	15	3
Po. varcus									**11**	31	5
Po. rhenanus									**1**		
I. obliquimarginatus										3	
total conodonts	**24**	**35**	**> 280**	**198**	**47**	**109**	**c. 40**	**48**	**50**	**120**	**26**

Tab. 1: Frequencies and ranges of conodonts in Section C3 of CYGAN et al. (1990), based on our new samples.

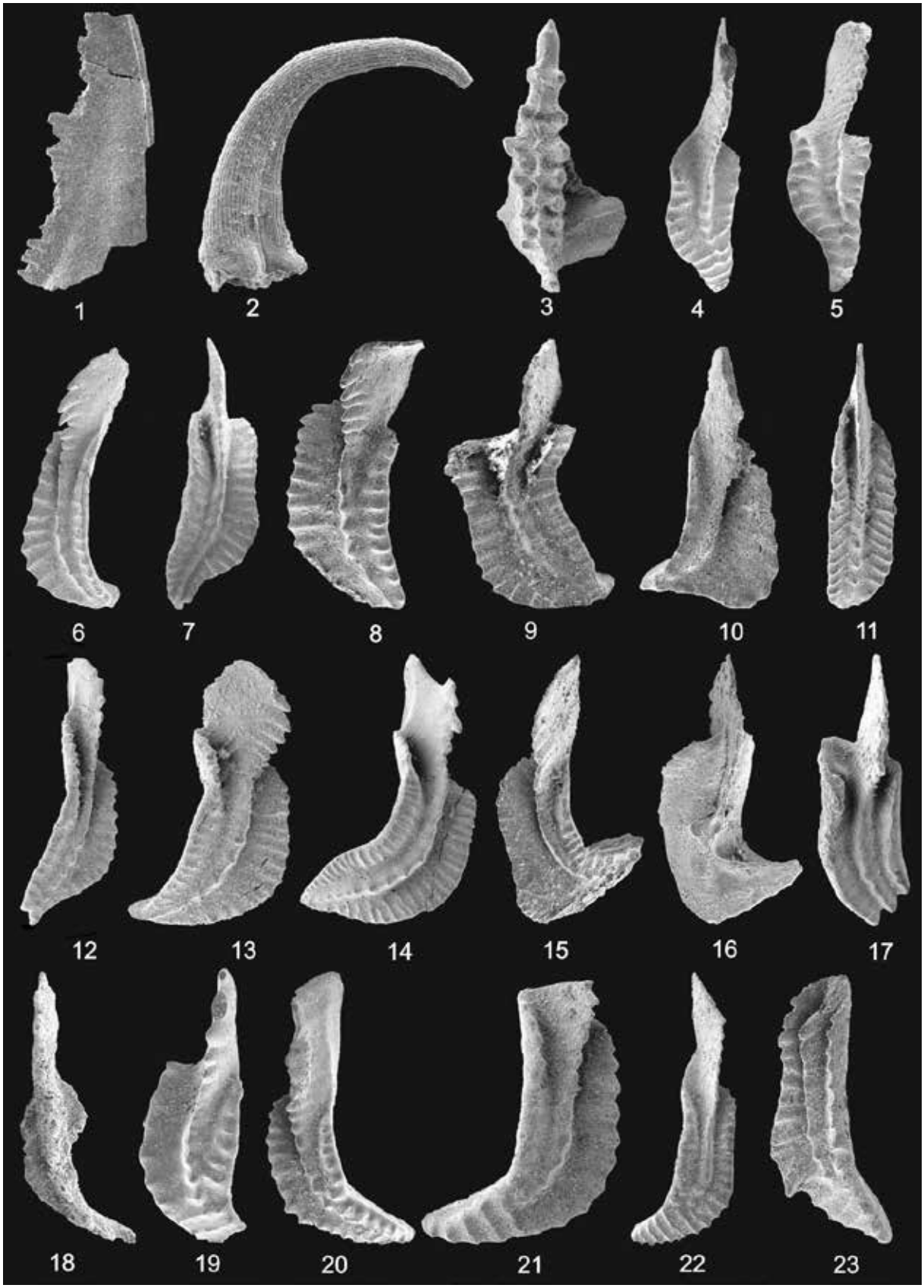

Fig. 11

Fig. 11: Upper Emsian and Eifelian conodonts from the (new) Ahmed-ben-Mellouk Formation at Immouzer-du-Kandar, Section C3 sensu CYGAN et al. (1990), Bed C3/1 (1-3), Bed C3/2 (4-5), Bed C3/6c (6-11), Bed C3/8a (12-17), Bed C3/9 (18, 23), Bed C3/10b (19-22). **1.** *Bel. resima*, x 35; **2.** *Neopand. perlineatus*, x 50; **3.** *Lat. Beckmanni beckmanni*, x 40; **4-5.** *Linguipolygnathus* n. sp., x 40 (4) and x 45 (5); **6.** *Po. costatus*, x 45; **7.** *Po. partitus*, x 30; **8-9.** *Po. praetrigonicus*, x 60, x 50; **10.** *L. serotinus*, x 75; **11.** *Polygnathus* n. sp. aff. *partitus*, x 50, unusually straight and long form; **12.** *Po*. aff. *Partitus*, x 30; **13:** *Po. costatus*, x 40; **14.** *Po. holynensis*, x 30; **15-16.** *L. serotinus*, x 65, upper and lower views; **17.** *Po.* aff. *Parawebbi*, x 35, with smooth platform margin; **18.** Juvenile *T. kockelianus*, x 75; **19.** *L. pinguis*, x 40; **20.** *Po. zieglerianus*, x 30; **21.** *L. bultyncki* ß, x 55; **22.** *L. bultyncki* α, x 35; **23.** *L. linguiformis*, x 50.

4.5. (new) **Ahmed-ben-Mellouk Formation** (upper Emsian-middle Givetian)

Previous authors did not assign the "Série carbonaté" to a formally named lithological unit. Based on the name for the small settlement just to the W (Fig. 2), we introduce here the new name Ahmed-ben-Mellouk Formation for all pelagic limestones ranging from the (higher) upper Emsian to the middle Givetian ("calcaires amygdalaires" of CHARRIÈRE & RÉGNAULT 1989; CYGAN et al. 1990: Unit 3b). Section C3 (Figs. 1, 10, 12, 13) is the type locality. The total thickness is ca. 18 m. The prevailing microfacies is bioturbated, flaser-bedded, bioclastic wackestone with micrite matrix and dark, clay and pyrite-enriched dissolution seams. Variably there are common trilobite remains (Bed 1, Fig. 9.1, Bed 4, Fig. 9.3, and Bed 8a, Fig. 9.6), gastropods (Bed 2, Fig. 9.2), or dominant dacryoconarids (Bed 6c, Fig. 9.5).

Fig. 12: Flaser-bedded lower part of the new Ahmed-ben-Mellouk Formation (Section C3 sensu CYGAN et al. 1990).

Fig. 13: Sampling in the solid Eifelian part of the new Ahmed-ben-Mellouk Formation.

In the lower part of Section C3 (Beds C3/0-2g, Fig. 10), beds are up to 70 cm thick. The abundance of pelagic fossils increases gradually from Bed 1 to Bed C3/2, which reflects a fast but gradual deepening. The neritic limestone environment of the upper Chabat Sitout Member turned into pelagic cephalopod limestone, as typical for open shelf seamount or deep offshore carbonate ramp settings. This is supported by the conodont biofacies, with faunas that are now dominated by polygnathids. CHARRIÈRE & RÉGNAULT (1989) pointed out some similarities with the "Orthoceratitico et Goniatitico-rosso" developed in the Rif,

which, however, was situated far away in the NE in Devonian time.

Bed 1 still has a large amount of shallow-water single cone genera (*Belodella resima,* Fig. 11.1*, Neopanderodus perlineatus*, Fig. 11.2). *Latericriodus beckmanni beckmanni* (Fig. 11.3) has persisted from the underlying formation. But *Linguipolygnathus bultyncki* is more common (> 50 % of the fauna, Tab. 1). It is an alternative index species of the *L. serotinus* Zone, ca. in the middle of the upper Emsian. In Morocco it is more widespread than the zonal species (e.g., ABOUSSALAM et al. 2015). The latter (*L. serotinus*) enters as the most common taxon in Bed C3/2a, in association with narrow forms identified as *L. pugiunculus* and rare *"Pandorinellina" expansa*. Two unusual specimens are assigned to a new, possibly endemic species, ***Linguipolygnathus* n. sp.** (Figs. 11.5-5). A single *L. cooperi* shows that the upper part of the *L. serotinus* Zone (*L. cooperi* Subzone of ABOUSSALAM et al. 2015) has been reached. Two small "ozarkodinids" with three isolated posterior denticles, small, very narrow basal cavity, and gently ascending, dense anterior denticles, may represent a new taxon.

An interval of more platy beds (Beds C3/3-4) is characterized by a sudden flood of polygnathids, especially of *Po. partitus* and *Po. gilklapperi*, followed in abundance by *L. ?cooperi* and *L. serotinus*. This signals a first, minor deepening in the basal Eifelian *Po. partitus* Zone. As in the Anti-Atlas (BECKER et al. 2018a), the Emsian-Eifelian boundary is not marked by any lithological change. A subsequent more solid Bed C3/5 is overlain by 60-65 cm marl with very thin limestone beds (Beds C3/6a-c), the local expression of the global and transgressive **Choteč Event** (CHLUPÀČ & KUKAL 1986, BERKYOVÁ 2009, and KOPTIKOVÁ 2011 for the Bohemian type region; BECKER & ABOUSSALAM 2013a for the Anti-Atlas). An increase of dacryoconarids is indicative of eutrophic conditions.

The re-onset of more solid limestone can be correlated with a similar change to solid lower Eifelian marker limestones in the Tafilalt (BULTYNCK 1986; KLUG 2002; BECKER & ABOUSSALAM 2013a). Conodonts support this correlation. Bed C3/6c yielded *L. serotinus* (Fig. 11.10), *Po. partitus* (Fig. 11.7), *Po. praetrigonicus* (Figs. 11.8-9), and the first, somewhat questionable *Po. costatus* (Fig. 11.6), the index species of the lower Eifelian *Po. costatus* Zone. A specimen provisionally called ***Polygnathus* n. sp. aff. *partitus*** (Fig. 11.11) is unique in its straight carina (which rules out any deformation), long, narrow, evenly ribbed platform, paired with unequal anterior platform ends on both sides. Since we have only one specimen, we refrain at this time from naming this apparently new species. Very peculiar is the sudden flood of *"Pandorinellina" expansa* (ca. 80 % of the fauna, Tab. 1). Current conodont biofacies models do not include a Lower Devonian **"Pandorinellid" Biofacies**. The close proximity to the Choteč Event suggests a palaeoecological connection that is not known from the type region (BERKYOVÁ 2009) or from the Anti-Atlas (BULTYNCK 1985; BECKER & ABOUSSALAM 2013a). The microfacies of Bed Ce3/6c is a dacryoconarid wacke-packstone with a strong overprint by pressure solution (Fig. 9.5).

Just above, Beds C3/7a and 7b contain abundant but poorly preserved goniatites. Based on three species, *Po. costatus, L. alveolus,* and *Po. angusticostatus*, the lower level (Sample Mae 1) can be assigned reliably to the *Po. costatus* Zone (compare composite range charts in BELKA et al. 1987 and GOUWY & BULTYNCK 2002, 2003). *Linguipolygnathus linguiformis* is often thought to enter slightly higher in the *costatus* Zone but an earlier range, even from below the Choteč Event Interval, was observed in

the Tafilalt (BECKER & ABOUSSALAM 2013a). This agrees with the Ardennes record. Specimens identified as *L.* cf. *linguiformis* display an unusually strongly bent lingua.

In Section 2, CYGAN et al. (1990) showed a rather early onset of Eifelian polygnathids, from ca. 60 cm above the base of the formation (with the first *L. linguiformis* in their Sample 231 and *Po. costatus, Po.* cf. *robusticostatus,* and *Po.* cf. *angustipennatus* in Sample 211). This implies that the upper Emsian and Choteč Event Interval is laterally missing in an unconformity at the base of the Ahmed-ben-Mellouk Formation. The Emsian-Eifelian transition at Immouzer-du-Kandar is rather condensed and, as noted above, marked by biofacies patterns that are not known from the Anti-Atlas.

The main part of the Eifelian (from Bed C3/8a on) and the lower/middle Givetian consist of more compact, light-grey micrites with flaser bedding. This lithological change was also shown by CYGAN et al. (1990: fig. 3, from their Sample 221 on). However, it is not evident in the microfacies, which still consists of flaser-bedded, micritic dacryoconarid wackestones with trilobite and shell debris (Bed C3/8a, Fig. 9.6).

Sample Em7 (later recognized as Bed C3/8a) is dominated (ca. 78 % of the fauna) by a different conodont species, *L. serotinus* (Tab. 1; Figs. 11.15-16, ***Linguipolygnathus* Biofacies**). Associated are *Po*. aff. *partitus* (Fig. 11.12), *Po. costatus* (Fig. 11.13), *Po. holynensis* (Fig. 11.14), and *Po. praetrigonicus*. An incomplete polygnathid with strongly asymmetric, smooth platform, bolstered, upturned margins, an anterior platform collar, and very narrow, deep adcarinal furrows may belong to a new species, here called ***Po.* aff. *parawebbi*** (Fig. 11.17). The only similarity is with some *L. parawebbi*, in which the concave outer anterior margin may be smooth, but not on both platform sides (see, e.g., CHATTERTON 1974 and VODRÁŽKOVÁ et al. 2011).

Ca. 80 cm higher, the solid Bed C3/9 yielded a smaller conodont fauna dominated again by linguipolygnathids, this time by *L. zieglerianus* and *L. linguiformis* (Fig. 9.23). Two small-sized *Tortodus kockelianus* (Fig. 11.18) prove the upper Frasnian *T. kockelianus* Zone. The so far missing *T. australis* Zone can be sought for in the unsampled interval. There is a minor change of microfacies: the shell debris of the bioclastic wackestone becomes very fine and matrix was partly washed out and microsparitized.

The microfacies of Bed C3/10b (Fig. 9.7) shows that the calm deeper-water sedimentation was occasionally interrupted by episodes of slightly increased bottom turbulence, perhaps by distal storms. Alternating bioturbated pack-and grainstones with dacryoconarids, many two-valved ostracods, and a lot fine shell hash are poor in larger fossils (Fig. 9.7). There is no flaser-bedding and the matrix varies between micrite and microsparite. There is no grading or sorting as indicators of distal turbidite deposition. The very small and light ostracods were probably washed in by slow currents from an adjacent (up-ramp) shallower setting. The conodont assemblage type has changed again. Characteristic is a late resurge (56 %) of *L. bultyncki* (both morphotypes, Figs. 11.21-22), which normally should not occur in the *T. kockelianus* Zone. Associated are *L. zieglerianus* (Fig. 11.20), *L. pinguis* (Fig. 11.19), and *I. rectirostratus* (Fig. 17.4). Because of their irregular ornamention, even on the lingua, some forms agree with the Chinese *L. qinjiaensis* XIONG (in XIAN et al. 1980) (Figs. 17.2-3). Two poorly preserved specimens represent *L. oviformis* KONONOVA & KIM, 2005 (Fig. 17.1), a species only known so far from the upper Eifelian of the Russian Platform. CYGAN et al. (1990) recorded from the lower part of the compact

limestones of Section C3 *Po. ensensis*, the index species of the top-Eifelian *ensensis* Zone, which was assumed to straddle the Eifelian-Givetian boundary. NARKIEWICZ et al. (2017) noted widespread inconsistencies in the identification of the species, which is more typically found in the basal Givetian *Po. hemiansatus* Zone. In the absence of illustrations, we cannot re-evaluate the local *Po. ensensis* record.

Fig. 14: Field photo of an upper Eifelian *Cabrieroceras* sp. (first record of the genus for the Moroccan Meseta).

Fig. 15: Weathered involute anarcestid *(?Subanarcestes*) from Section C2 of CYGAN et al. (1990).

Fig. 16: Weathered agoniatite from Section C2 of CYGAN et al. (1990) with fast expanding whorls and widely rounded flank lobe (max. diameter = 8 cm).

Laterally across a fault (Fig. 1), a bioclastic solid Eifelian limestone displays on its surface an evolute anarcestid, a *Cabrieroceras* sp. (Fig. 14). This genus is characteristic for the upper Eifelian of the eastern and western Anti-Atlas (e.g., BULTYNCK & HOLLARD 1980; BECKER & HOUSE 1994a; KLUG 2002; BAIRD et al. 2009) and other regions, such as the Montagne Noire or North America (see review in BECKER & HOUSE 2000b). Its first recognition in the Meseta was, therefore, to be expected in pelagic cephalopod facies. It is well possible that the record of "*Anarcestes lateseptatus*" by M. BENSAID (in CYGAN et al. 1990) refers to the same genus. To the southeastern side, ca. in the middle of the cliff of Section C2, there are also common goniatites: involute anarcestids with low whorls (Fig. 15, *?Subanarcestes*) and agoniatitids with fast expanding, high whorls and simple, wide flank lobe (Fig. 16; see record of *Agoniatites* sp. in CYGAN et al. 1990). A small loose block yielded a sectioned *Fidelites* cf. *verna*, known in the Tafilalt as a moderately common Eifelian agoniatitid species with relatively wide whorls (see KLUG 2002).

The still incomplete sampling did not yet enable us to fix locally the Eifelian-Givetian boundary. There is no macroscopic evidence

for the global Kačak Event Interval. This is unusual since the earlier Choteč Event is locally so well expressed as a deepening episode

.

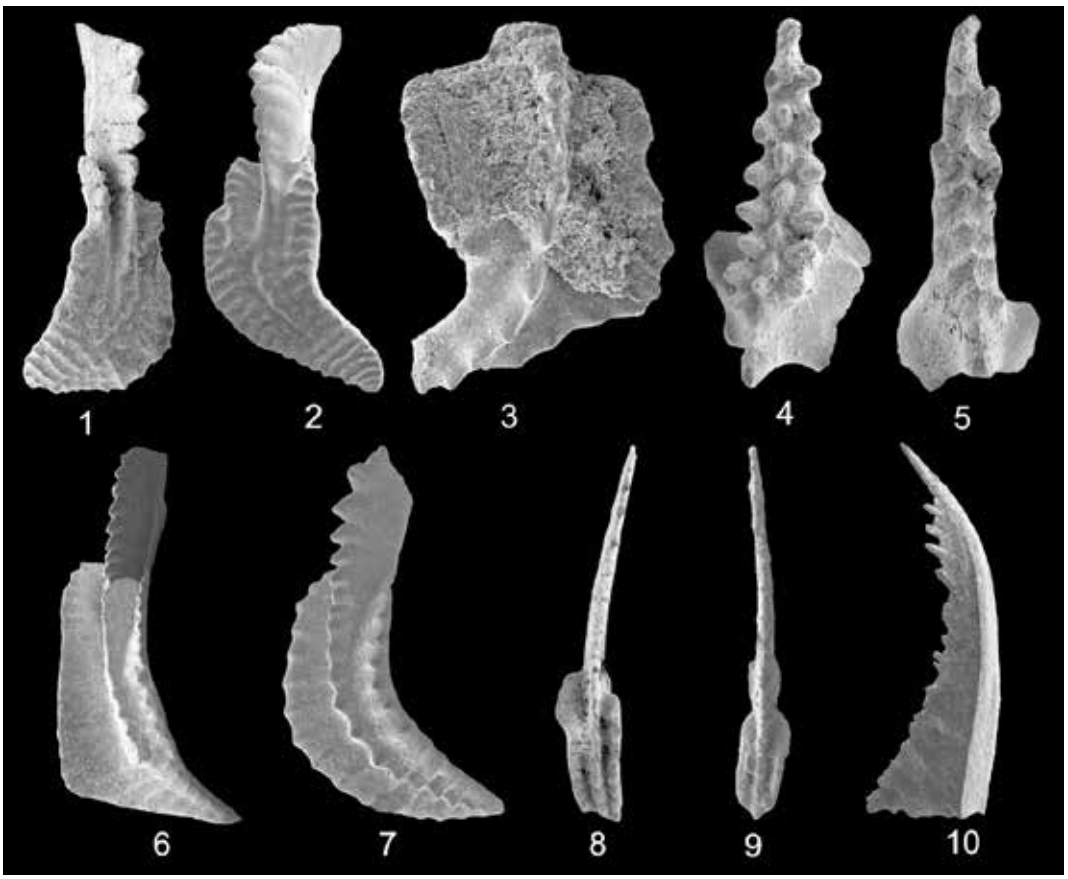

Fig. 17: Conodonts from the upper Eifelian (*T. kockelianus* Zone, Bed C3/10b, 1-4) and middle Givetian (*Po. rhenanus-varcus* Zone, Bed C3/36) of the Ahmed-ben-Mellouk Formation, Section C3, at Immouzer-du-Kandar. **1-2.** *L. qinjiaensis*, x 30; **3.** *L. oviformis*, x 55; **4.** *I. rectirostratus,* x 55; **5.** *I. obliquimarginatus*, x 45; **6.** *L. linguiformis* with reduced outer platform ornament, x 40; **7.** *L. weddigei*, x 45; **8.** *Po. timorensis*, x 35**; 9.** *Po. varcus*, x 60; **10.** *Bel. resima*, x 80.

The lower Givetian has not yet been re-sampled for conodonts and microfacies. The rather massive middle part of Bed C3/27 (a sample from 4 m below the top of the formation) yielded a rather diverse conodont fauna assigned to the lower part of the middle Givetian (sensu BULTYNCK 2005; *Po. rhenanus-varcus* Zone; Tab. 1). Apart from the index species *Po. varcus* and *Po. rhenanus*, we found two species that are more typical for the next younger *Po. ansatus* Zone, *L. transversus* and *L. mucronatus*. The first was shown by BULTYNCK & HOLLARD (1980) to range lower down in the Anti-Atlas. The second is restricted to the *ansatus* Zone in eastern North America (WORK et al. 2007; BRETT et al. 2018) but rare specimens were recorded by BULTYNCK (1987) from below the first *Po. ansatus* at Bou Tchrafine in the Tafilalt. Consequently, we date Bed C3/27 as upper part of the *Po. rhenanus-varcus* Zone. The microfacies (Fig. 9.8) is strongly reminiscent of the Eifelian: a flaser-bedded, slightly bioturbated dacryoconarid mud-wackestone with dense micrite to microsparite matrix. The constant repetition of this facies type proves that the lower ramp environment was stable for a very long period (at least 15 ma, BECKER et al. 2020). This

gives a big difference to the unstable lower Emsian to basal upper Emsian time.

The next higher local conodont record is from ca. 1.2 m below the formation top (Sample 233 of CYGAN et al. 1990). The only difference to our facies is another, rather late record of *Po. ensensis*. Elsewhere, the species (former subspecies of *Po. xylus*) is known to range to levels just below the global Taghanic Crisis (ABOUSSALAM 2003).

The top of the Ahmed-ben-Mellouk Formation consists first of very solid, light-grey flaserlimestone (Fig. 18) and finally of gradually thinner beds (Beds C3/35-37). Conodont faunas of Beds C3/367 and C3/37 (compare Sample 234 of CYGAN et al. 1990) are rather similar, with common *L. linguiformis* (Fig. 17.6; > 50 %, Tab. 1), followed in terms of abundance by *Po. varcus* (Fig. 17.9, 20-25 %) and *Po. timorensis* (Fig. 19.8, ca. 12 %). *Bel. resima* (Fig. 17.10) and *L. weddigei* (Fig. 17.7) are accessory. As in the Oued Cherrat region, there are some rather late/atypical representatives of the slender *I. obliquimarginatus* (Fig. 17.5). Although there are no characteristic species of the *Po. ansatus* Zone, the record of *L. mucronatus* from ca. 4 m below (see above) suggests that the upper part of the middle Givetian has been reached. NARKIEWICZ et al. (2016) noted in their late middle Givetian ("Taghanic") conodont biofacies analysis that the *L. linguiformis/Po. ansatus* ratio increases towards the outer shelf or in Anti-Atlas pelagic platform settings, where the second species becomes rather rare. Therefore, it is reasonable to infer that the absence of *Po. ansatus* at Immouzer-du-Kandar was controlled by palaeoecology. This implies some uncertainty for the "standard" zone application potential in deeper settings. The carbonate microfacies, the locally usual flaser-bedded micritic to microsparitic, bioturbated wackestone with sparse macrofauna (Fig. 19.1), is in complete agreement with the conodont biofacies evaluation.

Fig. 18: Top (middle Givetian) part of the new Ahmed-ben-Mellouk Formation (top of Section C3), grading by limestone-shale alternations (with the hammer for scale) into the overlying, hypoxic "plant shale" (Taghanic Event Interval). Note the sharp fault demarcation of the limestone along the slope (in the middle ground), followed by Givetian limestones of Section C4 lower on the slope (right middle ground).

The transition from the Ahmed-ben-Mellouk to the overlying (new) Immouzer-du-Kandar Formation was also studied in our new Section C4 (Figs. 1, 18, 21). The nodular to flaser-bedded Beds C4/1-3 correlate with the thick-bedded upper part of the adjacent Section C3 (ca. Beds C3/32-34). Bed C4/4 is an argillaceous interval with limestone nodules. The oldest conodont fauna of Section C4 comes from Bed 5, which is the top of the Ahmed-ben-Mellouk Formation. Its composition agrees with the faunas from the top of that unit in Section C3; *L. linguiformis* is by far dominant (85 %, Tab. 2). A minor difference is the presence of *I. difficilis*, the most common icriodid of the top middle Givetian.

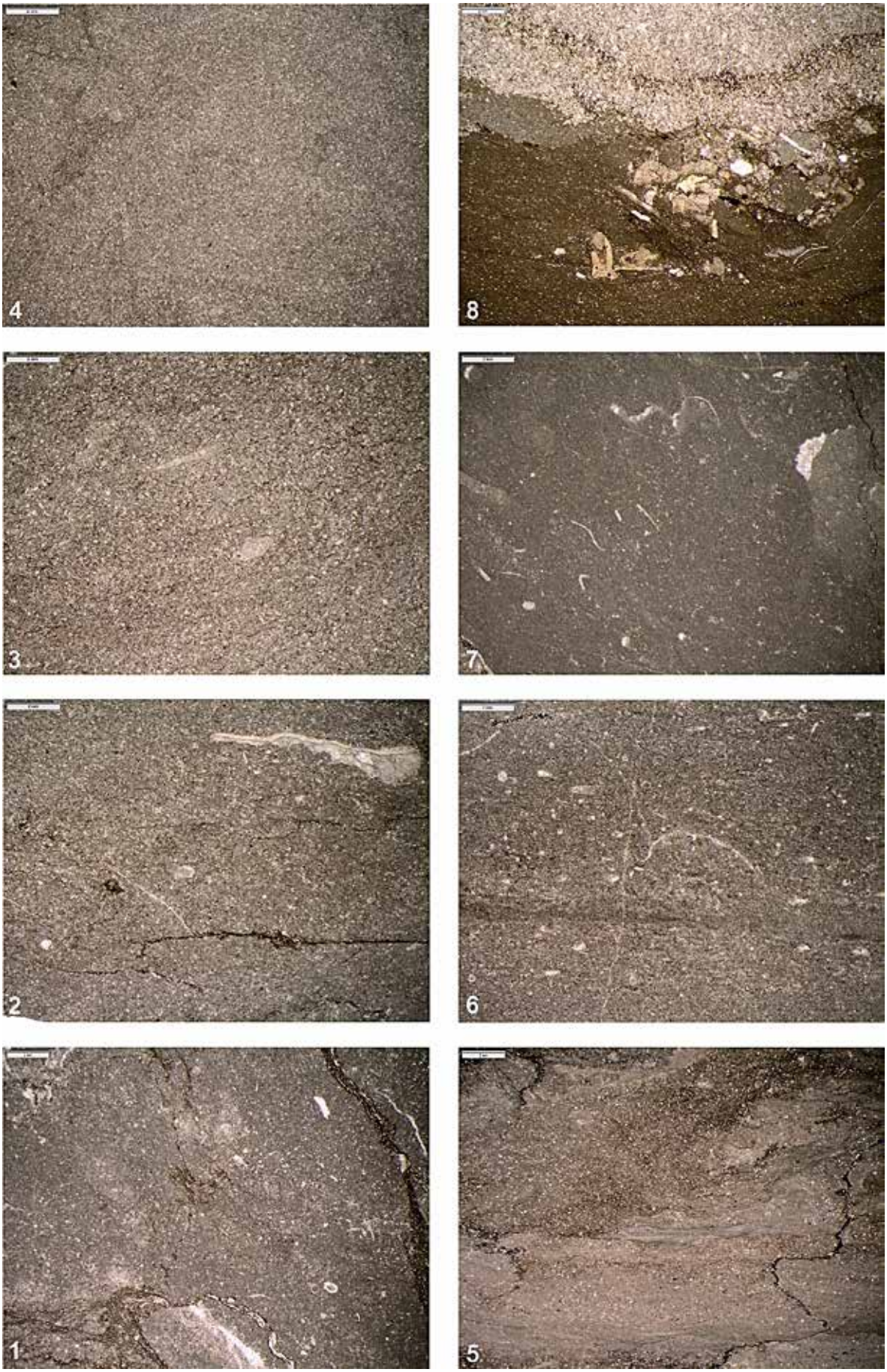
4
8
3
7
2
6
1
5

Fig. 19: Carbonate microfacies of middle Givetian (Ahmed-ben-Mellouk Formation, 1) to middle Frasnian (Immouzer-du-Kandar Formation, 2-8) limestones at Section C3 sensu CYGAN et al. (1990) and our Section C4 (scale bar = 2mm). **1.** Bioturbated, flaser-bedded wackestone with fine shell debris, micrite to microsparite matrix, and poor macrofauna, Bed C3/37, *?Po. ansatus* Zone; **2.** Bioturbated, silty calcisiltite with rare large shell fragments, Bed C4/7c, ? *ansatus* Zone, Member 1, Submember A; **3.** Detrital, silty calcisiltite with some styliolinids, Bed C4/13, top of Submember A, *?Po. ansatus* Zone; **4.** Unfossiliferous, bioturbated, detrital, silty calcisiltite, Bed C4/19, Member 1, middle Submember C, upper Givetian, MD III-C/D; **5.** Strongly flaser-bedded, bioturbated, silty mudstone, Bed C4/23, Member 1, upper Submember C, MN 1 Zone; **6.** Partly laminated, partly weakly bioturbated, silty, calcisiltitic wackestone with dacryoconarids (styliolinids) and mollusk shells, Bed C4/26a, Member 2, Submember B, top MN 4 Zone; **7.** Organic-rich, dark, weakly bioturbated mud-wackestone with shell filaments and fine silt, Bed C4/28a, Member 2, top Submember B, top MN 4 Zone; **8.** Organic-rich, dark mudstone, with sharp contact to an erosive calcisiltite that shows larger intraclasts at the channel base, Bed C4/35, base Member 3, top MN 6 Zone.

4.6. (new) **Immouzer-du-Kandar Formation** (upper Givetian-lower Famennian)

We assign the distinctive "lutites a plantes" (e.g., FAIRON-DEMARET & RÉGNAULT 1986; CHARRIÈRE & RÉGNAULT 1989; Unit 3c of CYGAN et al. 1990) and the overlying pelagic shales and limestones (Unit 3d) as well as the subsequent limestone breccias (Unit 3e) to a new formation named after our study region. In our type Section C4, the total thickness reaches up to 55 m but there is significant lateral (NW-SE) variation. The succession is so heterogeneous that a subdivision into five members, partly with further submembers, is inevitable. The oldest beds still fall in the middle Givetian, the main breccia was re-deposited after shales with lower Famennian goniatites (see below).

4.5.1. Member 1 (top middle/upper Givetian "plant shale")

Member 1 is easly identifiable by its predominant siltstones and silty shales, which yielded numerous, up to 15 cm long plant remains (FAIRON-DEMARET & RÉGNAULT 1986; Fig. 23). We place the formation and member base at the base of Bed 6 (Fig. 21). **Submember A** comprises a thin basal intercalation of silty shales and reddish weathering siltstones (e.g., Bed C4/8) with thin, detrital, silty limestones. Representative are Beds C4/7c (Fig. 19.2) and C4/13 (Fig. 19.3). They consist of slightly bioturbated, calcareous siltstones or silty calcisiltites with rare mollusk shells and some dacryoconarids (styliolinids). CHARRIÈRE & RÉGNAULT (1989) noted rare phacopids. The abundance of plants and the strong terrigenous influx may be interpreted as a significant regressive episode, changing gradually from a pelagic outer ramp to a siliciclastic nearshore realm. This sea-level fall could be related to the global pre-Taghanic Regression near the end of the middle Givetian (ABOUSSALAM 2003; ABOUSSALAM & BECKER 2011). However, the continuation of pelagic fauna (styliolinids, goniatites higher up), now diluted by a flood of silt, whilst benthic fauna is almost lacking, suggests that the setting remained rather distal marine. Fragmented plants were probably transported over a long distance. Increased weathering rates in the hinterland, perhaps by increasingly humid conditions, could have played a significant role to explain the facies change. Humidity would have supported a richer plant cover in the source region. Aneurophytales (progymnosperms), such as *Rellimia*, and the recorded fern *Protocephalopteris* were plants of a seasonally wet-dry tropical habitat (TAYLOR et al. 2009).

Conodonts from Submember A still fall in the middle Givetian. Beds C4/5 to C4/13 yielded similar assemblages as in the top Ahmed-ben-Mellouk Formation, again with dominant *L. linguiformis* (Tab. 2). There is also no evidence for marker species of the

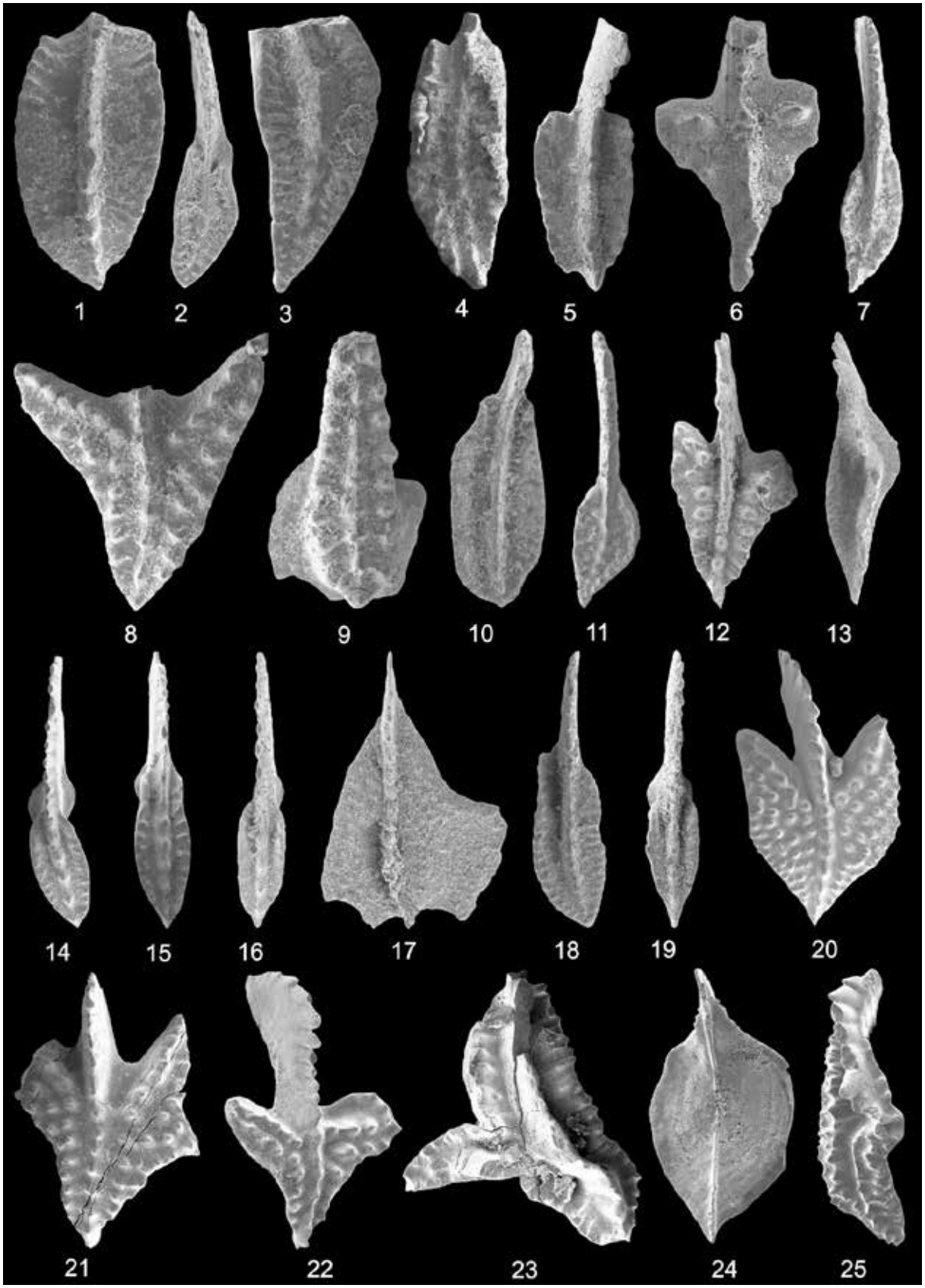

Fig. 20: Conodonts from the lower and middle Frasnian of Section C4 at Immouzer-du-Kandar, Bed C4/23 (1-6, MN 1 Zone), Bed C4/26a (7-11, top MN 4 Zone with *Ad. nodosa*), Bed C4/28a (12-16, top MN 4 Zone), Bed C4/32 (17-19, MN 5/6 Zone), and Bed C4/37 (20-26, MN 7 Zone). **1.** *M. guanwushanensis* M3, intermediate towards *Z. ovalis*, x 80; **2-3.** *Po. paradecorosus*, morphotype with slightly widened outer platform, x 50 and x 80; **4.** *Po.* cf. *pennatus*, eroded specimen, x 40; **5.** *Po*. n. sp. aff. *lanei* x 60; **6.** *Ad. rotundiloba pristina*, x 65; **7.** *Po.* aff. *paradecorosus*,

transitional towards *Av. decorosus*, x 45; **8.** *Ad. nodosa* (= *gigas* M1), x 75; **9.** *I. symmetricus*, x 55; **10.** *Po.* cf. *dengleri*, morphotype with incipient anterior rostrum, x 45; **11.** *Avignathus decorosus*, x 40; **12.** *Ad. africana*, x 40; **13.** *Nothognathella* sp., resembling *Tortodus*, x 70; **14.** *Po.* aff. *varcus* (sp. 1) with ribbed platform, x 85; **15.** *Po. jorfensis*, x 65; **16.** *Po. xylus*, x 90; **17.** *Palmatolepis* sp. indet., x 75; **18.** *Polygnathus* n. sp., x 70; **19.** *Po.* aff. *varcus* (sp. 2) with relative large, triangulat platform, x 80; **20.** *Ad. gigas* s. str., x 30; **21.** *Ad. lobata*, with incipient second outer side lobe, transitional towards *Ad. curvata*, x 45; **22.** *Ad. pramosica*, unusually late representative, x 60; **23.** *Ag. leonis*, x 40; **24.** *M. asymmetrica*, lower view showing the minute basal pit, x 50; **25.** Robust *Nothognathella* sp., x 30.

Po. ansatus Zone. But, as outlined above, we consider that this was the true age of the interval. CYGAN et al. (1990) reported a "*Polygnathus* sp. A" from a lenticular limestone (Sample 235) of their basal Unit 3c (basal Member 1 of the Immouzer-du-Kandar Formation) but did not explain this taxon.

Submember B embraces the up to 40 m thick main siltstone interval (Beds C4/14-16). In the middle is a calcareous, greenish-grey more solid cliff, which represents the peak of regression. A thin calcareous siltstone (Bed C4/17) did not produce any conodonts. Middle grey, limonitic (originally pyritic) silty shales at the top (around Bed C 4/19), surprisingly yielded several specimens of pharciceratids (Fig. 25). This is the first record of this goniatite superfamily for the Moroccan Meseta. Both *Synpharciceras* and *Stenopharciceras* are present. These genera occur abundantly in the upper Givetian *Synpharciceras* and *Taouzites* Genozones (MD III-C/D) of the eastern Anti-Atlas (e.g., BOCKWINKEL et al. 2008, 2013). In the conodont scale, the two zones correlate with the *Klapperina disparilis* to *Po. dengleri dengleri* Zones (BOCKWINKEL et al. 2017). Therefore, the main **Taghanic Crisis** Interval and the middle/upper Givetian boundary sensu ABOUSSALAM & BECKER (2002), which coincides with the global Geneseo Transgression (ABOUSSALAM & BECKER 2011), are locally masked by the siltstone shedding into a hypoxic, eutrophic and fully pelagic environment.

Bed C4/19 marks the re-onset of unfossiliferous calcisiltites (Fig. 19.4) and is taken as the base of **Submember C** (Fig. 24). CYGAN et al. (1990) found *Schmidtognathus hermanni* and *Kl. disparilis* in their Samples 237 and 236, their first limestones of Unit 3c (probably our Beds C4/21a-b, a poorly fossiliferous, silty mudstone). These are the index species of two successive zones in the lower part of the upper Givetian but both species range higher within the substage (ABOUSSALAM & BECKER 2007). Therefore, there is not necessarily a discrepancy between the goniatite and conodont ages.

Higher in Submember C, the calcareous Bed C4/23 is a flaser-bedded, partly laminated, partly bioturbated, fine-grained, silty mudstone (Fig. 19.5). It yielded a diverse (15 taxa) basal Frasnian conodont assemblage. *Ancyrodella rotundiloba pristina* is the zonal index of MN 1 Zone (or *Ad. rotundiloba pristina* Zone, Fig. 20.6). As emphasized by NARKIEWICZ & BULTYNCK (2010), *I. symmetricus* is an alternative marker (Tab. 2). Rare first *Po. praepolitus* are important for correlation into polygnathid-dominated shallow-water carbonate platforms (e.g., Russia, OVNATANOVA & KONONOVA 2008; Iran, GHOLAMALIAN et al. 2013). Associated are *Po. paradecorosus* (Figs. 20.2-3), poorly preserved *Po.* cf. *pennatus* (Fig. 20.4), *Po. dengleri dengleri*, and *I. tafilaltensis*. Characteristic for the basal Frasnian is an intermediate from *Mesotaxis guanwushanensis* M3 (sensu ABOUSSALAM & BECKER in PISARZOWSKA et al. 2020 in press) towards *Zieglerina ovalis* (Fig. 20.1). A still un-named species with quadrate platform and posteriorly extending carina, here provisionally called

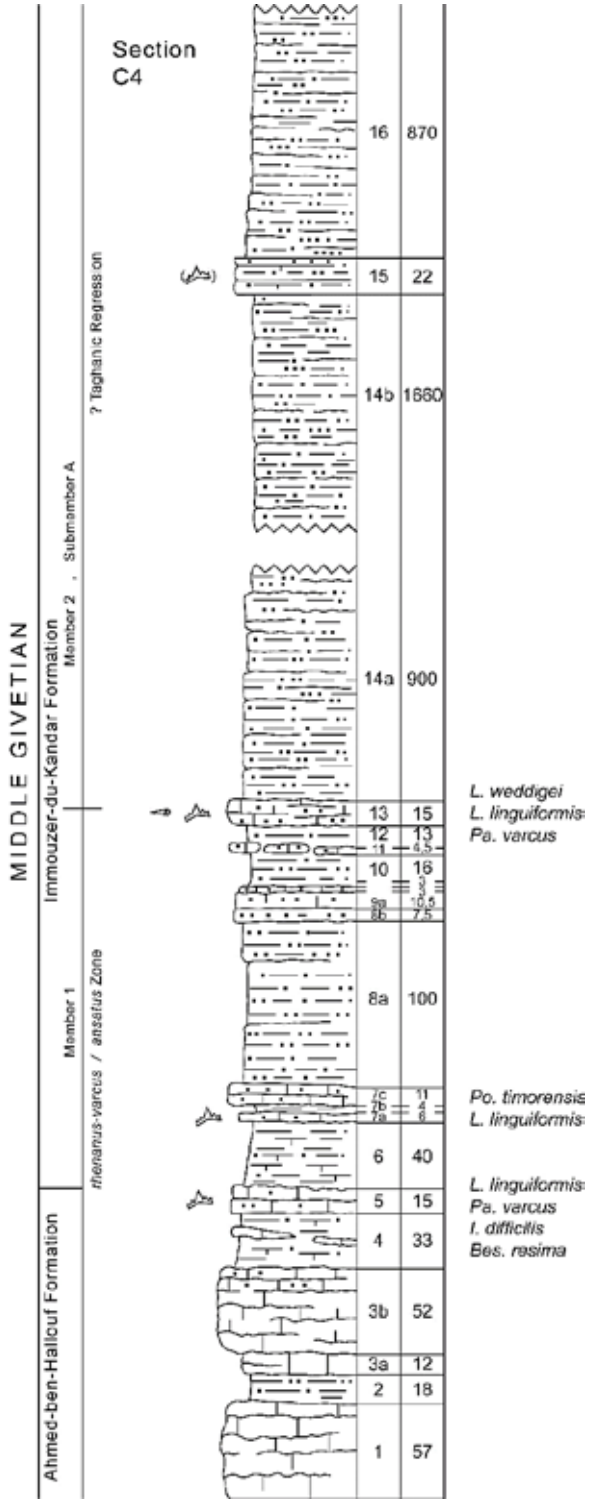

Fig. 21: Litho- and biostratigraphy (level of barren and productive conodont samples) of the lower part of Section C4, with the gradual transition from the Ahmed-ben-Mellouk to the overlying (new) Immouzer-du-Kandar Formation. For microfacies see Fig. 19.

Polygnathus* n. sp. aff. *lanei (Fig. 20.5), is also known from the Tafilalt (compare *Po. lanei* from MN 1 Zone in ABOUSSALAM & BECKER 2007, figs. 6l-m). The true Russian *Po. lanei* possesses a more strongly nodose and triangular platform. The conodonts are accompanied by some fish scales (probably from acanthodians). ***Polygnathus* aff. *cristatus*** refers to two very robust and coarsely nodose specimens with a marked concavity on one side of the thick anterior platform. ***Polygnathus* cf. *dengleri*** differs from typical members of the species in a reduced ornament and short anterior collar of the platform (compare Fig. 20.10). The dominance of *Polygnathus* supports a pelagic setting. Member 1 concludes with a last, up to 80 cm thick siltstone interval (Bed C4/24).

4.5.2. Member 2 (pelagic shale and limestone)

Member 2 is characterized by alternating, dark-grey, thin platy, originally pyritic (secondarily hematitic) shales, limonite-rich marls, and dark-grey, calcareous styliolinites (Fig. 26). Bedding planes show that the light-weighted dacryoconarids accumulated on bedding planes undisturbed by any currents (Fig. 27). This is a typical shelf basin lithofacies reflecting transgression and eutrophication, probably due to climate-controlled upwelling. Our conodonts from just below and above the main organic-rich shale package (Bed C4/25, **Submember A**) suggest that the sharp base of Member 2 can be correlated with the Upper Styliolinite of the Tafilalt (e.g., BULTYNCK 1986; ABOUSSALAM & BECKER 2007; NARKIEWICZ & BULTYNCK 2010). It expresses the main and second hypoxic pulse of the **global Frasnes Events** (BECKER & ABOUSSALAM 2004). Large hematite balls (oxidized from original pyritic) and the absence of any benthos indicate completely anoxic conditions that persisted apparently for a long time. **Submember B** (of Member 2) comprises the styliolinid-rich marl-limestone alternations, named by CHARRIÈRE & RÉGNAULT (1989) as "calcaires noirs à tentaculites".

sample no.																
bed no.	**5**	**7c**	**13**	**lense top23**	**b. bl. 26a**	**top bl. 28a**	**30**	**l. lst. 32**	**35**	**37**	**t. Fr. 38+**	**39**	**bl. 3**	**bl. 5 44-46**	**dis. bl.**	**top br. top 47**
stage	**m. Givetian**			**l. Fr.**	**middle Frasnian**								**(reworked faunas)**			
conodont zones	*?ansatus* Zone			**MN1**	**top MN4**		**MN5**		**MN6**	**MN7**			**Fr.**	**MN4**	**Fr.**	**MN7**
L. linguiformis	17	6	1													
L. weddigei	*	*	1													
I. difficilis	1															
Po. timorensis	*	1														
Po. varcus	1	*	1	8	*	*	4									
Bel. resima	1	*	*	4	*	*	3									
Po. xylus				11	*	2										
Po. cf. *pennatus*				2												
Po. n. sp. aff. *lanei*				1												
Ad. rotund. pristina				**2**												
M. guanwushanensis M3				1	*	4	*	*	2	1						
Po. dengl. dengleri				4	2											
Po. cf. *dengleri*				2	1											
I. symmetricus				**4**	5	9	3	11	61	49	7	8				12
I. tafilaltensis				2												
Po. paradecorosus				11	9	28	48	*	>10	xx	1	xx		3	1	27
Schm. latifossatus				1												
Po. n. sp. aff. *cristatus*				2												
Po. praepolitus				**1**	*	*	*	*	xx	24	*	4				
Z. ovalis					1	*	*	*	*	1						
Po. aff. *paradecorosus*					1											
Avign. decorosus					1											
Ad. nodosa					**2**	*	1	*	4	4						
Po. jorfensis						4										
Po. aff. *varcus* (sp. 1)						15	26	*	*	*	*	1				
Ad. africana						6								1		
Nothognathella sp.						2	*	*	3	4			1			
M. asymmetrica							45	*	*	1	1					
Z. unilabius							37	*	2	7	*	1				1
Pa. punctata							**1**	*	19	19						
Po. "aff. *angustidiscus*"							12	1	*	5						1
Palmatolepis sp.								1	1							
Po. aff. *varcus* (sp. 2)								9								
Po. n. sp. IdK-1								1								1
Ad. lobata									**7**	5						1?
Po. webbi									1	13	*		1	1		
M. falsiovalis										2						
Ad. gigas										5						

sample no.				**lense**	**b. bl.**	**top bl.**		**l. lst.**			**t. Fr.**		**bl. 3**	**bl. 5**	**dis. bl.**	**top br.**
bed no.	**5**	**7c**	**13**	**top23**	**26a**	**28a**	**30**	**32**	**35**	**37**	**38+**	**39**	**44-46**			**top 47**
stage	**m. Givetian**			**l. Fr.**	**middle Frasnian**								**(reworked faunas)**			
conodont zones	*?ansatus* Zone			**MN1**	**top MN4**		**MN5**		**MN6**	**MN7**			**Fr.**	**MN4**	**Fr.**	**MN7**
Pa. cf. *hassi*										1						
Pa. cf. *bohemica*										1						
Ad. pramosica										5						
Po. robustus										xx	*	8				8
"Oz." trepta										2						
"Oz." nonaginta										**1**						1
Ag. leonis										**1**						
Po. aequalis										xx						
I. aff. *symmetricus*										7				1		1
Po. alatus										1?						1
Z. orchardi												1				
Po. pollocki																1+1?
Po. aff. *sculptilis*																1
Po. n. sp. IdK-2																1
Po. zinaidae																1

Tab. 2: Ranges and frequencies of conodonts in the middle Givetian to middle Frasnian (including reworked faunas) in the upper part of Section C4 at Immouzer-du-Kandar.

They were also marked by CYGAN et al. (1990: lower part of Unit 3d; Figs. 26, 28; Beds C4/26a-28a). Characteristic are silty, partly laminated, partly weakly bioturbated wackestones with styliolinids and mollusk shells at the base (Bed C4/26a, Fig. 19.6), and organic-rich, dark, weakly bioturbated mud-wackestone with shell filaments at the top (Bed C4/28a, Fig. 19.7). Conodonts from both sampled beds fall in the top of MN 4 Zone with *Ad. nodosa* (= *gigas* M1; Fig. 20.8). This is the alternative *Ad. nodosa* Zone of ABOUSSALAM & BECKER (in PIZARKOWSKA et al. 2020) that shows the best potential to define a future formal lower/middle Frasnian boundary. The same interval is marked globally by one of the most significant positive carbon isotope excursions (PISARZOWSKA et al. 2006) and by the eustatic, transgressive **Middlesex Event** (HOUSE & KIRCHGASSER 1993; BECKER et al. 1993). This suggests to conduct future isotope studies at Immouzer-du-Kandar.

In Bed C4/26a, *Po. paradecorosus* is the most common species, grading via a transitional form with shortened and flattened platform (***Po.* aff. *paradecorosus***, Fig. 20.7) towards a specimen that closely resembles *Avignathus decorosus* (Fig. 20.11). An avignathan Pb element was not encountered but, due to hydraulic sorting, we hardly found anything than Pa elements. The so far oldest record of typical *Avignathus* is only slightly younger, from the basal MN 5 Zone (*Pa. punctata* Zone) of the Tafilalt (BECKER & ABOUSSALAM 2013b) but these were associated with a *Po. brevilamiformis* type Pa-element. The typical lowest range of *Avign. decorosus* is much younger, high in MN 10 Zone (KLAPPER 1997).

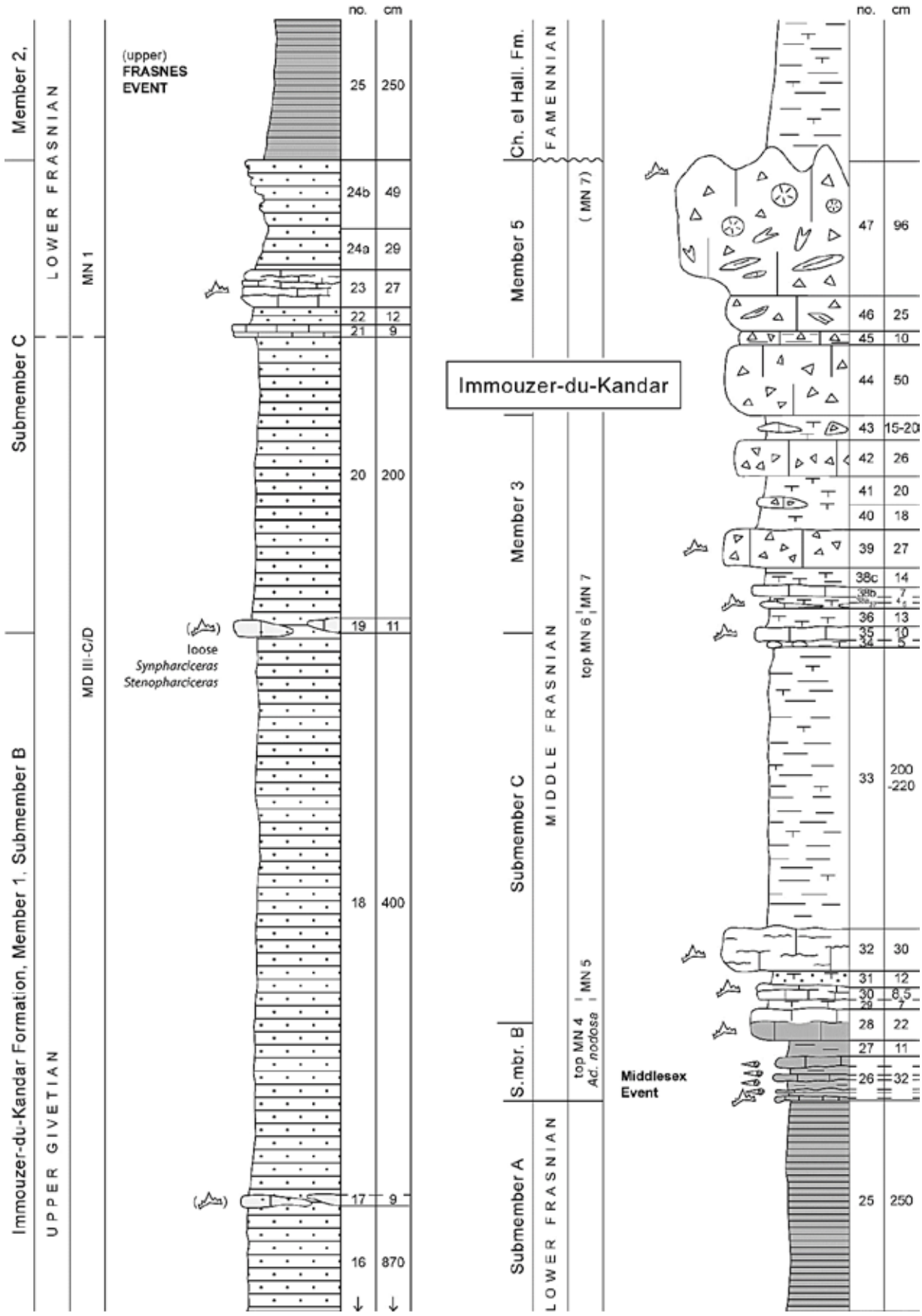

Fig. 22: Lithological log for the main/upper part of Section 4 (upper Member 1-5 of the Immouzer-du-Kandar Formation).

Fig. 23: Plant (Aneurophytales) from Member 1 of Immouzer-du-Kandar Formation (FAIRON-DEMARTET & RÉGNAULT 1986, pl. 3, fig. 7, picture width ca. 3 cm).

Fig. 25: Limonitized pharciceratids from Member 1 (top Submember B) of the Immouzer-du-Kandar Formation (loose at Bed C4/19): *Synpharciceras* sp. (left, dm = 31 mm) and *Stenopharciceras* sp. (right, dm = 26 mm).

Fig. 24: Thin-bedded, lenticular, silty limestones embedded in Submember C of Member 1.

Fig. 26: Laminated and cyclic alternation of limonite-rich marls and darker, calcareous limestones with styliolinids, lower Bed C4/26, lower Member 2 (Submember 2, top lower Frasnian, Middlesex Event Interval) of Immouzer-du-Kandar Formation.

Fig. 27: Styliolinid mass accumulation without current-orientation on the surface of Bed C4/26 (Submember 2, Member 2, top lower Frasnian; photo width 9 cm).

Fig. 28: Member 2 of Immouzer-du-Kandar Formation: alternating yellowish marls and thin grey limestones at the hammer (upper part of Bed C4/26), marker Bed C4/28, with a change from dark (28a, top of Submember B) to light-grey wackestone (28b, base Submember C), blocks of the thick, nodular Bed C4/32 in the background, and the main breccia at the top.

It needs to be emphasized that *Po. paradecorosus* continues to be confused by many authors (cf. in BAHRAMI et al. 2019; just recently in CABRERA-PORRAS et al. 2020) with *Av. decorous.* The Pb is not required for separation. Both Pa elements are not too similar, especially when type-specimens are respected. Other conodonts of Bed C4/26a are *I. symmetricus* (Fig. 20.9) and *Po.* cf. *dengleri* (Fig. 20.10).

The conodont fauna at the top of Submember B (Bed C4/28a) differs from below by a resurge of the Givetian survivor *Po. xylus* (Fig. 20.16). Relatives of *Po. varcus*, provisionally identified as ***Po.* aff. *varcus* (sp. 1)** (Fig. 20.14), display a slightly larger platform, a carina consisting of up to five large nodes, and regular transverse ribbing along the widened platform margins. In addition, there are some *Ad. africana* (Fig. 20.12) and a subtriangular *Nothognathella* with weekly ornamented platforms on both sides of the bent carina (Fig. 20.13), resembling ***Nothognathella* n. sp. of POLLOCK (1968)**. *Polygnathus jorfensis* was so far only known from the basal Frasnian (MN 1 Zone) of the northern Tafilalt (ABOUSSALAM & BECKER 2007). The absence of palmatolepids is intriguing and resembles the peculiar hypoxic conodont biofacies of the Upper Styliolinites of the Tafilalt (BULTYNCK 1986).

Submember C begins with Bed C4/28b, a light-grey weathering flaserlimestone. The styliolinid mass occurrences have disappeared. Above, alternating silty marls and griotte-type limestones follow (Beds C4/29-34). Bed C4/30 contains a different and distinctive conodont assemblage than known from below. Three species are near equally dominant, *M. asymmetrica*, *Z. unilabius*, and *Po. paradecorosus*, followed in terms of abundance by *Po.* aff. *varcus* (sp. 1). Such a middle Frasnian mesotaxid-polygnathid biofacies, without any *Palmatolepis* and almost without *Ancyrodella*, has been regarded by SANDBERG et al. (1989) as the deepest, most offshore facies. It occurs in comtemporaneous outer marginal reef slope settings of the Holy Cross Mountains, Poland (SOBSTEL et al. 2006: P-M facies, e.g., at Kostomloty and Śluchowice). A single *Pa. punctata* shows that the MN 5 Zone (*Pa. punctata* Zone) has been reached. There are moderately frequent ***Po.* "aff. *angustidiscus*" sensu HUDDLE (1981)**. This form is not related to *Ctenopolygnathus angustidiscus* because it has a short anterior free blade, as in the *Po. lanei*-*Po. aspelundi* Group, which members are all characterized by an only incipient free posterior blade.

Bed C4/32 is an up to 30 cm thick, yellowish-weathering marker unit with karstic upper surface (Fig. 28) that can be traced around the hill. CYGAN et al. (1990) noted it in the upper part of their Unit 3d as "calcaire massif". Our sampling confirmed a relatively sparse conodont fauna, in relation to the beds below, with only rare, fragmentary *Palmatolepis* (Fig. 20.17, possibly *Pa. punctata*) and dominant (50 % of the fauna) *I. symmetricus*. This short-termed icriodid-polygnathid biofacies indicates shallowing. However, *I. symmetricus* is not a shallow-water form but is regarded as a eurytopic species that flourished during environmental perturbations, for example during the lower/middle Frasnian transition (SOBSTEL et al. 2006).

Some polygnathids do not agree with described middle Frasnian species. ***Polygnathus* aff. *varcus* (sp. 2)** (Fig. 20.19) is characterized by smooth, narrow, posteriorly pointed platforms that are larger/longer than n in typical *varcus*. ***Polygnathus* n. sp. IdK-1** is characterized by a long, flat, narrow and finely ribbed platform with a hardly curved carina. Most characteristic are the uneven anterior platform ends. The outer side starts earlier and is slightly upturned while the inner end is shorter, flat and rounded. The new form falls in the lower Frasnian *Po. pollocki* Group; we wait

with formal naming until we have more material. CYGAN et al. (1990) reported in addition "*I.* cf. *eslaensis*". Typical *I. eslaensis* do not have a proven Frasnian range (NARKIEWICZ & BULTYNCK 2007), especially not in southern Morocco (ABOUSSALAM & BECKER 2007; GOUWY et al. 2007). The tabled "*Po. decorosus*" may have referred to our *Po.* aff. *varcus* (sp. 2).

4.5.3. Member 3 (middle Frasnian debris flows)

Within Bed C4/35 (Fig. 19.8), a sharp change from organic-rich, dark mudstone to erosive, sparitic calcisiltites, with small intraclasts filling a channel, marks the base of Member 3 of the Immouzer-du-Kandar Formation. The discharge of heterogeneous clasts reflects the onset of a second phase of significant Eovariscan block faulting, tilting and downslope deposition of reworked carbonate ramp material in debris and mass flows. The relatively diverse conodont assemblage probably comes from the mudstone. The abundance of *I. symmetricus* continues, followed by *Po. paradecorus* and *Po. praepolitus*. *Palmatolepis punctata* is finally more common, nothognathellids resemble *N. ziegleri*. The associated *Ad. lobata* enters elsewhere near the top of MN 6 Zone (KLAPPER 1997). Interesting is the locally oldest *Po. webbi* since this generally widespread species is elsewhere also not too common in the lower Frasnian and blossoms in the middle Frasnian (PISARZOWSKA et al. 2006; NARKIEWICZ & BULTYNCK 2010). The pelagic nature of Bed C4/35 is underlined by the presence of several goniatite ammonitellae in the conodont sample residue. There are also fish scales and shark teeth: one protacrodid (probably *Deihim mansoorae*) and one and a half *Wellerodus* sp. (Antarctilamnidae, Fig. 29), which is close to the Givetian type-species, *Well. wellsi*. In general, there is only little knowledge of middle Frasnian sharks.

Fig. 29: *Wellerodus* sp. from Bed C4/35 (top MN 6 Zone, middle Frasnian, tooth width = 1.6 mm).

Fig. 30: Member 3 of the Immouzer-du-Kandar Formation, starting with the still mostly micritic Bed C4/35 (upper MN 6 Zone), followed by lenticular detrital limestones (Beds C4/37-38, MN 7 Zone, at the hammer), and ending with more massive breccia beds (mass flow deposits, Bed C4/39, higher MN 7 Zone), all intercalated in yellowish weathering, strongly cleaved, limonitic (anoxic) shales.

Dark- or middle-grey lenticular, detrital limestones (Fig. 30) are embedded in greenish-grey, silty marls and shales of Beds C4/36-38. The conodont biofacies is similar to Bed C4/35 (polygnathid-icriodid), with a dominance of *Po. paradecorosus*, *Po. robustus* (Fig. 33.6, partly transitional from *Po. paradecorosus*, Fig. 33.11, or *Po. aequalis*, Fig. 33.12), and *I. symmetricus*. Markedly curved variants of the latter are identified as *I.* aff. *symmetricus*. There are no shallow water icriodids. The total number of taxa is unusually high (24 species, Tab. 2).

The age of the fauna, MN 7 Zone, is constrained by the distinctive, strongly bent *"Ozarkodina" trepta* (Fig. 33.2) and *"Oz." nonaginta* (Fig. 33.1; KLAPPER 1989; KLAPPER et al. 1996). Palmatolepids belong to *Pa. punctata* (most common, Tab. 2), rare *Pa.* cf. *bohemica* (Fig. 33.4) and *Pa.* cf. *hassi* (Fig. 33.3; still without a wide side lobe). Ancyrodellids include *Ad. nodosa* (= *gigas* M1), *Ad. lobata* (Fig. 20.21, intermediate towards *Ad. curvata* early form), *Ad. gigas* s.str. (Fig. 20.20, early form with many strong nodes; compare a cf. M2 specimen from MN 7 Zone of the Canning Basin, KLAPPER 2009, fig. 1.3.11), and **unusually late *Ad. pramosica*** (Fig. 20.22). The upper range of the latter ends normally much earlier (KLAPPER 1989, 1997). PISARZOWSKA et al. (2006) noted in Poland a just brief overlap with *Pa. punctata* at the base of MN 5 Zone. However, there is no evidence for reworking in our assemblage, no local occurrence in older beds, and no other middle Frasnian ancyrodellid our specimens could be confused with. A single *Ancyrognathus leonis* (Fig. 20.23) supports the MN 7 Zone age. Icriodids with relatively large, strongly asymmetric basal cavity and laterally connected posterior platform nodes are provisionally called *I.* aff. *symmetricus* (Tab. 2). Subordinate forms are robust nothognathellids with a strongly ornamented platform on one side only (Fig. 20.25), *M. asymmetrica* (Fig. 20.25), *Z. ovalis, Z. unilabius* (Fig. 33.5), *Po. praepolitus* (Figs. 33.7-8), *Po. aequalis* (Fig. 33.9), and *Po.* "aff. *angustidiscus*" sensu HUDDLE (1981).

Laterally, on the next hill to the W, there seem to be more non-brecciated limestone beds of Member 3. A conodont sample from the last limestone (Sample C4/38+) yielded only a sparse fauna (Tab. 2) that agrees in general with the richer faunas of Beds C4/35 and 37.

Bed C4/39 is the first coarse breccia Bed (Fig. 35.1). In thin-section, it is a strongly polymict extraclast grain-rudstone without any sorting or grading, typical for gravitational debris flow deposition. Crinoid debris, peloids, fragmented tabulate corals, brachiopods, calcareous algae, and conodonts lie free in a sparite matrix, together with variably large extraclasts, such as dark, organic-rich mudstones. The latter probably derived from eroded strata of Member 2. Most of the debris, however, stems from an adjacent shallow-water carbonate platform with reefal (biostromal) organisms that has today no preserved outcrop. Since the corals are not part of clasts, it can be assumed that they lived just prior to the seismically triggered reworking event. The conodont fauna is not mixed/reworked. It is dominated by *Po. paradecorosus*, accompanied by *Po. robustus* (Fig. 33.17), *Po.* aff. *varcus* (sp. 1) (Fig. 33.18), *Po. praepolitus*, and *I. symmetricus* (Fig. 33.14). In one *Zieglerina*, the shallow, asymmetric basal pit has expanded widely, as in the poorly known, Chinese *Z. orchardi* TIAN in HOU (1988; Figs. 33.15-16). There is no evidence for taxa that are younger than MN 7 Zone. Bed C4/39, therefore, proves the former existence of a **middle Frasnian reef/biostrome** in the Middle Atlas basement, which is **unique** for all of Morocco. All other Meseta reefs, including the bioherms of the Coastal Block or of the Oulmes region, died latest in the basal or at the end of the lower Frasnian (ABOUSSALAM et al. 2012). The

youngest known coral bank of the Anti-Atlas also falls in the Givetian-Frasnian transition (BECKER et al. 2013). Member 3 concludes with three more, similar breccia layers (Beds C4/41-43), which are partly lenticular and intercalated in grey shales; these have not yet been sampled for conodonts.

4.5.4. Member 4 (upper Frasnian-lower Famennian anoxic goniatite shale)

Just a few meters laterally to Section C4, Member 3 is overlain by a distinctive unit (5-6 m) of dark-grey to greenish, very pyrite-rich (weathering to yellow-ochre limonite) shale (Fig. 34). Its (for the Meseta) very unusual pelagic fauna shows that it is an extremely condensed, hypoxic/anoxic deep-water unit that straddles without any evidence of facies change or interruption the Frasnian-Famennian boundary. Goniatites in brown limonite preservation belong to *Costamanticoceras, Clauseniceras*, *Sphaeromanticoceras*, and the *Manticoceras cordatum* Group (Fig. 31). The first genus enters low in the upper Frasnian (sensu BECKER & HOUSE 1998; UD I-I, BECKER & HOUSE 1993) and does not reach the Lower Kellwasser level. The second enters in UD I-J and ranges into the interval between the two Kellwasser Events (UD I-K). The *Mant. cordatum* Group and *Sphaeromanticoceras* are long-ranging through the middle/upper Frasnian. Fragmentary orthocones, small-sized, smooth brachiopods, and the small gastropod *Platystoma*, which is typical for German goniatite shales, complete the hypoxic, muddy ecosystem. We correlate the onset of Member 4 tentatively with the basal upper Frasnian global eustatic rise known as the ***semichatovae* Transgression** (SANDBERG et al. 1992, 2002). In the Anti-Atlas, it introduced a long-lasting hypoxic interval (Kellwasser Facies s.l.), drowning the oxic middle Frasnian, pelagic Tafilalt Platform (e.g., WENDT & BELKA 1991; BECKER et al. 2018b). Based on neodymium isotopes, DOPIERALSKA (2009) and DOPIERALSKA et al. (2015) showed that this eustatic rise was associated with a major re-organisation of water masses in the western Prototethys, including the wide Moroccan shelf areas.

More or less next to the upper Frasnian manticoceratids, we collected three lower Famennian goniatites. However, these are differently preserved in black hematite (Fig. 32). There are two taxa, *Cheiloceras (Ch.) subpartitum crassum* and *Compactoceras (Com.) undulatum undulatum*. Both are common in the *(Ch.) (Ch.) subpartitum* Zone (UD II-C) of the Anti-Atlas (BECKER 1993a). In the Meseta, both generally widespread forms occur also in the ca. middle of the lower Famennian in the Oulmes region (e.g., TERMIER 1938; TERMIER & TERMIER 1950b; BECKER 1993a).

Since we have no local evidence for Kellwasser Beds or for the basal Famennian *Phoenixites* faunas, which are widespread in the Anti-Atlas (BECKER 1993a) or Mrirt allochthon (see Mrirt chapter of this volume), we assume that there is a hidden unconformity (non-deposition episode) within Member 4. But with respect to the long time involved, and in comparison with a strong peak of synsedimentary tectonics at the Frasnian-Famennian boundary in the eastern Anti-Atlas, the pelagic facies uniformity across that interval of global biotic crises at Immouzer-du-Kandar is remarkable.

Fig. 31: Three upper Frasnian, limonitic gephuroceratids from Member 4 of the Immouzer-du-Kandar Formation: a finely ribbed *Costamanticoceras* sp. (left, max dm. = 12 mm), *Clauseniceras* (middle, dm = 18 mm), and a *Manticoceras cordatum* (right, dm = 16 mm).

Fig. 32: Two black, hematitic *Cheiloceras (Ch.) subpartitum crassum* from the lower Famennian part of Member 4 of the Immouzer-du-Kandar Formation (max. dm = 7.2 mm, left, and 8 mm, right).

4.5.5. Member 5 (main reefal breccia, top lower Famennian)

The main breccia unit, our Member 5 of the Immouzer-du-Kandar Formation, eroded into gradually older Frasnian beds along the slope above Sections C4 to C2 (Fig. 34, upper photo; GPS N33°46‘7.2‘‘, W4°56‘51‘‘). From a better, distant perspective (Fig. 34, lower photo) it can be clearly seen that isolated breccia slump blocks overlie Member 4 and that they form an incised channel at Section C4 (Fig. 22). Therefore, the re-deposition age postdated UD II-C and can be assigned to the upper part of the lower Famennian. The base of Bed C4/44 is sharp, undulating, and disconformable (Fig. 36). There are only limestone clasts, which are up to 70 cm large, with decreasing maximum size towards the top. The lithology is strongly heterogeneous. There are abundant flat limestone blocks (Fig. 37), which are often oblique embedded (Fig. 38). A typical microfacies are polymict, unsorted coral-extraclast rudstones with stylolithic clast contacts (Figs. 35.3, 39). Based on field and thin-section examinations, we recognize the following clast types:

1. Isolated colonial rugose corals, such as *Phillipsastrea* (Figs. 35.4, 40; more than 20 cm large), hexagonariids (up to 20 cm large), and large “disphyllids” (phaceloid Rugosa, up to 70 cm large, Figs. 35.2, 41).
2. Isolated tabulate corals, such as *Thamnopora* branches (Fig. 39), alveolitids (Figs. 39, 43; up to 20 cm large), and nodular pachyfavositids.
3. Isolated, nodular, laminar, or fragmented stromatoporids.
4. Isolated crinoid stems (Fig. 44).
5. Isolated solitary rugose corals (Fig. 39).
6. Often large clasts of medium-bedded, laminated, fine-grained limestone (Figs. 37-38), partly with styliolinids, derived from lateral equivalents of Submember C of Member 2.
7. Dark, organic-rich, poorly fossiliferous mudstones (Fig. 35.1), probably derived from lateral parts of Submember B of Member 2.
8. Light-grey crinoidal limestones, sometimes with rugose corals.
9. Floatstones with solitary Rugosa and a variable amount of thamnoporids.
10 Floatstones with *Amphipora*, *Stachyodes*, and *Thamnopora*.
11. *Renalcis* limestone with brachiopods (Fig. 35.2).
12. *Alveolites*-stromatoporid boundstones.
13. Limonite clasts (Fig. 42), reworked from anoxic shale (upper Member 1 to lower Member 2).
14. Flaserlimestone with goniatite cross-sections (reworked from the mostly Middle Devonian Ahmed-ben-Mellouk Formation).

Corals are more frequent than stromatoporids. We observed reef debris clasts but no clear evidence for double reworking. The variability of microfacies types (e.g., EICHHOLT & BECKER 2016) suggests that the destructed reef was ecologically zoned, with agitated and more protected habitats. However, the evidence does not require a bioherm with a large protected lagoon. ***Renalcis* limestones** are recorded here for the first time from North Africa. They are more common in Frasnian than in Givetian reef complexes, which fits our conodont dating. In Australian, Canadian, and European (Ardennes) reefs, they characterize reef flat to marginal slope settings and especially small to medium-sized, open platform reef mounds (MOUNTJOY & JULL 1978; BURCHETTE 1981; PLAYFORD et al. 2009; GEORGE et al. 2009). They were important binder and cementer of coral-stromatoporid mounds (WHALEN et al. 2002), with possible cyanobacterial affinity.

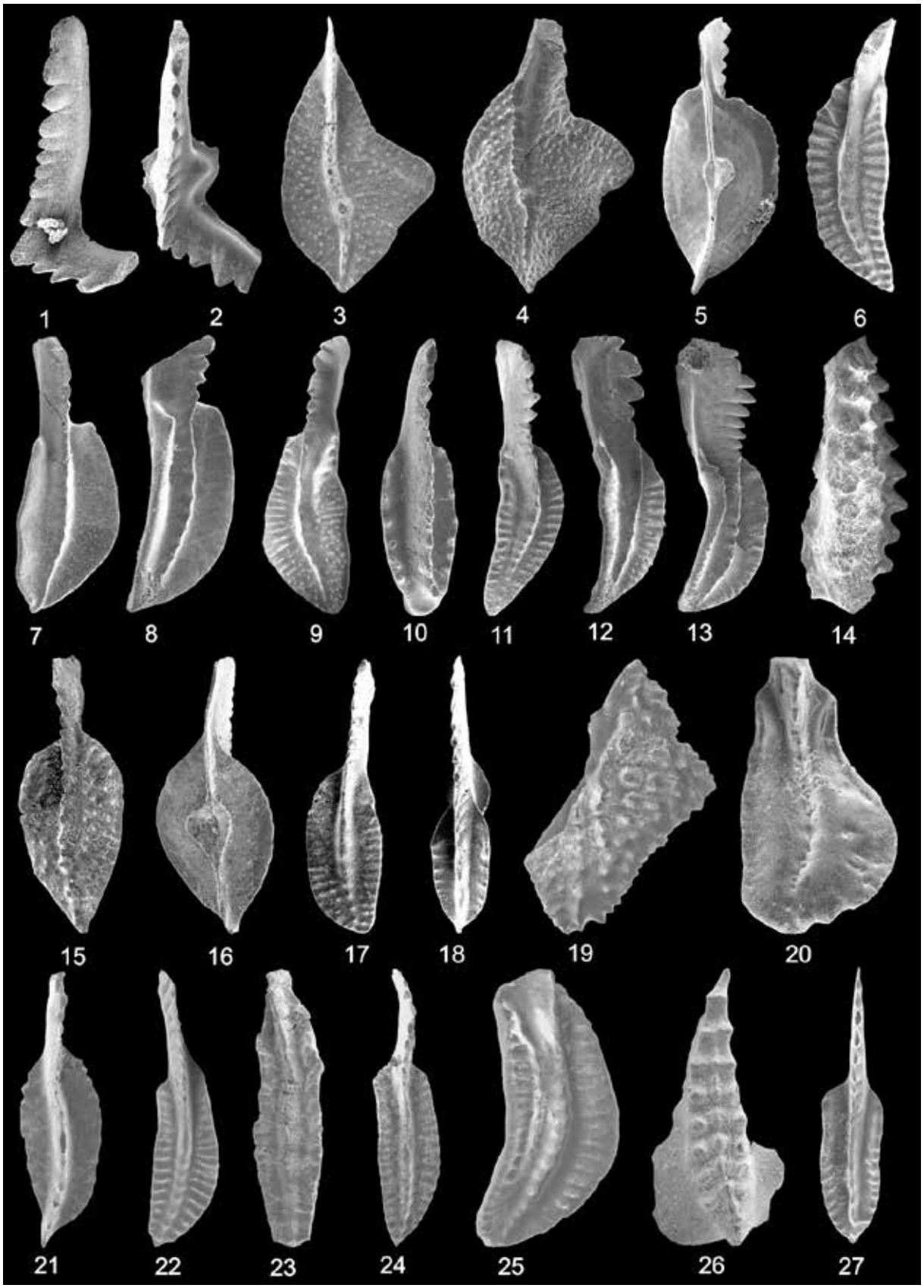

Fig. 33: Conodonts from Member 3 (Bed C4/37, 1-13, Bed C4/39, 14-18, all MN 7 Zone) and the main breccia, Member 5 (top Bed C4/47, 19-24 and 27, MN 7 Zone, individual blocks 3 (25), and 5 (26) from Beds C4/44-46), of the Immouzer-du-Kandar Formation. **1.** *"Oz." nonaginta*, x 70; **2.** *"Oz." trepta*, x 55; **3.** *Pa.* cf. *hassi*, x 60; **4.** *Pa.* cf. *bohemica*, x 40; **5.** *Z. unilabius*, x 50; **6.** *Po. robustus*, intermediate from *Po. aequalis*, x 50; **7-8.** *Po. praepolitus*, x 45 and x 50; **9.** *Po. aequalis*, x 30; **10.** *Po.* "aff. *angustidiscus*" sensu HUDDLE (1981), specimen with abnormal

(twisted) posterior end of carina, x 70; **11-12.** *Po. robustus*, intermediate from *Po. aequalis*, both x 35; **13.** *Po. webbi*, x 45; **14.** *I. symmetricus*, x 60; **15-16.** *Z. orchardi*, with strongly widened basal cavity, x 60; **17.** *Po. robustus*, x 50; **18.** *Po.* aff. *varcus* (sp. 1), x 90; **19.** *Ad. lobata*, fragmentary, x 35; **20.** *Po. zinaidae*, x 65; **21.** *Po.* "aff. *angustidiscus*" sensu HUDDLE (1981), x 80; **22.** *Po. paradecorosus*, x 60; **23.** *Po.* ?*pollocki*, x 60; **24**. *Po. pollocki*, x 55; **25**. *Po. webbi*, x 45; **26.** *I.* aff. *symmetricus*, curved form, x 50; **27.** *Polygnathus* n. sp. IdK-2, x 90.

Fig. 34: Upper photo: Thick breccia beds (Member 5) cutting off increasingly older parts of the middle Frasnian Members; lower photo: showing how Member 5 overlies the intensively ochre weathering F-F boundary shales (Member 4), cutting them off in the back and eroding as a channel into middle Frasnian strata.

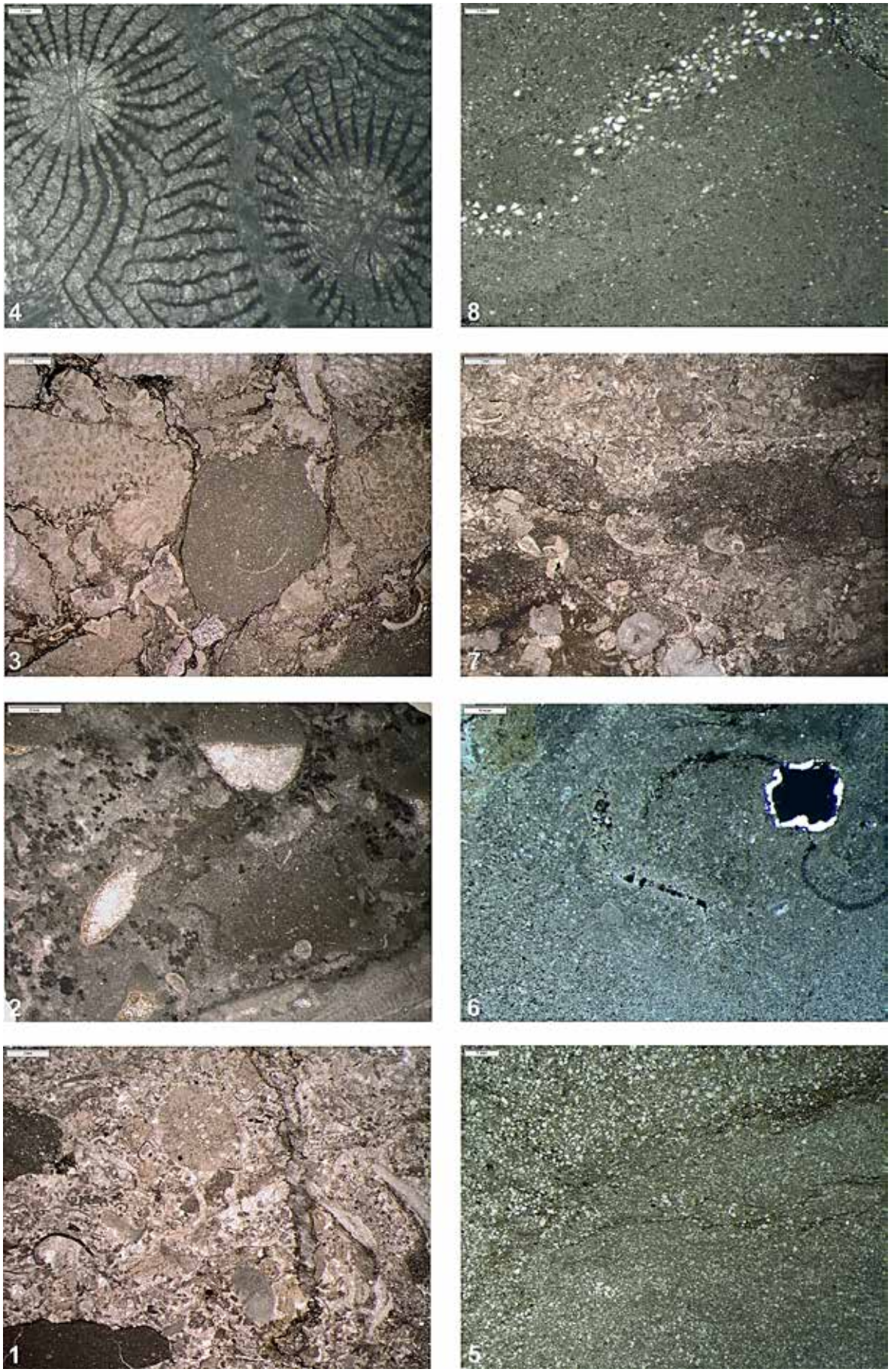

Fig. 35

Fig. 35: Microfacies of breccia beds in Member 3 (1) and Member 5 (2-4) and of upper Famennian thin carbonates (4-8), scale bar = 2 mm in 1-3 and 7, 1 mm in 4-8 and 8. **1.** Polymict, unsorted, extraclast grain-rudstone with crinoid debris, peloids, tabulate corals, brachiopods, reworked dark, organic-rich mudstones, conodonts (free in the sparite matrix), and calcareous algae, Bed C4/37, MN 7 Zone; **2.** Bioturbated *Renalcis*-coral floatstone with isolated or clumped *Renalcis* aggregates in dark micrite matrix, other microproblematica, sparite- or geopetally filled brachiopods, and large phaceloid rugose coral (lower right bar), block in Bed C4/47; **3.** Polymict, unsorted coral-extraclast rudstone with stylolithic clast contacts, various tabulate corals, crinoid debris, shell fragments, reworked, dark- or middle-grey silty mudstones and bioclastic wackestones, top of Bed C4/47; **4.** Extract of large *Phillipsastrea* colony, Bed C4/47; **5.** Flaser-bedded, unfossiliferous silty mudstone (lower part) to calcareous siltstone (upper part), Bed C5/Fa 1; **6.** Pyrite-rich, bioturbated, bioclastic wackestone with recrystallized ostracods, tabulate coral (middle right) and micrite/microsparite matrix, Bed C5/Fa 6; **7.** Flaser-bedded, bioturbated, strongly mixed dark mudstones and microsparitic crinoid wacke-packstones with tabulate corals, eroded by an overlying channel with strongly recrystallized crinoid-mollusk grainstone, Bed C5/Fa 13: **8.** Bioturbated, unfossiliferous, silty mudstone interrupted by a thin band of angular silt and mudclasts, Bed C5/Fa 15.

Fig. 36: Base of the main breccia (base Bed C4/42, base Member 5) at Immouzer-du-Kandar.

The erosion and reworking affected mostly Frasnian strata (Members 2-3 of the Immouzer-du-Kandar Formation and the destructed adjacent biostrome); clasts from the Ahmed-ben-Mellouk Formation are very subordinate. Uplift, excavation and re-sedimentation occurred after lithification, which may have been fast.

Age data come from conodont faunas obtained either from mixed breccia blocks or from individual larger clasts. As expected, the conodont yield is mostly poor. We found no reworked Emsian to Givetian conodonts but did not sample any flaserlimestone clast. Our Block 3 produced only *Po. webbi* (Fig. 33.25) and a nothognathellid (Pb element of *Mesotaxis/Palmatolepis*), indicative of the top lower to middle Frasnian. Block 5 contained the strongly curved representative of *I.* aff. *symmetricus* (Fig. 33.26), *Po. paradecorosus*, and *Ad. africana*. This suggests a top lower Frasnian (MN 4 Zone) age. The block with large phaceloid "disphyllid" colony (Fig. 35.2) only gave a single *Po. paradecorosus* (Tab. 2; topmost Givetian to Frasnian).

More intriguing is a breccia sample from the top of the breccia (top Bed C4/47). The abundance of *Po. paradecorosus, Po. robustus*, and *I. symmetricus* is the same as in Bed C4/37, with further similarity given by *"Oz." nonaginta*, the index species of MN 7 Zone, a fragmentary *Ad. lobata* (Fig. 33.19), and *Po.* "aff. *angustidiscus*" sensu HUDDLE (1981; Fig. 33.21). In accord with the clast spectrum, there was no change of the source of the mass/debris flow influx between Members 3 and 5. As minor differences, Bed C4/47 yielded some *Po. pollocki* (Figs. 33.23-24), characterized by a relatively short free blade, very narrow and long platforms with marginal ribbing, unlike as in the evenly curved *Po. paradecorosus* that has a longer free blade and always a small anterior platform collar.

Fig. 37: Block of main breccia (Member 5) showing large, flat lying blocks of laminated, light-grey limestone below unsorted, smaller-sized clasts.

Fig. 38: Oblique embedding of a large, fine-grained, laminated limestone block in the polymict, unsorted Bed C4/44.

Fig. 39: Disorganized, coarse extraclast-coral rudstone with a near-vertical block of laminated, fine-grained limestone (right), numerous rugose corals, pieces of stromatoporids, and angular clasts of crinoidal and reefal limestone.

Fig. 40: Field photo of a *Phillipsastrea* colony from the upper part of the main breccia.

Fig. 41: Large phaceloid rugose coral colony.

Fig. 42: Mass flow (Member 5) with angular reef limestone clasts, limonite pebbles, isolated *Thamnopora* branches, and alveolitids swimming in an argillaceous matrix.

Fig. 43: Isolated *Alveolites* colonies as clasts in the main breccia (Member 5).

There is also a second specimen of *Polygnathus* n. sp. IdK-1 (Fig. 33.22; see earlier record from Bed C4/32), which may be a relative of *Po. pollocki*. One specimen agrees closely with the holotype of *Po. zinaidae* (Fig. 33.20), apart from a few scattered platform nodes. This species occurs on the central Russian Platform, in the Timan in the hypoxic pelagic facies of the Middle Domanik (OVNATANOVA & KONONOVA 2008; MN 6 Zone, see HOUSE et al. 2000b), as well as in middle Frasnian shallow-watter settings of the SE Iran (e.g., GHOLAMALIAN & KEBRIAEI 2008).

Fig. 44: Thick crinoid stem parts lying isolated in breccia with argillaceous matrix.

A single, robust polygnathid with straight carina, coarse marginal platform nodes, asymmetric anterior platform ends, and short, free posterior carina is identified as ***Po.* aff. *sculptilis*** (Fig. 45). It is possibly a new species but too poorly preserved for formal naming. A second new species, ***Po*. n. sp. IdK-2**, is represented by a single polygnathid with straight carina, constricted narrow platform, which marginal ribbing becomes more regular in the posterior half (Fig. 33.27). The free blade occupies slightly more than 40 % of the total length and the anterior platform has a short smooth collar.

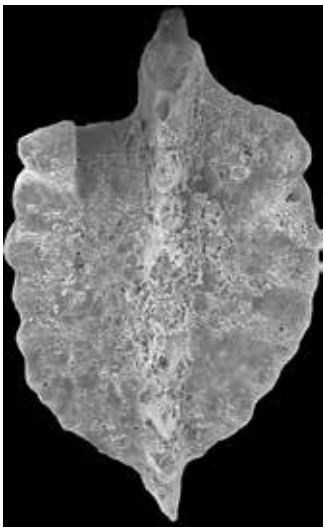

Fig. 45: The unique *Po.* aff. *sculptilis* specimen from Bed C4/47, the top of the brecciated Member 5 of the Immouzer-du-Kandar Formation (x 100).

CYGAN et al. (1990: Sample 25B) found in the breccia matrix *Po. webbi*, a questionable *Ad. rotundiloba* (perhaps one of the different, top lower Frasnian species), a "*Polygnathus* sp. A" and "*Po. decorosus*" (probably *Po. paradecorosus*). More interesting is their block with Sample 25A, allegedly with *I. alternatus* and *Apatognathus* sp. The first ranges from the upper Frasnian into the lower Famennian. If correctly identified (no figure available), the *Apatognathus* definitely proves an at least late lower Famennian age. This lends support to the observed depositional structure. The genus was revised by NICOLL (1980), who noted in the NW Australian reef complexes its first occurrence in the Middle/Upper *crepida* Zones (now including the *Pa. glabra pectinata* Zone = Uppermost *crepida* Zone; SPALLETTA et al. 2017). This gives a good fit with a level just above our UD II-C cheiloceratids (see goniatite-conodont correlation in BECKER 1993a).

4.6. (new) **Chabat el Hallouf Formation** (middle/upper Famennian)

The thick predominant siliciclastics, with interbedded thin limestones in the upper part, that occupy the main upper slope at Immouzer-du-Kandar (Figs. 1, 46), are assigned to the new Chabat el Hallouf Formation, using the name for the valley on the SE side of the mountain (Fig. 2). It comprises the "lutites à galets" of CHARRIÈRE & RÉGNAULT (1989) as well as Units 3f and 3g of CYGAN et al. (1990) that are assigned to formal Lower and Upper Members. The new formation begins with a regressive unit in comparison with the underlying Immouzer-du-Kandar Formation. However, the influx of clastic material is completely different than in the Emsian Chabat Jenanat Conglomerate or in the middle/upper Givetian "plant siltstones".

4.6.1. Lower Member (middle Famennian brachiopod-volcanite pebble siltstones)

The main breccia of Section C4 or laterally Member 4 are overlain by non-fossiliferous, mostly reddish, occasionally dark-grey to ochre weathering shales and siltstone, **Submember A** of the **Lower Member** of the Chabat el Hallouf Formation. In the absence of any fossils, a basal middle Famennian age is tentative. Both in Europe and in the Anti-Atlas, hypoxic and fossiliferous (eutrophic) sedimentation was terminated by the global Condroz Regressions at the top of the lower Famennian (BECKER 1993a, 1993b). These

may have ended the deposition of Member 4 of the Immouzer-du-Kandar Formation, too.

Submember B refers to the up to 30 m thick "lutites à galets" of BRICE et al. (1984), CHARRIÈRE & RÉGNAULT (1989), and CYGAN et al. (1990), which are partly covered by vegetation on the steep slope (Fig. 46).

Fig. 46: View from the main breccia (top of Immouzer-du-Kandar Formation, foreground) onto the upper slope occupied by the new Chabat el Hallouf Formation, with reddish silty shales at the base (Submember A) and the Upper Member at the crest. Note the ochre weathering Member 4 on the plateau to the middle right.

Fig. 47: Variably-sized, well-rounded, isolated volcanite pebbles weathering out of partly brachiopod-rich, volcaniclastic, greenish siltstones in the middle of the Lower Member (Submember B) of the Chabat el Hallouf Formation.

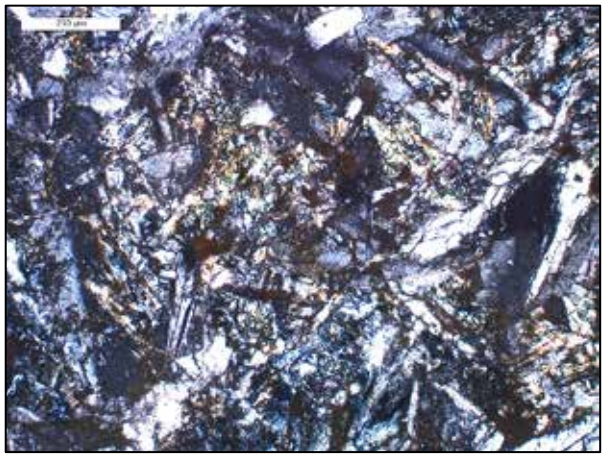

Fig. 48: Thin-section of feldspar-dominated, altered volcanite pebble from the "lutites à galets".

Fig. 49: Two examples of new brachiopods collected in-situ from volcaniclastic siltstones in Submember B of the Lower Member of the Chabat el Hallouf Formation (shell width = 11 and 13.5 mm, respectively).

The main lithology are greenish-grey siltstones with abundant, up to 10 cm large, well rounded, light greenish-grey, yellowish weathering pebbles consisting of argillaceous siltstone and, more frequently, volcanite pebbles (Figs. 47-48). The latter were briefly noted and were not explained by CHARRIÈRE & RÉGNAULT (1989, p. 33). They consist mostly of plagioklase, with some chlorite and pumpellyite (identified by M. BRÖCKER, Münster). This characterizes an altered composition of basaltic to, in this case more likely, intermediate volcanics.

BRICE et al. (1984) described brachiopods, which are typical for a neritic environment; these contrasts with the pelagic faunas from below. Records of *Cyrtospirifer* and "*Eodmitria*? sp." were used to suggest a possible lower Frasnian age, which can now be rejected. We found layers with univalved brachiopods (Fig. 49) and fragmented tabulate corals in the middle slope in greenish mudstones. They contain numerous, isolated or horizontally enriched, up to ca. 5 mm large (mostly as sand-sized fraction), angular clasts of light yellowish weathering (acid) magmatic particles. They also seem to represent reworked material since they are associated in epiclastitic sandstone layers with some angular quartz grains and siltstone micropebbles. However, they differ clearly from the well-rounded, much larger volcanic pebbles, as proof for a heterogeneous source. The age remains unclear; currently there is no published evidence for synsedimentary middle/upper Famennian volcanism in the Meseta (see review of Moroccan magmatic events by IKENNE et al. 2016).

The depositional mechanism of Submember B is odd. The siltstone and volcanite pebbles must have been reworked and rounded for a long time in a coastal or fluvial environment prior to re-deposition. A wide transport distance is impossible. The pebble age is currently unknown (Lower Palaeozoic to Devonian). The dropstone-type, isolated, not lumped, embedding in open marine, volcaniclastic brachiopod silt-sandstones can only be explained by a succession of mass flows along a shallow-water slope.

Fig. 50: Two views of the measured section through the Upper Member of the Chabat el Hallouf Formation, showing that beds dip near-parallel with the topography on the (ESE) back side of the mountain.

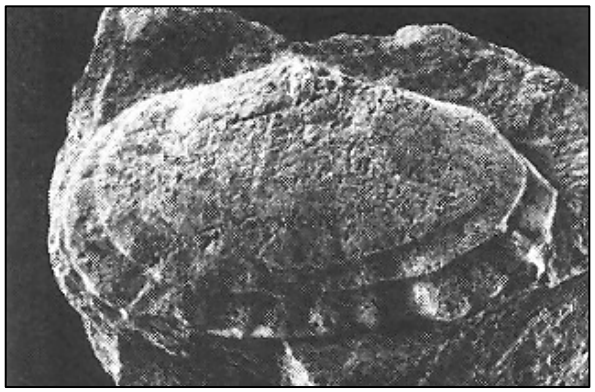

Fig. 51: Example for one of the brachiopods documented by BRICE et al. (1984) from the "niveau carbonates supérieur" (= Upper Member of Chabat el Hallouf Formation): a supposed *Planovatirostrum* sp., re-assigned by SARTENAER (2000) to *Phacoiderhynchus*.

4.6.2. Member 2 (upper Famennian limestone and shale)

Unit 3g, the "niveaux carbonate supérieur" of BRICE et al. (1984) and CHARRIÈRE & RÉGNAULT (1989), or "calcaires et marno-calcaires terminaux" of CYGAN et al. (1990), is here named as (new) Upper Member of the Chabat el Hallouf Formation. CYGAN et al. (1990) considered 40-50 m thickness but our detailed Section C5 includes only ca. 20 m of dominant greenish-grey or middle-grey, marly siltstones with intercalated, thin, lenticular, middle- to dark-grey limestone beds (Figs. 50, 53). The difference reflects the fact that we concentrated on the interval with limestones. BRICE et al. (1984) described brachiopods, such as the productid *Whidbornella* and rhynchonellids, supposed *Planovatirostrum* (Fig. 51). The latter was re-assigned to *Phacoiderhynchus*, possibly to its type-species, *Phac. antiatlasicus*, which occurs in the Maider (eastern Anti-Atlas) in zones UD III-B (higher middle Famennian) to UD IV-B (lower part of upper Famennian; SARTENAER 2000). Our new conodont data prove a younger (upper part of upper Famennian, UD V) age for the limestone interval. The combination of moderately fine siliciclastics and open neritic benthic fauna suggests a moderately deep (subtidal) setting at the outer margin of an inner shelf. Plant remains ("Psilophytales" in BRICE et al. 1984) may haved been transported over a long distance. CHARRIÈRE & RÉGNAULT (1989) mentioned a dark cephalopod limestone lense, which we did not re-discover. It indicates a deepening interval, possibly the global Dasberg Event (see HARTENFELS 2011).

In Section C5, the more than 1.2 m thick lower part (Bed C5/Fa 1) includes strongly bioturbated, unfossiliferous, silty mudstones and calcareous siltstones (Fig. 35.1). The same lithology continues for the next ca. 2 m (Beds C5/Fa 2-5a). The partly pyrite-rich, calcareous siltstone of Bed C5/5b yielded the first conodonts, but only two specimens of zonally undiagnostic forms within the long middle/upper Famennian interval (Fig. 53). In Bed C5/Fa 6a there are three layers of middle- to dark-grey limestone lenses, which represent a more fossiliferous microfacies: bioturbated, bioclastic wackestone with recrystallized ostracods, a tabulate coral, and silty micrite matrix. Among the conodonts, there are *Bispathodus aculeatus aculeatus* (Fig. 52.1), *Clydagnathus plumulus*, *Pa. perlobata schindewolfi* (Fig. 52.2), *"Po." diversus* (Fig. 52.3), and *Ctenopolygnathus* cf. *brevilaminus* (Fig. 52.4). The first is the index species of the *B. aculeatus aculeatus* Zone in the late upper Famennian (using the proposed substage definition of HARTENFELS et al. 2009). The second enters at the same level (ZIEGLER et al. 1974), the third does not range above that zone in well constrained, complete, pelagic successions (KAISER et al. 2009). *"Polygnathus" diversus* was so far not known to range above the *Po. styriacus* Zone (GLENISTER & KLAPPER 1966; SPALLETA et al. 2017). Since there are regionally no older Famennian conodonts, we do not think that the specimen was reworked. HARTENFELS (2011) extended the range of the *Ct. brevilaminus* Group to the *B. aculeatus aculeatus* Zone. The dominance of double-rowed bispathodids, which originally included *Cly. plumulus* (ZIEGLER et al. 1974), is normally typical for deep pelagic facies (part of the Palmatolepid-Bispathodid Biofacies of SANDBERG 1976). However, SÖTE et al. (2017) drew attention to bispathodid-dominated faunas occurring in much shallower crinoid shoals around uppermost Famennian islands in the eastern Anti-Atlas (section Lalla Mimouna, BECKER et al. 2013). Therefore, there was not necessarily a discrepancy between litho-, brachiopod and conodont biofacies at Immouzer-du-Kandar. The shallow-water Clydagnathid Biofacies of SANDBERG (1976) was based on high abundances of *Cly. ormistoni*, not on the facies distribution of *Cly. plumulus*.

.

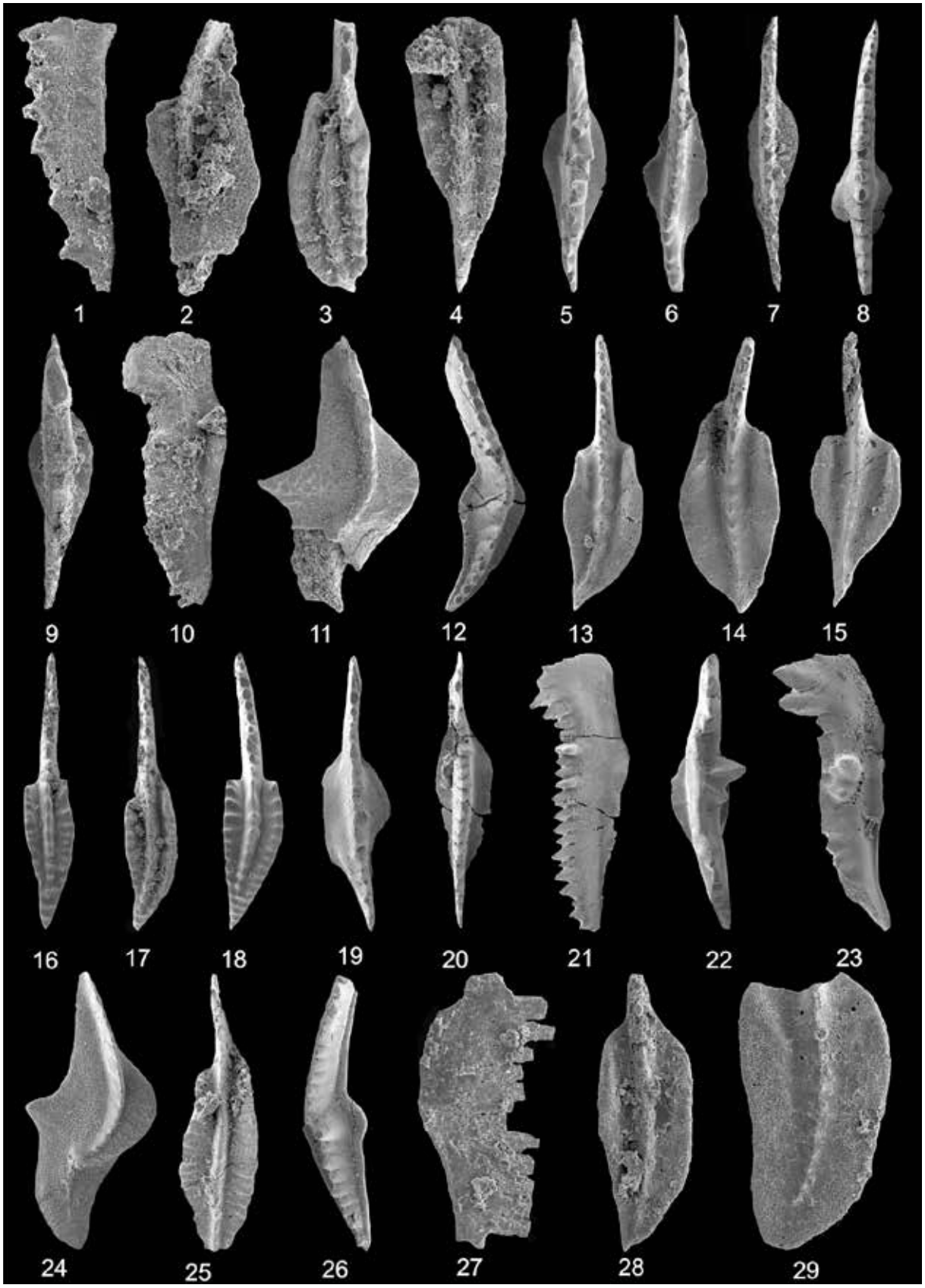

Fig. 52

Fig. 52: Upper Famennian conodonts from Immouzer-du-Kandar, Section C5, Bed Fa 6 (1-4), Bed Fa 13 (5-18), Bed Fa 15b (19-26), and base Bed Fa 17 (27-28). **1.** *Bispathodus aculeatus aculeatus*, x 85; **2.** *Pa. perlobata schindewolfi*, x 95; **3.** *"Po." diversus*, x 100; **4.** *Ctenopolygnathus* cf. *brevilaminus*, x 100; **5.** *B. bispathodus*, x 50; **6-7.** *B. stabilis vulgaris*, both x 60; **8.** *Branmehla fissilis*, x 50; **9-10.** *Clydagnathus plumulus*, both x 55; **11.** *Pa. perlobata schindewolfi*, x 30; **12.** *Pa. gracilis gracilis*, x 45; **13-15.** *Neopolygnathus* cf. *communis*, x 70, x 65, and a juvenile with posterior free blade (15, x 75); **16.** *Po. semicostatus* central morphotype; x 60 **17.** *Po.* cf. *semicostatus* with upturned platform margins and narrow adcarinal furrows, x 80; **18.** *Po. semicostatus* M6, x 55; **19.** *B. aculeatus aculeatus*, x 45; **20-21.** *B. bispathodus*, both x 50; **22-23.** *Cly. plumulus*, both x 35; **24.** *Pa. perlobata schindewolfi*, x 45; **25.** *Po. delicatulus*, x 45; **26.** *Pa. gracilis gracilis*, x 35; **27.** *Mehlina strigosa*; x 90; **28-29.** *Neo. communis communis*, x 95 and x 90.

All higher faunas seem to fall in the same zone and we did not encounter *B. costatus*, which defines an upper subzone (HARTENFELS 2011; *B. costatus* Zone in SPALLETTA et al. 2017). The detrital Bed C5/Fa 13 displays a complex microfacies: bioturbated, therefore strongly mixed, dark mudstones and microsparitic crinoid wackestones with tabulate corals were eroded by a channel filled by strongly recrystallized crinoid-mollusk grainstone. Such short intervals of increased bottom currents reflect the episodic, distal impact of large storms. The conodont fauna is rather diversified (15 taxa/morphotypes). *Bispathodus aculeatus aculeatus* is missing so far, but *Cly. plumulus* is present (Fig. 52.9-10). There are various single row spathognathodids, such as *B. stabilis stabilis*, *B. stabilis vulgaris* (Figs. 52.6-7), *Branmehla fissilis* (Fig. 52.8), as well as the long-ranging *B. bispathodus* (Fig. 52.5) with an incipient double row of carina nodes. Among the palmatolepids, there is, again, *Pa. perlobata schindewolfi* (Fig. 52.119 and the widespread, bradytelic *Pa. gracilis gracilis* (Fig. 52.12). Two polygnathid groups appear, various *Neopolygnathus*, including *Neo.* cf. *communis* with constricted, slightly upturned anterior platforms margins (giving a tendency towards *Neo. lectus*; Figs. 52.13-14), juveniles (Fig. 52.15), and the *Po. semicostatus* Group (Figs. 52.16-18). The latter species group possesses a platform lingua and is homoeomorphic to the Middle Devonian *Linguipolygnathus* (and should be separated as an own genus). The first represents ecological generalists (see discussion in SÖTE et al. 2017), the second is typical for neritic shallow-water biofacies (SANDBERG 1976). The upper range of the *semicostatus* Group is not well established. DREESEN & THOREZ (1994, tab. 5) have previously recorded a co-occurrence of *Po. semicostatus* and *Cly. plumulus* at Anseremme in the Belgian Ardennes. The unusual assemblage of Bed C5/Fa 13 (30 % *Bispathodus/Clydagnathus*, 21 % *Palmatolepis*, 17 % *Po. semicostatus*, 33 % *Neopolygnathus*) may reflect a sedimentary admixture of taxa living originally in different, adjacent environments, brought together at the outer margin of an inner shelf.

Unit C5/Fa 15 includes several lenses (original channels) of recrystallized crinoid debris (crinoid wacke-packstone or grain-rudstone), alternating with bioturbated, unfossiliferous, silty mudstone and thin bands of angular siltstone with mudclast (Fig. 35.8).

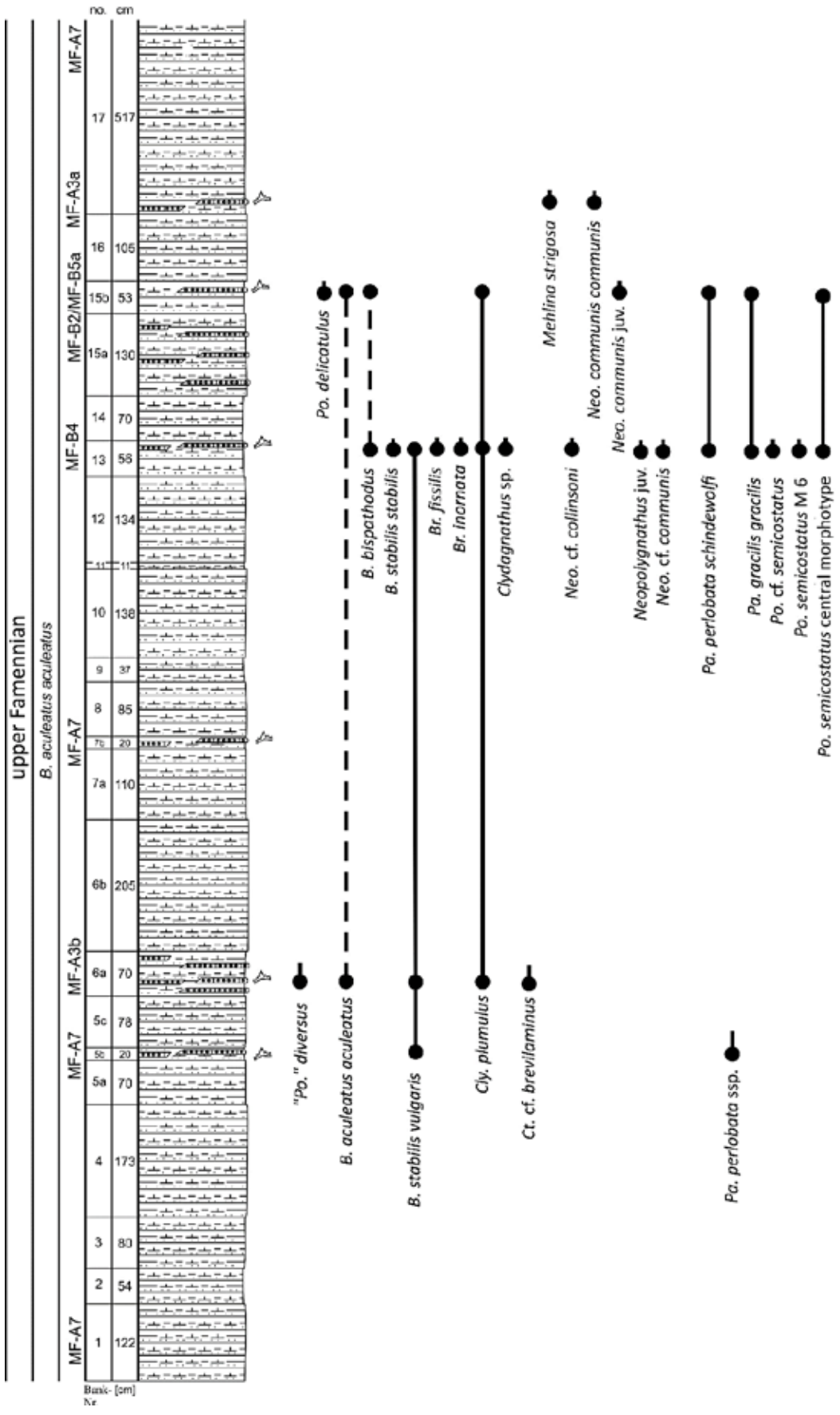

Fig. 53: Section log for the Upper Member of the Chabat el Hallouf Formation (Section C5) giving the conodont ranges.

The conodont fauna is sparse but with many taxa each represented by single specimens (e.g.; *B. aculeatus aculeatus*, Fig. 52.19 (very early form with incipient secondary nodes), *B. bispathodus*, Figs. 52.20-21, *Cly. plumulus*, Figs. 52.22-23, *Pa. perlobata schindewolfi*, Fig. 52. 24, *Pa. gracilis gracilis*, Fig. 52.26). *Polygnathus delicatulus* (Fig. 52.25) has previously been recorded from the *B. aculeatus aculeatus* Zone (former Middle *expansa* Zone, KLAPPER in ZIEGLER 1975).

Our logging of Section C5 (Fig. 53) ended with a ca. 5 m thick, grey to (upwards) greenish-grey siltstone package (Bed C5/17). A lense of strongly bioturbated, silty mud-wackestone, from the base yielded our so far youngest conodonts with the long-ranging spathognathodid *Mehlina strigosa* (Fig. 52. 27) and by far dominated by the opportunistic to generalistic *Neo. communis communis* (Fig. 52.28). It seems that the ecological conditions for conodonts worsened. At the top of the unit lies a last intercalation of bioclastic grainstone grading into slightly laminated silty mudstone.

A comparison of the Chabat el Hallouf Formation with contemporaneous strata of the Azrou region to the SW (BOHRMANN & FISCHER 1985; many new data) shows marked differences. The middle Famennian of Azrou lacks neritic faunas and is characterized by a thick sequence of shales and recurrent limestone breccias with mixed neritic-pelagic conodont taxa. Whilst the timing of Eovariscan uplift and reworking seems similar, the respective hinterland was very different (volcanic siliciclastic shelf versus a destructed carbonate ramp). The upper/uppermost Famennian of Azrou was also silty but strongly condensed, currently without a record of the *B. aculeatus aculeatus* Zone.

4.7. "Flyschoid Succession"

The wide area between the crest of Section C5 and Chabat el Sitout (Fig. 2) is occupied by a thick siliciclastic unit named in BRICE et al. (1984) "ensemble flyschoide" (see also CHARRIÈRE 1989, fig. 6, and Unit 4 of CYGAN et al. 1990). Its proposed top-Famennian to ?Tournaisian age is not based on any fossils but on the bracketing between upper Famennian and Viséan formations. A second, thick flyschoid unit ("série pélitique supérieure of CHARRIÈRE 1989) forms the matrix of lenticular Viséan limestone bodies. We did not re-study these un-named formations.

4.8. Viséan

Viséan shallow-water carbonates crop out as thick lenticular limestone bodies SE of Chabat el Sitout (e.g., CHARRIÈRE 1989, 1990; cross-section in OUARHACHE et al. 1991). They contain foraminiferes and calcareous algae, which first provided a supposed Middle Viséan (upper Molinacian, V2a = Cf4δ) age. This was changed by OUARHACHE et al. (1991) to lower Asbian (lower Warnantian, V3bα/ß = Cf 6α/ß), then to V3ßγ (BERKHLI 1999; BERKHLI et al. 2000). This "younging" of the limestones with ongoing research was also briefly commented on by COZAR et al. (2019). We cannot contribute to this question since we did not re-sample the Upper Viséan carbonate platform. Previous authors (e.g., BERKHLI et al. 2000) compared the Immouzer-du-Kandar Viséan with other Meseta regions and found that it fits well into the wider palaeogeographic patterns. Therefore, it seems that the rather peculiar facies development of Immouzer-du-Kandar ended in the Lower Carboniferous, latest with the Upper Viséan spread of carbonate platforms. The local Carboniferous macrofauna has not yet been studied sufficiently. We collected marly limestone slabs with numerous brachiopods and fenestellid bryozoans. CHARRIÈRE (1989) listed various brachiopod taxa, including schizophoriids, productids, and spiriferids.

References

ABOUSSALAM, Z. S. (2003): Das „Taghanic-Event“ im höheren Mittel-Devon von West-Europa und Marokko. – Münstersche Forschungen zur Geologie und Paläontologie, **97**: 1-332.

ABOUSSALAM, Z. S. & BECKER, R. T. (2002): The base of the *hermanni* Zone as the base of an Upper Givetian substage. – SDS Newsletter, **19**: 25-34.

ABOUSSALAM, Z. S. & BECKER, R. T. (2007): New upper Givetian to basal Frasnian conodont faunas from the Tafilalt (Anti-Atlas, Southern Morocco). – Geological Quarterly, **51** (4): 345-374.

ABOUSSALAM, Z. S. & BECKER, R. T. (2011): The global Taghanic Biocrisis (Givetian) in the eastern Anti-Atlas, Morocco. – Palaeogeography, Palaeoclimatology, Palaeoecology, **304**: 136-164.

ABOUSSALAM, Z. S., BECKER, R. T. & EICHHOLT, S. (2012): Conodont dating of reefs and carbonate platforms in the Middle and Upper Devonian of the Moroccan Meseta. – Terra Nostra, **2012** (3): 27-28.

ABOUSSALAM, Z. S., BECKER, R. T., EICHHOLT, S. & EL HASSANI, A. (2013a): Conodont biostratigraphy and the timing of facies changes at Ain-as-Seffah (Oued Cherrat Zone, Moroccan Meseta). – Documents de l´Institut Scientifique, Rabat, **26**: 11-13.

ABOUSSALAM, Z. S., BECKER, R. T., EICHHOLT, S., EL HASSANI, A., BENFRIKA, M. EL. & EL KAMEL, F. (2013b): The precise timing of Devonian reef growth and extinctions in the Moroccan Meseta. – In: REITNER, J., YANG, Q, WANG, Y.-D. & REICH, M. (Eds.), Palaeobiology and Geobiology of Fossil Lagerstätten through Earth History, A joint Conference of the “Paläontologische Gesellschaft” and the “Palaeontological Society of China”, Göttingen, Germany, September 23-27, 2013, Abstract Volume: 13; Universitätsverlag Göttingen.

ABOUSSALAM, Z. S., BECKER, R. T. & BULTYNCK, P. (2015): Emsian (Lower Devonian) conodont stratigraphy and correlation of the Anti-Atlas (Southern Morocco). – Bulletin of Geosciences, **94** (4): 893-980.

ABOUSSALAM, Z. S., BECKER, R. T., EL HASSANI, A., EICHHOLT, S. & BAIDDER, L. (2017): Late Early Carboniferous conodonts from a supposed Middle Devonian reef limestone of the Marrakech region (Morocco). – Stratigraphy, **14** (1/4): 7-14.

ACOTTO, C., MARTÍNEZ POYATOS, D., AZOR, A., JABALOY, A., AZDIMOUSA, A., TAHIRI, A. & EL HADI, H. (2018): First U/Pb detrital zircon age populations from the Eastern Variscan Moroccan Meseta. – In: EGU General Assembly 2018. Geophysical Research Abstracts, **20**: 1 p.

ACOTTO, C., MARTÍNEZ POYATOS, D. J., AZOR, A. & JABALOY-SÁNCHEZ, A. (2019): Structural and geochronological constraints on the Early Variscan evolution of the Eastern Moroccan Meseta. – Geological Society of America, Abstracts with Programs, **51** (5), 1 p., doi: 10.1130/abs/2019AM-332308.

AGARD, J., MORIN, P. & TERMIER, H. (1955): Exquisse d´une histoire géologique de la région de Mrirt (Maroc central). – Notes et Mémoires du Service Géologique du Maroc, **12** (125): 15-28.

AGARD, J., BALCON, J.-M. & MORIN, P. (1958): Etude géologique et metallogenique de la region mineralisée du Jebel Aouam (Maroc central). – Notes et Mémoires du Service Géologique du Maroc, **132**: 1-127.

AGER, D. V., COSSEY, S. P. J., MULLIN, P. R. & WALLEY, C. D. (1976): Brachiopod ecology in mid-Palaeozoic sediments near Khenifra, Morocco. – Palaeogeography, Palaeoclimatology, Palaeoecology, **20**: 171-185.

ALBERTI, G. K. B. (1969): Trilobiten des jüngeren Siluriums sowie des Unter- und Mittel-Devons. I. Mit Beiträgen zur Silur-Devon-Stratigraphie einiger Gebiete Marokkos und Oberfrankens. – Abhandlungen der senckenbergischen naturforschenden Gesellschaft, **520**: 1-692.

ALLARY, A., ANDRIEUX, J., LAVENU, A. & RIBEYROLLES, M. (1972): Les nappes hercyniennes de la Meseta sud orientale (Maroc central). – Comptes Rendus de l´Academie des Sciences Paris, **274**: 2284-2287.

ÀLVARO, J. J., ARETZ, M., BOULVAIN, F., MUNNECKE, A., VACHARD, D. & VENNIN, E. (2007): Fabric transition from shell accumulations to reefs: an introduction with Palaeozoic examples. – In: ÀLVARO, J. J., ARETZ, M., BOULVAIN, F., MUNNECKE, A., VACHARD, D. & VENNIN, E. (Eds.), Palaeozoic Reefs and Bioaccumulations: Climatic and Evolutionary Controls. Geological Society, London, Special Publications, **275**: 1-16.

AMLER, M. R. W. & HERBIG, H.-G. (2006): Ostrand der Kohlenkalk-Plattform und Übergang in das Kulm-Becken im westlichsten Deutschland zwischen Aachen und Wuppertal. – Schriftenreihe der Deutschen Gesellschaft für Geowissenschaften, **41**: 441-477.

ARETZ, M. & HERBIG, H.-G. (2010): Corals from the Upper Viséan of the southern Azrou-Khenifra Basin (Carboniferous, Central Moroccan Meseta). – Palaeoworld, **19**: 294-305.

AVERBUCH, O., TRIBOVILLARD, N., DEVLEESCHOUWER, X., RIQUIER, L., MISTIAEN, B. & VAN VLIET-LANOE, B. (2005): Mountain building-enhanced continental weathering and organic carbon burial as major causes for climatic cooling at the Frasnian-Famennian boundary (c. 376 Ma)? – Terra Nova, **17**: 25-34.

BACHTADSE, V., VAN DER VOO, R. & HAELBICH, I. W. (1987): Paleozoic paleomagnetism of the western Gondwana. – Earth and Planetary Sciece Letters, **84**: 487-499.

BAHRAMI, A., KÖNIGSHOF, P., VAZIRI-MOGHADDAM, H., SHAKERI, B. & BOMNCHEVA, I. (2019): Conodont stratigraphy and conodont biofacies of the shallow-water Kuh-e-Bande-Abdol-Hossein section (Anarak, Central Iran). – Palaeodiversity and Palaeoenvironments, **99**: 477-494.

BAIDDER, L., RADDI, Y., TAHIRI, M. & MICHARD, A. (2008): Devonian extension of the Pan-African crust north of the West African craton, and its bearing on the Variscan foreland deformation: evidence from eastern Anti-Atlas (Morocco). – In: ENNIH, N. & LIÉGEOIS, J.-P. (Eds.), The Boundaries of the West Africxan Craton. Geological Society, London, Special Publications, **297**: 453-465.

BAIRD, G. C., BRETT, C. E., BECKER, R. T., ABOUSSALAM, Z. S., DESANTIS, M. & BARTHOLOMEW, A. J. (2009): Comparatitive stratigraphy of Eifelian successions in southern Morocco and the Appalachian Basin; implications for global events. – Palaeontoigraphica Americana, **63**: 193-194.

BALBUS, S. (2015): Devonian tides and some of their consequences. – Proceedings of the Royal Society, A, 11 pp.

BALINSKI, A. & BIERNAT, G. (2003): New observations on rhynchonellid brachiopod *Dzieduszyckia* from the Famennian of Morocco. – Acta Palaeontologica Polonica, **48** (3): 463-474.

BALTER, V., MARTIN, J. E., TACAIL, T., SUAN, G., RENAUD, S. & GIRARD, C. (2019): Calcium stable isotopes place Devonian conodonts as first level consumers. – Geochemical Perspectives Letters, **10**: 36-39, Supplement with 5 tabs., 3 figs, and references.

BAMOUMEN, H. AARAB, M. & SOULAIMANI, A. (2008): Evolution tectono-sédimentaire et magmatique des bassins viséen supérieur d´Azrou-Khénifra et des Jebilet orientales (Meseta marocaine). – Estudios Geológicos, **64** (2): 1-16.

BARHAM, M., MURRAY, J., SEVASTOPULO, G. D. & WILLIAMS, M. (2015): Conodonts of the genus *Lochriea* in Ireland and the recognition of the Viséan-Serpukhovian (Carboniferous) boundary. – Lethaia, **48** (2): 151-171.

BARBERO, L., JABALOY, A., GÓMEZ-ORTIS, D., PÉREZ-PEÑA, J. V., RODRÍGUEZ-PECES, M. J., TEJERO, R., ESTUPIÑÁN, J., AZDIMOUSA, A., VÁZQUEZ, M. & ASEBRIY, L. (2011): Evidence for surface uplift of the Atlas Mountains and the surrounding peripheral plateux: Combining apatite fission-track results and geomorphic indicators in the Western Moroccan Meseta (coastal Variscan Paleozoic basement). – Universidad Complutense, E-Prints, 15 pp., online at https://eprints.ucm.es/17114/1/1-s2.90.pdf; Madrid.

BEAUCHAMP, J. & IZART, A. (1987): Early Carboniferous basins of the Atlas-Meseta domain (Morocco): Sedimentary model and geodynamic evolution. – Geology, **15**: 797-800.

BECKER, R. T. (1992): Zur Kenntnis von Hemberg-Stufe und *Annulata*-Schiefer im Nordsauerland (Oberdevon, Rheinisches Schiefergebirge, GK 4611 Hohenlimburg). – Berliner geowissenschaftliche Abhandlungen, Reihe E, **3**: 3-41.

BECKER, R. T. (1993a): Stratigraphische Gliederung und Ammonoideen-Faunen im Nehdenium (Oberdevon II) von Europa und Nord-Afrika. – Courier Forschungsinstitut Senckenberg, **155**: 1-405, 26 pls.

BECKER, R. T. (1993b): Kellwasser Events (Upper Frasnian, Upper Devonian) in the Middle Atlas (Morocco) – implications for plate tectonics and anoxic event generation. – In: Global Boundary Events. An Interdisciplinary Conference, Kielce – Poland, September 27-29, 1993, Abstracts: 9.

BECKER, R. T. (1993c): Anoxia, eustatic changes, and Upper Devonian to lowermost Carboniferous global ammonoid diversity. – In: HOUSE, M. R. (Ed.), The Ammonoidea: Environment, Ecology, and Evolutionary Change. Systematics Association Special Volume, **47**: 115-163.

BECKER, R. T. (1994): Faunal and sedimentary succession around the Frasnian-Famennian boundary in the eastern Moroccan Meseta. – 64. Jahrestagung der Paläontologischen Gesellschaft, 26-30. September 1994, Budapest, Vortrags- und Posterkurzfassungen: 44.

BECKER, R. T. (2013): Membership News: The Münster Devonian Team. – SDS Newsletter, **28**: 59-63

BECKER, R. T. (2015): Membership News: TM R. Thomas BECKER and the Münster Group. – SDS Newsletter, **30**: 50-55.

BECKER, R. T. & ABOUSSALAM, Z. S. (2004): The Frasne Event – a phased 2nd order global crisis and extinction period around the Middle-Upper Devonian boundary. – In: Devonian neritic-pelagic correlation and events, International Meeting on Stratigraphy, Rabat, Morocco 1-10, 2004, IUGS

Subcommission on Devonian Stratigraphy and Institute Scientifique, University Mohammed V – Agdal, Rabat, Morocco, Abstracts: 8-9.

BECKER, R. T. & ABOUSSALAM, Z. S. (2013a): The global Chotec Event at Jebel Amelane (western Tafilalt Platform) – preliminary data. – In: BECKER, R. T., EL HASSANI, A. & TAHIRI, A. (Eds.), International Field Symposium "The Devonian and Lower Carboniferous of northern Gondwana", 22nd to 29th March 2013, Field Guidebook. Document de l´Institute Scientifique, Rabat, **27**: 129-133.

BECKER, R. T. & ABOUSSALAM, Z. S. (2013b): Middle Givetian – middle Frasnian event stratigraphy at Mdoura-East (western Tafilalt). - In: BECKER, R. T., EL HASSANI, A. & TAHIRI, A. (Eds.), International Field Symposium "The Devonian and Lower Carboniferous of northern Gondwana", 22nd to 29th March 2013, Field Guidebook. Document de l´Institute Scientifique, Rabat, **27**: 143-150.

BECKER, R. T. & ABOUSSALAM, Z. S. (2014): Devonian global events in the Moroccan Meseta – an update. – In: 4th International Palaeontological Congress, "The history of life: A view from the Southern Hemisphere", Septemner 28 – October 3, 2014, Mendoza, Argentina, (digital) Abstract Volume: 1 p.

BECKER, R. T. & ABOUSSALAM, Z. S. (2019): Impact of Emsian/Eifelian global events on faunas and biofacies in the Moroccan Meseta. – In: Paleo & Life, Abstracts of the 90th Annual Meeting of the Paläontologische Gesellschaft, Munich 2019, 15-18 September 2019: 20; Bayrische Staatssammlung für Geologie und Paläontologie, München.

BECKER, R. T. & HOUSE, M. R. (1993): New early Upper Devonian (Frasnian) goniatite genera and the evolution of the "Gephuroceratáceae". – Berliner geowissenschaftliche Abhandlungen, Reihe E, **9**: 111-133.

BECKER, R. T. & HOUSE, M. R. (1994a): International Devonian goniatite zonation, Emsian to Givetian, with new records from Morocco. – Courier Forschungsinstitut Senckenberg, **169**: 79-135.

BECKER, R. T. & HOUSE, M. R. (1994b): Kellwasser Events and goniatite successions in the Devonian of the Montagne Noire with comments on possible causations. – Courier Forschungsinstitut Senckenberg, **169**: 45-77.

BECKER, R. T. & HOUSE, M. R. (1998): Prospects for an international substage subdivision of the Frasnian. – SDS Newsletter, **15**: 17-22.

BECKER, R. T. & HOUSE, M. R. (2000a): Sedimentary and faunal successions of the allochthonous Upper Devonian at Gara d´Mrirt (Eastern Moroccan Meseta). – Notes et Mémoires du Service Géologique du Maroc, **399**: 109-114.

BECKER, R. T. & HOUSE, M. R. (2000b): Devonian ammonoid zones and their correlation with established series and stage boundaries. – Courier Forschungsinstitut Senckenberg, **220**: 113-151.

BECKER, R. T. & HOUSE, M. R. (2009): Devonian ammonoid stratigraphy of the Canning Basin. – Geological Survey of Western Australia, Bulletin, **145**: 415-438.

BECKER, R. T., FEIST, R., FLAJS, G., HOUSE, M. R. & KLAPPER, G. (1989): Frasnian-Famennian extinction events in the Devonian at Coumiac, southern France. – Comptes Rendus de l`Academie des Sciences Paris, Série II, **309**: 259-266.

BECKER, R. T., HOUSE, M. R. & KIRCHGASSER, W. T. (1993): Devonian goniatite biostratigraphy and timing of facies movements in the Frasnian of the Canning Basin, Western Australia. – In: HAILWOOD, E. A. & KIDD, R. B. (Eds.), High Resolution Stratigraphy. Geological Society Special Publication, **70**: 293-321.

BECKER, R. T., HOUSE, M. R. & MARSHALL, J. E. (1997): The allochthonous Upper Devonian at Mrirt (eastern Moroccan Meseta) – North African continuation of a Montagne Noire carbonate platform? – In: FEIST, R. (Ed.), First International Conference on North Gondwanan Mid-Palaeozoic Biodynamics, IGCP Project 421, Vienna, 17-21 Septembre 1997, Meeting Program and Abstracts: 7-8.

BECKER, R. T., HOUSE, M. R., MENNER, V. V. & OVNATANOVA, N. (2000): Revision of ammonoid biostratigraphy in the Frasnian (Upper Devonian) of the Southern Timan (Northeast Russian Platform). – Acta Geologica Polonica, **50** (1): 67-97.

BECKER, R. T., HOUSE, M. R., BOCKWINKEL, J., EBBIGHAUSEN, V. & ABOUSSALAM, Z. S. (2002): Famennian ammonoid zones of the eastern Anti-Atlas (southern Morocco). – Münstersche Forschungen zur Geologie und Paläontologie, **93**: 159-205.

BECKER, R. T., BOCKWINKEL, J., EBBIGHAUSEN, V., ABOUSSALAM, Z. S., EL HASSANI, A. & NÜBEL, H. (2004): Lower and Middle Devonian stratigraphy and faunas at Bou Tserfine near Assa (Dra Valley, SW Morocco). – In: EL HASSANI, A. (Ed.), Devonian neritic-pelagic correlation and events in the Dra Valley (western Anti-Atlas, Morocco). International Meeting on Stratigraphy, Rabat, March 1-10, 2004. Dopcuments de l´Institute Scientifique, Rabat, **19**: 99-110.

BECKER, R. T., GRADSTEIN, F. M. & HAMMER, O. (2012): The Devonian Period. – In: GRADSTEIN, F. M., OGG, J. G., SCHMITZ, M. & OGG, G. (Eds.), The Geologic Time Scale 2012, Volume **2**: 559-601; Elsevier, Amsterdam, Boston etc.

BECKER, R. T., EL HASSANI, A. & TAHIRI, A. (Eds., 2013): International Field Symposium „The Devonian and Lower Carboniferous of northern Gondwana“, Field Guidebook. – Document de l´Institut Scientifique, Rabat, **27**: 1-150.

BECKER, R. T., ABOUSSALAM, Z. S., EL HASSANI, A., HARTENFELS, S. & BAIDDER, L. (2015): The timing of Eovariscan block faulting, reworking and re-deposition in the Moroccan Meseta. – Strata, Série 1, **16**: 14-15.

BECKER, R. T., ABOUSSALAM, Z. S., STICHLING, S., MAY, A. & EICHHOLT, S. (2016a): The Givetian-Frasnian Hönne Valley Reef Complex (northern Sauerland) – an outline of stratigraphy and facies development. – Münstersche Forschungen zur Geologie und Paläontologie, **108**: 126-140.

BECKER, R. T., HARTENFELS, S., HELLING, S. & SCHREIBER, G. (2016b): The „Nehden Goniatite Shale“ (lower Famennian, Brilon Reef Complex, NE Rhenish Massif). – Münstersche Forschungen zur Geologie und Paläontologie, **108**: 179-195.

BECKER, R. T., PIECHA, M., GEREKE, M. & SPELLBRINK, K. (2016c): The Frasnian/Famennian boundary in shelf basin facies north of Diemelsee-Adorf. – Münstersche Forschungen zur Geologie und Paläontologie, **108**: 220-231.

BECKER, R. T., ABOUSSALAM, Z. S., EL HASSANI, A. & HARTENFELS, S. (2016d): The distribution of Devonian pelagic facies in the western Moroccan Meseta as a key for palaeogeographic reconstructions in the Prototethys. – In: International Geoscience Programme Project 591 – Closing Meeting “The Early to Mid Palaeozoic Revolution”, Ghent University, Ghent, Belgium, 6-9 July 2016, Abstracts: 24-25.

BECKER, R. T., EL HASSANI, A., ABOUSSALAM, Z. S., HARTENFELS, S. & BAIDDER, L. (2018a): The Devonian and Lower Carboniferous of the eastern Anti-Atlas: introduction to a „cephalopod paradise“. – Münstersche Forschungen zur Geologie und Paläontologie, **110**: 145-157.

BECKER, R. T., ABOUSSALAM, Z. S., HARTENFELS, S., EL HASSANI, A. & BAIDDER, L. (2018b): Bou Tchrafine – central Tafilalt reference section for Devonian stratigraphy and cephalopod succession. – Münstersche Forschungen zur Geologie und Paläiontologie, **110**: 158-187.

BECKER, R. T., ABOUSSALAM, Z. S. & HARTENFELS, S. (2018): The Frasnian-Famennian boundary mass extinction – widespread seismic events, the timing of climatic pulses, „pelagic death zones“, and opportunistic survival. – In: The Fossil Week, 5th International Palaeontological Congress, July 9th to 13th, 2018, Abstract Book: 107; Paris.

BECKER, R. T., MARSHALL, J. E. A. & DA SILVA, A.-C. (2020 in press): Devonian. – In: GRADSTEIN, F. et al. (Eds.), The Geological Time scale 2020; Elsevier (Amsterdam).

BELKA, Z., KAUFMANN, B. & BULTYNCK, P. (1987): Conodont-based quantitative biostratigraphy for the Eifelian of the eastern Anti-Atlas. – Geological Society of America, Bulletin, **109** (6): 643-651.

BENFRIKA, M. EL (1999): Some upper Silurian – middle Devonian conodonts from the northern part of Western Meseta of Morocco: systematic and palaeogeographical relationships. – Bolletino della Società Paleontologica Italiana, **37** (2/3): 311-319.

BENFRIKA, M. EL & BULTYNCK, P. (2001): Lower to Middle Devonian conodonts from Oued Cherrat – North-Western Meseta (Morocco). – In: JANSEN, U., KÖNIGSHOF, P., PLODOWSKI, G. & SCHINDLER, E. (Eds.), 15th International Senckenberg Conference, Mid-Palaeozoic Bio- and Geodynamics – The North Gondwana-Laurussia Interaction, May 11-121, 2001, Frankfurt a. M., Abstracts: 13; Forschungsinstitut Senckenberg, Frankfurt a. M.

BENFRIKA, M. EL & BULTYNCK, P. (2003): Lower to Middle Devonian conodonts from the Oued Cherrat area and its southern extension (North-Western Meseta, Morocco). – Courier Forschungsinstitut Senckenberg, **242**: 209-215.

BENFRIKA, M. El, BULTYNCK, P. & EL HASSANI, A. (2007): Upper Silurian to Middle Devonian conodont faunas from the Rabat-Tiflet area (northwestern Moroccan Meseta). – Geological Quarterly, **51** (4): 393-406.

BENSAID, M. (1979): L´Ordovicien supérieur, le Silurien et le Dévonien dans l´Est du Maroc Central. – Mines, Géologie et Energie, Rabat, **46**: 83-86.

BERKHLI, M. (1999): Sédimentologie, biostratigraphie et stratigraphie séquentielle du NE de la Mèseta occidentale marocaine le Carbonifère inférieur (Viséen-Serpukhovien). – Thèse État, Université Moulay Ismail de Meknes, 290 pp.

BERKHLI, M., VACHARD, D., PAICHELER, J.-C. & TAHIRI, A. (2000): Modèle sédimentaire et évolution géodynamique du Nord-Est de la Méseta occidentale marocaine au cours du Carbonifère inférieur. – Comptes Rendus de l´Academie des Sciences Paris, Sciences de la Terre et des planètes, **331**: 251-256.

BERKYOVÁ, S. (2009): Lower-Middle Devonian (upper Emsian-Eifelian, *serotinus-kockelianus* zones) conodont faunas from the Prague Basin, the Czech Republic. – Bulletin of Geosciences, **84** (4): 667-686.

BEUN, N., HUVELIN, P., BRICE, D., BULTYNCK, P., DESTOMBES, J., MERGL, M. & MORZADEC, P. (1992): Le Paléozoique de Khemis-n´Ga:

discordance du Silurien supérieur sur l´Arenig (region de Safi, Maroc). – Annales de la Société Géologique du Nord, 2éme Série, **1**: 171-177.

BIERNAT, G. (1967): New data on the genus *Dzieduszyckia* SIEMIRADZKI, 1909 (Brachiopoda). – Acta Palaeontologica Polonica, **12** (2): 133-155, pls. I-II.

BLIECK, A., CLEMENT, G., BLOM, H., LELIEVRE, H., LUKSEVICZ, E., STREEL, M., THOREZ, J. & YOUNG, G. C. (2007): The biostratigraphical and palaeogeographical framework of the earliest diversification of tetrapods (Devonian). – In: BECKER, R. T. & KIRCHGASSER, W. T. (Eds.), Devonian Events and Correlations. Geological Society, London, Special Publications, **278**: 219-235.

BOCKWINKEL, J., BECKER, R. T. & EBBIGHAUSEN, V. (2008): Upper Givetian ammonoids from Dar Kaoua (Tafilalt, SE Anti-Atlas, Morocco). – Berliner paläobiologische Abhandlungen, **10**: 61-128.

BOCKWINKEL, J., BECKER, R. T. & EBBIGHAUSEN, J. (2013): Late Givetian ammonoids from Hassi Nebech (Tafilalt Basin, Anti-Atlas, southern Morocco). – Fossil Record, **16** (1): 5-65 + online supplement, 58 pp.

BOCKWINKEL, J., BECKER, R. T. & ABOUSSALAM, Z. S. (2017): Ammonoids from the late Givetian *Tazouites* Bed of Ouidane Chebbi (eastern Tafilalt, SE Morocco). – Neues Jahrbuch für Geologie und Paläontologie, Abhandlungen, **284** (3): 307-354.

BOGOSLOVSKIY, B. I. (1969): Devonskie Ammonoidei, I. Agoniatity. – Trudy Paleontologicheskiy Institut, **124**: 1-341, 29 pls.

BOHRMANN, G. & FISCHER, G. (1985): Stratigraphie und Fazies des Paläozoikums nördlich von Azrou. Ein Beitrag zur Geologie der nordöstlichen marokkanischen Meseta. – Geologica et Palaeontologica, **19**: 15-37.

BOLLELI, E., DESTOMBES, J. & KARPOFF, R. (1953): Découverte du Tournaisien à goniatites dans la Meseta côtière marocaine. – Comptes Rendus hebdomadaires des Séances de l`Academie des Sciences, **1953**: 1906-908.

BOUABDELLI, M. (1989): Tectonique et sédimentation dans un bassin orogénique: Le sillon viséen d´Azrou-Khénifra (Est du massif hercynien central du Maroc). – Unpublished Thesis, University Straßbourg, 256 pp.

BOUABDELLI, M. (1994): Tectonique de l´Est du Massif hercynien central (zone d´Azrou-Khénifra). – Bulletin de l`Institute Scientifique, Rabat, **18**: 145-168.

BOUABDELLI, M., FAIK, F. & HABIBI, M. (1989): Tectonique en blocs basculés et glissement contemporains dans le Dévonien moyen et supérieur du Jebel Bouechot: un nouvel élément pour la comprehension de l´évolution ante-viséenne de l´Est du Maroc central. – Comptes Rendus de l´Academie des Sciences Paris, **308**: 761-766.

BRETT, C. E., ZAMBITO, J. J. IV, BAIRD, G. C., ABOUSSALAM, Z. S., BECKER, R. T. & BARTHOLOMEW, A. J. (2018): Litho-, bio-, and sequence stratigraphy of the Boyle-Portwood Succession (Middle Devonian, Central Kentucky, USA). – Palaeodiversity and Palaeoenvironments, **98** (2): 331-368.

BRICE, D., CHARRIÈRE, A., DROT, J. & REGNAULT, S. (1984): Mise en evidence, par des faunes de Brachiopodes, de l´extension des formations dévoniennes dans la boutonnière d´Immouzer du Kandar (Sud de Fès, Maroc). - Annales de la Sociètè Géologique du Nord, **103**: 445-458.

BUDIL, P., HÖRBINGER, F. & MENCL, R. (2009): Lower Devonian dalmanitid trilobites of the Prague Basin (Czech Republic). – Earth and Environmental Science Transactions of the Royal Society of Edinburgh, **99**: 61-100.

BUGGISCH, W. (1972): Zur Geologie und Geochemie der Kellwasserkalke und ihrer begleitenden Sedimente (Unteres Oberdevon). – Abhandlungen des Hessischen Landesamtes für Bodenforschung, **62**: 1-68, 13 pls.

BUGGISCH, W. & JOACHIMSKI, M. M., 2006. Carbon isotope stratigraphy of the Devonian of Central and Southern Europe. - Palaeogeography. Palaeoclimatology, Palaeoecology, **240**: 68-88.

BULTYNCK, P. (1985): Lower Devonian (Emsian) – Middle Devonian (Eifelian and lowermost Givetian) conodont successions from the Ma´der and the Tafilalt, southern Morocco. – Courier Forschungsinstitut Senckenberg, **75**: 261-286.

BULTYNCK, P. (1986): Accuracy and reliability of conodont zones: the *Polygnathus asymmetricus* "zone" and the Givetian-Frasnian boundary. - Bulletin de l´Institute Royal des Sciences Naturelles de Belgique, Sciences de la Terre, **57**: 149-181.

BULTYNCK, P. (1987): Pelagic and neritic conodont successions from the Givetian of pre-Sahara Morocco and the Ardennes. – Bulletin de l´Institute Royal des Sciences Naturelles de Belgique, Sciences de la Terre, **57**: 149-181.

BULTYNCK, P. (2005): Proposal for a threefold subdivision of the Givetian. – SDS Newsletter, **21**: 20-22.

BULTYNCK, P. & HOLLARD, H. (1980): Distribution comparée de Conodontes et Goniatites dévoniens des plaines du Dra, du Ma´der et du Tafilalt (Maroc). – Aardkundige Mededelingen, **1**: 1-73.

BULTYNCK, P. & SARMIENTO, G. N. (2003): Reworked Ordovician and autochthonous Siluro-Devonian conodonts from Khemis-n`Ga (Moroccan Meseta) – Depositional, environmental, and palaeogeographic implications. – Courier Forschungsinstitut Senckenberg, **242**: 257-283.

BURCHETTE, T. P. (1981): European Devonian reefs: a review of current concepts and models. – SEPM Special Publication, **30**: 85-142.

BURKHARD, M., CARITG, S., HELG, U., ROBERT-CHARRUE, C. & SOULAIMANI, A. (2006): Tectonics of the Anti-Atlas of Morocco. – Comptes Rendus Geoscience, **338**: 11-24.

CABRERA-PORRAS, Á., RODRÍGUEZ-CAÑERO, R. & MARTÍN-ALGARRA, A. (2019): Primeros conodontos del Frasniense en el Complejo Maláguide de Granada (Cordillera Bética). – Spanish Journal of Palaeontology, **34** (2): 163-186.

CARLS, P., SLAVÍK, L. & VALENZUELA-RÍOS, J. I. (2008): Comments on the GSSP for the basal Emsian stage boundary: the need for its redefinition. – Bulletin of Geosciences, **83** (4): 383-390.

CARLS, P., SLAVÍK, L. & VALENZUELA-RÍOS, J. I. (2009): Request and comments concerning the GSSP for the basal Emsian stage boundary. – SDS Newsletter, **24**: 20-27.

CASIER, J.-G., LEHMAMI, M. & PREAT, A. (1997): Ostracodes et sédimentologie du Givétien à Ain Khira (Meseta nord-occidentale du Maroc). - Revue de Paléobiologie, **16** (1): 151-167.

CATTANEO, G., TAHIRI, A., ZAHRAOUI, M. & VACHASRD, D. (1993): La sedimentation récifale du Givétien dans la Meswta Marocaine nord-occidentale. - Comptes Rendus de l´Academie des Sciences Paris, Série II, **1993**: 73-80.

CHAKIRI, S. (2002): Sédimentologie et géodynamique du Maroc Central Hercynien pendant le Dévonien. – Unpublished Ph. D. Thesis, Ibn Tofail University, Khenitra.

CHAKIRI, S. & TAHIRI, A. (2000): La formation chaotique famenno-tournaisiene du Grou: témoin de la bordure orientale du bassin de Sidi Bettache (Meseta marocain). – Bulletin de l´Institute Scientifique, Rabat, **22**: 9-15

CHALOUAN, A. (1981): Stratigraphie et structure du Paléozoique de l´Oued Cherrat: un segment du couloir de cisaillement de Meseta occidentale (Maroc). - Notes et Mémoires du Service géologique du Maroc, **42** (308): 33-100, 4 pls.

CHALOUAN, A. & HOLLARD, H. (1979). Stratigraphie des terrains du Paléozoique moyen de l´oued Cherrat (Meseta occidentale marocaine). - Comptes Rendus de l´Academie des Sciences Paris, Série D, **288**: 199-202.

CHARLOT, R., RHALIB, M. & TISSERANT, D. (1973): Etude géochronologique préliminaire des granites de la region de Rabat-Tiflet (Maroc occidental). – Noters et Mémoires du Service Géologique Maroc, **249**: 55-58.

CHARRIÈRE, A. (1989): Mise en évidence de différents ensembles lithostratigraphiques et structuraux dans le socle du Moyen Atlas tabulaire (Msroc). - Notes et Mémoires du Service géologique du Maroc, **335**: 37-48.

CHARRIÈRE, A. (1990): Héritage hercynien et évolution géodynamique alpine d´une chaîne intracontinentale: le Moyen-Atlas au SE de Fès (Maroc). – Unpublished Ph. D. Thesis, University Toulouse, 589 pp.

CHARRIÈRE, A. & RÉGNAULT, S. (1983): Stratigraphie du Dévonien de la boutonnière d´Immouzer-du-Kandar (Sud de Fès). Conséquences paléogéographiques. – Symposium P.I.G.C. 27, Rabat.

CHARRIÈRE, A. & RÉGNAULT, S. (1989): Stratigraphie du Dévonien de la boutonnière d´Immouzer du Kandar (Sud de Fès); conséquences paléogeographiques. - Notes et Mémoires du Service géologique du Maroc, **335**: 25-35.

CHARRIÈRE, A., CYGAN, C. & REGNAULT, S. (1984): Un exemple d´évolution de facies carbonaté dans le Dévonien marocain. – 10è Réunion, Annales de l`Sciences de la Terre, Bordeaux: 133; Société Géologique du France.

CHATTERTON, B. F. (1974): Middle Devonian Conodonts from the Harrogate Formation, Southeastern British Columbia. – Canadian Journal of Earth Sciences, **11**: 1461-1484.

CHLUPÁČ, I. & KUKAL, Z. (1986): Reflection of possible global Devonian events in the Barrandian area, C.S.S.R. – Lecture Notes in Earth Sciences, **8**: 171-179.

CHLUPÁČ, I. & KUKAL, Z. (1988): Possible global events and the stratigraphy of the Palaeozoic of the Barrandian (Cambrian-Middle Devonian), Czechoslowakia). – Sborník geologických věd, Geologie, **43**: 83-146.

CHLUPÁČ, I. & LUKEŠ, P. (1999): Pragian/Zlíchovian and Zlíchovian/Dalejan boundary sections in the Lower Devonian of the Barrandian area, Czech Reopublic. – Newsletters on Stratigraphy, **37** (1/2): 75-100.

COCKS, L. R. M. & TORSVIK, T. H. (2002): Earth geography from 500 to 400 million years ago: a faunal and palaeomagnetic review. – Journal of the Geological Society London, **159**: 631-644.

COGNEY. G. (1967): Sur le Dévonien de la région d´Oulmès (Maroc central). – Comptes Rendus

Somnaires et Séances, Société Géologique du France, **7é série** (9): 283-284.

CORNÉE, J.-J. (1989): Le Haut Atlas Occidental Paleozoique: un reflet de l´histoire hercynienne du Maroc occidental. – Unpublished Ph.D. Thesis, Université de Droit, d´Economique et des Sciences, d`Aix-Marseille, 335 pp.

CORNÉE, J. J., RACHEBEUF, P. R., TAYEBI, M. & WILLEFERT, S. (1990): Les Formations dévoniennes de la nappe des Aït Tounart (partie occodentale du massif ancient du Haut Atlas, Maroc hercynien). – Géologie Méditerrannéenne, **17** (3/4): 331-342.

CORRADINI, C. & CORRIGA, M. G. (2012): A Přídolí-Lochkovian conodont zonation in Sardinia and the Carnic Alps: implications for a global zonation scheme. – Bulletin of Geosciences, **87** (4): 635-650.

CORRIGA, M. G., CORRADINI, C., HAUDE; R. & WALLISER, O. H. (2013): Conodont and crinoid stratigraphy of the upper Silurian and Lower Devonian scyphocrinoid beds of the Tafilalt, southeastern Morocco. – GFF, **2013**: 1-5.

COZAR, P., VACHARD, D., IZART, A. & CORONADO, I. (2019 online): Survival of early Viséan foraminifers in the Western Meseta of Morocco. – Palaeoworld, 33 pp., doi.org/10.1016/j.palwor.2019.06.001.

CRONIER, C., FEIST, R. & AUFFRAY, J.-C. (2004): Variation in the eye of *Acuticryphops* (Phacopina, Trilobita) and its evolutionary significance: a biometric and morphometric approach. – Paleobiology, **30** (3): 471-481.

CYGAN, C., CHARRIÈRE, A. & REGNAULT, S. (1990): Datation par Conodontes du Dévonien (Emsien – Frasnian basal) dans le substratum du Moyen-Atlas au Sud de Fés (Maroc); Implications paléogéographiques. - Géologie Méditerranéennne, **17** (3/4): 321-330.

DALZIEL, I. W. D., DALLA SALIDA, L. H. & GAHAGAN, L. M. (1994): Paleozoic Laurentia-Gondwana interaction and the origin of the Appalachian-Andean mountain system. – Geological Society of America, Bulletin, **106**: 243-252.

DAVYDOV, V. I., KORN, D., SCHMITZ, M. D., GRADSTEIN, F. M. & HAMMER, O. (2012): The Carboniferous Period. – In: GRADSTEIN, F. M., OGG, J. G., SCHMITZ, M. & OGG, G. (Eds.), The Geologic Time Scale 2012, Volume **2**: 603-651; Elsevier, Amsterdam, Boston etc.

DE BAETS, K., KLUG, C. & PLUSQUELLEC, Y. (2010): Zlíchovian faunas with early ammonoids from Morocco and their use for the correlation of the eastern Anti-Atlas and the western Dra Valley. – Bulletin of Geosciences, **85** (2): 317-352.

DE KONING, G. (1957): Geologe des Ida ou Zal (Maroc) – Stratigraphie, Petrographie et Tectonique de la partie SW du Bloc Occidental du Massif Ancien du Haut Atlas. – Leidse Geologische Mededelingen, **23**: 1-209.

DELCHINI, S., LAHFID, A., LACROIX, B., BAUDIN, T., HOEPFFNER, C., GUERROT, C., LACH, P., SADDIQI, O. & RAMBOZ, C. (2018): The Geological Evolution of the Variscan Jebilet Massif, Morocco, Inferred From New Structural and Geochronological Analyses. – Tectonics, **37**: 1-24.

DENCKMANN, A. (1905): Über das Devon und Carbon des Sauerlandes. – Jahrbuch der Preußischen Geologischen Landesanstalt, **23**: 534-596.

DESTOMBES, J. & JEANETTE, A. (1966): Mémoire explicative de la carte géotechnique de la Meseta Cotière à l´Est de Casablanca au 1/50 000. – Notes et Mémoires du Service Géologique du Maroc, **180bis**: 1-104.

DOPIERALSKA, J. (2003): Neodymium isotopic composition of conodonts as a palaeoceanographic proxy in the Variscan oceanic system. – Unpublished Ph. Thesis, Justus-Liebig-University Gießen, 111 pp.

DOPIERALSKA, J. (2009): Reconstructing seawater circulation on the Moroccan shelf of Gondwana during the Late Devonian: Evidence from Nd isotope composition of conodonts. – Geochemistry, Geophysics, Geosystems, **10** (3): 1-13, doi:10.1029/2008GC002247.

DOPIERALSKA, J., BELKA, Z. & WALCZAK, A. (2015 online): Nd isotope composition of conodonts: An accurate proxy of sea-level fluctuations. – Gondwana Research, **34**: 284-295.

DREESEN, R. & THOREZ, J. (1994): Parautochthnous – allochthonous carbonates and conodont mixing in the Late Famennian (Uppermost Devonian) Condroz Sandstones of Belgium. – Courier Forschungsinstitut Senckenberg, **168**: 159-182.

EBBIGHAUSEN, V., BECKER, R. T. & BOCKWINKEL, J. (2000): Morphometric Analyses and Taxonomy of Oxyconic Goniatites (Paratornoceratinae n. subfam.) from the Early Famennian of the Tafilalt (Anti-Atlas, Morocco). – Abhandlungen der Geologischen Bundesanstalt, 57: 167-180.

ECHARFAOUI, H., HAFID, M. & Aït Salem, A. (2002): Structure sismique du socle paléozoique du basin des Doukkala, Môle côtier, Maroc occidental. Indication en faveur de l´existence d´une phase éo-varisque. – Comptes Rendus Geoscience, **334**: 13-20.

EICHHOLT, S. & BECKER, R. T. (2016): Middle Devonian reef facies and development in the Oued Cherrat Zone and adjacent regions (Moroccan Meseta). - Facies, **62** (7): 29 pp.

EICHHOLT, S., BECKER, R. T. & STICHLING, S. (2013): Microfacies and Devonian reef development in the Oued Cherrat Zone (Aïn Khira South and Aïn-as-

Seffah), Moroccan Meseta. – Documents de l´Institut Scientifique, Rabat, **26**: 37-39.

EL HASSANI, A. (1990): La Zone de Rabat-Tiflet: Bordure nord de la chaîne calédono-hercynienne du Maroc. – Bulletin de l´Institute Scientifique, **15**: 134 pp.

EL HASSANI, A. (1994): Tectonique de la Meseta nord occidentale. – Bulletin de l´Institute Scientifique, **18**: 107-124.

EL HASSANI, A. (Ed., 2004): Devonian neritic-pelagic correlation and events in the Dra Valley (western Anti-Atlas, Morocco). International Meeting on Stratigraphy, Rabat, March 1-10, 2004. – Documents de l´Institute Scientifique, **19**: 1-100.

EL HASSANI, A. & BENFRIKA, M. EL (1995): Biostratigraphy and correlations of the Devonian of the Morfoccan Meseta: a synopsis. – Bulletin de l`Institut Scientifique, Rabat, **19**: 29-44.

EL HASSANI, A. & BENFRIKA, M. EL (2000): The Devonian of the Moroccan Meseta: biostratigraphy and correlations. – Courier Forschungsinstitut Senckenberg, **225**: 195-209.

EL HASSANI, A. & EL KAMEL, F. (2000): Tectonic control of Devonian reef building in Mechra ben Aboou area (northern Rehamna, Morocco). – In: TAHIRI, A. & EL HASSANI, A. (Eds.), Proceedings of the Subcommission on Devonian Stratigraphy (SDS) – IGCP 421 Morocco Meeting. Travaux de l. Institute Scientifique, Rabat, **20**: 25-30.

EL HASSANI, A. & TAHIRI, A. (Eds., 1994): Géologie du Maroc central et de la Meseta orientale. – Bulletin de l´Institute Scientifique, **18**: 1-214.

EL HASSANI, A. & TAHIRI, A. (Eds., 1999): SDS-IGCP 421 Morocco Meeting, April 24th – May 1st 1999, Excursion Guidebook, Part I: Tafilalt and Maider (eastern Anti-Atlas). – 107 pp., Institute Scientifique, Rabat (see also Notes et Mémoires du Service Géologique du Maroc, **399**, 2000).

EL HASSANI, A. & TAHIRI, A. (2000): The Eastern part of Central Morocco (Western Meseta). - Notes et Mémoirs du Service géologique Maroc, **399**: 89-92.

EL HASSANI, A., DESTOMBES, J. & WILLEFERT, S. (1988): Le problème de l´Arenig-Llanvirn (Ordovicien), la discordance calédonienne et la preparation de l´orogenèse hercynienne dans la region de Rabat-Tiflet (Maroc occidental). – Bulletin de l´Institute Scientifique, Rabat, **12**: 27-45.

EL HASSANI, A., TAHIRI, A. & WALLISER O. H. (2003). The Variscan Crust between Gondwana and Laurasia. - Courier Forschungsinstitut Senckenberg, **242**, pp: 81-87.

EL HASSANI, A., ABOUSSALAM, Z. S., BECKER, R. T., EL WARTITI, M. & EL HASSANI, F. (2017): Patrimoine géologique marocain et développement durable: l´exemple du Dévonien du Tafilalt, Anti-Atlas oriental. – Géologues, Revue Officielle de la Société Géologique de France, **194**: 112-117.

EL KAMEL, F. (2004): Études géologiques du Paléozoique de Mechra Ben Abbou et d´Oulad Abbou, Meseta occidentale, Maroc. – Notes et Mémoires du Service Géologique, **462**: 1-187.

EL KAMEL, F., EL HASSANI, A. & DAFIR, J. E. (1992): Présence d´une tectonique synsédimentaire dans le Dévonien inférieur des Rehamna septentrionaux (Meseta marocaine occidentale). – Bulletin de l`Institute Scientifique, Rabat, 16: 37-43.

ERNST, A. & RODRIGUEZ, S. (2010): Broyozoan fauna from the oolithic limestone from Pajarejos, SW Spain. – Revista Española de Paleontologia, **25** (2): 83-88.

FADLI, D. (1990): Evolution sédimentaire et structural des massifs de Mdakra et du Khatouat; deux segments hercyniens de la Meseta marocaine nord-occidentale. - Unpublishhed Ph.D. Thesis, University Rabat, 272 pp.; Rabat.

FADLI, D. (1994a): Le Fameno-Tournaisian. – Bulletin de l´Institut Scientifique, Rabat, **18**: 57-70.

FADLI, D. (1994b): Le Viséen. - Bulletin de l´Institut Scientifique, Rabat, **18**: 71-83.

FADLI, D., BOUABDELLI, M., CAILLEUX, Y., EL HASSANI, A., EL WARTITI, M;, HOEPFFNER, CH., KHARBOUCH, F., TAHIRI, A. & ZAHRAOUI, M. (2008): Hercynian geological map of Central Morocco. Presented at IGC-Oslo-2008.

FAIK, F. (1988): Le Paléozoique de la région de Mrirt (Est du Maroc central). Evolution stratigraphique et structurale. – Unpublished Thesis of the 3rd Cycle, University P. SABATIER, Tolouse, 233 pp.

FAIRON-DEMARET, M. & REGNAULT, S. (1990): Macroflores dévoniennes dans le Nord du Maroc (Boutonnière d´Immouzer-du-Kandar, Sud de Fés). Etude Paléobotanique – Implications stratigraphiques et paléogéographiques. – Annales de la Société géologiques de Belgique, **109**: 499-513.

FEDOROWSKI, J. (1973): Rugose corals Polycoelaceae and Tachylasmatina subord. n. from Dalnia in the Holy Cross Mts. - Acta Geologica Polonica, **23** (1): 89-133, 6 pls.

FEIST, R. (1985): Devonian Stratigraphy of the Southeastern Montagne Noire (France). – Courier Forschungsinstitut Senckenberg, **75**: 331-352.

FEIST, R. (2002): Trilobites from the latest Frasnian Kellwasser crisis in North Africa (Mrirt, Central Moroccan Meseta). – Acta Palaeontologica Polonica, **47** (2): 203-210.

FEIST, R. (2003): Biostratigraphy of Devonian tropidocoryphid trilobites from the Montagne Noire

(southern France). – Bulletin of Geosciences, **78** (4): 431-446.

FEIST, R. (2019): Post-Kellwasser event recovery and diversification of phacopid trilobites in the early Famennian (Late Devonian). – Bulletin of Geosciences, **94** (1): 1-22.

FERONI, A., ELLERO, A., MALUSÀ, M. G., MUSUMECI, G., OTTRIA, G., POLINO, R. & LEONI, L. (2010): Transpressional tectonics and nappe stacking along the Southern Variscan Front of Morocco. – Internationa Journal of Earth Sciences, **99**: 1111-1122.

FRANCOIS, J.-M., REGNAULT, S. & CHEILLETZ, A. (1986): Mise au point concernant les series de l´Ordovicien-Silurien-Dévonien inférieur du Djebel Aouam (Maroc Central). – Bulletin de l´Société Géologique du France, **1986** (2): 293-297.

FRANKE, W. (2000): The mid-European segment of the Variscides: tectonostratigraphic units, terrane boundaries and plate tectonic evolution. – Geological Society, London, Special Publications, **179**: 35-61.

FRANKE, W., COCKS, L. R. M. & TORSVIK, T. H. (2017): The Palaeozoic Variscan oceans revisited. – Gondwana Research, **48**: 257-284.

FRECH, F. (1887): Die palaeozoischen Bildungen von Cabrières (Languedoc). – Zeitschrift der Deutschen Geologischen Gesellschaft, **39**: 360-488, pl. 24.

GARCÍA-ALCALDE, J. (1997): North Gondwanan Emsian events. – Episodes, **20** (4): 241-246.

GENDROT, C. (1973): Environnements du Dévonien récifal au Maroc. – Notes du Service géologique du Maroc, **34**: 55-86.

GENDROT, C., KERGOMARD, D. & RABATÉ, J. (1969): Etude des formations récifale du dévonien de la meseta occidentale. – Vol. I: 68 pp. + 5 figs., vol. II: 16 pls.; Charia Moulay Hassan, Rabat.

GENTIL, L. (1918): Notice sur les titres et travaux scientifiques de L. GENTIL. – 132 pp., Larose, Paris.

GEORGE, A. D., TRINAJSTIC, K. M. & CHOW, N. (2009): Frasnian reef evolution and palaeogeography, SE Lennard Shelf, Canning Basi, Australia. – In: KÖNIGSHOF, P. (Ed.), Devonian Change: Case Studies in Palaeogeography and Palaeoecology. The Geological Society, London, Special Publications, **314**: 73-107.

GERRIENNE, P., MEYER-BERTHAUD, B., LARDEUX, H. & RÉGNAULT, S. (2010): First record of *Rellimia* LECLERQ & BONAMO (Aneurophytales) from Gondwana, with comments on the earliest lignophytes. – In: VECOLI, M., CLÉMENT, G. & MEYER-BERTHAUD, B. (Eds.), The Terrestrialisation Process: Modelling Complex Interactions in the Biosphere-Geosphere Interface. Geological Society, Special Publication, **339**: 81-92.

GHOLAMALIAN, H. & KEBRIAEI, M.-R. (2008): Late Devonian conodonts from the Hojedk Section, Kerman Province, southeastern Iran. – Rivista Italiana di Paleontologia e Stratigrafia, **114** (2): 179-189.

GHOLAMALIAN, H., HAIRAPETIAN, V., BARFEHEI, N., MANGELIAN, S. & FARIDI, P. (2013): Givetian-Frasnian boundary conodonts from Kerman Province, Central Iran. – Rivista Italiana di Paleontologia e Stratigrafia, **119** (2): 133-146.

GINTER, M. & IVANOV, A. (2000): Stratigraphic distribution of chondrichthyans in the Devonian on the East European Platform margin. – Courier Forschungsinstitut Senckenberg, **223**: 325-339.

GINTER, M., HAIRAPETIAN, V. & KLUG, C. (2002): Famennian chondrichthyans from the shelves of North Gondwana. – Acta Geologica Polonica, **52**: 169-215.

GIRARD, C. & ALBARÈDE, F. (1996): Trace elements in conodont phosphates from the Frasnian/Famennian boundary. – Palaeogeography, Palaeoclimatology, Palaeoecology, **126**: 195-209.

GIRARD, C. & RENAUD, S. (2008): Disentangling allometry and response to Kellwasser anoxic events in the Late Devonian conodont genus *Ancyrodella*. – Lethaia, **41**: 383-394.

GIRARD, C., KLAPPER, G. & FEIST, R. (2005): Subdivision of the terminal Frasnian *linguiformis* conodont Zone, revision of the correlative interval of Montagne Noire Zone 13, and discussion of stratigraphically significant associated trilobites. – In: OVER, D. J., MORROW, J. R. & WIGNALL, P. B. (Eds.), Understanding Late Devonian and Permian-Triassic Biotic and Climatic Events; Towards an Integrated Approach. Developments in Palaeontology & Stratigraphy, **20**: 181-198.

GIRARD, C., PHUONG, T. H., SAVAGE, N. & RENAUD, S. (2010): Temporal dynamics of the geographic differentiation of Late Devonian *Palmatolepis* assemblages in the Prototethys. – Acta Palaeontologica Polonica, **55** (4): 675-687.

GLENISTER, B. F. (1958): Upper Devonian amonoids from the *Manticoceras* Zone, Fitzroy Basin, Western Australia. – Journal of Paleontology, 32 (1): 58-96, pls. 5-15.

GLENISTER, B. F. & KLAPPER, G. (1966): Upper Devonian conodonts from the Canning Basin, Western Australia. – Journal of Paleontology, **40** (4): 777-482.

GOLONKA, J. (2007): Phanerozoic paleoenvironment and paleolithofacies maps. Late Paleozoic. – Geologia, **33**: 145-209.

GOMEZ, F., BEAUCHAMP, W. & BARAZANGI, M. (2000): Role of the Atlas Mountains (northwest Africa) within the African-Eurasian plate-boundary zone. – Geology, **28** (9): 775-778.

GOUWY, S. & BULTYNCK, P. (2002): Graphic correlation of Middle Devonian sections in the Ardene region (Belgium) and the Mader-Tafilalt region (Morocco): development of a Middle Devonian composite standard. – In: Proceedings of the first Geologica Belgica International Meeting, Leuven, 11-15 September 2002. Aardkundige Mededelingen, **12**: 105-108.

GOUWY, S. & BULTYNCK, P. (2003): Conodont based graphic correlation of the Middle Devonian formations of the Ardenne (Belgium): implications for stratigraphy and construction of a regional composite. – Revista Española de Micropaleontología, **35** (3): 315-344.

GOUWY, S., HAYDUKIEWICZ, J. & BULTYNCK, P. (2007): Conodont-based graphic correlation of upper Givetian-Frasnian sections of the Eastern Anti-Atlas (Morocco). – Geological Quarterly, **51** (4): 375-392.

GRABAU, A. W. (1928): Palaeozoic Corals of China. Part I. Tetraseptata II. Second contribution to our knowledge of the Streptelasmoid Corals of China and Adjacent Territories. - Palaeontologica Sinica, series B, **2** (2): 1-175, 6 pls.

GRAHAM, J. R. & SEVASTOPULO, G. D. (2008): Mississippian Platform and Basin Successions from the Todrha Valley (northeastern Anti-Atlas), southern Morocco. – Geological Journey, **43**: 361-382.

GROBE, M. (1993): Stratigraphie, Fazies, Tektonik und Maturität des Paläozoikums von Dchar-Ait-Abdallah (östliches Zentral-Marokko), unter besonderer Berücksichtigung der faziellen Entwicklung des Mittel- und Oberdevons. – Unpublished Diplomarbeit, Universität Tübingen, 104 pp.

GROBE, M. (1997): The allochthonous Devonian units of Dchar-Aït-Abdallah, southeastern Meseta, east-central Morocco: a facies model. – Gaea heidelbergensis, **3**: 149.

HAHN, G., MÜLLER, P. & BECKER, R. T. (2012): Unter-karbonische Trilobiten aus dem Anti-Atlas (S-Marokko). – Geologica et Palaeontologica, **44**: 37-74.

HALL, J. (1874): Descriptions of new species of Goniatitidae. With a list of previously described species. – Annual Reports of the Regents of the University of the State New York, **26**: 1-4.

HARTENFELS, S. (2011): Die globalen *Annulata*-Events und die Dasberg-Krise (Famennium, Oberdevon) in Europa und Norda-Afrika – hochauflösende Conodonten-Stratigraphie, Karbonat-Mikrofazies, Paläoökologie und Paläodiversität. – Münstersche Forschungen zur Geologie und Paläontologie, **105**: 17-527.

HARTENFELS, S. & BECKER, R. T. (2016): The global *Annulata* Events: review and new data from the Rheris Basin (northern Tafilalt) of SE Morocco. – In: BECKER, R. T., KÖNIGSHOF, P. & BRETT, C. E. (Eds.), Devonian Climate, Sea Level and Evolutionary Events. Geological Society, London, Special Publications, **423**: 291-354.

HARTENFELS, S., BECKER, R. T. & TRAGELEHN, H. (2009): Marker conodonts around the global *Annulata* Events and the definition of an Upper Famennian substage. – SDS Newsletter, **24**: 40-48.

HARTENFELS, S., BECKER, R. T., EL HASSANI, A. & LÜDDECKE, F. (Eds., 2018): 10th International Symposium „Cephalopods – Present and Past", Fes, 26th March – 3rd April 2018, Field Guidebook. – Münstersche Forschungen zur Geologie und Paläontologie, **110**: 110-306.

HARTENFELS, S., BECKER, R. T. & ABOUSSALAM, Z. S. (2016): Givetian to Famennian stratigraphy, Kellwasser, *Annulata* and other events at Beringhauser Tunnel (Messinghausen Anticline, eastern Rhenish Massif). – Münstersche Forschungen zur Geologie und Paläontologie, **108**: 196-219.

HAUDE, R., CORRIGA, M. G., CORRADINI, C. & WALLISER, O. H. (2014): Bojen-Seelilien (Scyphocrinitidae, Echinodermata) in neu-datierten Schichten vom oberen Silur bis untersten Devon Südost-Marokkos. – Göttingen Contributions to Geosciences, **77**: 129-145.

HAVLÍČEK, V. (1956): Brachiopods of the Bráník and Hlubočepy limestones in the immediate vicinity of Prague. – Sborník Ústředního ústavu geologického, **22**: 535-565.

HECKEL, P. H. & WITZKE, B. J. (1979): Devonian world palaeogeography determined from distributions of carbonates and related lithic palaeoclimatic indicators. – Special Papers in Palaeontology, **23**: 99-123.

HELLING, S. & BECKER, R. T. (2015): A new Pragian trilobite assemblage from Aïn-al-Aliliga (western Meseta, NW Morocco). – In: MOTTEQUIN, B., DENAYER, J., KÖNIGSHOF, P., PRESTIANNI, C. & OLIVE, S. (Eds.), IGCP 596 – SDS Symposium "Climate change and Biodiversity patterns in the Mid-Palaeozoic", September 20-22. 2015, Brussels – Belgium, Abstracts. Strata, Travaux de Géologie sédimentaire et Paléontologie, Série 1: communications, **16**: 68-69.

HINDERMEYER, J. (1954): Découverte du Tournaisian, et tectonique prémonitoire hercynienne dans la region

de Tinerhir (flanc nord du Sarho-Ougnat). – Comptes Rendus hebdomadaires des Séances de l´Academie des Sciences, Paris, **239**: 1824-1826.

HINDERMEYER, J. (1955): Sur le Dévonien et l´existence de mouvements calédoniens dans la region de Tinerhir. – Comptes Rendus de l´Academie des Sciences, Paris, **240** (26):2547-2549.

HOEPFFNER, C., SOULAIMANI, A. & PIQUE, A. (2005): The Moroccan Hercynides. – Journal of African Earth Sciences, **43**: 144-165.

HOEPFFNER, C., HOUASRI, M. R. & BOUABDELLI, M. (2006): Tectonics of the North African Variscides (Morocco, western Algeria): an outline. – Compte Rendus Geosciences, **338**: 25-40.

HOLLARD, H. (1967): Le Dévonien du Maroc et du Sahara nord-occidentale. – In: OSWALD, D. H. (ed.), International Symposium on the Devonian System, Calgary, 1967, **I**: 203-244; Alberta Society of Petroleum Geologists, Calgary.

HOLLARD, H. & MORIN, P. (1973): Les gisements de *Dzieduszyckia* (Rhynchonellida) du Famennien inférieur du Massif hercynien central du Maroc. – Notes et Mémoires du Service Géologique du Maroc, **33** (249): 7-14.

HOLLARD, H. (1978): Corrélations entre niveaus à brachiopods et á goniatites au voisinage de la limite Dévonien inférieur – Dévonien moyen dans les plaines du Dra (Maroc présaharien). – Newsletters on Stratigraphy, **7** (1): 8-25.

HOLLARD, H., LYS, M., MAUVIER, A. & MORIN, P. (1970): Précisions sur l´age famennien inférieur des *Dzieduszyckia* (Rhynchonellida) du Massif hercynien central du Maroc. – Comptes Rendus de l´Academie des Sciences Paris, Série D, **270**: 3177-3180.

HOLLARD, H., MICHARD, A., JENNY, P., HOEPFFNER, C. & WILLEFERT, S. (1982): Stratigraphie du Primaire de Mechra-Ben-Abbou, Rehamna. – In: MICHARD, A. (Ed., 1982), Le massif Paléozoique des Rehamna (Maroc). Stratigraphie, Tectonique et Petrogenese d´un segment de la Chaine Varisque. - Notes et Mémoires du Service Géologique, **303**: 180 pp.

HORON, O. (1954): Note sur la géologie des affleurements de Primaire de la region du Kandar. – Unpublished Report, Archive of B.R.P.M.

HOU, H.-F. (1988, Ed.): Devonian stratigraphy, Paleontology and Sedimentary Facies of Longmenshan, Sichuan. – Chengdu Institute of Geology and Mineral Resources; Geological Publishing House, Beijing.

HOUSE, M. R. (1975): Facies and Time in Devonian Tropical Areas. – Proceedings of the Yorkshire Geological Society, **40** (2): 233-288.

HOUSE, M. R. & KIRCHGASSER, W. T. (1993): Devonian goniatite biostratigraphy and timing of facies movements in the Frasnian of eastern North America. – In: HAILWOOD, E. A. & KIDD, R. B. (Eds.): High Resolution Stratigraphy. Geological Society Special Publication, **70**: 267-292.

HOUSE, M. R. & KIRCHGASSER, W. T. (2009): Late Devonian goniatites (Cephalopoda, Ammonoidea) from New York State. – Bulletins of American Paleontology, **374**: 1-285.

HOUSE, M. R. & ZIEGLER, W. (1977): The Goniatite and Conodont sequences in the early Upper Devonian at Adorf, Germany. – Geologica et Palaeontologica, **11:** 69-108.

HOUSE, M.R., BECKER, R.T., FEIST, R., FLAJS, G., GIRARD, C. & KLAPPER, G. (2000a): The Frasnian/Famennian boundary GSSP at Coumiac, southern France. - Courier Forschungsinstitut Senckenberg, **225**: 59-75.

HOUSE, M.R., MENNER, V.V., BECKER, R.T., KLAPPER, G., OVNATANOVA, N.S., KUZ´MIN, V., (2000b): Reef episodes, anoxia and sea-level changes in the Frasnian of the southern Timan (NE Russian platform). - In: INSALACO, E., SKELTON, P.W., PALMER, T.J. (Eds.), Carbonate Platform Systems: components and interactions. Geological Society, London, Special Publications, **178**: 147-176.

HUDDLE, J. W., assisted by REPETSKI, J. E. (1981): Conodonts from the Genesee Formation in Western New York. – Geological Survey Professional Paper, **1032-B**: 1-66 + 31 pls.

HUDSON, R. G. S. (1936): On the Lower Carboniferous Corals: *Rhopalolasma*, gen. nov. and *Cryptophyllum*, CARR. - Proceedings of the Yorkshire Geological Society, **23** (2): 91-102, pls. 4-5.

HÜNEKE, H. (2001): Gravitative und strömungsinduzierte Resedimente devonischer Karbonatabfolgen im marokkanischen Zentralmassiv (Rabat-Tiflet-Zone, Decke von Ziar-Mrirt). – Unpublished Habilitation Thesis, Ernst-Moritz-Arndt-Universität Greifswald, 230 pp.

HÜNEKE, H. (2006): Erosion and deposition from bottom currents during the Givetian and Frasnian: Response to intensified oceanic circulation between Gondwana and Laurussia. – Palaeogeography, Palaeoclimatology, Palaeoecology, **234**: 146-167.

HÜNEKE, H. (2007): Pelagic carbonate ooze reworked by bottom currents during Devonian approach of the continents Gondwana and Laurussia. – In: VIANA, A. R. & REBESCO, M. (Eds.), Economic and Palaeoceanographic significance of Contourite Deposits. Geological Society, London, Special Publication, **276**: 299-328.

HÜNEKE, H. (2013): Facies and sedimentary architecture of Upper Devonian limestones at Gara de Mrirt, Eastern Moroccan Central Massif: Resedimentation in response to block faulting. – In: EL HASSANI, A., BECKER, R. T. & TAHIRI, A. (Eds.), International Field Symposium "The Devonian and Lower Carboniferous of northern Gondwana", Abstract Book. Documents de l´Institut Scientifique, **26**: 62-64.

HUVELIN, P. (1970): Mouvements hercyniens précoces dans le region de Mrirt (Maroc). – Comptes Rendus de l´Academie des Sciences, Paris, **271**: 953-955.

HUVELIN, P. (1977): Etude géologique et gitologique du massif hercynien des Jebilet (Maroc occidental). – Notes et Mémoires du Service Géologique, **232 bis**: 307 pp.

HUVELIN, P. & MAMET, B. (1997): Transgressions, faulting and redeposition phenomenon during the Visean in the Khenifra area; Western Moroccan Meseta. – Journal of African Earth Sciences, **25** (3): 383-389.

IKENNE, M., SOUHASSOU, M., ARAI, S. & SOULAIMANI, A. (2016): A historical overview of Moroccan magmatic events along northwest edge of the West African Craton. – Journal of African Earth Sciences, **127**: 3-15.

IZART, A. & VIESLET, J. L. (1988): Stratigraphie, Sédimentologie et Micropaléontologie des sédiments du bassin de Sidi Bettache et ses bordures (Meseta marocaine nord-occidentale) du Famennien au Viséen supérieur. – Notes et Mémoirs du Service géologique du Maroc, **334**: 7-41.

JANSEN, U. (2001): Morphologie, Taxonomie und Phylogenie unter-devonischer Brachiopoden aus der Dra-Ebene (Marokko, Prä-Sahara) und dem Rheinischen Schiefergebirge (Deutschland). – Abhandlungen der Senckenbergischen Naturforschenden Gesellschaft, **554**: 1-389-

JANSEN, J., LAZREQ, N., PLODOWSKI, G., SCHEMM-GREGORY, M., SCHINDLER, E. & WEDDIGE, K. (2007): Neritic-pelagic correlation in the Lower and basal Middle Devonian of the Dra Valley (Southern Anti-Atlas, Moroccan Pre-Sahara). – In: BECKER, R. T. & KIRCHGASSER, W. T. (Eds.), Devonian Events and Correlations. Geological Society, London, Special Publications, **278**: 9-37.

JEANETTE, D. & PIQUE, A. (1981): Le Maroc hercynien: plate-forme disloquée du craton oust-africain. – Comptes Rendus de l´Academie des Sciences, Paris, Série II, **293**: 79-82.

JOACHIMSKI, M. M. & BUGGISCH, W. (1993): Anoxic events in the late Frasnian - Causes of the Frasnian-Famennian faunal crisis? - Geology, **21**: 657-678.

JOACHIMSKI, M. M., OSTERTAG-HENNING, C., PANCOST, R. D., STRAUSS, H., FREEMAN, K. H., LITTKE, R., SINNINGHE DAMSTÉ, J. S. & RACKI, G. (2001): Water column anoxia, enhanced productivity and concomitant changes in $\delta^{13}C$ and $\delta^{34}S$ across the Frasnian-Famennian boundary (Kowala – Holy Cross Mountains / Poland). - Chemical Geology, **175**: 109-131.

JOACHIMSKI, M. M., PANCROST, R. D., FREEMAN, K.A., OSTERTAG-HENNING, C. & BUGGISCH, W. (2002): Carbon isotope geochemistry of the Frasnian - Famennian transition. - Palaeogeography, Palaeoclimatology Palaeoecology, **181**: 91-109.

KAISER, S. I., BECKER, R. T. & EL HASSANI, A. (2007): Middle to Late Famennian succession at Aïn Jemaa (Moroccan Meseta) – implications for regional correlation, event stratigraphy and synsedimentary tectonics of NW Gondwana. – In: BECKER, R. T. & KIRCHGASSER, W. T. (Eds.), Devonian Events and Correlations. Geological Society, London, Special Publications, **278**: 237-260.

KAISER, S. I., BECKER, R. T., SPALLETTA, C. & STEUBER, T. (2009): High-resolution conodont biostratigraphy, biofacies, and extinctions around the Hangenberg Event in pelagic successions from Austria, Italy, and France. – In: OVER, J. D. (Ed.), Studies in Devonian Stratigraphy: Proceedings of the 2007 International Meeting of the Subcommission on Devonian Stratigraphy and IGCP 499. Palaeontographica Americana, **63**: 99-143.

KAISER, S. I., BECKER, R. T., STEUBER, T. & ABOUSSALAM, Z. S. (2011): Climate-controlled mass extinctions, facies, and sea-level changes around the Devonian-Carboniferous boundary in the eastern Anti-Atlas (SE Morocco). – Palaeogeography, Palaeoclimatology, Palaeoecology, **310**: 340-364.

KELLING, G. & MULLIN, P. R. (1975): Graded limestones and limestone-quartzite couplets. possible storm-deposits from the Moroccan Carboniferous. – Sedimentary Geology, **13**: 161-190.

KERGOMARD, D. (1970): Contribution à l´ètude du Siluro-Dévonien de la Meseta occidentale. – Unpublished Report B.R.P.M., Rabat.

KLAPPER, G. (1989): The Montagne Noire Frasnian (Upper Devonian) conodont succession. – In: MCMILLAN, N. J., EMBRY, A. F. & GLASS, D. J. (Eds.), Devonian of the World, Proceedings of the Sercond International Symposium on the Devonian System, Calgary, Canada. Canadian Society of Petroleum Geologists, Memoir, **14** (III): 449-468 [imprint 1988].

KLAPPER, G. (1997): Graphic correlation of Frasnian (Upper Devonian) sequences in Montagne Noire,

France, and western Canada. – In: KLAPPER, G., MURPHY, M. A. & TALENT, J. A. (Eds.), Paleozoic Sequence Stratigraphy, Biostratigraphy, and Biogeography: Studies in Honor of J. Granville ("Jess") JOHNSON. Geological Society of America, Special Paper, **321**: 113-129.

KLAPPER, G. (2009): Upper Devonian conodonts in the Canning Basin. - Geological Survey of Western Australia, Bulletin, **145**: 405-413.

KLAPPER, G. & KIRCHGASSER, W. T. (2016): Frasnian Late Devonian conodont biostratigraphy in New York: graphic correlation and taxonomy. – Journal of Paleontology, **90** (3): 525-554.

KLAPPER, G., KUZ´MIN, A. & OVNATANOVA, N. S. (1996): Upper Devonian conodonts from the Timan-Pechora region, Russia, and correlation with a Frasnian Composite Standard. – Journal of Paleontology, **70** (1): 131-152.

KLAPPER, G. & VODRÁŽKOVÁ, S. (2013): Ontogenetic and intraspecific variation in the late Emsian – Eifelian (Devonian) conodonts *Polygnathus serotinus* and *P. bultyncki* in the Prague Basin (Czech Republic) and Nevada (western U.S.). – Acta Geologica Polonica, **63** (2): 153-174.

KLUG, C. (2002): Quantitative stratigraphy and taxonomy of late Emsian and Eifelian ammonoids of the eastern Anti-Atlas (Morocco). – Courier Forschungsinstitut Senckenberg, **238**: 1-109.

KONONOVA, L. I. & KIM, S.-Y. (2003): Eifelian Conodonts from the Central Russian Platform. – Paleontological Journal, **39**, Supplement 2: 55-134.

KOPTIKOVÁ, L. (2011): Precise position of the Basal Choteč event and evolution of sedimentary environments near the Lower-Middle Devonian boundary: the magnetic susceptibility, gamma-ray spectrometric, lithological, and geochemical record of the Prague Synform (Czech Republic). – Palaeogeography, Palaeoclimatology, Palaeoecology, **304**: 96-112.

KREBS, W. (1974): Devonian carbonate complexes of Central Europe. - SEPM Special Publication, **18**: 155-208.

KREBS, W. (1979): Devonian basinal facies. – Special Papers in Palaeontology, **23**: 125-139.

LAAMRANI ELIDRISSI, A. (1993): Relations deformations-deplacements le long de failles hercyniennes: Systeme de Bouznika et Systemes du Cherrat-Ben Slimane et du Cherrat-Yquem. – Unpublished Diplom Thesis, Université Mohammed V, Rabat, 200 pp., online at http://archives.cnd.hcp.ma/uploads/news/017942.pdf.

LAVENU, A. (1976): Etude tectonique et microtectonique d´un segment de chaine hercynienne dans la partie sud-orientale du Maroc central (Région situeé entre Khénifra et Kef-en-Nsour). – Notes et Mémoires du Service Géologique, **261**: 57-111.

LAVILLE, E. (1980): Tectonique et Microtectonique d´une partie du versant sud du Haut Atlas marocain (Boutonnière de Skoura, Nappe de Toundout). – Notes et Mémoires du Servioce géologique du Maroc, **41** (285): 81-183.

LAZREQ, N. (1990): Devonian Conodonts from Central Morocco. – Courier Forschungsinstitut Senckenberg, **118**: 65-79.

LAZREQ, N. (1992a): Le Dévonien du Maroc central: biostratigraphie des Conodontes. Biofaciès et événement Kellwasser. – Unpublished Ph. D. Thesis, University Marrakech, 260 pp.

LAZREQ, N. (1992b): The Upper Devonian of Mrirt (Morocco). Courier Forschungsinstitut Senckenberg, **154**: 107-123.

LAZREQ, N. (1999): Biostratigraphie des conodontes du Givétien au Famennien du Maroc central – Biofaciès et événement Kellwasser. – Courier Forschungsinstitut Senckenberg, **214**: 1-111.

LAZREQ, N. (2017): A propos de l´existence du Famennien au sud des Jebilet Centrales et altération des conodontes: cas de Koudiat Laabid (Jbel Guéliz, Marrakech, Maroc). – Bulletin de l´Institute Scientifique, Rabat, Section Sciences de la Terre, **39**: 79-86.

LECOINTRE, G. (1926) Recherches géologiques dans la Meseta marocaine. – Mémoires de l´Société des Sciences Naturelles du Maroc, **14**: 1-158.

LE HOUEDEC, S., GIRARD, C. & BALTER, V. (2013): Conodont Sr/Ca and $\delta^{18}O$ record seawater changes at the Frasnian-Famennian boundary. – Palaeogeography, Palaeoclimatology, Palaeoecology, **376**: 114-121.

LINDSKOG, A., ERIKSSON, M. E., BERGSTRÖM, S. M., TERFELT, F. & MARONE, F. (2017): Palaeozoic ´conodont pearls` and other phosphatic microsphaerules. – Lethaia, **50**: 26-40.

MAMET, B., PREAT, A. & LEHMAMI, M. (1999): Algues calcaires marines du Dévonien marocain (Meseta). – Revue de Micropaléontologie, **42** (4): 301-314.

MATTE, P. (2001): The Variscan collage and orogeny (480-290 Ma) and the tectonic definition of the Armorica microplate: a review. – Terra Nova, **13**: 122-128.

MAY, A. (1993): Korallen aus dem höheren Eifelium und unteren Givetium (Devon) des nordwestlichen Sauerlandes (Rheinisches Schiefergebirge). Teil I: Tabulate Korallen. - Palaeontographica, Abt. A, **227**: 87-224, pls. 5-19.

MAY, A. (2005): Die Stromatoporen des Devons und Silurs von Zentral-Böhmen (Tschechische Republik)

und ihre Kommensalen. - Zitteliana, **B25**: 117-250, pl. 1-43.

McKERROW, W. S., MAC NIOCAILL, C., AHLBERG, P. E., CLAYTON, G., CLEAL, C. J. & EAGAR, R. M. C. (2000): The Late Palaeozoic relations between Gondwana and Laurussia. – Geological Society, London, Special Publications, **179**: 9-20.

MICHARD, A. (1976): Eléments de géologie marocaine. – Notes et Mémoires du Service Géologique du Maroc, 252: 408 pp.

MICHARD, A. (Ed., 1982): Le massif Paléozoique des Rehamna (Maroc). Stratigraphie, Tectonique et Petrogenese d´un segment de la Chaine Varisque. – Noters et Mémoires du Service Géologiquw, **303**: 180 pp.

Michard, A., Yazidi, A., Benziane, F., Hollard, H. & Willefert, S. (1982): Foreland thrusts and olistostromes on the pre-Sahara margin of the Variscan orogen, Morocco. – Geology, 10: 253-256.

MICHARD, A., HOEPFFNER, C., SOULAIMANI, A. & BAIDDER, A. (2008): The Variscan Belt. – In: MICHARD, A., SADDIQI, O., CHALOUAN, A. & FRITZ DE LAMOTTE, D. (Eds.), Continental Evolution: The Geology of Morocco. Lecture Notes in Earth Sciences, **116**: 65-132.

MICHARD, A., SOULAIMANI, A., HOEPFFNER, C., OUZANAIMI, H., BAIDDER, L., RJIMATI, E. C. & SADDIQI, O. (2010): The South-Western Branch of the Variscan Belt: Evidence from Morocco. – Tectonophysics, **492**: 1-24.

MORZADEC, P. (1988): Le genre *Psychopyge* (Trilobita) dans de Dévonien inférieur du nord de l´Afrique et l´ouest de l´Europe. – Palaeontographica, Abt. A, **200** (4/6): 153-161, 2 pls.

MOTTEQUIN, B. & POTY, E. (2016): Kellwasser horizons, sea-level changes and brachiopod-coral crises during the late Frasnian in the Namur-Dinant Basin (southern Belgium): a synopsis. – In: BECKER, R. T., KÖNIGSHOF, P. & BRETT, C. E. (Eds.), Devonian Climate, Sea Level and Evolutionary Events. Geological Siciety, London, Special Publications, **423**: 235-250.

MOUNTJOY, E. W. & JULL, R. K. (1978): Fore-reef carbonate mud bioherms and associated reef-margin, Upper Devonian, Ancient Wall Reef complex, Alberta. – Canadian Journal of Earth Sciences, **15**: 1304-1325.

MÜNSTER, G., Graf zu (1831): Über das geognostische Vorkommen der Ammoneen in Deutschland. – Jahrbuch für Mineralogie, Geognosie, Geologie und Petrefaktenkunde, **1831**: 367-375.

MÜNSTER, G., Graf zu (1832): Ueber die Planuliten und Goniatiten im Uebergangs-Kalk des Fichtelgebirges. – 38 pp., 6 pls.; Birner, Bayreuth.

MÜNSTER, G., Graf zu (1839): Nachtrag zu den Goniatiten im Fichtelgebirge. – Beiträge zur Petrefaktenkunde, **1**: 43-55, pls. 3-5.

MULLIN, P., BEDSAÏD, M. & KELLING, G. (1976): Les nappes hercyniennes au sud-est du Maroc central; une nouvelle interpretation. – Comptes Rendus de l´Academie des Sciences, Paris, Série D, **282**: 827-830.

NAHRAOUI, F. Z., WARTITI, M. EL, BOUKILI, B., MOUTAOUAKKIL, N. EL, KACIMI, I., AMRANI IDRISSI, H., KHARCHOF, A. EL K. & MAALAM, B. (2012): The cement Temara: needs a new deposit of limestone (case the deposit of oued Cherrat). – MATEC Web of Conference, **2** (05003): 1-7.

NANCE, R. D., GUTIÉRREZ-ALONSO, G., KEPPIE, J. D., LINNEMANN, U., MURPHY, J. B., QUESADA, C., STRACHAN, R. A., WOODCOCK, N. H. (2012): A brief history of the Rheic Ocean. – Geoscience Frontiers, **3** (2): 125-135.

NARKIEWICZ, K. & BULTYNCK, P. (2007): Conodont biostratigraphy of shallow marine Givetian deposits from the Radom-Lublin area, SE Poland. – Geological Quarterly, **51** (4): 419-442.

NARKIEWICZ, K. & BULTYNCK, P. (2010): The upper Givetian (Middle Devonian) *subterminus* conodont zone in North America, Europe and North Africa. – Journal of Paleontology, **84** (4): 588-625.

NARKIEWICZ, K., NARKIEWICZ, M. & BULTYNCK, P. (2016): Conodont biofacies of the Taghanic transgressive interval (middle Givetian): Polish record and global comparisons. – In: BECKER, R. T., KÖNIGSHOF, P. & BRETT, C. E. (Eds.), Devonian Climate, Sea Level and Evolutionary Events. Geological Society, London, Special Publications, **423**: 201-222.

NARKIEWICZ, K., NARKIEWICZ, M., BULTYNCK, P. & KÖNIGSHOF, P. (2017): The past, present and future of the upper Eifelian conodont zonation. – In: LIAO, J.-C. & VALENZUELA-RÍOS, J. I. (Eds.), Fourth International Conodont Symposium, ICOS IV "Progress on Conodont Investigation". Cuadernos del Museo Geominero, **22**: 137-140.

NAZIK, A. & GROOS-UFFENORDE, H. (2016): Notes on beyrichiacean ostracods from the Early Devonian of NW Turkey and their palaeobiogeographical relations. – Turkish Journal of Earth Sciences, **25**: 201-226.

NEQQAZI, A., RAJI, M. & BENFRIKA, M. El (2014): Conodontes du Carbonifère inférieur de la région de l`Oued Cherrat (Meseta nord-occidentale, Maroc). – International Journal of Innovation and Applied Studies, **9** (1): 81-88.

NEUGEBAUER, J. (1988): The Variscan plate tectonic evolution: an improved „Iapetus model". –

Schweizerische Mineralogische und Petrographische Mitteilungen, **68**: 313-333.

NICOLL, R. S. (1980): The multielement genus *Apatognathus* from the Late Devonian of the Canning Basin, Western Australia. – Alcheringa, **4**: 133-152.

OUANAIMI, H. & PETIT, J. P. (1992): La limite sud de la chaîne hercynienne dans le Haut-Atlas marocain: reconstitution d´un saillant non déforme. – Bulletin de l`Société Géologie du France, **163**: 63-73.

OUANAIMI, H., SOULAIMANI, A., HOEPFFNER, C. & MICHARD, A. (2019): The "Eovariscan Synmetamorphic Phase" of the Morioccan Meseta Domain Revisited; A Hint for Late Devonian Extensional Geodynamics Prior to the Variscan Orogenic Evolution. – In: ROSSETTI, F. et al. (Eds.), The Structural Geology Contribution to the Africa-Eurasia Geology: Basement and Reservoir Structure, Ore Mineralisation and Tectonic Modelling: 259-261; Advances in Science, Technology & Innovation.

OUARHACHE, D. (1987): Ètude géologique dans le Paléozoique et le Trias de la bordure NW du causse Moyen-Atlasique (S et SW de Fès, Maroc). – Thèse 3ème cycle, Université de Toulouse, 130 pp.

OUARHACHE, D., BAUDELOT, S., CHARRIÈRE, A., PERRET. M. F. & VACHARD, D. (1991): Nouvelles datations micrpaléontologiques et palynologiques dans le Viséen de la bordure nord occidentale du Causse moyen-atlasique (Maroc). – Géologie Méditerranéenne, **18** (1/2): 43-59.

OVNATANOVA, N. S. & KONONOVA, L. I. (2008): Frasnian Conodonts from the Eastern Russian Platform. – Paleontological Journal, **42** (10): 997-1166.

PÉREZ-CÁZERES, I., MARTÍNEZ POYATOS, SIMANCAS, J. F. & AZOR, A. (2017): Testing the Avalonian affinity of the South Portuguese Zone and the Neoproterozoic evolution of SW Iberia through detrital zircon populations. – Gondwana Research, **42**, 177-192.

PETTER, G. (1959): Goniatites dévoniennes du Sahara. – Publications du Service de la Carte Géologique de l´Algérie, Nouvelle Série, Paléontologie, **2**: 1-313, 26 pls.

PIQUE, A. (1975): Différenciation des aires de sédimentation au Nord-Ouest de la Meseta marocaine; la distension dévono-dinantienne. – Comptes Rendus de l´Academie des Sciences Paris, **281**: 767-770.

PIQUE, A. (1979): Évolution structural d´un segment de la chaîne hercynienne: La Meseta Marocaine nord-occidentale. – Sciences Géologiques, Mémoire, **56**: 243 pp.

PIQUE, A. (1984): Facies sédimentaire et evolution d´un basin: le Bassin dévono-dinantien de Sidi Bettache (Maroc nord-occidental). – Bulletin de l`Société Géologique du France, (7), **26** (6): 1015-1023.

PIQUE, A. & MICHARD, A. (1981): Les zones structurales du Maroc hercynien. – Sciences Géologiques, Bulletin, **34** (2): 135-146.

PIQUE, A. (1994): Géologie du Maroc. Les domaines régionaux et leur évolution structurale. – 284 pp., Marrakech.

PIQUE, A. (2001): Geology of Northwest Africa. – 310 pp., Bornträger, Berlin.

PIQUE, A. & MICHARD, A. (1989): Moroccan Hercynides: a synopsis. The Paleozoic sedimentary and tectonic evolution at the northern margin of West Africa. – American Journal of Science, **289**: 286-330.

PIQUE, A., JEANETTE, D. & MICHARD, A. (1980): The Western Meseta Shear Zone, a major and permanent feature of the Hercynian belt in Morocco. – Journal of Structural Geology, **2** (1/2): 55-61.

PISARZOWSKA, A., SOBSTEL, M. & RACKI, G. (2006): Conodont-based event stratigraphy of the Early-Middle Frasnian transition on the South Polish carbonate shelf. – Acta Palaeontologica Polonica, **51** (4): 609-646.

PISARZOWSKA, A., BECKER, R. T., ABOUSSALAM, Z. S., SZCZERBA, M., SOBIEN, K., KREMER, B., OWOCKI, K. & RACKI, G. (2020 in press): Middlesex/*punctata* Event in the Rhenish Basin (Padberg section, Sauerland, Germany) – multidisziplinary clues to the early-middle Frasnian global biogeochemical perturbation. – Global and Planetary Change.

PLAYFORD, P. E., HOCKING, M. R. & COCKBAIN, A. E. (2009): Devonian Reef Complexes of the Canning Basin, Western Australia. – Geological Survey of Western Australia, Bulletin, **145**: 1-403.

POLLOCK, C. A. (1968): Lower Upper Devonian conodonts from Alberta, Canada. – Journal of Paleontology, **42** (2): 415-443, pls. 61-64.

POTTHAST, I. & OEKENTORP, K. (1987): Eine Favositiden-Fauna aus dem Emsium/Eifelium des Hamar Laghdad, Tafilalt (SE-Marokko). – Münstersche Forschungen zur Geologie und Paläontologie, **66**: 57-93.

PRESTIANNI, C., MEYER-BERTHAUD, B., BLANCHARD, R., RÜCKLIN, M., CLÉMENT, G. & GERRIENNE, P. (2012): The Middle Devonian plant assemblage from Dechra Aït Abdallah (Central Morocco) revisted. – Review of Palaeobotany and Palynology, **179**: 44-55.

RACHEBEUF, P. R. (1990a): Chonetacés (Brachiopodes) éo- et mésodévoniens de la Meseta Hercynienne et

de l´Anti-Atlas, Maroc. - Géologie Méditerranéenne, **17** (3/4): 301-319.

RACHEBEUF, P. R. (1990b): Silurian to Middle Devonian chonetacean brachiopods from the northwestern Gondwanaland margin: A review in time and space. – In: MACKINNON, D. I., LEE, D. E. & CAMPBELL, J. D. (Eds.), Brachiopods through time: 319-323; A. A. Balkema (Rotterdam, Brookfield).

RAJI, M. & BENFRIKA, E. M. (2009): L´indice de l´altération de la couleur des conodontes: Indicateur d´activité hydrothermale. L´exemple du Dévonien de Mrirt (Maroc central oriental). – Notes et Mémoires du Service Géologique du Maroc, **530**.

RAUMER, J. F. VON, BUSSY, F. & STAMPFLI, G. M. (2009): The Variscan evolution in the External massifs of the Alps and place in their Variscan framework. – Comptes Rendus Geoscience, **341**: 239-252.

RÈGNAULT, A. (1985): Les Scyphocrinitidae (Crinoidea, Camerata) du Silurien terminal-Dévonien basal au Maroc. Répartition stratigraphique et paléogeographique. Discussion. – Actes 110e Congress des Naturelle Société du Savantes, Montpellier Sciences, **4**: 9-20.

RÉGNAULT, S. & CHAUVEL, J. (1987): Découverte d´un échinoderme carpoide (Stylophora – Mitrata) dans le Dévonien Inférieur du Maroc. – Geobios, **20** (5): 669-674.

RIBEYROLLES, M. (1976): Etude tectonique et microtectonique d´un segment de chaine hercynienne dans la partie sud-orientale du Maroc central (Region située entre Aguelmous et Mrirt) – Notes et Mémoires du Service Géologique du Maroc, **261**: 9-56.

RICHTER, J. (2017): Biostratigraphie und Fazies im Devon von Immouzer-du-Kandar südlich von Fes (Marokkanische Meseta). – Unpublished M. Sc. Thesis, WWU Münster, 112 pp.

RICHTER, J., HARTENFELS, S., ABOUSSALAM, Z. S., BECKER, R. T. & EL HASSANI, A. (2016): Biostratigraphy of the isolated Devonian (Emsian to Famennian) at Immouzer du Kandar (south of Fes, Moroccan Meseta). – In: International Geoscience Programme Project 591 - Closing Meeting "The Early to Mid palaeozoic Revolution", Ghent University, Ghent, Belgium, 6-9 July 2016, Closing Meeting Abstracts: 127.

RIQUIER, L., TRIBOVILLARD, N., AVERBUCH, O., JOACHIMSKI, M. M., RACKI, G., DEVLEESCHOUWER, X., EL ALBANI, A. & RIBOULLEAU (2005): Productivity and bottom water redox conditions at the Frasnian-Famennian boundary on both sides of the Eovariscan Belt: constraints from trace-element geochemistry. – In: OVER, D. J., MORROW, J. R. & WIGNALL, P. B. (Eds.), Understanding Late Devonian and Permian-Triassic Biotic and Climatic Events; Towards an Integrated Approach. Developments in Palaeontology & Stratigraphy, **20**: 199-224.

RIQUIER, L., AVERBUCH, O., TRIBOVILLARD, N., EL ALBANI, A., LAZREQ, N. & CHAKIRI, S. (2007): Environmental changes at the Frasnian-Famennian boundary in Central Morocco (Northern Gondwana): integrated rock-magnetic and geochemical studies. – In: BECKER, R. T. & KIRCHGASSER, W. T. (eds.), Devonian Events and Correlations. Geological Society, London, Special Publications, **278**: 197-217.

ROBARDET, M. (2003): The Armorica ´microplate` fact or fiction? Critical review of the concept and contradictory palaeobiogeographical data. – Palaeogeography, Palaeoclimatology, Palaeoecology, **195**: 125-148.

ROBARDET, M., PARIS, F. & RACHEBEUF, P. R. (1990): Palaeogeographic evolution of southwestern Europe during Early Palaeozoic times. – In: MCKERROW, W. S. & SCOTESE, C. R. (Eds.), Palaeozoic Palaeogeography and Biogeography. Geological Society, Memoir, **12**: 411-419.

ROCH, E. (1939): Descxriptions géologiques des montagne à l´Est de Marrakech. – Notes et Mémoires du Service des Mines et Carte géologiques du Maroc, **51**: 438 pp.

ROCH, E. (1950): Histoire Stratigraphique du Maroc. – Notes et Mémoires du Service Géologique du Maroc, **80**: 1-435, 11 maps.

RYTINA, M.-K., BECKER, R. T., ABOUSSALAM, Z. S., HARTENFELS, S., HELLING, S., STICHLING, S. & WARD, D. (2013): The allochthonous Silurian-Devonian in olistostromes at "the Southern Variscan Front" (Tinerhir region, SE Morocco) – preliminary data. – Documents de l´Institut Scientifique, Rabat, **27**: 11-21.

SANDBERG, C. A. (1976): Conodont biofacies of Late Devonian *Polygnathus styriacus* Zone in Western United States. – The Geological Association of Canada, Special Paper, **15**: 171-186.

SANDBERG, C. A., ZIEGLER, W., DREESEN, R. & BUTLER, J. L. (1992): Conodont Biochronology, Biofacies, Taxonomy, and Event Stratigraphy around Middle Frasnian Lion Mudmound (F2h), Frasnes, Belgium. – Courier Forschungsinstitut Senckenberg, **150**: 1-87.

SANDBERG, C. A., MORROW, J. A. & ZIEGLER, W. (2002): Late Devonian sea-level changes, catastrophic events, and mass extinctions. – In: KOEBERL, C. & MACLEOD, K. G. (Eds.), Catastrophic Events and Mass Extinctions: Impacts

and Beyond. Geological Society of America, Special Paper, **356**: 473-487.

SANDBERGER, G. (1855): *Clymenia subnautilina* (nova species), die erste und bis jetzt einzige Art aus Nassau. – Jahrbücher des Vereins für Naturkunde im Herzogthum Nassau, **10**: 127-136, pl. 1.

SANDBERGER, G. & SANDBERGER, F. (18450-1856): Die Versteinerungen des rheinischen Schichtensystems in Nassau. Mit einer kurzgefassten Geognosie dieses Gebietes und mit steter Berücksichtigung analoger Schichten anderer Länder. – XIV + 564 pp., 41 pls.; Wiesbaden.

SANDY, M. R. (1995): A review of some Palaeozoic and Mesozoic brachiopods as members of cold seep chemosynthethic communities: "unusual" palaeoecology and anomalous palaeobiogeographic patterns explained. – Földtani Közlöny, **125** (3/4): 241-258.

SAVAGE, N. (2013): Late Devonian conodonts from northwestern Thailand. – 48 pp., Trinity Press, Eugene, Oregon.

SCHINDEWOLF, O. H. (1942): Zur Kenntnis der Polycoelien und Plerophyllen. Eine Studie über den Bau der "Tetrakorallen" und ihre Beziehungen zu den Madreporarien. - Abhandlungen des Reichsamts für Bodenforschung, Neue Folge, **204**: 1-324, 36 pls..

SCHINDLER, E. (1990): Die Kellwasser-Krise (hohe Frasne-Stufe, Ober-Devon). – Göttinger Arbeiten zur Geologie und Paläontologie, **46**: 1-115.

SCHÜLKE, I. (1999): Conodont multielement reconstructions from the early Famennian (Late Devonian) of the Montagne Noire (Southern France). – Geologica et Palaeontologica, SB **3**: 1-124.

SCHUMACHER, E. (1971): Conodonts from the Middle Devonian Lake Church and Milwaukee Formations. – In: CLARK, D. L. (Ed.), Conodonts and Biostratigraphy of the Wisconsin Paleozoic. Wisconsin Geological and Natural History Survey, Information Circular, **19**: 55-67, 90-99.

SCHWERMANN, K. (2014): Devonische Haizähne aus Marokko – Taxonomie, Stratigraphie und fazielle Verbreitung. – Unpublished M.Sc. Thesis, WWU Münster, 80 pp.

SIMANCAS, J., AZOR, A., MARTÍNEZ-POYATOS, D., TAHIRI, A., EL HADI, H., GONZÁLEZ-LODEIRO, F., PÉREZ-ESTAÚN, A. & CARBONELL, R. (2009): Tectonic relationships of Southwest Iberia with the allochthonous of Northwest Iberia and the Moroccan Variscides. – Comptes Rendus Geosciences, **341**: 103-113.

SOBSTEL, M., MAKOWSKA-HAFTKA, M. & RACKI, G. (2006): Conodont ecology in the Early-Middle Frasnian transition on the South Polish carbonate shelf. – Acta Palaeontologica Polonica, **51** (4): 719-746.

SÖTE, T., HARTENFELS, S. & BECKER, R. T. (2017): Uppermost Famennian stratigraphy and facies development of the Reigern Quarry near Hachen (northern Rhenish Massif)′, Germany). – Palaeodiversity and Palaeoenvironments, **97**: 633-654.

SOULAIMANI, A. & BURKHARD, M. (2008): THE ANTI-ATLAS CHAIN (MOROCCO): the southern margin of the Variscan belt along the edge of the West African craton. – In: ENNIH, N. & LIÉGEOIS, J.-P. (Eds.), The boundaries of the West African craton. Geological Society, London, Special Publications, **279**: 433-452.

SPALLETTA, C., PERRI, M. C., OVER, D. J. & CORRADINI, C. (2017): Famennian (Upper Devonian) conodont zonation: revised global standard. – Bulletin of Geosciences, **92** (1): 31-57.

TAHIRI, A. (1983): Lithostratigraphie et structure du Jebel Ardouz – Maroc hercynien. – Bulletin de l´Institute Scientifique, Rabat, **7:** 1-16.

TAHIRI, A. (1994): Tectonique hercynienne de l´anticlinorium de Khouribga-Oulmès et du synclinorium de Fourhal. – Bulletin de l´Institute Scientifique, Rabat, **8**: 125-144.

TAHIRI, A. & HOEPFFNER, C. (1988): Importance des mouvements distensifs au Dévonien supérieur en Meseta nord-occidentale (Maroc); les calcaires démantelés de Tiliouine et la ride d`Oulmès, prolongement oriental de la ride des Zaèr. – Comptes Rendus de l`Academie des Sciences, Paris, **306** (Série II): 223-226.

TAHIRI, A. & LAZREQ, N. (1988): Précisions stratigraphiques sur le Dévonien de la ride d´El Hammam (Nord d´Oulmès), consequences paléogeographiques. – Bulletin de l´Institute Scientifique, Rabat, **12**: 47-51.

TAHIRI, A., EL HASSANI, A., EL HADI, H., SIMANCAS, F., LODEIRO, F. G., AZOR, A., POYATOS, D. M. & SAIDI, A. (2011): Circuit C13: Meseta nord-occidentale. – Notes et Mémoires du Service Géologique du Maroc, **563** (8): 9-44.

TAHIRI, A., MONTERO, P., EL HADI, H., MARTÍNEZ POYATOS, D., AZOR, A., BEA, F., SIMANCAS, J. F. & GONZÁLEZ LODEIRO, F. (2010): Geochronological data on the Rabat-Tiflet granitoids: Their bearing on the tectonicvs of the Moroccan Variscides. – Journal of African Earth Sciences, **57**: 1-13.

TAHIRI, A., BELFOUL, A. & BAIDER, L. (2013): Chaotic deposits in the Lower Carboniferous formations of the Merzouga area (Tafilalet, Eastern Anti Atlas,

Morocco): Geodynamic importance. – Documents de l´Institute Scientifique, Rabat, **27**: 103-108.

TAHIRI, A., EL HADI, H., POCELET, A., POYATOS, D., AZOR, A., LODEIRO, F. & SIMANCAS, F. (2017): Ediacarian to Cambrian U-Pb ages of granite pebbles in the Lower Devonian conglomerate of Immouzer Kandar (Northwestern Middle Atlas, Morocco). – In: The First West African Craton and Margins International Workshop "WACMA1", Dakhla, Morocco, 24 to 29th April, 2017, Abstracts, 1 p.

TAIT, J., SCHÄTZ, M., BACHTATDSE, V. & SOFFEL, H. (2000): Palaeomagnetism and Palaeozoic palaeogeography of Gondwana and European terranes. – In: FRANKE, W., HAAK, V., ONCKEN, O. & TANNER, D. (Eds.), Orogenic Processes: Quantification and Modelling in the Variscan Belt. Geological Society, London, Special Publications, **179**: 21-34.

TAYLOR, E. L., TAYLOR, T. N. & KRINGS, M. (2009): Paleobotany: The Biology and Evolution of Fossil Plants. – 1252 pp., Academic Press.

TERMIER, H. (1927a): Sur la stratigraphie du Maroc central. – Bulletin de la Société Géologique du France, 4è série, **27**: 21.

TERMIER, H. (1927b): Observations nouvelles en Maroc central. - Bulletin de la Société Géologique du France, 4è série, **27**: 100-102.

TERMIER, H. (1936): Etudes géologiques sur le Maroc central et le Moyen-Atlas septentrional. Tome III. Paléontologie, Pétrographie. – Notes et Mémoires, Service des Mines et Carte géologique du Maroc, **33**: 1-1566.

TERMIER, H. (1938a): Sur l´existence des *Halorella* au Dévonien supérieur. – Comptes Rendus somnaire des Séances de la Société Géologique de France, 5è série, **7**: 108.

TERMIER, H. (1938b): Noveaux affleurements de Famennien dans le Maroc central. - Comptes Rendus somnaire des Séances de la Société Géologique de France, 5è série, **8**: 40-42.

TERMIER, H. & TERMIER, G. (1948): Les phénomènes de speciation dans le genre *Halorella*. Notes et Mémoires du Service Géologique du Maroc, **71**: 47-63.

TERMIER, H. & TERMIER, G. (1949): Sur les genres *Halorella* et *Dzieduszyckia*. – Notes et Mémoires du Service Géologique du Maroc, **74**: 113-115.

TERMIER, H. & TERMIER, G. (1950a): Paléontologie Marocaine. II. Invértebrés de l´ère Primaire. Fascicule II. Bryozoaires et brachiopodes. Notes et Mémoires du Service géologique du Protectorate Francaise de Maroc, **77**: 21-252.

TERMIER, H. & TERMIER, G. (1950b): Paléontologie Marocaine. II. Invértebrés de l´ère Primaire. Fascicule III. Mollusques. – Notes et Mémoires, Service géologique du Protectorate Francaise de Maroc, **78**, 246 pp. (pls. 123-183).

TERMIER, H. & TERMIER, G. (1951): Stratigraphie et Paléobiologie des Terraions Primaires de Benhamed (Chaouïa sud, Maroc). – Notes et Mémoires du Service Géologique Maroc, **5** (85): 47-104.

TERMIER, H. & TERMIER, G. (1970): Sur la géologie de la région de Dchar-Aït-Abdallah (Maroc Central). – Comptes Rendues de l´Academie des Sciences, Paris, Série D, **271**: 1612-1614.

TERMIER, H., TERMIER, G. & VACHARD, D. (1975): Recherches micropaléontologiques dans le Paléozoïque supérieur du Maroc central. - Cahiers de Micropaléontologie, **4**: 1-99 + 10 pls.

TIDTEN, G. (1972): Morphogenetisch-ontogenetische Untersuchungen an Pterocorallia aus dem Permo-Karbon von Spitzbergen. - Palaeontographica, Abt. A, **139** (1-3): 1-63, 15 pls.

TOTO, E. A., KAABOUBEN, F., ZOUHRI, L., BELARBI, M., BENAMMI, M., HAFID, M. & BOUTIB, L. (2007): Geological evolution and structural style of the Paleozoic Tafilalt subbasin, eastern Anti-Atlas (Morocco, North Africa). – Geological Journal, **43**: 59-73.

TRIBOVILLARD, N., AVERBUCH, O. DEVLEESCHOUWER, X., RACKI, G. & RIBOULLEAU, A. (2004): Deep-water anoxia over the Frasnian-Famennian boundary (La Serre, France): as tectonically induced oceanic snoxic event? – Terra Nova, **16**: 288-295.

VACHARD, D., ZAHRAOUI, M. & CATTANEO, G. (1994): Parathuramminines et Moravamminides (Foraminiferes ?) du Givetien du Maroc central. – Revue de Paléobiologie, **14** (1): 1-19.

VALENZUELA-RÍOS, J. I., SLAVÍK, L., LIAO, J.-C., HUŠKOVÁ, A. & CHADIMOVÁ, L. (2015): The middle and upper Lochkovian (Lower Devonian) conodont successions in key peri-Gondwana localities (Spanish Central Pyrenees and Prague Synform) and their relevance for global correlations. – Terra Nova, **27**: 409-415.

VANDELAER, E., VANDORMAEL, C. & BULTYNCK, P. (1989): Biofacies and Refinement of Conodont Succession in the Lower Frasnian (Upper Devonian) of the Type Area (Frasne-Nismes, Belgium). – Courier Forschungsinstitut Senckenberg, **117**: 321-351.

VAN DER VOO, R. (1988): Paleozoic paleogeography of North America, Gondwana, and intervening displaced terranes: Comparisons of paleomagnetism with paleoclimatology and biogeographical patterns. – Geological Society of America, Bulletin, **100**: 311-324.

VODRÁŽCOVÁ, S., KLAPPER, G. & MURPHY, M. A. (2011): Early Middle Devonian conodont faunas (Eifelian, *costatus-kockelianus* zones) from the Roberts Mountains and adjacent areas in central Nevada. – Bulletin of Geosciences, **84** (4): 737-764.

WALLISER, O. H. (1990): Marble Quarry at Pic de Bissous. – Document submitted to the Subcommission on Devonian Stratigraphy (ICS, IUGS), Frankfurt/M., September 1990, 2 pp.

WALLISER, O. H., EL HASSANI, A. & TAHIRI, A. (1995): Sur le Dévonien de la Meseta marocaine occidentale. – Courier Forschungsinstitut Senckenberg, **188**: 21-30.

WALLISER, O. H., EL HASSANI, A. & TAHIRI, A. (2000): Mrirt: A Key Area for the Variscan Meseta of Morocco. – Notes et Mémoires du Service Géologique du Maroc, **399**: 93-108.

WALLISER, O. H. & BULTYNCK, P. (2011): Extinctions, survival and innovations of conodont species during the Kacák Episode (Eifelian-Givetian) in south-eastern Morocco. – Bulletin de l´Institut royal des Sciences naturelles de Belgique, **81**: 5-25.

WANG, Z. H., BECKER, R. T., ABOUSSALAM, Z. S., HARTENFELS, S., JOACHIMSKI, M. M. & GONG, Y. M. (2016): Conodont and carbon isotope stratigraphy near the Frasnian/Famennian (Devonian) boundary at Wulankeshun, Junggar Basin, NW China. – Palaeogeography, Palaeoclimatology, Palaeoecology, **448**: 279-297.

WANG, Q.-L, KORN, D., NEMYROVSKA, T. & QI, Y.-P. (2018): The Wenne river bank section – an excellent section for the Viséan-Serpukhovian boundary based on conodonts and ammonoids (Mississippian; Rhenish Mountains, Germany). – Newsletters on Stratigraphy, **51**: 427-444.

WARD, D., BECKER, R. T., ABOUSSALAM, Z. S., RYTINA, M. & STICHLING, S. (2013): The Devonian at Oued Ferkla (Tinejdad region, SE Morocco). – In: BECKER, R. T., EL HASSANI, A. & TAHIRI, A. (Eds.), International Field Symposium „The Devonian and Lower Carboniferous of northern Gondwana", Field Guidebook. Document de l´Institut Scientifique, Rabat, **27**: 23-29.

WEDEKIND, R. (1913a): Die Goniatitenkalke des unteren Oberdevon von Martenberg bei Adorf. – Sitzungsberichte der Gesellschaft naturforschender Freunde, Berlin, **1913** (1): 23-77, pls. IV-VI.

WEDEKIND, R. (1913b): Beiträge zur Kenntnis des Oberdevons am Nordrande des Rheinischen Gebirges. 2. Zur Kenntnis der Prolobitiden. – Neues du Jahrbuch für Mineralogie, Geologie und Paläontologie, **1913**: 78-95, pl. 8.

WEDEKIND, R. (1918): Die Genera der Palaeoammonoidea (Goniatiten). Mit Ausschluß der Mimoceratidae, Glyphioceratidae und Prolecanitidae. – Palaeontographica, **62**: 85-184, pls. 14-22.

WENDT, J. & BELKA, Z. (1991): Age and Depositional Environment of Upper Devonian (Early Frasnian to Early Famennian) Black Shales and Limestones (Kellwasser Facies) in the Eastern Anti-Atlas, Morocco. - Facies, **25**: 51-90.

WHALEN, M. T., DAY, J., EBERLI, G. P. & HOMEWOOD, P. W. (2002): Microbial carbonates as indicators of environmental change and biotic crisis in carbonate systems: examples from the Late Devonian, Alberta basin, Canada. – Palaeogeography, Palaeoclimatology, Palaeoecology, **181**: 127-151.

WILLEFERT, S. (1963): Graptolites du Silurien et du Lochkovien de Touchchent (anticlinorium de Kasba-Tadla – Azrou, Maroc central). – Notes et Mémoires du Service Géologique du Maroc, **23**: 69-98.

WILLEFERT, S. & CHARRIÈRE, A. (1990): Les formations à Graptolithes des boutonnières de Moyen-Atlas tabulaire (Maroc). – Géologie Méditerranéennne, **17** (3/4): 279-299.

WORK, D. M., MASON, C. E. & KLAPPER, G. (2007): The Middle Devonian (Givetian) ammonoid *Pharciceras* from the New Albany Shale, Kentucky. – Journal of Paleontology, **81** (6): 1510-1515.

XIAN, S., WANG, S., ZHOU, X., XIONG, J. & ZHOU, T. (1980): Nandan typical stratigraphy and paleontology of the Devonian in South China. – Guihou People´s Publishinh House (Guyang).

XU, G. (1977): Fossil Atlas of South-Central China, part 2, Cephalopoda. – Yichang Institute of Geological Science: 537-582, pls. 204-218; Geological Publishing House, Beijing.

YOUNG, G. C. (1981): Biogeography of Devonian vertebrates. – Alcheringa, **5**: 225-243.

YOUNG, G. C. (2003): North Gondwana mid-Palaeozoic connections with Euramerica and Asia: Devonian vertebrate evidence. – Courier Forschungsinstitut Senckenberg, **242**: 169-185.

ZAHRAOUI, M. (1991): La plate-forme carbonate dévoniene du Maroc occidentale et sa dislocation hercynienne. – Unpublished Ph. D. Thesis, University of the Bretagne Occidentale, 261 pp.; Brest.

ZAHRAOUI, M. (1994a): Le Silurien. - Bulletin de l´Institut Scientifique, Rabat, **18**: 38-42.

ZAHRAOUI, M. (1994b): Le Dévonien inférieur et moyen. – Bulletin de l´Institut Scientifique, Rabat, **18**: 43-56.

ZAHRAOUI, M., EL HASSANI, A. & TAHIRI, A. (2000): Devonian outcrops of the Oued Cherrat shear zone. – Notes et Mémoires du Service géologique du Maroc, **399**: 123-128.

ZIEGLER, P. A. (1989): Laurussia – The Old Red Continent. - In: MCMILLAN, N. J., EMBRY, A. F. & GLASS, D. J. (Eds.), Devonian of the World, Proceedings of the Sercond International Symposium on the Devonian System, Calgary, Canada. Canadian Society of Petroleum Geologists, Memoir, **14** (I): 15-48 [imprint 1988].

ZIEGLER, W. (Ed., 1975): Catalogue of conodonts, Volume **2**. – 404 pp.; Schweizerbart, Stuttgart.

ZIEGLER, W. & SANDBERG, C. A. (1990): The Late Devonian standard conodont zonation. – Courier Forschungsinstitut Senckenberg, **121**: 1-115.

ZIEGLER, W., SANDBERG, C. A. & AUSTIN, R. L. (1974): Revision of *Bispathodus* group (Conodonta) in the Upper Devonian and Lower Carboniferous. – Geologica et Palaeontologica, **8**: 97-112.

ZONG, P., BECKER, R. T. & MA, X. (2015): Upper Devonian (Famennian) and Lower Carboniferous (Tournaisian) ammonoids from western Junggar, Xinjiang; northwestern China – stratigraphy, taxonomy and palaeobiogeography. – Palaeobiodiversity and Palaeoenvironments, **95**: 159-202.

Dépôt légal : 2012 PE 0007
ISSN : 2028 - 7615

ACADEMY Press MA

Email : fse@academiesciences.ma
www.academiesciences.ma/fse/